THE HYDROSALINITY MODULE OF *ACRU* AGROHYDROLOGICAL MODELLING SYSTEM (*ACRUSalinity*) :

MODULE DEVELOPMENT AND EVALUATION

AYNOM TESFAY TEWELDEBRHAN

DISSERTATION

Submitted in partial fulfilment of the requirements
for the degree of MSc in Hydrology

School of Bioresources Engineering and Environmental Hydrology
University of Natal
Pietermaritzburg

June 2003

ABSTRACT

Water is characterised by both its quantity (availability) and its quality. Salinity, which is one of the major water quality parameters limiting use of a wide range of land and water resources, refers to the total dissolved solutes in water. It is influenced by a combination of several soil-water-salt-plant related processes. In order to develop optimum management schemes for environmental control through relevant hydrological modelling techniques, it is important to identify and understand these processes affecting salinity. Therefore, the various sources and processes controlling salt release and transport from the soil surface through the root zone to groundwater and streams as well as reservoirs are extensively reviewed in this project with subsequent exploration of some hydrosalinity modelling approaches.

The simulation of large and complex hydrological systems, such as these at a catchment scale, requires a flexible and efficient modelling tool to assist in the assessment of the impact of land and water use alternatives on the salt balance. The currently available catchment models offer varying degrees of suitability with respect to modelling hydrological problems, dependent on the model structure and the type of the approach used. The *ACRU* agrohydrological modelling system, with its physically-conceptually based characteristics as well as being a multi-purpose model that is able to operate both as a lumped and distributed model, was found to be suitable for hydrosalinity modelling at a catchment scale through the incorporation of an appropriate hydrosalinity module.

The main aim of this project was to develop, validate and verify a hydrosalinity module for the *ACRU* model. This module is developed in the object-oriented version of *ACRU, viz. ACRU2000,* and it inherits the basic structure and objects of the model. The module involves the interaction of the hydrological processes represented in *ACRU* and salinity related processes. Hence, it is designated as *ACRUSalinity*. In general, the module is developed through extensive review of *ACRU* and hydrosalinity models, followed by conceptualisation and design of objects in the module. It is then written in Java object-oriented programming language. The development of *ACRUSalinity* is based mainly on the interaction between three objects, *viz.* Components, Data and Processes. Component objects in *ACRU2000* represent the physical features in the hydrological system being modelled. Data objects are mainly used to store data or information. The Process objects describe processes that can take place in a

conceptual or real world hydrological system. The Process objects in *ACRUSalinity* are grouped into six packages that conduct:

- the initial salt load determination in subsurface components and a reservoir
- determination of wet atmospheric deposition and salt input from irrigation water
- subsurface salt balance, salt generation and salt movement
- surface flow salt balance and salt movement
- reservoir salt budgeting and salt routing and
- channel-reach salt balancing and, in the case of distributed hydrosalinity modelling, salt transfer between sub-catchments.

The second aim of the project was the validation and verification of the module. Code validation was undertaken through mass balance computations while verification of the module was through comparison of simulated streamflow salinity against observed values as recorded at gauging weir U1H005 which drains the Upper Mkomazi Catchment in KwaZulu-Natal, South Africa. Results from a graphical and statistical analysis of observed and simulated values have shown that the simulated streamflow salinity values mimic the observed values remarkably well. As part of the module development and validation, sensitivity analysis of the major input parameters of *ACRUSalinity* was also conducted. This is then followed by a case study that demonstrates some potential applications of the module. In general, results from the module evaluation have indicated that *ACRUSalinity* can be used to provide a reasonable first order approximation in various hydrosalinity studies.

Most of the major sources and controlling factors of salinity are accommodated in the *ACRUSalinity* module which was developed in this project. However, for a more accurate and a better performance of the module in diversified catchments, further research needs to be conducted to account for the impact of salt loading from certain sources and to derive the value of some input parameters to the new module. The research needs include incorporation in the module of the impact of salt loading from fertilizer applications as well as from urban and industrial effluents. Similarly, further research needs to be undertaken to facilitate the module's conducting salt routing at sub-daily time step and to account for the impact of bypass flows in heavy soils on the surface and subsurface salt balances.

DISCLAIMER

I wish to certify that the work reported in this dissertation is my own original and unaided work except where specific acknowledgement has been made. In addition I wish to declare that this dissertation has not been submitted for a degree in any other university.

Signed: 

Signed: 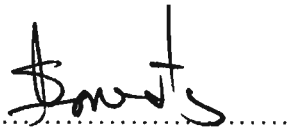

Supervisor

ACKNOWLEDGEMENTS

I would like to express my sincere thanks and appreciation to the following persons and institutions for their invaluable contribution to the work presented in this thesis:

Dr. S. A. Lorentz, School of Bioresources Engineering and Environmental Hydrology, for supervision and assistance throughout this research;

Professor R. E. Schulze, School of Bioresources Engineering and Environmental Hydrology, for co-supervision and assistance throughout this research;

Mr. A. Pike, for his patient and constructive advice throughout the module development and at early stage of the verification phases of this research;

Mr. D. Clark, Land Resources International (LRI), for his advice and assistance when I started learning the Java object oriented programming language and for answering my many *ACRU2000* and Java related questions;

Professor, J. Smithers, head, School of Bioresources Engineering and Environmental Hydrology, for his continual encouragement throughout the research project;

Dr. G. Kiker, for his warm welcome when I first arrived to the school in 2001, for his encouragement and providing me helpful *ACRU2000* related papers;

Ms. V. Taylor, School of Bioresources Engineering and Environmental Hydrology, for supplying me with input files for the *ACRU 300*, helpful materials and information related to the Mkomazi Catchment;

The staff of Ninham Shand Consulting Engineers (especially Professor A. H. M. Görgens) for providing me with helpful data and a FORTRAN program for data patching;

The Human Resources Development Project, in Eritrea, for the postgraduate study grant.

TABLE OF CONTENTS

LIST OF FIGURES

LIST OF TABLES

LIST OF SYMBOLS AND ABREVIATIONS

θ = soil water content

λ = dispersivity

A_{adj} = adjunct impervious area

A_{dam} = dam area

A_{dis} = disjunct impervious area

A_{gls} = gross net land segment area

A_{irrig} = irrigated land area

A_s = the surface area at various storage volumes of the reservoir

BF = volume of baseflow release for the day

BTC = break-through curves

C = solute concentration

C_{bf} = baseflow salt concentration

C_{chnl} = TDS concentration of flow at the channel reach

CDE = convection-dispersion equation

C_{dsf} = salt concentration of delayed stormflow

C_e = solute equilibrium

C_{gw} = salt concentration of the groundwater store before salt generation

C_i = salt concentration of the i-th horizon before salt generation or reservoir salinity at the end of the current day of simulation

C_{i-1} = reservoir salinity at the end of the previous day

C_{in} = TDS concentration in water infiltrating to a particular layer

Cin_i = average salt concentration of reservoir inflowing water on the current day of simulation

C_{iw} = irrigation water salinity

C_{nf} = salt concentration of normal (legal) flow release

C_{of} = salt concentration of overflow

C_{qf} = quickflow salinity

C_r = rainfall salinity

C_{run} = salt concentration of runoff water

C_{run_adj} = salt concentration of runoff from adjunct impervious areas

C_{run_imp} = salt concentration of runoff water from impervious areas

C_{run_irr} = salt concentration of runoff water from irrigated areas

C_{run_ni} = Salt concentration of runoff from non-irrigated lands

C_{sat} = the equilibrium value

C_{seep} = salt concentration of seepage water

C_{sf} = stormflow salinity

CSIR = council for scientific research

C_{upd_gw} = updated groundwater salinity (after salt generation)

C_{upd_i} = updated horizon salinity (after salt generation)

D_* = coefficient of molecular or ionic diffusion for the liquid phase of the soil

D_{dis} = coefficient of mechanical dispersion

D_o = coefficient of molecular diffusion for a free or bulk solution

DUL = drained upper limit

DWAF = department of water affairs and forestry

EC = electrical conductivity

ECe = soil salinity

ECw = electrical conductivity of applied irrigation water

ER = volume of effective rainfall

Fc_i = drained upper limit of the i-th layer

f_{dam} = fraction of the gross catchment area contributing its flow to the dam

GW = volumetric groundwater content after baseflow release

Ia = initial abstractions before stormflow commences

I_{dam} = total water inflow to the dam on the day including rain falling on surface of the dam

IW = volume of irrigation water

IWR = institute for water research

Jc = convective flux of solute

J_{dif} = solute flux due to molecular diffusion

J_{dis} = dispersive solute flux

Js = total solute flux due to the joint effects of diffusion and convection

k = salt uptake rate constant

L = straight length of the soil

L_* = actual path length for diffusion in the soil

LAI = leaf area index

LF = fraction of applied volume of water leached below the root zone

$LNLSA\_i$ = lower net land segment area under the i-th sub-catchment configuration

MAP = mean annual precipitation

NF_{dam} = legal flow release volume

$NLSA$ = total area of the non-irrigated land in a sub-catchment

OF_{dam} = dam overflow volume

Pg = gross daily precipitation amount

PW_i = volume of percolated water out of the i-th horizon

Q = discharge

q = rate of volumetric water flow

Q_a = local concentration of solute in the adsorbed phase

QF = quickflow volume

QF = total quickflow volume

QF_a = actual quickflow, i.e. fraction of the total stormflow leaving the land on the same day

Qin_i = water inflow to the reservoir on the current day of simulation

$Qout_i$ = water outflow from the reservoir for the current day of simulation (excluding evaporation loss)

R = volumetric ratio of "new" to "old" water

RFL_{dam} = volume of rain falling on the dam surface

RUN = the total runoff volume from non-irrigated land in a sub-catchment

RUN_{adj} = runoff volume from the adjunct impervious areas

RUN_{adj_dam} = runoff from adjunct impervious areas inflowing to the dam

RUN_{chnl} = runoff volume inflowing to the channel

RUN_{dam} = runoff volume entering to the dam

RUN_{dis} = runoff volume from disjunct impervious area

RUN_{imp} = depth of runoff from impervious area

RUN_{irr} = runoff from irrigated areas

RUN_{ni} = runoff flowing into the dam from non-irrigated lands

S = solute loss (sink) or gain (source)

$SEEP_{dam}$ = volume of seepage water from the dam

SF_d = fraction of delayed stormflow contributing to quickflow

$Sgen$ = total daily salt mass generated per soil layer

S_i = volume of water stored in the reservoir at the current day of simulation

S_{i-1} = volume of water stored in the reservoir at the end of the previous day

SL = total salt load associated with runoff from the non-irrigated land

SL_{adj_chnl} = salt load flowing into the channel from adjunct impervious areas

SL_{adj_dam} = the salt load flowing into the dam from adjunct impervious areas

SL_{aiw} = salt load input to topsoil associated with irrigation water

SL_{bf} = salt load associated with baseflow release

SL_{chnl} = salt load entering to the channel

SL_{dam} = salt load inflowing to the dam

SL_{dam_of} = total salt load released from the dam to downstream reaches

SL_{dis} = salt load associated with runoff from disjunct impervious areas

SL_{er} = salt load input to topsoil associated with rainfall

SL_{gen_gw} = salt load generated for the day in groundwater store

SL_{gen_i} = salt load generated for the day in the i-th soil horizon

SL_{gw} = groundwater store salt load before salt generation

SL_i = current salt load of the i-th horizon before salt generation

SL_{inf_t} = daily total salt load stored in the channel reach

SL_{p_i} = the salt load associated with the percolation water out of the i-th horizon

SL_{qf} = salt load associated with the total quickflow volume for the day

SL_{run} = the salt load associated with runoff water

SL_{upd_gw} = salt load of groundwater store after salt generation

SL_{upd_i} = salt load in the i-th horizon after salt generation

SL_{upf} = upward salt flux from topsoil to quickflow

$SMCs$ = soil moisture content

SP_i = saturation water content

$STFL$ = volume of streamflow at the channel reach

Sv = storage (volume) of water

SW_i = volumetric soil water content of the i-th horizon after percolation has taken place out of the horizon

TDS = total dissolved solutes

UML = unified modelling language

$UNLSA\_i$ = upper net land segment area under the i-th sub-catchment configuration

V = average flow velocity

x = distance

$X(LF)$ = concentration factor

1. INTRODUCTION

Water is characterised by both its quantity (availability) and its quality (for example, its salinity). The significance of an integrated management of water quantity and quality is stated in Principle 15 of the South African National Water Act of 1998 as "Water quality and quantity are interdependent and shall be managed in an integrated manner, which is consistent with broader environmental management approaches" (Pegram *et al.*, 1998). In arid and semi-arid areas it may seem that water quantity is the primary concern. However, quantity and quality issues are so interwoven that attempting to address one without the other is an exercise in futility (Seelig *et al.*, 2001).

Salinity, as a result of natural and anthropogenic solute inputs, is causing serious water quality problems in many parts of the world, such as the Breede and Fish-Sundays River systems in South Africa (Jonker, 1995), the Murray Darling Basin in Australia (Blackmorea *et al.*, 1999) and the eastern and western lowlands of Eritrea. Salinity causes loss of yield and degradation of agricultural lands. History relates that ancient civilizations based on irrigated agriculture in river valleys (e.g. Mesopotamia) collapsed, as they did not provide drainage systems for leaching of the accumulated salt (Aswathanarayana, 2001). Salinity is also reported to cause road and wall damage in many parts of Australia (Blackmorea *et al.*, 1999). Furthermore, salinity also limits domestic and industrial water uses. It has a direct influence on the industrial and domestic water users through corrosion of water reticulation systems such as water delivery pipes.

Salinity is related to the total dissolved solid (TDS) concentration of water (Walling and Webb, 1986). According to Michael (1997a), the main soluble constituents in water are calcium, magnesium, sodium and, sometimes, potassium as cations and chloride, sulphate, bicarbonate and carbonate as anions. The standard method of measuring salinity is the use of electrical conductance (EC), sometimes referred to as specific conductance (Seelig *et al.*, 2001). Salinity is expressed in various units which include, millimho per centimetre (mmho/cm), deci-siemens per metre (ds/m), moles per cubic metre of solution (mol/m^3), grams per cubic metre of solution (g/m^3) and milliequivalents per litre of solution (meq/l). The fate and transport of salts in the soil is described mathematically with hydrosalinity models (Moolman, 1993).

Studies dealing with hydrosalinity are essential for assessing the effects of land and water uses on salinisation. Research focused on soil salinity has been carried out internationally for more than a century (Shouse *et al.*, 1997). Similarly, the development and application of computer operated mathematical models to simulate the movement of pollutants, and thus to anticipate environmental problems, has been the subject of extensive research by government agencies, universities and private companies for many years (Jayatilaka and Connel, 1995). Models dealing with salt loading in streams and across impoundments are of global interest because such models can provide a wide range of support for salinity management: from helping to understand the cause-effect relation between various sources and salinity impacts, to design of control measures and subsequent assessment of their effectiveness. However, knowledge about the main sources and controlling factors is important for the development of hydrosalinity models.

Salinity is affected by a combination of several soil-water-salt-plant factors. Therefore, in order to accurately estimate the magnitude of the hazard posed by salinity, it is important to identify and understand the processes that control salt movement from the soil surface through the root zone to the groundwater and streamflow. Knowing these processes makes it possible to develop optimum management schemes for environmental control for the purpose of preventing groundwater, streamflows and farm land salinisation (Bresler, 1981). For the above reasons, an extensive literature review was undertaken (Chapters 2 and 3) to assess the governing processes in hydrosalinity, to examine how these processes interact with various factors to influence water salinisation and to explore some modelling techniques employed to describe these processes.

The main aim of this research was to develop and evaluate a catchment hydrosalinity module that could provide information for use in planning, design and management of water and land uses through modelling surface and subsurface salinisation, including reservoir and streamflow. In general, the module makes two basic assumptions, *viz.* salt is a conservative substance, and reservoirs and flow in streams are completely mixed systems. The *ACRU* agrohydrological modelling system (Schulze, 1995a), with its physically-conceptually based structure and its multi-purpose capability as a lumped or distributed model, was found to be a suitable model within which the hydrosalinity module could be developed for its intended uses. The hydrosalinity module was developed in the object oriented version of the model, *viz. ACRU2000*. It inherits the basic structure and objects of the model. The new module was

designed with the help of Rational Rose Software and is encoded with Java object-oriented programming language. The specific objectives of this project were:

a. to develop a catchment hydrosalinity module within the *ACRU* agrohydrological modelling system to:
    i. simulate TDS concentration and salt loading of surface and subsurface flows from a number of land use categories including irrigated, non-irrigated and impervious areas and, to
    ii. simulate reservoir storage as well as outflow salinity and salt loading;

    in order for predictions from the module to assist catchment planners to:
    - assess effects of climatic and hydrologic variability on future TDS concentration and salt loading
    - assess effects of future land use changes on future salinity levels and salt loading
    - assess the effects of water resources developments on future salinity levels and salt loading and to
    - analyse how operating policies or water allocation such as reservoir releases designed to dilute high TDS concentration at downstream reaches, may need to change to mitigate effects of exceeding salinity standards, especially in critical low flow periods; and furthermore
b. to test the hydrosalinity module both for its underlying codes and through comparison of simulated streamflow TDS concentration against the available observed values.

As part of the development and evaluation of the new module, a sensitivity analysis is undertaken to assess model response to changes in the main hydrosalinity input parameters. A case study is also carried out for the Upper Mkomazi Catchment to illustrate some potential applications of the module. This dissertation documents the development and evaluation of the hydrosalinity module (Chapters 5, 6 and 7). Some important points that need further explanation are discussed and general conclusions are presented in Chapter 8. Further research to enhance the performance of the hydrosalinity module is recommended in Chapter 9.

2. SOURCES AND CONTROLLING FACTORS OF HYROSALINITY

High levels of dissolved salts make some of South Africa's rivers unsuitable as a supply source for growing crops. Major sources of saline water are municipal, mining and industrial effluents and seepage from waste disposal sites (DEAT, 1996). In the semi-arid parts of the country low precipitation, coupled with high evaporation, further increase the salt concentrations of both surface and groundwater resources. Identification of the various sources of salinity, the factors controlling it and knowledge on the interrelationships between sources and factors are most important for the development of a hydrosalinity model. This chapter, therefore, reviews the main sources and controlling factors of hydrosalinity.

2.1 Sources of Hydrosalinity

The main sources of hydrosalinity may differ from one area to another depending on governing environmental and social factors in that particular area. However, an assessment made by different researchers to identify the various sources has revealed the main sources of hydrosalinity to be rock and soil weathering, wet and dry atmospheric inputs, irrigation return flows as well as urban and industrial effluents. These sources can broadly be categorised into natural and anthropogenic sources.

2.1.1 Natural sources

Soil and rock weathering, as well as atmospheric inputs, are natural sources for most of the salts added to the soil solution and open water bodies. The weathering of parent material of soil or rocks, which includes hydrolysis, hydration, solution, oxidation and carbonation is reported to be the primary source of salinity in irrigation water (Michael, 1997a). Most rocks consist of an assemblage of minerals. The mechanism and rate of reaction of these minerals in the presence of water depends on how the minerals themselves react (Spears, 1986). Interactions between water and surrounding rocks involves reactions which generally include chemical weathering of rock forming minerals, dissolution-precipitation of secondary minerals and ion exchange between water and secondary minerals (Njitchoua *et al.*, 1997).

Atmospheric inputs can be of marine or continental origin and can be deposited as wet or dry inputs. Atmospheric inputs can vary according to the relative influence of major sources such as oceanic aerosols, continental dust, living and decaying vegetation and active volcanoes (Meybeck, 1983). Oceanic aerosols are the main contributors of atmospheric inputs, particularly in coastal areas (Walling and Webb, 1986). The common constituents of atmospheric inputs derived from continental sources include Ca^{2+}, NH_4, SO_4^{2-}, HCO_3^- and NO_3^-, while marine sources contribute Na^+, Cl^-, Mg^{2+} and K^+ (Raymond, 2001). Atmospheric inputs can greatly influence water salinity, especially when the rate of weathering is very low (Meybeck, 1983).

Different studies have reported the complexity of predicting atmospheric inputs based on atmospheric processes. First, it is difficult to trace the origin of most atmospheric salts, because they may be carried hundreds of kilometres from their sources (Johnston, 1993). Moreover, according to Walling and Webb (1986), the relative importance of atmospheric material removal mechanisms varies in response to change in droplet size distribution, atmospheric conditions, droplet life times and precipitation duration and intensity. Thus the complexity and variability of atmospheric input mechanisms make any attempt to model wet deposition from a knowledge of its component processes difficult. For above reasons it is common practice to use relatively simple empirical analysis of collected wet deposition samples mainly because of the easy measurement techniques which are available, compared to the more complex mechanistic approach which has proved less valuable in a predictive sense because of difficulties of obtaining all the input variables (Walling and Webb, 1986).

2.1.2 Anthropogenic sources

Return flows from irrigated lands as well as urban and industrial effluents are the main sources of hydrosalinity from anthropogenic influences. According to Johnston (1993), drainage effluent, especially from arid or semi-arid agricultural land, almost always contains some amount of dissolved mineral salts. These salts either originate in the irrigation water or the soil, or are present as a result of fertiliser application. The concentration of these salts increase as water is lost from soil and plants in the form of evaporation and transpiration. Water applied in excess of plant requirement dissolves and leaches the salts through either natural or artificial drainage systems.

Most irrigation water contains certain amounts of salt that generally range from 70 to 3500 mg/l (Luthin, 1997) and water uptake by plants and evaporation from the soil surface further concentrates the salt. Thus the salinity level of drainage water is usually higher than that of the applied irrigation water. The salt content of mountain streams increases as the streams pass through alluvial areas which receive water from upstream irrigation activities. Hence drainage water from agricultural lands always contains some amount of dissolved mineral salts and, according to Ayers and Westcot (1985), drainage systems are usually constructed without consideration of the adverse impacts on receiving surface waters. Therefore irrigated agriculture, especially in arid and semi-arid regions, is the primary diverter of water and donor of salts to water resources (Johnston, 1993).

Salinity problems in irrigation areas and in rivers can be exacerbated by poor management systems. For example, they can get worse by downstream irrigators having to use water already containing high salt concentrations, drawn from rivers which drain salt-affected dry land areas (NSW, 2000). The same applies to pumping from saline groundwaters.. Other major causes of irrigation salinity include over-irrigation of farmlands, inefficient water use, poor sub-surface drainage, irrigating on unsuitable or "leaky" soil, allowing water to pond for long periods and allowing seepage from irrigation channels, drains and storage (NSW, 2000). Thus the type of irrigation and leaching practices are likely to affect the salt contribution through subsurface return flows. For example, basin and border types of irrigation practices are reported to result in soluble salts moving through the soil with the irrigation water because of their relatively poorer efficiencies, and thereby increasing subsurface salt concentrations. Most subsurface return flow problems, however, result from unlined water delivery and drainage ditches (Seelig *et al.*, 2001).

Urban sewage and industrial waste effluents can also be significant sources of water salinity. Some industrial processes concentrate salts in the water they use. For example, in coal fired power stations water used for cooling is partly evaporated and concentrates the salt in the water discharged from coolers (NSW, 2000). Similarly, sulphate emissions from energy and industrial facilities cause an "acid rain" effect (Pegram and Görgens, 2001). Abandoned mines are also reported as major sources of salinity in some areas. Wiechers *et al.* (1996), from their research on Nigel Dam in South Africa, noted high concentrations of salts dominated by sulphate concentrations of up to 780 mg/l attributed to seepage from gold mines. Similarly, in more densely populated urban areas, the annual levels of stream

chemistry are reported to reflect the varying effect of sewage inputs (Walling and Webb, 1986). An increase in sodium and chloride ion concentrations by 40 and 45 mg/l respectively, was reported by Wiechers *et al.* (1996) when direct discharge into Nigel Dam from sewage treatment works was commenced. Studies in the Vaal River Catchment in South Africa have also shown a similar rise of total dissolved solid concentrations from 125 to 700 mg/l in the period 1935-1980 (Furness, 1989). The increased salinisation of this river was mainly attributed to increased urbanisation and industrialisation. Industries and sewage works alone contribute about 35% of the total load entering the Vaal River (Cowan and Skivington, 1993).

2.2 Factors Controlling Hydrosalinity

The factors involved in hydrosalinity are highly inter-linked. The basic factors reported by various studies can, however, be broadly grouped into soil and geologic formations, hydrological and climatic factors, land use and land cover as well as topographic characteristics and time.

2.2.1 Soil and geologic formations

Certain soils and rock types are more likely to contribute to land and stream salinity problems than others because of their composition, texture, structure, location or other physical and chemical characteristics. For example, there is a high degree of association of salinity with certain classes of sedimentary rocks compared with that from other rock formations (Blackmorea *et al.*, 1999). A frequency distribution analysis of specific conductance level in relation to major rock types by Walling and Webb (1986) has shown a clear contrast of the distributions between most rock types. This was related to the varying susceptibility of the major rock types to chemical weathering. Weatherablity of a mineral depends on the basicity of the mineral, the degree of linkage of tetrahedrons, as well as structure and the degree of crystallinity and purity of the mineral (Michael, 1997a). The differences in major rock types not only affects the variation in the magnitude of total solute concentrations, as expressed by specific conductance, but also the balance between the concentrations of individual cations in receiving streams, as shown in Table 2.1.

Table 2.1 Influence of rock type on the average composition of world river waters (Meybeck, 1981)

Constituents	Average concentration (mg/l)		
	Plutonic and highly metamorphosed rocks	Volcanic rocks	Sedimentary rocks
SiO_2	1.5x	3.5x	x
Ca^{2+}	4	8	30
Mg^{2+}	1	3	8
K^-	1	1.5	1
Na^-	Oceanic influences dominant		
Cl^-	Oceanic influences dominant		
SO_4^{2-}	2	6	25
HCO_3^-	15	45	100

NB. x denotes average SiO_2 content of water from rivers draining sedimentary rocks at a given temperature.

Furthermore, even small-scale changes in bedrock geology can have a large impact on stream water chemistry. For example, according to Billett *et al.* (1996) and Raymond (2001), parent material such as evaporites or carbonates, which on a catchment scale may be spatially insignificant, will have a disproportionally large effect on stream water chemistry (Table 2.2).

Table 2.2 The influence of rock type on dissolved river loads (Raymond, 2001)

Rock Type	World Outcrop Area (%)	Dissolved River Load (%)
Crystalline igneous and metamorphic	34.0	12.0
Evaporites	1.3	15.0
Carbonates	16.0	50.0

The physical characteristics of geological formations also affect the movement of water and dissolved solids to receiving streams. Frequently, discharge points will first appear where there is a change in rock type or along a fracture (NSW, 2000). Moreover, according to Blackmorea *et al.* (1999), groundwater movement is usually independent of local landforms, being determined more by the regional rock structures. Thus, in the presence of saline groundwater, these factors can make important contributions to the processes involved in water salinisation. Similarly the chemical and physical properties of a soil can also influence water salinity both in terms of composition and movement of draining water. For example, Rhoades *et al.* (1997) have observed greater increases in salt concentration of irrigation water as it flowed across heavy textured soils with large cracks and fractures than across non-cracking soils. However, in order to simplify calculations of water losses below the root zone, some researchers assume that the amount of water that flows directly below the root zone through the cracks (by pass flow) in cracking soils does not contribute to leaching (for example, Crescimanno *et al.*, 2002).

2.2.2 Hydrologic and climatic factors

Hydrologic and climatic factors are the major factors that control water salinisation. The following sections review some of the factors grouped under these categories, on how they influence water salinisation.

2.2.2.1 Rainfall

Rainfall is the fundamental driving force and pulsar input to most hydrological processes (Schulze *et al.*, 1995c), resulting also in water quality impacts from non-point sources (Pegram and Görgens, 2001). Rainfall plays a major role during wet atmospheric deposition. Flügel (1987) has suggested that rainfall salt input could account for about 10 to 20% of the total salt output measured in the Sandspruit River, South Africa. Similarly, Michael (1997b) has reported a positive correlation between rainfall depth and chloride content in coastal stations of the UK. According to Gibbs (1992), the chemical composition of low-salinity waters is controlled by the amount of dissolved salts furnished by precipitation. This principle has been observed in moorland areas, where there are low solute inputs from weathered local material. In these areas seasonal variation in stream solute concentrations are strongly related to annual variations in the chemistry of incoming precipitation (Walling and Webb, 1986).

Under certain circumstance rainwater composition can play a substantial role in rain-derived flood and mineral chemical interaction. Generally, according to Nativ *et al.* (1997), in rainwater the concentrations of sodium are higher than those of potassium. Sodium ion is more electronegative than potassium and thus there is a higher affinity of this ion to be absorbed by the soil particle surfaces as compared to potassium. It was suggested, therefore, that sodium could be sorbed from the rain-derived floodwater on to mineral surfaces releasing sorbed potassium to the floodwater and thereby affecting the composition of receiving streams.

2.2.2.2 Irrigation water

The volume of irrigation water is also a key management issue for proper salinity control in irrigated areas. According to Tedeschi *et al.* (2001), over-irrigation is the main cause of two alternative negative scenarios: (1) areas with limited drainage experience rising water tables, "evapoconcentration" of water and soil salinisation, and (2) areas with unlimited drainage result in deep percolation of surplus water, mineral dissolution, mobilisation of salts and salinisation of the receiving subsurface and surface water bodies.

2.2.2.3 Total evaporation

A reduction in water content of the soil in the field at water contents below drained upper limit (DUL) and consequent increase in salt concentration would normally arise from evaporative drying, either as a result of evaporation from the soil surface, or due to water uptake by plant roots in response to transpiration by the leaves (Johnston, 1994). Different studies have shown the presence of some chemical constituents in irrigation and rainwater and the loss of this water through evaporation from the soil and vegetation tends to increase salt concentration. Irrigation water drawn from surface or groundwater sources can typically contain 200 to 2000 mg/l of salts (Aswathanarayana, 2001). Dissolved solids are added to agricultural land by way of irrigation and rainwater. However, neither surface water evaporation nor absorption by plants appreciably reduces the amount of these salts added to the soil (Kay, 1986). Rather, the continuous upward movement of water from a subsurface system results in salt accumulation near the soil surface as water is lost by evaporation (Hoffman *et al.*, 1990). An increase in evaporation can also cause a lowering of the water

table during the day time hours. This, in turn, can result in a daily cycle of accumulation and re-dissolution of soluble materials (Walling and Webb, 1986).

2.2.2.4 Runoff volume and flow components

Different researchers have noted the rise of salt concentrations during periods of low flows and a corresponding decrease during high flow periods. Kelbe and Germishuyse (1999), for example, have noted a drop in electrical conductivity of runoff immediately as discharge rates started to increase. The conductivity of runoff reached a minimum value at almost the same time as the peak flow occurred. However, according to Datta (1983), there may be a lag or lead effect in the drop of TDS concentration after or before a rise in discharge. Usually the trough in solute concentration in water progressively lags behind the peak of water discharge as the flood hydrograph moves downstream.

Several natural and anthropogenic factors can influence hydrosalinity through their effect on reducing the levels of flow. Increasing regulation of river flows and the abstraction of water for consumptive uses are some of the aggravating anthropogenic factors resulting in a decrease in natural flushing of salts out of a particular catchment. Irrigation practices reduce the diluting flows of natural runoff. The use of water for irrigation not only reduces dilution flows, but also speeds up the rise in groundwater levels, bringing salts to the surface and increasing salt flushes to rivers (Blackmorea *et al.,* 1999).

Unlike the relationship between TDS concentration and runoff volume, a positive correlation exists between salt load and annual runoff. According to Crabtree (1986) this can be partly explained by the increased rate of salinity related chemical reactions with increased water availability. High runoff volumes result in increased moisture availability, this in turn provides an increase in the total quantity of dissolved material released or available for transport. Moreover, the erosive power of high runoff volumes may also cause an exposure of saline subsoil and consequent washing away of solutes to watercourses (NSW, 2000).

One of the main reasons for the difference in solute concentrations of high and low flows, with a mainly inverse relationship between flow volume and salinity, are the different sources of runoff components contributing to the total flow. During low flows runoff is generated from the lower soil profile and the groundwater reservoir and has a relatively high

concentration of dissolved solids (Walling and Webb, 1986). Ferguson *et al.* (1994) suggest that the pathways are slow through soil and rock in low flow conditions and faster near or over the land surface during rainfall events and floods. Thus the longer residence time of slow–moving groundwater allows solute enrichment. On the other hand, during high flow much of the runoff is translated rapidly to the channel and has little opportunity for solute pickup. It is this variable mixture in the stream of enriched "old" water and more diluted "young" surface water that leads generally to an inverse relationship between solute concentration and water discharge.

As a rule runoff components reflect the pathway of water. Thus, variation of solute concentrations in runoff water occur as a result of the changing contributions of the different pathways. Although, the soil chemistry of deeper mineral soils is strongly influenced by the underlying geology, this influence becomes less evident on receiving streams at high flows as water flow paths become increasingly dominated by surface and subsurface flow passing through organic top soils (Billet *et al.* 1996).

2.2.3 Land use and land cover

Land use and development in a catchment can have a significant impact on the quantity and quality of the surface and groundwater resources (Pegram *et al.*, 1998). In most areas of Australia, for example, increased salinity was found to result from a particular land use practice such as deforestation, urban development, river regulation, irrigation or cultivation of crops and pasture (NSW, 2000). The effect of land use on salinisation is mainly associated with intensive use and re-use of water as a result of increasing urbanisation, industrialisation, mining and irrigation (Furness, 1989). Some researchers have also reported the role of land use on hydrosalinity through its effect on dry and wet atmospheric deposition, weathering and other sources of salinity (for example, Walling and Webb, 1986).

Any land use practice which allows excess moisture to migrate downward through the soil profile beneath the root zone, can contribute to the rise of the groundwater table and consequent formation and growth of dry land salinity (Johnston, 1993). Trees and shrubs consume more water than annual crops and grasses. Moreover, because of their deep rooting system, they usually extract water from greater depths. Research in high rainfall areas (more than 600 mm per annum) of the Murray-Darling basin in Australia has shown that land use

change from native vegetation to grazing land has increased the amount of water entering the groundwater system by 10 mm per annum (Blackmorea *et al.*, 1999). The same authors have also reported that the "leakage" rate for grazing areas in medium rainfall areas is two to three times greater than under woodland vegetation. Similarly, an increase in amount of water entering the groundwater system as a result of removal of vegetation for urban development has been reported by NSW (2000). The entrance of this additional water into the groundwater system leads to an accumulation of soluble salts at or near the surface along with the rising water table (Johnston, 1993). As to the effect of fallow land, Miller *et al.* (1981) suggest that most soils store limited amounts of water in the root zone during a fallow period. Thus, once recharged by precipitation, any additional water entering the soil moves to the water table and may appear downslope as a saline seep. Generally the basic cause of dryland salinity in Australia is clearing of natural vegetation for agricultural land use (Hillman, 1981). Once dry land salinity is developed, leaching of salts stored in the landscape causes serious problem on the quality of water resources.

Management practices associated with certain land use types can also influence hydrosalinity, depending on whether the particular land use or management practice has soil disturbing or stabilising effect. According to Collins and Jenkins (1996), higher weathering rates as a result of soil tillage practices in agricultural lands can promote high concentrations of base cations. Some studies have indicated the existence of a strong contrast in solute level of streams draining from agricultural land and other land uses, which are less disturbed by agricultural practices. For example, Walling and Webb (1986) noted a progressive decline in total solute level with increase in percentage of moorland cover from 50% to 90% (Figure 2.1 a), with a subsequent shift in the composition of water from Ca^{2+} and Mg^{2+} (mainly as a result of weathering) to Na^{+} and K^{+} (mainly as a result of atmospheric input) as major constituents (Figure 2.1 b). This phenomenon is associated with the lower soil disturbing effects of moorland compared to those of agricultural lands. The addition of mineral fertilizers on drainage basins can also result in an elevated concentration of some solutes on the receiving streams draining agricultural lands.

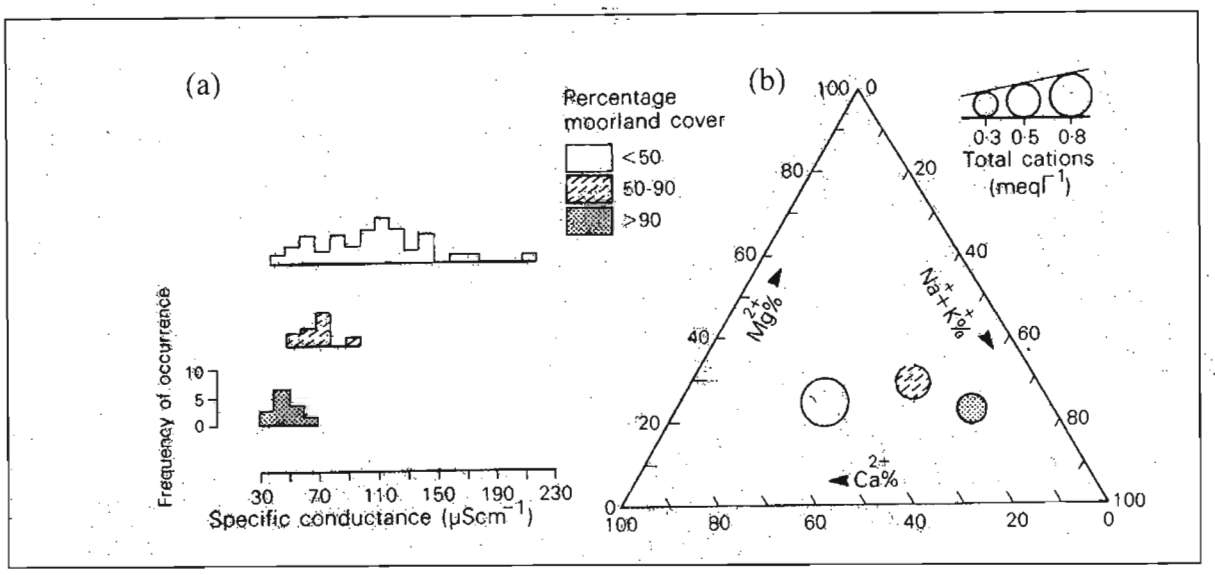

Figure 2.1 The influence of land use on (a) specific conductance levels and (b) cation composition of streams (Walling and Webb, 1986)

Depending on their type and size, plants can play a significant role in the solute balance of soil water and receiving streams through their uptake, storage and release mechanisms. Thus, according to Meybeck (1983), not all the solute inputs from weathering or other sources necessarily reach the watercourse. In some ecosystems and for some elements, the stream output may be less than these inputs from the atmosphere alone, or from atmospheric and weathering sources together. For example, Froehlich (1983) has observed a difference in calcium concentration from 3.6 μeq/l in rainwater to 1.9 μeq/l in stream water mainly as a result of plant accumulation. Solutes may accumulate either as surface deposits on vegetation surfaces or as labile ions within plant bodies. The passage of rainfall through a vegetation canopy thus considerably modifies the solute concentration of receiving streams by washing off surface deposits from vegetation surfaces or by the leaching of labile ions and compounds from within as a result of mineralisation (Foster *et al.*, 1983).

The type and nature of land cover also have a significant influence on dry and wet atmospheric deposition. For example, the capture of hill cloud by forests is observed to be an important deposition pathway for marine ions (Reynolds *et al.*, 1997). The nature of the surface is very important in dry atmospheric deposition. Its configuration, roughness, wetness and chemical characteristics have all been reported as affecting dry deposition rates. Thus the rough surface presented by a forest associated with high wind speed and frequent wet surface conditions increases the capture efficiency of the vegetation for particles and small droplets

(Cryer, 1986). According to Kinross (2001), this is one of the main factors in the apparent change in chemistry of lakes and streams in some afforested upland areas.

2.2.4 Topographic characteristics

Various reports have indicated that topographic characteristics of a drainage basin, including slope, size and elevation can influence the release, transportation and deposition of solutes, thereby influencing land and stream salinity. Meybeck (1983) has reported a ten-fold decrease in chloride concentrations of streams at similar distances from the sea but which vary between 100 and 150m in mean altitude. This observation was attributed to the combined effects of variation in both the water budget and concentration of chloride in precipitation at higher and lower altitudes. Similarly, Walling and Webb (1986) have identified a positive correlation between catchment slope and stream salinity. Both stormflow and baseflow salt concentrations are dependent on basin area. Dissolved solutes in surface runoff increase proportionally with increase in basin area (Froehlich, 1983). Similarly, the conductance levels of baseflow was reported to rise with increasing catchment area until a threshold size of approximately 2 km^2 is attained. However, solute levels are observed to be independent of basin scale beyond this threshold catchment size (Walling and Webb, 1986). High stream density is also noted to increase delivery ratios for eroded material as well as creating opportunities for stream bank erosion and consequent increases in concentrations of some solutes (Archeimer *et al.*, 1996).

2.2.5 The effect of time

The release, transportation and deposition of solutes are also subject to temporal influences and are reflected in annual, seasonal and even storm period cyclic variation of dissolved solid concentrations. Kelbe and Germishuyse (1999) have noted solute concentrations showing an initial rise with increasing flow for a rainstorm following prolonged dry conditions. On the other hand, a series of closely spaced and similar high discharges exhibit progressively lower total dissolved solute concentrations (Figure 2.2). Similarly, Loah and Stoikes (1981) observed major salinity fluctuations as a result of different sequences of flood and drought years on partially cleared catchments, which far outweighed the long term increases caused by clearing. This reflects a temporary exhaustion in the supply of soluble salts from the same sources during the sequence of events (Froehlich, 1983).

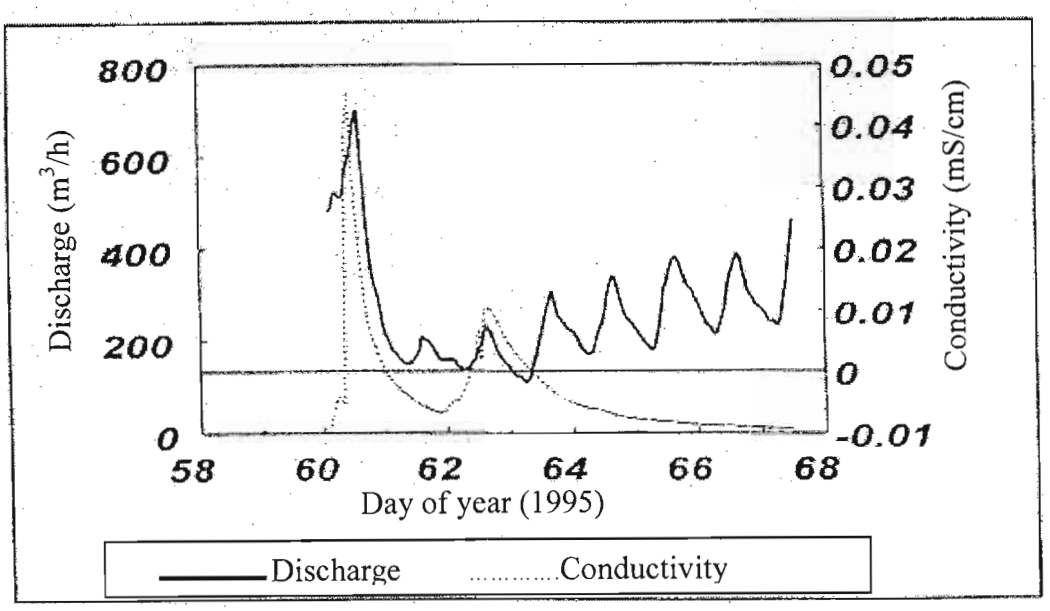

Figure 2.2 Changes in conductivity following prolonged drought conditions (after Kelbe and Germishuyse, 1999)

Temporal variation of water salinity can occur as a result of the various sources of flows contributing in different seasons of the year. According to Davis and Keller (1983), in some areas this temporal variation may reveal underlying seasonal influence on the varying contribution of water from rain, snowmelt and groundwater during the course of the year. Since each of these sources has a markedly different range of solute concentrations, it may be considered a logical consequence that cyclic behavior will also characterise the concentration of most solutes found in stream water. For example, Walling and Webb (1986) have reported that, rivers characterised by very low solute concentrations and dominated by atmospheric solute sources occasionally show a positive salinity–flow relationship, since in this situation maximum dissolved solute concentrations may occur during storm events.

This chapter has reviewed the major sources and factors that control the release, transport and deposition of salts from various sources. Despite the fact that most of these sources and processes of hydrosalinity are highly interrelated, knowledge about the main sources and how the dominating processes influence water salinity is vitally important for the development of hydrosalinity models. The next chapter deals with the basic approaches used to describe salt movement from the soil surface through the subsoil to groundwater and stream flows as well as reservoirs as conceptualised in different hydrosalinity models.

3. REVIEW OF HYDROSALINITY MODELLING APPROACHES

A hydrosalinity model is a mathematical description of the fate and transport of water and chemicals in the soil (Moolman, 1993). Addiscot and Wagenet (1985) suggest that, before making further attempts to model solute movement, it is important to place existing modelling approaches in perspective, comparing and classifying them on several levels, indicating those cases for which they were intended to be applied, and discussing the accuracy of model predictions under field situations in which solute transport models have been tested. This helps for future modelling efforts to proceed with a clear recognition of modelling approaches as a function of the modeller's purpose, realising in the process the inherent strengths and weaknesses of each method. Therefore, this chapter will attempt to review the basic types of water quality and quantity models followed by a review of processes involved in hydrosalinity with special emphasis on soil salt balance and movement and the commonly used modelling approaches to describe these processes.

3.1 Types of Hydrosalinity Models

Various researchers have attempted to classify hydrosalinity models. However, most of the models fall into one of the types described in the following sections. *ACRUSalinity* is a hydrosalinity module, i.e. it is premised around the dominance of the hydrological "forcing" processes, which links the fate of salt to the fate of water. This section, therefore, classifies hydrosalinity models mainly based on physical processes rather than chemical processes such as sorption, dissolution and precipitation. According to Kienzle *et al.* (1997), hydrological and water quality modelling are commonly performed using one or more of the following four different modelling approaches.

3.1.1 Calibration and parameter optimizing models

These are models in which parameters of the model are adjusted to enable the model output to match observations as closely as possible. The major drawbacks of these models are that they are data demanding (for the calibration procedure) and that parameters are identified for a particular catchment. This makes parameter transfers to ungauged catchments problematic and speculative.

3.1.2 Parametric models

These are so-called "grey box" models which are sometimes referred to as conceptual models. Parametric models represent a partial understanding of processes. However, the system's spatial heterogeneity (e.g. of soils, vegetation, terrain) is not taken into account explicitly because inputs (and hence outputs) are spatially averaged (lumped). Consequently, hydrological processes and their variability are integrated in such a way that their parameter expressions are often indices rather than having strictly physically meaningful values. Thus an underlying problem in using parametric models is that these models use parameters to represent catchments as a whole, whereas data on catchment characteristics are collected at multiple field locations and are difficult to transform into one measure of collective impact (Song and James, 1992).

3.1.3 Stochastic models

These are so-called "black-box" models, in which inputs (e.g. rainfall) are transformed to outputs (e.g. runoff) with little or no understanding of the processes involved in the transformation. This type of model relies on historical records of both input and output variables that are a representative sample over time.

According to Quilez *et al.* (1992), an improvement has recently been observed on simple regression models with the incorporation of random noise theory for application in modelling water quality variables. In most of these regression based water quality models, streamflow has been considered as the most important driving variable. In general, water quality variables, and in particular salinity, are known to be related to streamflow. Regression models for this relation have been proposed and applied in different basins. These models do not consider the temporal and dynamic relationships between the primary variables. However, the random noise theory based models try to introduce a stochastic (noise) component into the model, based on the fact that water quality variables do not behave in a completely deterministic manner with respect to streamflow. This approach was employed to study the flow-salinity relationships on the Ebro River Basin in Spain (Quilez *et al.*, 1992) and by Herold and Eeden (2001) in an effort to relate river water quality and diffuse loads to a range of land uses in South Africa.

The empirically developed and commonly used function to describe flow-salinity relationship assumes, among other conditions, that mixing is complete and there is no hysterics in the flow salinity relationship. This expression is commonly described as: $EC = aQ^b$, where EC is the electrical conductivity, Q is the discharge, a and b are regression coefficients. This regression equation is referred to as a dilution model (Walling and Webb, 1986).

Transfer function-noise models are similar to regression models such as the above named dilution model, the main difference being the addition of the noise component. In order to account the stochastic nature of water quality variables, the above equation is, in most cases, reduced to a linear form by taking natural logarithms. Random noise is then added to the regressed values for each day. The random noise is computed through a series of steps. Herold and Eeden (2001), for example, have used a random number generator to provide a random number for each day of the record. These random numbers were then normalised in order to conform to a normal distribution. The normalised random number for each day simulated is then multiplied by the standard error for the observed data set.

In general, according to Quilez *et al.* (1992), transfer function-noise approach models represent an improvement over simple regression models in terms of higher explained variance, and they represent the advantage of having a related flow series. They also represent marked improvement over classical regression models for cases in which the relation between salinity and flow is not instantaneous. The effect of not including random noise to the regression line is reflected in the research results of Herold and Eeden (2001), where the use of a regression line alone, with no allowance for the observed variance about the regression, has affected the results very severely, with the result that the peak values were much too low.

3.1.4 Deterministic, physically conceptually based models

These belong to the group of near "white box" models, in which the behaviour of the hydrological system is described in terms of mathematical relationships which represent the interactions and linkages of the various components of spatially and temporally varying hydrological processes. Deterministic hydrosalinity models may further be classified to mechanistic and functional models.

For the purpose of this dissertation these models are more important than the other types of hydrosalinity models. Therefore, the following sections will attempt to review with more detail the two subdivisions of deterministic models, *viz.* mechanistic and functional models.

3.1.4.1 Mechanistic models

Physically based flow and transport models use as a basis, continuum mechanics theory for the way in which substances migrate. Since these models attempt to represent the coupled flow system that is operating, the mathematical description also usually results in a system of coupled partial differential equations (Connel *et al.*, 2001).

Mechanistic models are broadly characterised by the use of rate parameters and their use as research tools. The use of rate parameters for solute movement combines the description of several transport processes (Addiscot and Wagenet, 1985). It first defines the instantaneous flux of water content in terms of the product of a hydraulic gradient and a rate parameter, *viz.* hydraulic conductivity (based on Darcy's Law), and then defines the flux of solute concentration in terms of two other rate processes, *viz.* convection and diffusion. Thus, they describe the fundamental mechanisms of the physical processes involved in the leaching of solutes (Hall, 1993). Mechanistic models are often described as research (rather than operational) tools, in that they are developed to aid the testing of hypotheses and the exposure of areas of incomplete understanding. Although mechanistic models have a solid theoretical basis and have been widely used, when compared to the other soil-water-solute models their predictions can be misleading unless their inputs are well characterised with respect to variability. Thus, they require a detailed knowledge of the soil's pore-size distribution and hydraulic properties. Moreover, it is not yet established that they necessarily give more reliable or more accurate simulations of water and solute movement than the simpler, more functional models (Addiscot and Wagenet, 1985).

3.1.4.2 Functional models

The term functional is used for models that incorporate simplified treatments of solute and water flows and make no claim to fundamentality. They require less input and computer expertise for their use (Addiscott and Wagenet, 1985). According to Hall (1993), functional models use a simplified approach to describe water flow and solute transport and generally

divide the soil profile into layers, with water and solute being passed from one layer to the next, usually on a daily basis. The amount of water passing through each layer depends on the pore volume available for mobile water, which is defined by the moisture release characteristics of the soil. Another important characteristic of functional models is their use of capacity parameters such as the volumetric water content at drained upper limit (DUL), instead of rate parameters. Thus, they define changes (rather than rates of changes) in amounts of solute and water content. Furthermore, unlike mechanistic models which are driven by rates, functional models are usually driven by the amounts of rainfall, evaporation or irrigation and only consider rates indirectly.

Functional models are generally used for management purposes. They are less rigorous than mechanistic models in terms of describing the processes involved in release, transportation, and deposition of salts. However, their input requirements are simpler and more readily available for a wider range of soils. Their reliance on capacity-type soil water inputs enables them to avoid the spatial variability problems associated with the rate inputs, but could result in failure to simulate variation in leaching that might be of practical importance (Addiscot and Wagenet, 1985). The *ACRU* agrohydrological modelling system, for example, belongs to this group of hydrological models (Schulze, 2001).

The procedure followed by Kienzle *et al.* (1997) classified hydrology and water quality models into four classes. In another classification by Addiscott and Wagenet (1985), hydrosalinity models are broadly classified as deterministic and stochastic models (Figure 3.1). The general concepts behind these models are similar to those in the preceding classification. Deterministic models presume that a system, or process, operates such that the occurrence of a given set of events leads to a uniquely definable outcome, whereas stochastic models presuppose that the outcome is uncertain and are structured to account for this uncertainty. Addiscott and Wagenet (1985) also classify deterministic models into mechanistic and functional models that are recognised by the characteristics described in the preceding sections. They also make a distinction between rate and capacity, as well as research and management models, which again corresponds broadly to the distinctions between mechanistic and functional models.

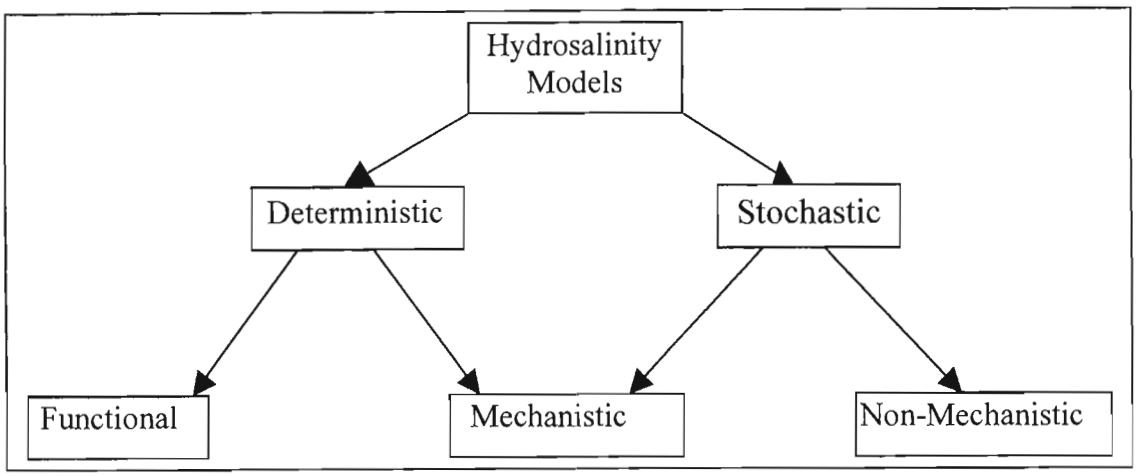

Figure 3.1 Classification of hydrosalinity models according to Addiscot and Wagenet (1985)

3.2 Classification of Hydrosalinity Models Commonly Used in South Africa

Some of the hydrosalinity models commonly used in South Africa are shown in Table 3.1, according to a classification by Jonker (1995). The classification is based on Addiscott and Wagenet's (1985) procedure.

Table 3.1 Classification of some hydrosalinity models used in South Africa according to Addiscott and Wagenet's classification procedure (after Jonker, 1995)

Model	Deterministic/ Stochastic	Functional/ Mechanistic	Research/ Management	Lumped or Distributed parameter
NACL (Herold, 1981)	Deterministic	Functional	Management	Lumped
FLOSAL (Hall and Du Plessis, 1981)	Deterministic	Functional	Research	Lumped
IRRIS (Forster, 1987)	Deterministic	Functional	Management	Lumped
LEACHM (Wagenet and Hutson, 1989)	Deterministic	Mechanistic	Research	Lumped
DISA (NSI, 1990)	Deterministic	Functional	Research and Management	Lumped and Distributed

From Table 3.1 it can be noticed that most of the hydrosalinity models commonly used in South Africa are deterministic functional models. However, most of the models listed in the table are lumped models. Therefore, this calls the need for a distributed hydrosalinity model which is applicable in complex land use or larger catchments.

In the preceding sections an attempt was made to review the common types of water quantity and quality models in general and hydrosalinity models in particular. In the following sections some of the deterministic hydrosalinity modelling approaches are reviewed in more detail with special emphasis on describing the basic processes that influence salt balance and movement through the soil profile.

3.3 Mechanistic Modelling Approaches of Salt Balance and Movement in Soils

Despite the difficulties involved in obtaining the necessary soil, water and salt measurements required for mechanistic models, they are nevertheless widely used, especially for research purposes. The main salt transport and mixing mechanisms such as diffusion, dispersion and convection, as well as associated processes, are described below.

3.3.1 Diffusion

According to Leij and Genuchten (1999), solute molecules in a free solution possess random thermal motion which causes an exchange of molecules between adjacent volume elements. A net transfer of molecules of a solute species usually occurs when the concentration of the species differs in adjacent volume elements, i.e. more particles move from the elements with higher concentrations to those with lower concentrations than vice versa. The resulting process is referred to as diffusion. Diffusion is an important mechanism for the transport of solutes in the liquid phase in directions of low mean pore-water velocities with relatively little, or no, water flow. The maximum flux (J_{dif}) due to molecular diffusion has the dimension of mass per unit area per unit time ($ML^{-2}T^{-1}$) and it is usually expressed by Fick's first law which states that the transport of the substance in a space direction is proportional to the gradient of the concentration of this substance in that direction, with the proportionality factor being the coefficient of diffusion (Jolankai, 1997). This law, for one dimentional diffusion, yields:

$$J_{dif} = -\theta D_o \frac{\partial c}{\partial x} \tag{3.1}$$

where x is distance (L), θ is water content, c is the solute concentration and D_o is the coefficient of molecular diffusion for a free (or bulk) solution (L^2T^{-1}) whose value depends on properties of both the solute and solvent (Leij and Genuchten, 1999).

The path of diffusion becomes more tortuous when there is less water available to move through, which further reduces the actual values of D_0 (Herald, 1999). As the water content of a soil decreases, the cross-sectional area available for diffusion becomes smaller and the ions have to travel a longer distance to reach a given point. Other factors such as viscosity and anion exclusion become more influential as water content decreases (Herald, 1999). Therefore, to describe diffusion in a porous medium such as soil, the diffusivity in a free solution is typically adjusted to account for a reduced solution phase (a smaller cross-sectional area available for diffusion), and an increased path length. The macroscopic diffusive flux per unit area of soil can be written as (Leij and Genuchten, 1999):

$$J_{dif} = -\theta D_* \frac{\partial c}{\partial x} \tag{3.2}$$

where D_* is the coefficient of molecular, or ionic, diffusion for the liquid phase of the soil. The diffusion coefficients for the soil liquid and a free liquid are related by $D_* = D_0/(L_*/L)^2$, where L_* is the actual path length for diffusion in the soil (which depends on θ), L is the (straight) length of the soil and L_*/L is the tortuosity.

3.3.2 Mechanical dispersion

The macroscopic convective transport of a solute is usually described by an equation that takes into account two modes of transport, *viz.* the average flow velocity and mechanical dispersion (resulting from local variations in flow velocities). The mechanical dispersion component is similar to diffusion in the sense that there is a net movement of solute from zones of high concentration to zones of low concentration (Bresler, 1981).

Variation in water flow in a porous medium leads to mechanical dispersion. Several factors contribute to mechanical dispersion, and hence, to increased spreading. Initially steep concentration fronts will become smoother during movement along the main flow direction. Dispersion may occur as a consequence of one or more of the following factors (Wild, 1981; Leij and Genuchten, 1999):

- the development of a velocity profile in an individual pore, such that the highest velocity occurring in the center of the pore, and presumably little or no flow at the pore walls,
- different mean flow velocities in pores of different sizes,
- the mean water direction in the porous medium being different from the actual streamlines within individual pores, which differ in shape, size and orientation, and
- particles originating from different pores ending up in the same pore, and vice versa.

Although molecular diffusion and mechanical dispersion are different processes, the macroscopic solute flux due to mechanical dispersion is often conveniently expressed with Fick's first law of diffusion (Leij and Genuchten, 1999). For one dimensional dispersion in a uniform porous medium this leads to:

$$J_{dis} = -\theta D_{dis} \frac{\partial c}{\partial x} \tag{3.3}$$

where J_{dis} is the dispersive solute flux ($ML^{-2}T^{-1}$) and D_{dis} is the coefficient of mechanical dispersion (L^2T^{-1}). The dispersion coefficient (D_{dis}) is proportional to first power of the average velocity (Bresler, 1981), i.e. $D_{dis} = \lambda|V|$, where λ is the dispersivity and $|V|$ is the absolute value of the average flow velocity. The dispersivity is an intrinsic physical property of the porous medium and has unit of length (Herbert and Mary, 1982). Dispersion coefficients can be estimated with semi-empirical formulae or with the aid of *in situ* tracer measurements (Reichert *et al.*, 2001).

The macroscopic similarity between diffusion and mechanical dispersion enables both processes to be described with one coefficient of hydrodynamic dispersion. This practice is consistent with results from typical laboratory and field experiments, which do not distinguish between mechanical dispersion and molecular diffusion (Leij and Genuchten, 1999).

3.3.3 Convection and combined convective-diffusion transport

Solute transport is made up of two convective or mass flow components. In larger pores, turbulent flow dominates and fast convection occurs. On the other hand slow laminar transport occurs adjacent to particle surfaces and in micropores (Herald, 1999). In the case of conservative solutes no gains or losses and no solute-with-soil surface or solute-with-solute interactions occur. Under such circumstances the convective flow of solutes associated with water movement is expressed by $Jc = q.c$, where Jc = convective flux of solute, q = rate of volumetric water flow and c is solute concentration (Wild, 1981).

In the preceding discussion three types of solute transport mechanisms have been described, *viz.* molecular diffusion and the two modes of convective flow. However, these three components of solute transport occur simultaneously in natural soils (Bresler, 1981). Thus solute transport in soils has generally been described with the convection-dispersion equation. This equation incorporates two constitutive transport processes (Leij and Genuchten, 1999), *viz.* solute movement as a result of liquid flow, and spreading as a result of known and unknown processes such as diffusion and small-scale variations in water flow velocity.

An inherent assumption made by different modellers, in order to make their models simpler for the simulation of convective-diffusion transport of solutes is that the soil is an inert porous medium. In that case the total solute flux (Js) due to the joint effects of diffusion and convection can be described as (Bresler, 1981)

$$Js = -\theta D \frac{\partial c}{\partial x} + qc \qquad (3.4)$$

where c is salt concentration in the soil solution, D is hydrodynamic dispersion coefficient, θ is volumetric water content, x is flow direction and q is volumetric water flux. However, water and solutes move at different rates through soil and may be acted upon, transformed or retarded during their movement through the soil (Herald, 1999). Therefore an expression for one-dimentional transient conditions should be derived from a consideration of continuity or mass conservation (Bresler, 1981). This states that the rate of change of solute within a given soil element must be equal to the difference between the amounts of solute that enter and leave that element. For the case of one dimensional vertical flow the following expression has

been derived by equating the difference between outflow and inflow to the amount of salt that has accumulated in the soil element (Bresler, 1981; Runkel, 1998):

$$\frac{\partial(Q_a + \theta c)}{\partial t} = \frac{\partial}{\partial x}(\theta D \frac{\partial c}{\partial x}) - \frac{\partial(qc)}{\partial x} + S \qquad (3.5)$$

where t is time, Q_a is the local concentration of solute in the adsorbed phase (meq.cm^{-3} soil), S is any solute loss (sink) or gain (source) due to salt uptake, sorption, precipitation or dissolution, and x is the vertical space co-ordinate (considered to be positive downward). S can be dealt through linear or nonlinear isotherms (Leij and Genuchten, 1999). The above equation is applicable for both reactive and non-reactive solutes, including the case when there is loss or gain of salt inside the flow system.

In general, the convection-dispersion equation (CDE) is the foundation upon which numerous mathematical analyses of solute transport in porous media have been based (Russo, 2002). Questions have, however, been raised regarding the applicability of the CDE at the field scale in which there are large variations in pore water velocities caused by spatial variability in soil hydraulic properties.

3.3.4 Miscible displacement

Miscible displacement experiments are important tools in the quantitative analysis of solute concentration changes in soils (Smettem, 1986). According to Bresler (1981), most works on miscible displacement phenomena are limited to steady state water flow with constant flow velocities and water contents. As such, these studies provide a means of determining hydrodynamic dispersion coefficients, evaluating macroscopic flow velocities and giving physical explanations for mixing phenomena that occur when salts flow through soils.

Miscible displacement phenomena in soils are illustrated by a classical experiment in which a solute is continuously introduced at the up-gradient end of a laboratory soil column (Herbert and Mary, 1982). When a salt-free soil solution is displaced through a column of soil by a solution containing an inert (non-reacting) solute of concentration C_0 at pore water velocity V and water content θ, the fraction of this solute in the effluent at time t can be designated as C/C_0, where C is solute concentration of the effluent. Plots of C/C_0 versus pore volumes of

effluent are commonly called break-through curves, BTC (Figure 3.2). Pore volume refers to ratio of volume of effluent to volume of solution contained in the soil column.

The shape and development of the BTCs are very important to the understanding of solute behaviour when the solute percolates through porous media and when pore volume is set to unity as a reference (Matos *et al.*, 1999). It is then possible to derive important conclusions about the soil solute interactions simply by the position of the curves in relation to this reference. As to the physical explanation of the resulting different types of break-through curves, Bresler (1981) states that if piston displacement were operative, no mixing would occur between the displacing and displaced solutions and a vertical line would represent solute break through. A sigmoidal shape of break-through curve, on the other hand, indicates mixing (longitudinal dispersion) of the solution. Shifting of the curve to the left indicates exclusion from, or by-pass of, a significant portion of the soil solution. Displacement to the right indicates adsorption or retention of the solute by soil (Figure 3.2).

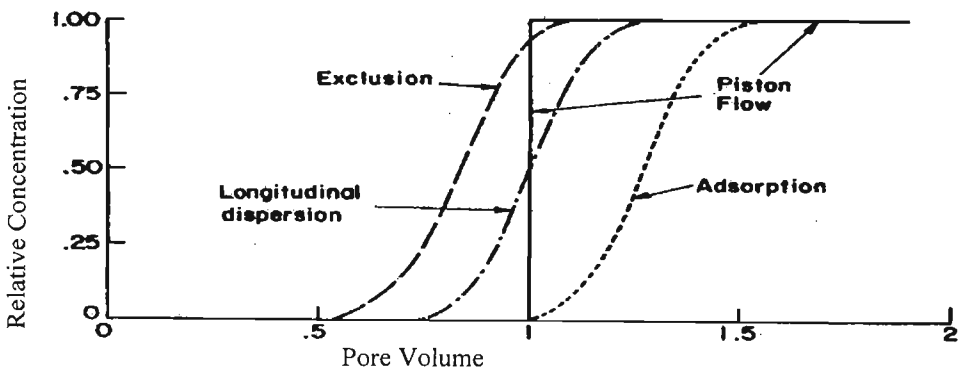

Figure 3.2 Schematic break-through curves for various miscible displacement conditions (after Bresler, 1981)

According to Lorentz (1986), break-through curves can be symmetrical or asymmetrical and can be influenced by other factors in addition to the governing soil-solute interaction mechanisms. Some of these factors affecting the shape of the BTC include soil particle and aggregate size, the ratio of micro- to macro-space volume and the length of the soil column (Lorentz, 1987).

3.3.5 Anion exclusion

In some cases part of the liquid phase, especially near the solid end, does not participate in the transport processes. This occurs when anion exclusion takes place, or when relatively immobile liquid regions are present in the soil, for example, inside aggregates (Leij and Genuchten, 1999). Certain anions interact with the solid phase of the soil and are excluded from liquid zones adjacent to negatively charged soil particle surfaces (Shukla and Cepuder, 2000). Soil clay particles and humus surfaces exhibit negative charges that repel anions electrostatically. Anions are repelled from such surfaces and accumulate in the centre of pores. Thus, the volume of immobile water into which anionic solutes can diffuse is effectively decreased. The resultant reduction in anion concentration close to particle surfaces, which result from repulsion by electrostatic forces, is termed anion exclusion (Hall, 1993). Wild (1981) reported that anion exclusion resulted in a 10-20% reduction in pore volume available for anion transport when compared to that available for cations.

The above effect of anion exclusion suggests that anions move more rapidly than cations. For example, a study by Leij and Genuchten (1999) based on analysis of break-through curves for an anion (Cl^-), a nearly non-reactive solute (^3H_2O), and an adsorbing solute (Ca^{2+}) has shown that the Cl^- curve was strongly affected by anion exclusion, with a consequent shift of its BTC to the left, while ^3H_2O transport was subject to relatively minor adsorption or exchange. The different types of break-through curves observed for the three solutes are shown in Figure 3.3.

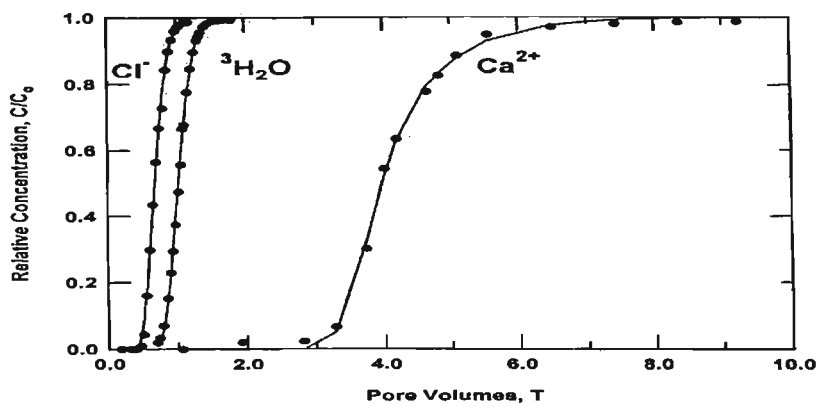

Figure 3.3 Break-through curves for Cl^-, ^3H_2O and Ca^{2+} (after Leij and Genuchten, 1999)

The main factors affecting anion exclusion are as follows (Ross, 1989; Herald, 1999):

- Anion exclusion increases with increasing anion concentration.
- Exclusion increases with increasing anion valency. More electronegative ions will be more strongly repelled by the soil particle surfaces, and to a greater distance, than less electronegative ions.
- Exclusion decreases with soil pH, since this decreases the net negative charge on soil colloids. At low pH, there are more hydrogen (H^+) ions in solution, which readily occupy the cation exchange sites, rendering the soil particle neutral. The particles will no longer be able to repel anions, hence reducing the anion exclusion effect.
- Exclusion also decreases with increasing cation saturation of the soil. This is a similar effect to increased pH, except the exchange sites are filled with cations other than H^+.
- Exclusion increases with increased density of negative charge on the particle surface. This means the particle can exert a greater repulsive force on the anions.

In general, most mechanistic solute transport models use the convection-dispersion equation to describe salt movement and leaching in the soil. However, this solute transport equation is difficult to solve numerically, largely because the mathematical properties of the transport equation vary according to the dominance of specific terms in the equation under particular situations. Moreover, this equation does not account for different management practices and soil properties. Shouse *et al.* (1997), for example, have observed large differences in water flow and salt transport between two soils with different shrink-swell characteristics. They further noticed that the salt distribution and transport in the non-cracking soil were consistent with the generally accepted principle of water and chemical transport through porous media. Conversely, this theory of water and salt transport through porous media was found to be less adequate in describing the flow of solutes through soils with large cracks that appeared as the soil dried out. This is because by-pass flow provides the primary mechanism for leaching on a heavy clay soil (Crescimanno *et al.*, 2002). Thus, the generally accepted concepts describing salt movement and leaching typically described in textbooks do not account for soils that are highly susceptible to serious cracking (Rhoades *et al.*, 1997). Some of the simplified solute transport modelling approaches are described below.

3.4 Simplified Modelling Approaches of Soil Salt Balance and Movement

Simplified approaches to assessing the soil total dissolved solute (TDS) balance have been used, ranging from simple empirical equations to conceptual functional models like the DISA hydrosalinity model. Some of these approaches are described in the following sections.

3.4.1 Empirical and simplified functional approaches

According to Aswathanarayana (2001), a steady-state value of soil salinity (*ECe*) resulting from the application of water with conductivity (*ECw*) can be estimated from knowledge of the leaching fraction (*LF*). *LF* is the fraction of applied volume of water leached below the root zone. Soil salinity in the root zone can be computed from *ECw* of applied water as:

$$ECe = X(LF) * ECw \tag{3.6}$$

where *X(LF)* is an empirically estimated parameter based on experience with irrigated, cropped soils. Some of these empirically determined *X(LF)* factors for different values of *LF* and applied water are presented in Table 3.2. These concentration factors are determined using a constant crop water use pattern along the soil profile (Ayers and Westcot, 1985).

Table 3.2 Concentration factors, *X(LF)* for predicting soil salinity, *ECe* (Ayers and Westcot, 1985)

Leaching Fraction *LF*	Irrigation Water Needed (% of total evaporation)	Concentration Factor *X(LF)*
0.05	105.3	3.2
0.10	111.1	2.1
0.15	117.6	1.6
0.20	125.0	1.3
0.25	133.3	1.2

Soil vertical heterogeneity complicates the analysis of salt transport, and a complete description of the mechanism often requires that each soil horizon be examined separately

(Schwartz *et al.*, 1999). Some researchers have adopted a modelling approach that takes into account this heterogeneity. Laudelout (1975), for example, has described a simplified salt transport and mixing model, in which the soil profile is partitioned into a number of layers. The movement of water is expressed by the fact that a given layer fills up to saturation and then empties into the layer below, returning to drained upper limit (DUL) before filling up again. If the saturation content of layer i is denoted by SP_i and its DUL by Fc_i then, applying mass conservation to each layer and supposing that perfect mixing occurs in each layer, the salt concentration of a given layer i at present time step j is expressed as:

$$C_{i,j} = [1-(\frac{Fc_i}{Sp_i})]\, C_{i-1,j} + (\frac{Fc_i}{Sp_i}) C_{i,j-1} \qquad (3.7)$$

The drawback of this model, however, is in its inherent assumption that a given layer fills up to saturation and then drains the water above its DUL into the layer below. However, drainage of the excess water is unlikely to be an instantaneous process. Moreover, this expression does not take into account that in the case of a multi-layered soil at any time step; a given layer may receive percolated water, not only from its immediate upper layer but also from two or more overlying layers. This consideration is particularly important when longer time steps are used. The salinity level of water draining from different layers varies according to the governing processes operating on a specific layer. Although some of the simplifications of this expression are unrealistic in most cases, there is a fairly wide use of this formulation, since the retention factor defined by *Fc/Sp* will be close to 0.5 for most soils (Laudelout, 1975). A more rigorous functional salt balance model with water and salt movement from multiple layers is described below.

3.4.2 Soil water and TDS balance modelling in the DISA hydrosalinity model

DISA is the acronym for the Daily Irrigation and Salinity Analysis model which was developed by Ninham Shand Inc based on extensive research that had been conducted in the Breede River basin (Wolf-Piggott, 1995). Some of the underlying modelling concepts and assumptions of DISA with respect to subsurface water and TDS balance include (NSI, 1990) the following:

- The irrigated soil profile consists of a layered soil structure, allowing for a root zone, unsaturated zone and a saturated zone.
- The model takes into account the capillaric rise of water and salts in the unsaturated zone
- Movement of water between layers occurs only when the DUL is exceeded and it depends on a percolation factor.
- Groundwater movement in the saturated zone is controlled by a one dimensional Dupuit approximation.

According to Görgens *et al.* (2001), the soil profile in the model is divided into a number of layers of equal thickness. Each layer is broken down into smaller units in a horizontal plane. These units define the basic scale at which the model calculates the movement of water and salt within the root zone. In general a similar concept to that of *ACRU*'s soil water budgeting was adopted in DISA to describe water movement in the soil profile.

After calculating the soil moisture balance of each layer at the end of the day, the model determines the corresponding final salt concentration within each unit from a consideration of the salt concentration of the soil moisture at the end of previous time step, the salt concentration of inflowing and percolating (out flowing) water and soil moisture status at the present time step.

In order to ensure a realistic simulation of salt movement within the soil profile, the model divides the total volume of water entering a unit (layer) into sub-volumes, each with a different salt concentration, depending on the unit from which the water originated. Figure 3.4 is a diagrammatic representation of salt movement within the root zone. It shows that if the volume of water that enters a unit (*Qin*) is more than the initial soil moisture content of the unit immediately above, $SMCs_{(i-1)}$ (with corresponding salt concentration $Ss_{(i-1)}$), the remaining excess water from that entering the unit, after deducting the initial soil moisture content of the unit immediately above, has a salt concentration equal to that of the layer immediately above the overlying unit $Ss_{(i-2)}$. If *Qin* is more than ($SMCs_{(i-1)}$+ $SMCs_{(i-2)}$), the process continues until the total volume which constitutes *Qin* has been accounted for.

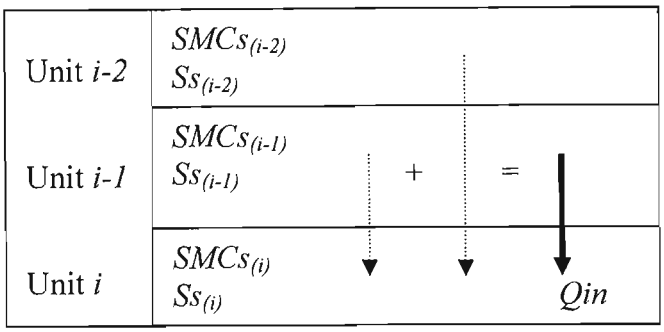

Figure 3.4 Salt movement in the soil profile (after Görgens *et al.*, 2001)

3.4.3 Salt generation

Salt generation in a soil horizon is the result of different weathering processes, mainly chemical weathering taking place in the soil profile with a subsequent release of solutes to the soil solution. Some of the chemical processes involved during weathering of rock and soil materials include hydrolysis, hydration, carbonation, dissolution and precipitation.

The level of salt generation models ranges from simple regression equations that simulate salt generation without having a clear understanding of the underlying processes to complex models that account the chemical processes taking place in the soil profile. According to Jonker (1995), various hydrosalinity models have adopted different approaches to simulate salt generation. Some of these models attempt to account for chemical processes in great detail. The LEACHM (Wagenet and Hutson, 1989) model, for example, uses a mechanistic approach, requiring detailed field information and is suited for small-scale application.

3.4.3.1 Salt generation in DISA model

According to Görgens *et al.* (2001), the DISA model does not account for dynamic salinity related soil processes such as chemical weathering processes. Although this simplification does not significantly affect the results when the model is used for single season simulations, with multiple seasons the simulated salinities in the system do, however, experience a steady decline from the second season onwards. Therefore, an attempt was made to develop a salt generation function in DISA so as to obtain a realistic representation of salinity for simulation periods of more than one season. The salt generation function is based on a simple empirical equation, which was expressed by Jonker (1995) as

$$Sgen = a(1 - e^{-bQin}) \quad (3.8)$$

where $Sgen$ = total daily salt mass generated per soil layer ($t.ha^{-1}.d^{-1}$)

a = calibration constant (upper limit for water percolation-related salt mass generated) ($t.ha^{-1}.d^{-1}$)

b = constant controlling water percolation-related salt mass

if $Cin > 50$, then $b = 1/\ln C_{in}$

if $Cin \leq 50$, then $b = 1/\ln 50$

C_{in} = TDS concentration in water infiltrating the layer (mg/l)

Q_{in} = daily volume of water infiltrating the layer (l).

Development of the salt generation function in DISA is governed by various principles. Some of the principles underlying this function are given below (Jonker, 1995; Görgens *et al.*, 2001):

- The mass of salt generated in the soil profile increases asymptotically with the volume of water infiltrating the soil profile, up to a limit above which more water does not generate more salt.
- The mass of salt generated depends on the salt concentration of the water entering the soil. As shown in the preceding equation the constant, b depends on concentration of water infiltrating to the layer (C_{in}). The higher TDS concentration of infiltrating water, the smaller value of calibration constant (b) and thus the lesser salt generated will be.
- The function accommodates net salt dissolution rather than the precipitation of salts. This is based on the assumption that in an irrigation scheme where water is applied continuously, more salt is being dissolved than precipitated and it is this difference (net dissolution) that is being modelled.
- It further assumes that there exists an infinite solid salt reservoir in each layer from which salt is dissolved by the infiltrating water, instead of a finite soluble salt store.

3.4.3.2 Combined salt generation and mixing models

First order equations generally have a widespread use in describing practical chemistry related processes, as in studies of biochemical reactions and weathering processes. According to Ross

(1989), many of the processes involved during weathering of rock and soil materials are controlled by chemical kinetics. These processes include adsorption of reactants on the surface of the weathering material, chemical reactions on the surface and desorption of products from the surface. Ferguson *et al.* (1994) have proposed the application of first order rate kinetics to simulate an increase in salt concentration of the soil solution due to solute uptake by the soil water. Hence the model indirectly simulates salt generation. This solute uptake process based on first order kinetics with subsequent simple mixing of the "new" and enriched "old" water is reviewed in this section.

The salt uptake by soil solution (salt generation) model is based on first-order kinetics where the rate of increase over time in the concentration, C, of a solute is proportional to how far C falls short of its equilibrium value C_e. Introducing the rate constant (k) this may be expressed as:

$$\frac{\partial C}{\partial t} = k(Ce - C) \tag{3.9}$$

This equation describes an initially rapid, but progressively slower, uptake of solute so that the concentration approaches asymptotically a maximum value C_e (Figure 3.5). The rate of uptake is controlled by the rate constant k.

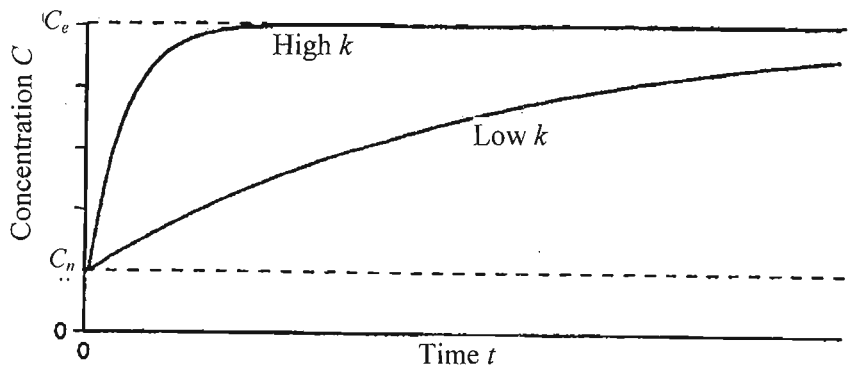

Figure 3.5 Salt uptake curves over time, showing both rapid (high k) and slow (low k) salt uptake (after Ferguson *et al.*, 1994)

The variable mixing of chemically dilute "new" (event) water (Q_n) with more enriched "old" (pre-event) water (Q_0) has been reported by different authors (e.g. Walling and Webb, 1986).

These concepts can be represented in the case of conservative mixing by $Q = Q_n + Q_0$ and the associated mixture concentration by the following equation:

$$C = C_n R + C_o(1 - R) \tag{3.10}$$

where subscripts n and o refer to "new" and "old" water respectively and R is the volumetric ratio of "new" to "old" water (Q_n / Q).

Between rainfall or irrigation events, the water in the ground is enriched chemically. During an event this "old" water is mixed with "new" water. The mixture becomes enriched until the next event, as shown in Figure 3.6 (a). This conceptual model combines the solute mixing and uptake models, and is represented mathematically as:

$$C = C_e - (C_e - C_n)\exp(-kt)[R + \exp(-ku)(1 - R)] \tag{3.11}$$

where t and u respectively refer to age of the "new" water and that of "old" water before the occurrence of the new event. Equation (3.11) describes mixing with uptake under instantaneous events. However, mixing is unlikely to be instantaneous, first, since rainfall or irrigation are not instantaneous and secondly, as a result of the time taken for the "new" water to infiltrate and mix with the "old" soil water. Consequently, the concentration will not drop immediately to the value given by the preceding equation. Rather it will decline slowly to a minimum and then increase as shown in Figure 3.6 (b).

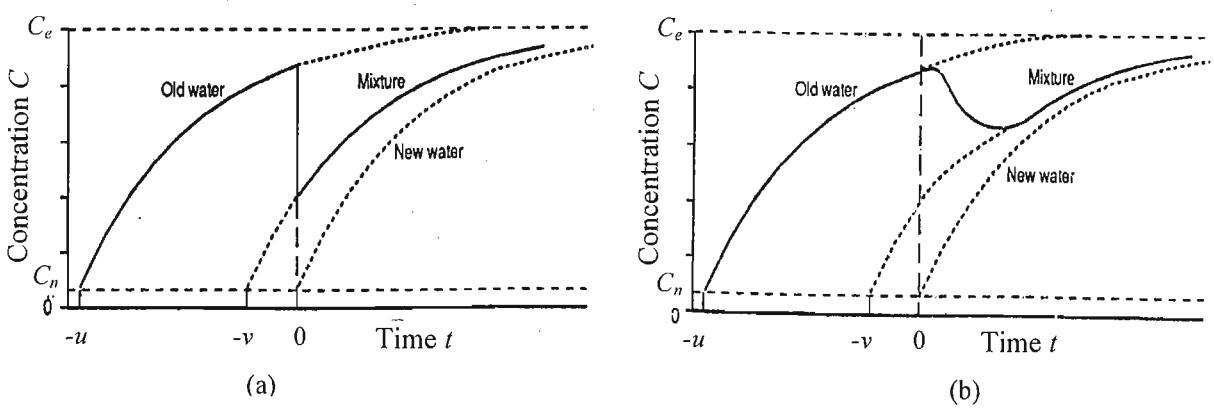

Figure 3.6 Sequence of enrichment of "old" water prior to an event: (a) instantaneous mixing of "new" water during an event and (b) non-instantaneous mixing (after Ferguson *et al.*, 1994)

3.5 Conclusions

From the various studies reviewed in this chapter it can be concluded that mechanistic solute transport models are more efficient in terms of describing the fundamental physical processes involved in the transport of solutes when compared to functional models. However, most mechanistic models do not take into account the impact of various management and land use practices. Moreover, because of the significant influence of field heterogeneity such as variability in soil hydraulic properties, and due to difficulties involved in obtaining the necessary soil, water and salt measurements required for mechanistic models, a simplified modelling procedure seems to be more appropriate for most management purposes.

Most of the hydrosalinity models commonly used in South Africa operate as lumped models. However, hydrosalinity studies at a catchment level usually require discretization of the catchment into a number of sub-catchments (distributed hydrosalinity modelling) in order to accurately model the impact of various land uses and water resources developments. Such distributed hydrosalinity modelling is particularly important in areas with complex land use or soils and in bigger catchments. Therefore, this calls for a conceptual-physical based hydrosalinity model that can operate both as lumped and distributed model. The following chapter will review the background and concepts of the *ACRU* agrohydrological modelling system, into which a hydrosalinity module has been developed in this project.

4. DESCRIPTION OF THE *ACRU* AGROHYDROLOGICAL MODELLING SYSTEM

The literature review in the previous chapter has revealed that most of the existing hydrosalinity models that are commonly used in South Africa operate only as lumped model. However, catchment based hydrosalinity modelling usually requires discretisation of the catchment into a number of sub-catchments, especially when modelling larger catchments or catchments with complex land use and soils. Therefore, the hydrosalinity module is decided to be developed within the *ACRU* model, since *ACRU* can operate as a distributed cell-type model and with widely tested multi-purpose hydrological modules.

ACRU is a conceptually-physically based agrohydrological modelling system (Schulze, 2001). The model was initially written in FORTRAN 77. However, as will be described in this chapter, this programming language had some drawbacks when applied to modelling the hydrological system. In order to overcome some of these difficulties, and to accommodate future model additions, the model was recently rewritten in an object-oriented framework using Java programming language (Kiker and Clark, 2001). The new object oriented version of *ACRU* is named *ACRU2000*. Thus, in this chapter and subsequent chapters, the *ACRU* model prior to the development of the object oriented version (*ACRU2000*), will be referred to as the *ACRU 300 series*. This chapter commences with a review of the general background and concepts of the *ACRU* model in which the hydrosalinity module is developed. It will also explain some of the structural limitations associated with the *ACRU 300 series,* followed by an overview of object-oriented programming and the *ACRU2000*. The overview of object-oriented programming explains some of the concepts and terminologies to which there will be a frequent mention in the subsequent chapter that deals with development of the hydrosalinity module.

4.1 Background and Concepts of *ACRU* Model

The acronym *ACRU* is derived from the Agricultural Catchments Research Unit in the Department of Agricultural Engineering, now School of Bioresources Engineering and Environmental Hydrology of the University of Natal in Pietermaritzburg, South Africa (Schulze, 1995a). According to Schulze (1995a), agrohydrology seeks to evaluate the

influence of available water on the agricultural potential, with the objective of promoting a high efficiency for the use of the water. Thus, it can be seen not only as a branch, but also as an extension, of the terrestrial hydrological system when it comes to production information for planning and management of water resources in the broader sense. *ACRU* is an agrohydrological modelling system, which integrates the fields of scientific hydrology, applied engineering and water resources related hydrology with subsequent linking of these fields with agrohydrology. The origin of *ACRU* dates back to detailed studies in the Natal Drakensberg in 1975, where it started as an energy driven catchment evapotranspiration model (Schulze, 1975).

ACRU is centered on a number of concepts that characterise the model. First, it is a conceptual-physical model. It is conceptual in that it conceives of a system in which important processes are idealised, and it is physical in that physical processes are represented in the model explicitly. In order to capture relevant processes, the model uses daily time steps and thus uses daily rainfall and reference potential evaporation data as primary inputs. *ACRU* operates on a daily multi-layered soil water budget (Figure 4.1). This enables the model to simulate land use and climate change impacts on the hydrological system of an area. The model also provides multiple options in many of its routines that can be used depending on the level of input data available or the detail of output required. It can operate either as a lumped small catchment model or as a distributed cell-type model for larger catchments or in areas of complex land use and soils.

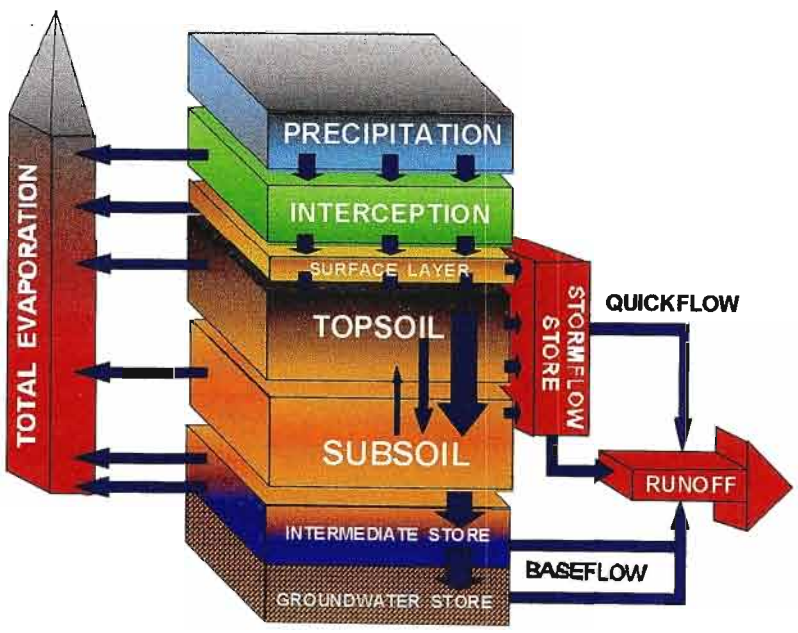

Figure 4.1 General structure of the *ACRU* agrohydrological modeling system (Schulze, 1995a)

ACRU is a multi-purpose model that simulates one or more facets of the terrestrial hydrological system and, according to Schulze (1995a), the model has been widely used by numerous groups of people since 1986, ranging from students to researchers. Typical applications of the model include water resources assessment, design flood estimation, irrigation water requirements and supply, crop yield and primary production modeling, assessment of land use and climate change impacts on water resources, and hydrological impacts of wetlands (Figure 4.2). A detailed explanation on the background, concepts and applications of the *ACRU* model is given by Schulze (1995a) in Chapter 2 of the text accompanying the *ACRU 300* modeling system.

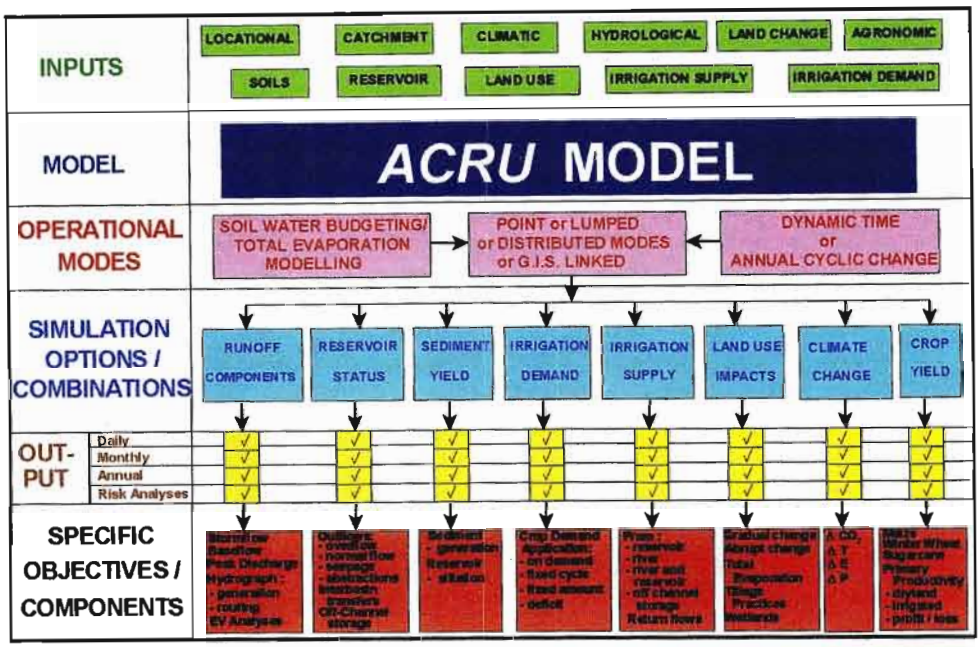

Figure 4.2 The *ACRU* agrohydrological modelling system: Concepts (Schulze, 1995a)

4.2 *ACRU 300 Series* and Its Structural Limitations

The *ACRU 300 series* have been written in the FORTRAN 77 programming language. Although this programming language has many merits in terms of computational efficiency, it also has limitations in developing a modular, easily expandable program design (Campbell *et al.*, 2001) which otherwise could be achieved by any object-oriented programming language such as Java. In his comparison between object oriented and procedural simulation models, such as FORTRAN and BASIC, from the view of their suitability for simulating an ecosystem, Silvert (1993) has described object-oriented simulation models as consisting of objects with complex internal dynamics that interact with each other. Furthermore, he

suggests the existence of a strong resemblance between object-oriented models and the ecosystem, which these models represent, as compared to the resemblance between procedural simulation models and the ecosystem.

Since its inception, *ACRU* has been expanding from being a rainfall: runoff model to its present status with several hundred routines and a complex internal structure. However, according to Campbell *et al.* (2001) it was becoming difficult to make new additions to the model. These structural limitations of the *ACRU 300 series* necessitated a rewriting of the model using an object-oriented programming language and restructuring it into a more extensible and modular structure.

4.3 *ACRU2000*

According to Clark *et al.* (2001) the two main reasons for restructuring the model were to make it easily extendible and to better represent the individual spatial elements of the model and the order of processing to facilitate the modelling of artificial water flows. The restructured *ACRU* model is designated as *ACRU2000*. It is implemented with the help of object-oriented programming techniques and the Java programming language.

Restructuring of the model in general was aimed at satisfying the requirements of both model developers and users. According to Campbell *et al.* (2001), the present modular structure of *ACRU2000* allows different individuals involved in model development to work independently without causing conflicts within the model when their contributions are combined. The structuring of *ACRU2000* was also partially driven by the increased social and governmental interest in water related issues. Various stakeholder groups were requesting new capabilities and tools that could allow them effective management of hydrological information.

4.3.1 Object-oriented programming and the *ACRU2000*

Model development in *ACRU2000* comprises two consecutive steps, object design (including analysis) and the subsequent code development (Campbell *et al.*, 2001). According to Quatrani (1998) the Unified Modeling Language (UML) provides a very robust notation, which grows from analysis into design. UML is a language used to specify, visualise, and

document the artifacts of an object-oriented system under development. UML is widely used in the development of *ACRU2000* for the abovementioned uses. The second step, code development, is implemented with the help of the Java object-oriented programming language. Detailed descriptions of object-oriented programming techniques and the Unified Modeling Language are given in various modelling tools (for example, Quatrani (1998) and Rational Software Corporation (1998)). However, this section is aimed at introducing the reader with some basic concepts and terminologies of object-oriented programming technique, which will be mentioned frequently in the rest of the document.

The object-oriented programming technique is an intuitive way of modelling real world systems such as the hydrological system, in a conceptual manner (Clark *et al.*, 2001). From the modelling point of view, an Object can be described as a concept, abstraction, or matter with well-defined boundaries and meaning for a certain application. A Class is a description of a group of objects with common properties and relationships to other objects and semantics (Quatrani, 1998). Since objects are a representation of either a real world or conceptual entity, there is always an interaction between objects.

Three main relationship types are used in *ACRU2000* to describe interactions between classes or objects, *viz.* inheritance, aggregation and association relationships (Kiker and Clark, 2001). According to Quatrani (1998) and Rational Software Corporation (1998), inheritance defines a relationship among classes where one class shares the structure and / or behavior of one or more other classes. This type of relationship is also called an "is-a" or " kind-of" hierarchy. In the literature two classes linked by an inheritance are described as child and parent, sub-class and super-class as well as client and supplier (for example, Rational Software Corporation 1998). A child class inherits all attributes, operations, and relationships defined in any of its parent classes. The inheritance relationship is diagrammatically denoted by a line with a triangle at one end connecting the parent class. An association relationship may represent a uni-directional or bi-directional relationship between two objects and for the case of bi-directional relationship it is represented by a line. An aggregation relationship, on the other hand, is a specialised form of association in which a whole is related to its part. Aggregation is also known as a "part of" relationship. It is denoted in UML by a line, connecting the "part" and the "whole", with a diamond next to the class showing a whole.

The three main relationship types are employed in *ACRU2000* to describe the interactions between various classes or objects. However, in order to help the reader appreciate the applicability of these relationships in conceptual physical based models, a simplified example is presented in Figure 4.3 that depicts the concept of objects and relationships as applied to the soil system and associated objects.

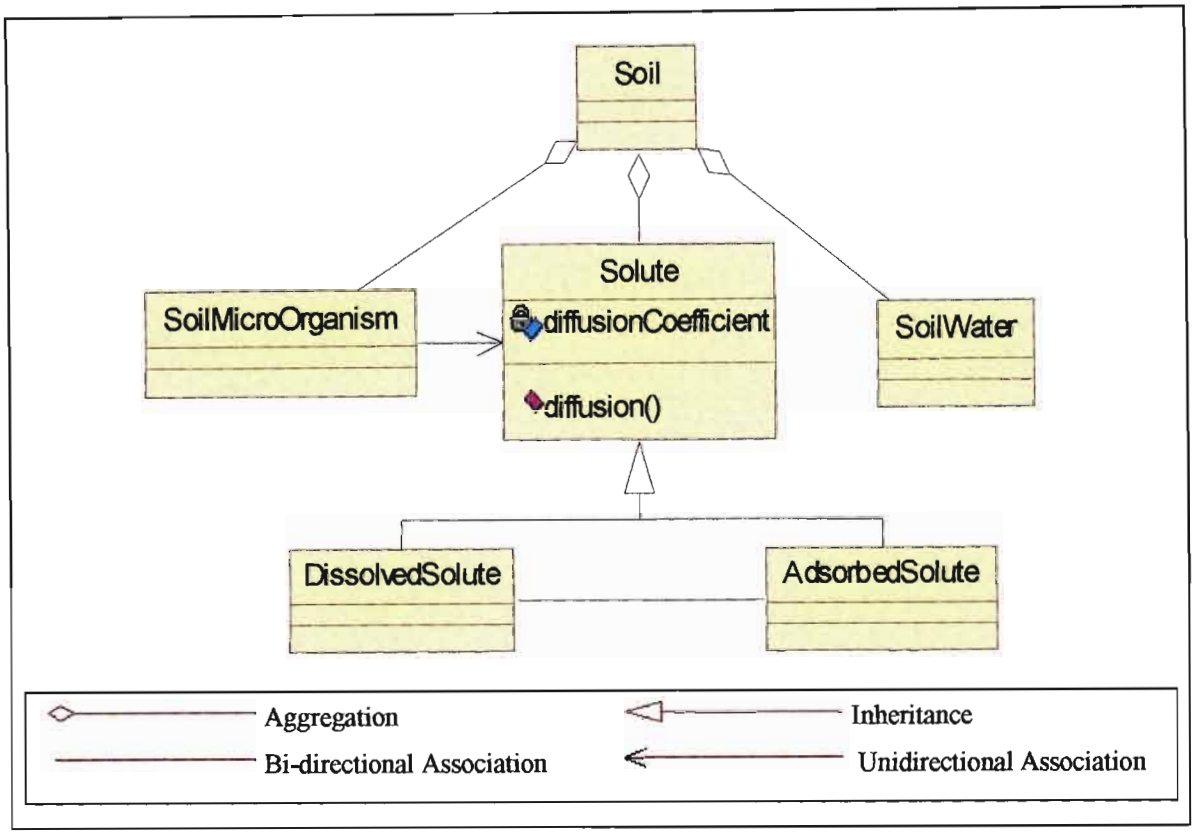

Figure 4.3 An example of objects and their relationships as applied in a simplified soil system

The soil object, among other objects, is comprised of soil microorganisms, solutes and soil water that are represented in Figure 4.3 by SoilMicroOrganism, Solute and SoilWater classes respectively. Thus, these three objects are "part of" the soil object and their relationship with the "whole" (soil object) is represented by an aggregation. A solute, in turn, can be either dissolved, in the form of soil solution or adsorbed on the soil particles. Therefore, depending on their mode of appearance and other associated characteristics, there are two "types of" solute. Hence, the DissolvedSolute and AdsorbedSolute classes are linked to the Solute classes by an inheritance relationship. Like all other objects a solute has attributes and

behaviours that characterise the object. As it is depicted in Figure 4.3, the Solute Class owns "diffusionCoefficient" and "diffusion" which respectively are its attribute and behaviour (operation). Thus, the two child classes (DissolvedSolute and AdsorbedSolute), being linked with their parent class (Solute) by an inheritance relationship, will be able to inherit the attribute and behavior of the Solute Class. From the diagram it can be seen there also exists an interaction between the SoilMicroOrganism and Solute as well as between DissolvedSolute and AdsorbedSolute classes. The interaction between these classes is an association. Solutes can change from the dissolved phase to an adsorbed phase, and vise versa, through the operation of diffusion. This movement of solutes, however, depends on the concentration gradient. Thus, in order for a solute to diffuse from one phase to another, these two objects need to exchange information regarding the solute load and concentration of both sides. Hence, the interaction between these two objects is described as a bi-directional association. Assuming a Solute Class does not need any information from the SoilMicroOrganism Class, while the SoilMicroOrganism needs information on the amount and state of a solute, then the relationship between these two objects can be represented by a unidirectional association.

4.3.2 Basic structure and objects of *ACRU2000*

Since *ACRU2000* is written with an object-oriented programming language, it is composed of Objects. There are seven main objects that constitute the model (Table 4.1). According to Kiker and Clark (2001), four of these objects: Model, Control, Interface and Exception operate out of sight to developers of new module. The Model Object starts model simulation through paving the way for other model objects. The Control Object, on the other hand, is responsible for managing the input and output systems of the Model. The Interface Object is used in *ACRU2000* for grouping of similar objects. The Exception Object handles errors that can emanate from conflicts between the new object under development and objects that belong to the programming language (Java). Such errors can result, for example, through a division by zero. It can also be used to handle errors that can arise due to the non compliance of the new object with the requirements already set by another *ACRU2000* object. For example, if a new data object is trying to add or deduct a value to or from a data object whose upper and lower value limits are already set, then the Exception object would handle and send an error message that the quantity requested by the object under development is out of the limits specified by another existing object. The remaining three objects, *viz.* Components, Processes and Data, are the most important objects as far as modelling of hydrology is

concerned (Clark *et al.*, 2001). Most of the coding phase of this research project is also based on these three objects. Therefore, this section will attempt to describe these objects with the help of an example.

Table 4.1 Basic objects in *ACRU2000* (after Campbell *et al.*, 2001)

Object Name	**Example Classes in *ACRU2000***
Model	MAcru2000Extensible
Control	AAcru2000ModelInput, AAcru2000ModelOutput
Interface	IWaterFlow, INutrientCycle, ISaltFlow
Exception	EArithmeticException, EFileNotFoundException
Components	CLandSegment, CReach, CDam, CChannel
Processes	PSCSRunoff, PMUSLEErosion, PSaltInput
Data	DArea, DPrecipitation, DBaseflowSalinity

In order to maintain model consistency and for ease of differentiating which class belongs to which object, a convention has been adopted in *ACRU2000* that all class names should start with a capital letter (which is also the Java language convention) indicating the class type. Thus, all classes that belong to Component Object start with C, Process classes start with P and Data classes start with D (Clark *et al.*, 2001). The Control object, however, is an exception to this rule. Instead of starting with the letter C its object classes start with A. This was done to avoid confusion that could arise due to having the same starting letter as the Component Object. Further, Butler (2001) has used italic letters to show class names in his dissertation. Therefore, this dissertation will also adhere to all the above conventions so as to maintain model consistency both in the coding and documentation of *ACRU2000.*

According to Clark *et al.* (2001), the Component objects represent the physical component of the hydrological system being modelled and form the building blocks of *ACRU2000.* Objects such as *CVegetation*, *CClimate* and *CLandSegment* are examples of the Componet Objects (Figure 4.4). These objects, in turn, may contain other smaller objects that together constitute the whole. The *CVegetation* Object, for example, is composed of *CLeafCanopy*, *CStem* and *CRoots* objects. The term "land segment", represented as a *CLandSegment* Object, in *ACRU2000* replaces the term sub-catchment in *ACRU 300 Series.* This is done in order to

show that an area need not be self contained hydrologically and could be created from a digital elevation grid (Kiker and Clark, 2001).

Each Component Object contains data objects that can store and describe attributes inherent to the component. For example, as shown in Figure 4.4, the *CClimate* object contains *DPrecipitation* and *DRainfallSaltLoad* data objects. The *DPrecipitation* stores information pertaining to daily depth of precipitation and the *DRainfallSaltLoad* stores the quantity of salt associated with wet atmospheric deposition (rainfall salt load). According to Clark *et al.* (2001), data objects can also perform additional functions such as range checking and specification of data units.

The Process Object, as its name implies, is responsible for describing processes that can take place in a conceptual or real world hydrological system. Thus, process objects shown in Figure 4.4, such as *PSurfaceFlow*, *PSubsurfaceFlow* and *PGroundwaterFlow*, along with other associated process objects, describe the flow of water from the soil surface through soil horizons to groundwater store and runoff. Similarly, process objects other than those responsible for water flow do exist in *ACRU2000,* such as those responsible for the transport of sediment and nutrients from one component to another. For example, the *PSaltGeneration* Process (in the hydrosalinity module of *ACRU2000*) describes an increase in salinity level of soil solution and groundwater store because of the addition of salts as a result of the weathering processes acting upon the surrounding soil and rock materials.

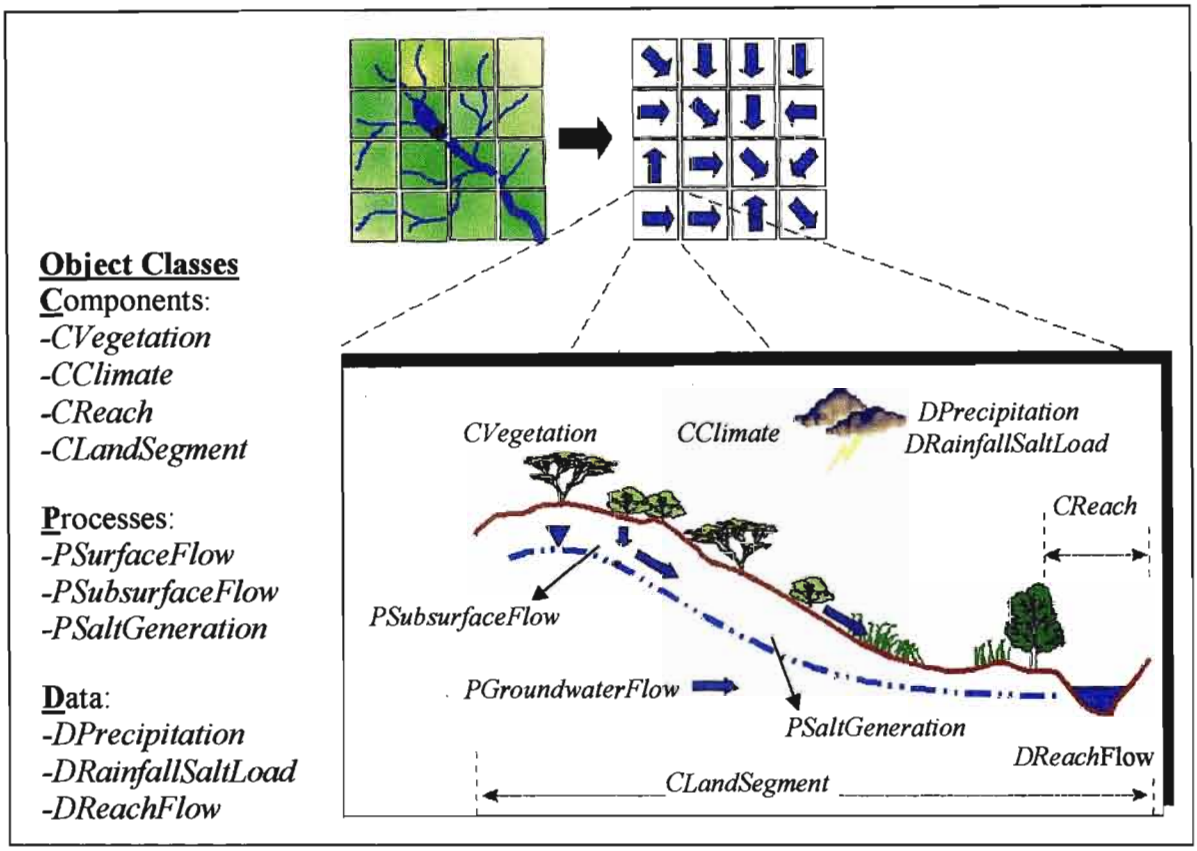

Figure 4.4 Examples of object classes as conceptualised in *ACRU2000* (after Clark *et al.*, 2001)

The hydrosalinity module of *ACRU* is developed within the *ACRU2000* environment. Therefore, it inherits the basic objects and structure of *ACRU2000* that have been described in this chapter. The following chapter deals with development of the hydrosalinity module of *ACRU* with special emphasis on description of the processes and associated data and component objects involved in the module.

5. DEVELOPMENT OF THE HYDROSALINITY MODULE

As mentioned in the preceding chapter one of the main reasons for restructuring the *ACRU* model was to make it easily extendable and modular. The hydrosalinity module of *ACRU* is developed in the restructured version of *ACRU, viz. ACRU2000*. The new structure of *ACRU* has facilitated development of the hydrosalinity module with little interference with the existing modules. The term "module" in *ACRU2000* refers to groups of objects with a common overall purpose (Kiker and Clark, 2001). Since this module is developed in the *ACRU2000* environment, it inherits the basic structure and objects of the model. Hydrosalinity models, in general, involve the interaction of hydrological and salinity related processes. Thus, the hydrosalinity module of *ACRU* also involves the interaction of hydrological processes, as determined by the hydrological modules of *ACRU*, and salinity related processes. Hence, the hydrosalinity module of *ACRU* is designated as *ACRUSalinity*. This chapter describes the development of the module with special emphasis on the processes and the interaction between various objects involved in these processes.

5.1 Modelling Approach and Basic Objects in *ACRUSalinity*

A series of steps is followed in the development of *ACRUSalinity*. First, an extensive review of the *ACRU* and hydrosalinity models was undertaken so as to get the basic idea on the way processes are represented in these models (Chapters 2 and 3). The next step was conceptualisation, where hydrological processes from *ACRU* and relevant salinity processes from the hydrosalinity models are conceptually linked to accomplish the required tasks. This step was then followed by a review of relevant UML designs and corresponding Java Classes in *ACRU2000*. Some of the major classes are described in Chapter 4.

After the conceptualisation and review of relevant UML diagrams and Java Classes in *ACRU2000*, the design of *ACRUSalinity* objects is implemented in the Rational Rose Software (Rational Software Corporation, 1995) with subsequent primary code generation using the same software. The generated primary code was further edited in JBuilder (Borland Software Corporation, 2001) to accomplish the required tasks for which the respective class was intended. The abovementioned stages are followed during the building process of all classes in *ACRUSalinity*. However, these steps were not followed step-wise since the

significance of adding some new classes was emerging during the development process. Rather, the development process was iterative.

The development of *ACRUSalinity* is based mainly on the interaction between three objects, *viz.* Components, Data and Processes. Thus, the following topics will briefly introduce for these basic objects. This will be followed by details of each process representing the various real hydrosalinity processes, starting from salt input from wet atmospheric deposition and irrigation water to salt balance and transport in surface and subsurface components of the hydrological system, as well as the associated component and data objects.

5.1.1 Component objects

No new component (physical feature) was added to the hydrological system in *ACRUSalinity*. However, attributes that belong to a certain physical feature and hydrosalinity processes taking place in a particular physical feature are described from a reference of the component object to which these attributes belong and in which the processes take place. According to Clark *et al.* (2001), all component objects are part of the abstract *CComponent* Class and most of them represent either surface features such as *CIrrigatedArea*, *CImperviousArea* and *CDam* or, alternatively vertical layers such as the *CHorizon* subcomponents of the *CSoil* layer and *CGroundwater*.

5.1.2 Data objects

The role of data objects in *ACRU2000* is described in Chapter 4. Data objects in *ACRUSalinity* also serve a similar purpose. For example, simple data objects, such as *DRainfallSaltLoad*, *DTopsoilSalinity* and *DBaseflowSalinity* are used to store data pertaining, respectively, to the *CClimate*, *CSoil* and *CGroundwater* component objects. Some data objects still hold information about certain processes. For example, the *DSalinityOption* stores information on whether the hydrosalinity module is to be executed or not in a particular simulation, whereas the *DSaltFluxRecord* Object serves not only to store the salt load of a particular component, but also to conduct internal salt balance computations with the help of its parent classes. Such computations are automatically executed whenever salt transport occurs from one component to another. Like all the data objects in *ACRU2000*, data objects in

ACRUSalinity also extend to the *DData* Class. This module is comprised of a number of new data objects that describe the various hydrosalinity attributes (Appendix A).

5.1.3 Process objects

A number of process classes have been built to describe salt input, salt balance and movement taking place on the surface and subsurface components, including reservoirs and channels. All the process objects in *ACRUSalinity* extend ("are type of") the *PProcess* Class, which is the parent class of all process objects in *ACRU2000*. The processes taking place within a particular component are executed based on a predetermined order. However, the order of execution for hydrosalinity processes in different component objects follows the direction of water flow as determined by the hydrological modules of *ACRU2000*. According to Clark *et al.* (2001), on each day of simulation, the processes for the land segment on the edge (head water) of the simulated catchment are executed first, followed by land segments in progression towards the catchment exit. Thereafter, processes for each *CReach* type are executed, starting with reaches on the edge of the flow network and moving progressively downstream. Processes responsible for accomplishing the various hydrosalinity computations are grouped into six objects. These objects are briefly described below.

I. Initializing Salt Load

For the ease of module use by users, most inputs to the module are prepared in units that are readily available from physical measurements rather than in a way that can readily be used for internal computations. For example, in most cases, data for the initial TDS level of the soil solution is usually available as a concentration (mg/l) rather than a mass (mg). Therefore, the module is structured in such a way that it can accept inputs in readily available unit (mg/l). However, internal computations of the hydrosalinity processes involve salt load (mg). Hence, the main aim of this object is to set the initial salt load through computations based on the initial salt concentration and volumetric water content of the soil layers in irrigated and non-irrigated lands. This object also sets the initial salt load of reservoirs based on the initial reservoir water storage and its associated TDS concentration.

II. Salt Input

This object contains classes that are responsible for salt load input from rainfall and irrigation water to the topsoil horizon of irrigated and non-irrigated lands as well as to reservoirs. External salt input to non-irrigated lands and reservoirs has rainfall as its origin. However, irrigated lands receive additional salt input from irrigation water. Processes which undertake the salt input mechanism to irrigated land, non-irrigated land and a reservoir, respectively, are *PIrrigSaltInput*, *PLandSegSaltInput* and *PReservoirSaltInput*.

III. Surface Salt Movement

This object generally contains such process classes that describe the stormflow and runoff salinity as well as distribution of salt load from irrigated, non-irrigated and impervious areas and also reservoirs to an appropriate destination component. Some of the process classes contained in this object include *PRunoffSalinity*, *PIrrigAreaSaltMovement* and *PLandSegSaltMovement*.

IV. Subsurface Salt Movement

This object includes process classes that handle the salt balance and salt generation computations in subsurface components. Thus, processes in this object describe the movement of salts from the topsoil through subsoil to the groundwater store with subsequent salt generation taking place in each soil horizon and the groundwater store. This object also supports upward movement of salt load from the bottom horizon to stormflow through the overlying horizons, in the case of saturated upward flow. *PIrrigUpwardSaltTransport*, *PSubsurfaceSaltMovement* and *PSaltUptake* are some example classes from this object.

V. Reservoir Salt Budget

Processes included with in this object describe the reservoir salt budget with subsequent determination of the current reservoir storage salinity and salt concentration of the various outflow components, such as overflow and seepage. In the case of distributed hydrosalinity modelling, if the reservoir under consideration is situated at a particular sub-catchment's outlet, this object also carries out the transport of salt load associated with the various

outflows from the reservoir to an appropriate sub-catchment. The main classes in this object are *PReservoirComponSalinity* and *PSaltStacking*.

VI. Channel Salt Movement

This object contains classes that describe the salt balance at the channel outlet of a particular sub-catchment. This object also performs the transfer of salt load from one sub-catchment to the relevant downstream sub-catchment, in the case of distributed hydrosalinity modelling. The main process class contained in this object is the *PCatchmentSalinity*.

5.2 Subsurface TDS Balance and Baseflow Salinity

Subsurface TDS balance and movement through the soil profile is based on the concepts used in the DISA model. However, the Lagranian salt lagging approach used in the DISA model to account for the varying sources of percolated water and its influence on TDS balance of the various layers is not employed in *ACRUSalinity*. This is not expected to have a significant impact on the subsurface TDS balance if the subsurface system is divided into only two layers, i.e. topsoil and subsoil, plus the groundwater store as vertical components of the subsurface system. Therefore, it is based on the assumption that each layer is deep enough to store more volume of water in comparison to the percolated water out of the layer for the day, and hence at a particular time step (day) the source of percolated water into a given layer is only from its immediate overlying layer.

5.2.1 Total evaporation and the soil water balance as conceptualised in the *ACRU* model

An increase in soil- and groundwater salinity is attributed mainly to the combined effects of hydrological and geochemical processes. Two of the main hydrological processes that influence the subsurface salt balance include precipitation and total evaporation. In most cases, the recharge of the soil horizons and groundwater store by precipitation has a dilution effect on subsurface water TDS concentration. On the other hand, the removal of water through evaporation and transpiration has a concentrating effect. Therefore, these processes coupled with the physiographic characteristics of the catchment, such as drainage of the soil, have a substantial effect on the subsurface water balance, and thereby on its salt balance.

5.2.1.1 Total evaporation

In the dryland routines of *ACRU,* total evaporation consists of evaporation from the plant tissue (transpiration) and soil water evaporation (Schulze, 1995c). Both transpiration and soil water evaporation occur at maximum rates when the plant is not under environmental stress. Maximum transpiration can be calculated either from LAI (leaf area index) values or water use coefficients (formerly termed crop coefficients). Similarly, maximum soil water evaporation is estimated either as a residual of the available energy remaining after estimating maximum transpiration, or from considerations of shading of the soil surface by aboveground biomass.

In *ACRU,* maximum transpiration is expressed as a function of reference potential evaporation and the fraction of total available transpiration. Maximum transpiration is allocated among the different soil horizons in proportion to the fraction of root mass density and degrees of colonisation of that specific horizon. However, when one of the horizons experiences a greater soil water deficiency than the other, the unstressed horizon contributes more to transpiration than computed by its proportion of root mass available for transpiration.

Actual transpiration may take place at its maximum rate or below. Plants may transpire below maximum rate under saturated or deficit soil water conditions. In *ACRU,* actual evaporation from the soil surface is calculated in two stages. In the first stage, when the soil is wet, evaporation from the soil surface is limited only by the energy which is available at the surface, and is thus equal to maximum soil water evaporation. Once the accumulated soil water evaporation exceeds the stage 1 upper limit, the stage 2 evaporative process starts, after which evaporation from the soil declines rapidly. Actual evaporation may be suppressed by surface cover such as mulch, litter or surface rocks. *ACRU* accounts for this effect by a linear relationship between the surface cover and soil water evaporation (AT7-10) (Schulze, 1995c).

Mathematical expressions that describe the preceding principles of total evaporation are given in the soil water budgeting and total evaporation as well as irrigation crop water demand chapters (Chapters 7 and 17) of the *ACRU* model documentation (Schulze, 1995c).

5.2.1.2 Soil water balance

The standard *ACRU* water budgeting routines for general use operate within a surface layer and two "active" soil horizons in which rooting development and hence soil water extraction, as well as soil water uptake and drainage can take place (*ACRU* Theory, pp AT5-4) (Schulze *et al.*, 1995b).

The soil water budgeting process in *ACRU* takes place in a sequence of steps. First, the soil water content at total porosity, drained upper limit and permanent wilting point need to be stipulated for each of the active soil horizons. After the soil water content of the topsoil horizon is adjusted by the addition of net rainfall, the soil water content of the topsoil horizon is re-assessed. If it exceeds the topsoil's drained upper limit, a proportion of the excess water drains into the subsoil horizon. Similarly, if the subsoil water content is above its drained upper limit (DUL), a fraction of the excess water drains below the root zone and to the groundwater store. Thereafter baseflow releases are calculated as the product of the previous day's groundwater store and a user specified baseflow recession coefficient, which depends on factors such as geology, catchment area and slope. On the other hand, if the drainage rate of the lower soil layer is very low (for example, because of a subsurface impervious layer), the soil water content may accumulate to a level exceeding its porosity. In such cases the water accumulates from the lower soil layer in an upward direction, filling first the subsoil horizon to porosity and thereafter contributing to the topsoil horizon from below. Should the topsoil's water content exceed porosity, excess water contributes directly to stormflow as saturated overland flow.

Unsaturated soil water redistribution can take place in the model as a result of differences between soil water conditions of the respective horizons. This slow movement of water will occur from the top soil horizon, when the soil water content is below its drained upper limit (DUL), to the subsoil horizon if the topsoil horizon is relatively wetter than the subsoil horizon. Unsaturated redistribution depends on the soil water gradient, the head of water and soil texture. Upward soil water redistribution in *ACRU* mimics capillary movement, and takes place when the subsoil horizon contains a higher relative soil water fraction compared to that of the topsoil (*ACRU* Theory, pp AT7-19) (Schulze, 1995c).

Various options are provided by *ACRU* decision support system to estimate soil water content at permanent wilting point and drained upper limit, depending on the level of available soil information (*ACRU* Theory, Chapter 5) (Schulze *et al.*, 1995b).

5.2.2 Rainfall and irrigation water salt input

The source of dissolved solutes in the soil solution, other than the primary source, i.e. due to *in situ* weathering processes, is assumed to be from solutes added along with rainfall (wet atmospheric deposition) and irrigation water. In irrigated areas, solute input includes both that from applied irrigation water and that from rainfall. The average TDS concentration of rainfall and irrigation waters are input to the model and are stored in the *DRainfallSalinity* and *DIrrigationWaterSalinity* data objects for subsequent computations.

In most cases, it is difficult to obtain a time series of rainfall salinity. Therefore, salt concentration of rain water is assumed to have a constant value at a specific location and can be taken as the average observed value at the site. However, time series irrigation water salinity is available for most irrigated areas and is characterised by seasonal variations in some areas. Therefore, irrigation water salinity is input to the model on monthly basis.

These processes of salt input to the soil are carried out in two similar process classes functioning on irrigated and non-irrigated lands. The *PLandSegSaltInput* Process carries out the daily input of salt load associated with rain falling on non-irrigated lands. On the other hand, the *PIrrigSaltInput* Process determines the daily salt load from rain falling on irrigated areas and applied irrigation water, with subsequent addition of this salt load to the topsoil horizon. The quantity of salt load added from a rainfall source is described as the product of effective rainfall volume and rainfall salinity (Equation 5.1). Similarly, the salt load associated with irrigation water is determined as the product of the volume of applied irrigation water and its average TDS concentration (Equation 5.2). The flow diagram in Figure 5.1 represents the main steps included in the *PIrrigSaltInput* Process.

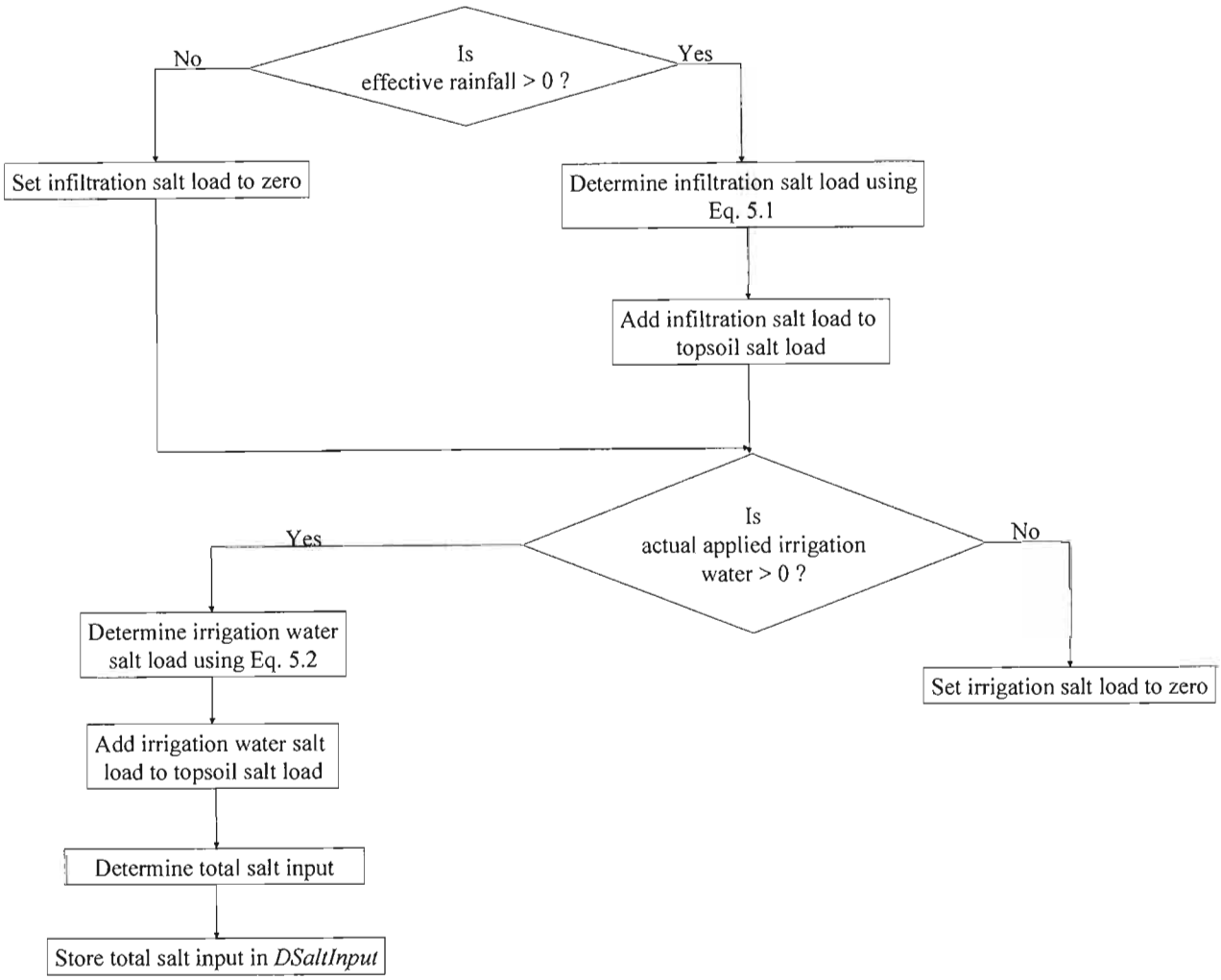

Figure 5.1 Flow diagram of salt input mechanism to irrigated lands as accounted in the *PIrrigSaltInput* Process Object

$$SL_{er} = ER * C_r \tag{5.1}$$

$$SL_{aiw} = IW * C_{iw} \tag{5.2}$$

where SL_{er} = salt load input to topsoil associated with rainfall (mg)

ER = volume of effective rainfall (l)

C_r = rainfall salinity (mg/l)

SL_{aiw} = salt load input to topsoil associated with irrigation water (mg)

IW = volume of irrigation water (l) and

C_{iw} = irrigation water salinity (mg/l).

In *PIrrigSaltInput*, effective rainfall refers to the volume of rainfall infiltrated into the topsoil horizon on a particular day and is expressed in litres. Similarly, actual applied irrigation water refers to the volume of irrigation water infiltrated into the soil, i.e. the total applied irrigation water excluding the various irrigation losses. This process assumes that irrigation water is applied only to the topsoil horizon and hence its direct contribution is only to the topsoil TDS balance. Therefore, the daily calculated salt load both for irrigated and non-irrigated lands is added to salt load of the topsoil horizon. The *PIrrigSaltInput* and *PLandSegSaltInput* processes are similar in structure. Figure 5.2 shows the various data and component objects associated with the *PIrrigSaltInput* Process Object and the interaction between these objects. Notations representing the relationship types in the figure are described in Chapter 4. For a definition of the class names in the diagram see Appendices A, B and C.

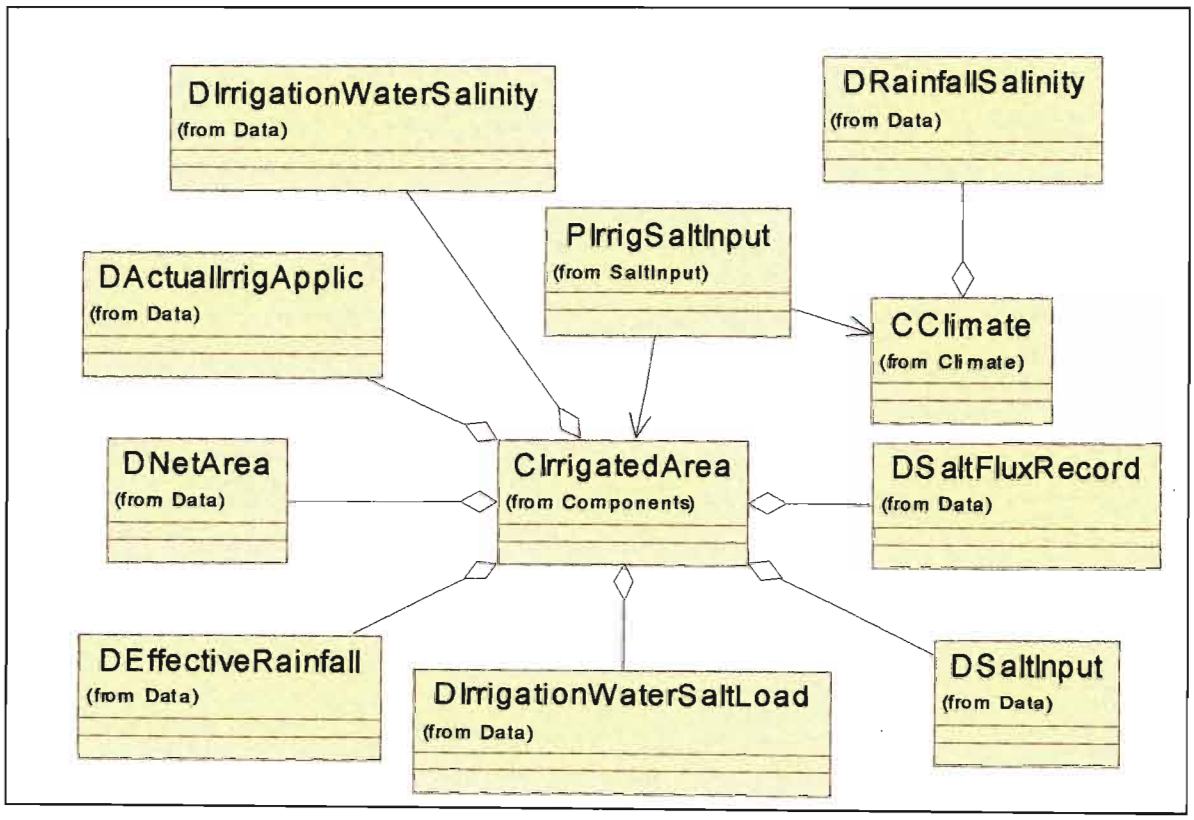

Figure 5.2 Class diagram of *PIrrigSaltInput* Process and associated data and component objects

5.2.3 Subsurface salt movement

Subsurface salt movement occurs in both irrigated and non-irrigated lands. It can be either downward or upward, depending on the direction of soil moisture movement. Downward salt

movement occurs as a result of percolation of water from the topsoil to underlying horizons and the groundwater store. On the other hand, upward salt movement is associated with saturated upward flow of water from a bottom horizon to the overlying layer under conditions of poor drainage.

5.2.3.1 Downward subsurface salt movement

The downward salt movement from any layer in the soil profile occurs when the saturated downward flow of water from that layer is greater than zero. In *ACRU,* saturated downward flow takes place when the soil moisture store exceeds drained upper limit. Hence, downward salt movement can also take place only when the drained upper limit is exceeded. *ACRU* includes an option for unsaturated water movement in the soil profile, i.e. flow from topsoil to subsoil horizon or *vice versa* when the soil water content is below DUL. However, at present *ACRUSalinity* is not linked to this optional process. Therefore, this option needs to be switched off when conducting hydrosalinity simulations in order to avoid salt imbalances.

The subsurface system is composed of vertical layers. Thus, the algorithms that perform subsurface salt balance and movement computations are written assuming a multi-layered soil profile. In non-irrigated lands, for example, downward salt movement takes place from the topsoil through the subsoil to the groundwater store. Thus, in these conditions *ACRU* considers three subsurface components (two soil horizons and the groundwater store). However, the algorithm that carries out this salt balance process and in most other subsurface TDS balance processes are written in a way that they can be used for multi-layered soils with more than three stores.

The downward subsurface salt movement and salt balance computations are accomplished by the *PSubsurfaceSaltTra* and *PIrrigSubsurfaceSaltTransport* processes on non-irrigated and irrigated lands respectively. The component, process and data objects associated with the *PSubsurfaceSaltTra* Process are depicted in Figure 5.3. Definitions for the data objects are given in Appendices A and B. Similarly definitions for the component objects are presented in Appendix-C.

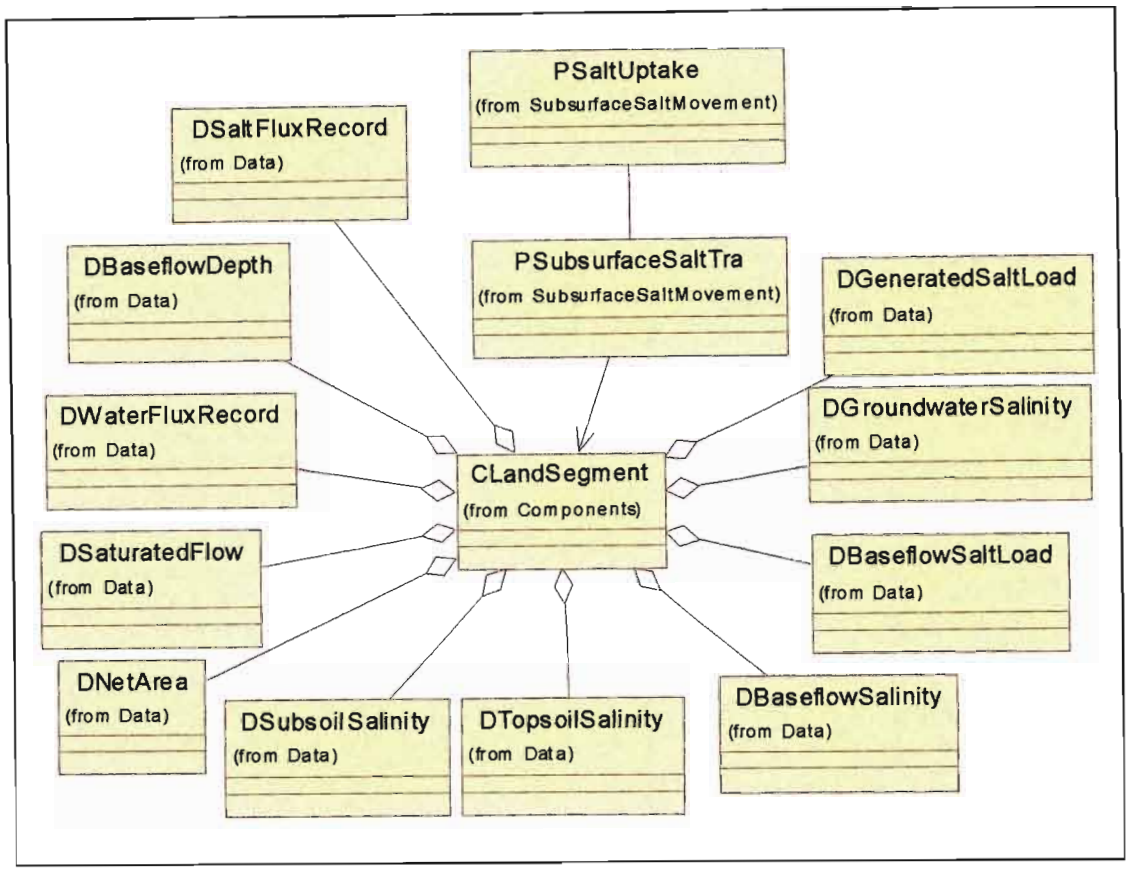

Figure 5.3 Class diagram of *PSubsurfaceSaltTra* Process and its associated component and data objects

The *PSubsurfaceSaltTra* Process determines the subsurface TDS balance in non-irrigated lands. In this process salt is transported from the topsoil to an underlying horizon and finally to the groundwater store depending on the volume of percolating water and its salinity. It also determines the TDS concentration of each horizon, salt load associated with percolation water and baseflow salt concentration.

The *ACRUSalinity* module and other water quality related modules of *ACRU2000*, such as sediment yield and nutrient simulations (Nitrogen and Phosphorous), are executed after the relevant hydrological processes are executed and the associated data objects are set for the day. Therefore, the salt concentration and salt load in a particular horizon are computed after percolation of water to an underlying layer has taken place for the day. Hence, taking into account the effect of this phenomenon the salinity of each horizon, before salt generation, is estimated using the following equation:

$$C_i = \frac{SL_i}{SW_i + PW_i} \tag{5.3}$$

where C_i = salt concentration of the i-th horizon before salt generation (mg/l)

SL_i = current salt load of the i-th horizon before salt generation (mg)

SW_i = volumetric soil water content of the i-th horizon after percolation has taken place out of the horizon (l) and

PW_i = volume of percolated water out of the i-th horizon (l)

The salt load of the subsurface components (layers) is replenished from internal and external sources. The salt load of the topsoil horizon is replenished from rainfall salt input, whereas, in the case of subsoil and groundwater store, it is replenished by the salt load added from an overlying layer along with the percolating water. The internal source of salt load to a particular layer, or the groundwater store, is through salt generation within the layer or the groundwater store. The increase in salt concentration of each horizon due to salt generation is determined in a separate process (*PSaltUptake*) and is described in Section 5.2.4. However, the *PSaltUptake* Process only updates the salt concentration of a given layer according to first order rate kinetics. Thus, once the *PSubSurfaceSaltTra* Process has received the updated salinity level as determined by the *PSaltUptake* Process, the salt load after the update of the horizon's salinity is calculated using Equation 5.4. The quantity of salt added to the particular layer due to salt generation is then determined as the difference of the salt load after and before the update of that horizon's salinity has taken place (Equation 5.5).

$$SL_{upd\_i} = C_{upd\_i} * (SW_i + PW_i) \tag{5.4}$$

$$SL_{gen\_i} = SL_{upd\_i} - SL_i \tag{5.5}$$

where SL_{upd_i} = salt load in the i-th horizon after salt generation (mg)

C_{upd_i} = updated horizon salinity (mg/l) and

SL_{gen_i} = salt load generated for the day in the i-th horizon (mg).

The water percolating on a daily basis from each horizon has the same salt concentration as the particular layer from which percolation took place. Thus, this process assumes that the

volume of water entering each layer for the day originates only from its immediate overlying layer. This assumption seems to hold true in *ACRU*, since the soil profile is commonly divided only into topsoil and subsoil horizons. In this case, the layers are deep enough such that at a daily time step the amount of percolated water is likely to be less than the storage of the layer immediately above the current layer. The salt load associated with the percolation water out of the i-th horizon (SL_{p_i}) is described by Equation 5.6 and is transported to the underlying layer or groundwater store (if the current layer is the bottom horizon) before any salt balance computation commences for the underlying layer.

$$SL_{p\_i} = C_{upd\_i} * PW_i \tag{5.6}$$

The groundwater salt balance and baseflow salinity are determined after the salt balance of the soil horizons has been set for the day. Within the soil profile, salt load associated with percolation water is added to an underlying horizon. However, if the layer under consideration is the bottom horizon, the salt load of the percolated water is transported to the groundwater store and replenishes the groundwater salt load. If, on a particular day, the groundwater store is not empty, its daily salinity and salt load are determined in a similar way to that of soil horizons. In this case, however, the salt load leaving the groundwater store is a function of the baseflow volume and groundwater salinity. The daily groundwater salt concentration before salt generation is computed based on the current groundwater volume and salt load, as well as the volume of water released from the groundwater store as baseflow. This is expressed by the following equation:

$$C_{gw} = \frac{SL_{gw}}{GW + BF} \tag{5.7}$$

where C_{gw} = salt concentration of the groundwater store before salt generation (mg/l)

SL_{gw} = groundwater store salt load before salt generation (mg)

GW = volumetric groundwater content after baseflow release (l) and

BF = volume of baseflow release for the day (l).

Besides the salt load source associated with percolation water from the bottom soil horizon, the salt load of the groundwater store is also replenished by the salt generated from within the

groundwater system as a result of the different weathering processes acting upon the soil and geological formations. This salt generation process in the groundwater store is also performed in conjunction with the *PSaltUptake* Class in a similar way as is done for soil horizons. The groundwater store TDS concentration is updated by the *PSaltUptake* Process (section 5.2.4). The groundwater salt load after update of the salt concentration is calculated in *PSubsurfaceSaltTra* using Equation 5.8 and the generated salt load is calculated as the difference of groundwater salt load before and after the salt concentration is updated (Equation 5.9).

$$SL_{upd\_gw} = C_{upd\_gw} * (GW + BF) \tag{5.8}$$

$$SL_{gen\_gw} = SL_{upd\_gw} - SL_{gw} \tag{5.9}$$

where SL_{upd_gw} = salt load of groundwater store after salt generation (mg)
C_{upd_gw} = updated groundwater salinity (after salt generation) (mg/l) and
SL_{gen_gw} = salt load generated for the day in groundwater store (mg).

Baseflow volume released from the groundwater store is assumed to have the same salinity level as the updated groundwater TDS concentration for the day. The associated salt load for baseflow release is then calculated as:

$$SL_{bf} = BF * C_{bf} \tag{5.10}$$

where SL_{bf} = salt load associated with baseflow release (mg) and
C_{bf} = baseflow salt concentration (mg/l).

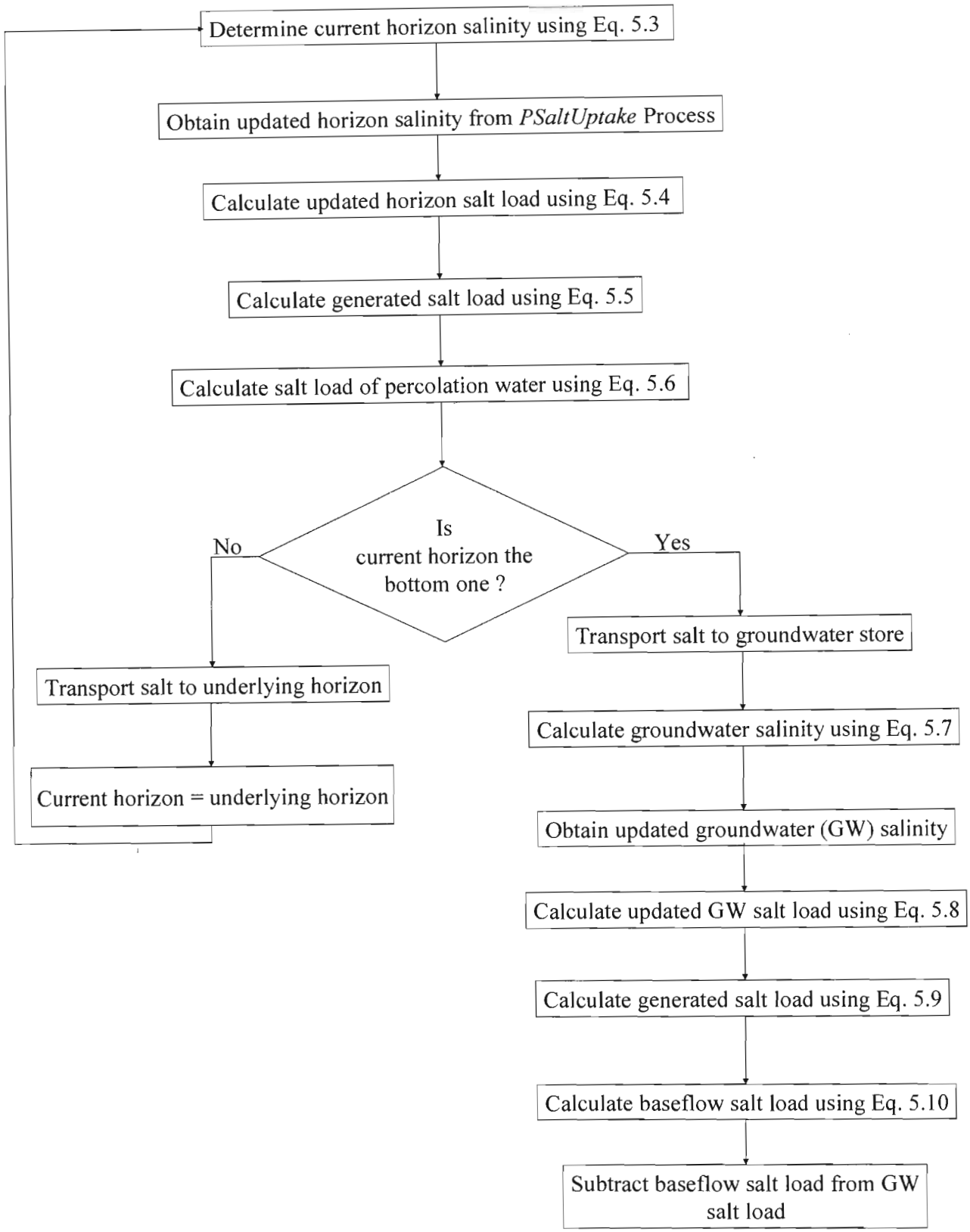

Figure 5.4 Flow diagram of subsurface salt movement in non-irrigated lands

The *PIrrigSubsurfSaltTransport* Process serves a similar purpose as that of *PSubsurfaceSaltTra*. This process, however, handles subsurface TDS balance and movement in irrigated lands. Generally it has similar algorithms to that of *PSubsurfaceSaltTra*, but in

this case, only a single horizon and the groundwater store are considered as *ACRU* considers only these subsurface components in irrigated lands. In *ACRU* the months in which irrigation take place are specified by the user. Thus, this algorithm is invoked only for months in which irrigation is taking place. Component and data objects associated with this process are depicted in the following figure and definition of each class is given in Appendices A, B and C.

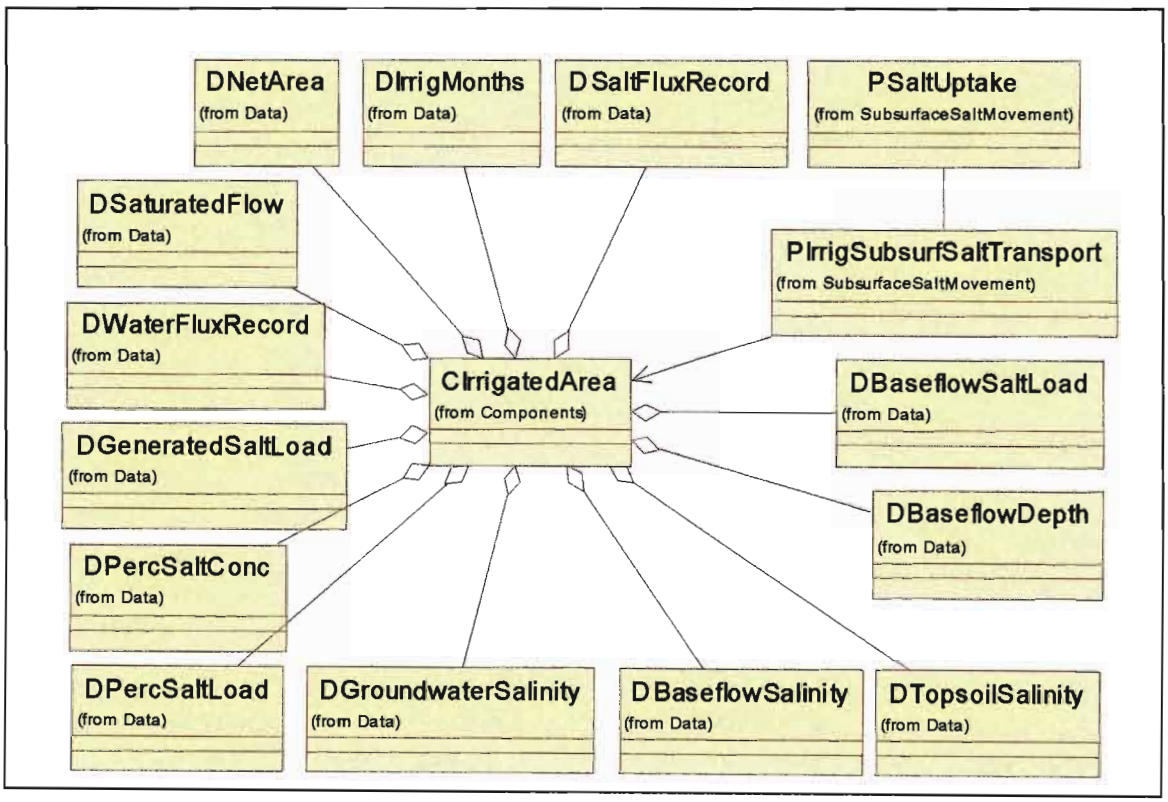

Figure 5.5 Class diagram of *PIrrigSubsurfSaltTransport* and its associated data and component objects

5.2.3.2 Upward subsurface salt movement

Upward salt movement through the soil profile and its influence on surface and subsurface salt balance is determined by the *PUpwardSaltTransport* Process. In this process, salt load moves from the bottom horizon through the overlying horizons to quickflow. The upward movement of salt is dependent on the moisture status and drainage of a particular layer. This process accounts upward subsurface salt movement only under a saturated condition. Hence, upward salt movement under this process occurs only if the rate of water recharge to a layer

exceeds the rate of water loss from that particular layer. Information on the quantity of upward moving water is retrieved from the *DSatUpwardFlow* Data Object whose value is determined and assigned in *PSatUpwardFlow*. This data object is created in *ACRUSalinity* for hydrosalinity computations. Data and component objects associated with this process are shown below. Definitions for the data and component objects are given in Appendices A, B and C.

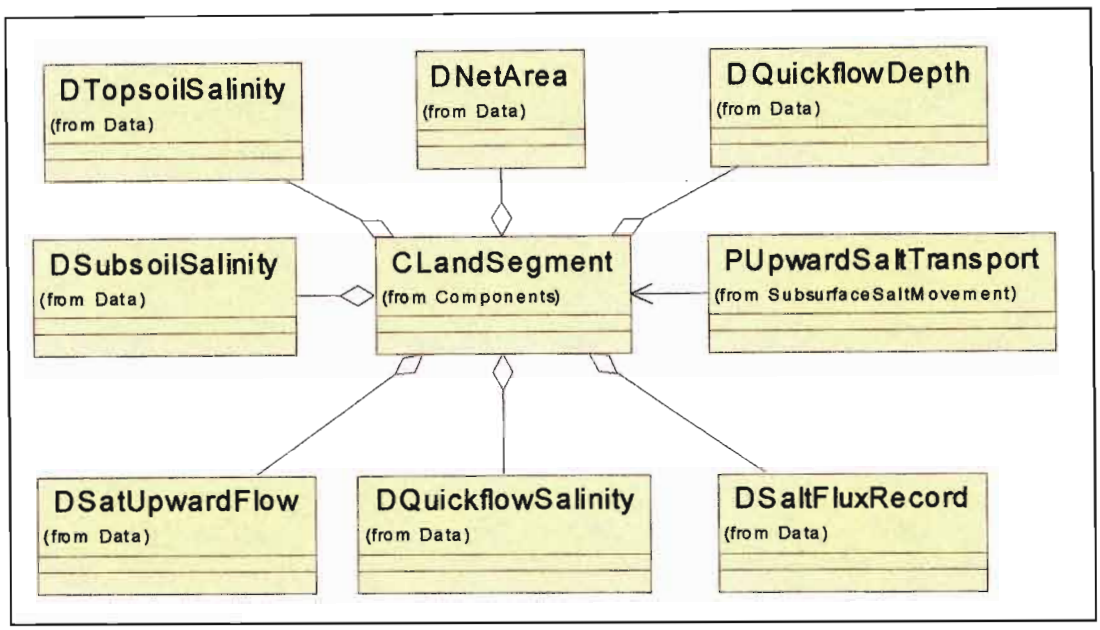

Figure 5.6 Class diagram of *PUpwardSaltTransport* Process and associated data and component objects

If, on any particular day, the upward movement of water from a given horizon is greater than zero, then the salt load entering an overlaying layer is expressed as the product of the volume of water entering the layer and the current salt concentration of the layer from which this volume of water commences. The upward flow of water is expressed in litre (l) and the salt concentration value in mg/l. Thus, the salt load entering the layer is expressed in milligram (mg). This is so in the case of salt movement being within the soil profile. If the origin of the upward moving salt is from the topsoil horizon, the salt load is added to the quickflow salt load. The TDS concentration of quickflow is subsequently updated under this process using Equation 5.11 in order to account for the effect of the salt flux from the topsoil associated with saturated upward flow. The concept of quickflow in *ACRU* model and determination of its initial salinity and salt load are discussed in Section 5.3.

$$C_{qf} = \frac{SL_{qf} + SL_{upf}}{QF} \tag{5.11}$$

where C_{qf} = the updated quickflow salinity (mg/l)

SL_{qf} = salt load of the quickflow before upward salt flux from the topsoil (mg)

SL_{upf} = upward salt flux from topsoil to quickflow (mg) and

QF = quickflow volume (l).

The following figure shows a flow diagram of an upward salt movement in non-irrigated lands as accounted in *ACRUSalinity*.

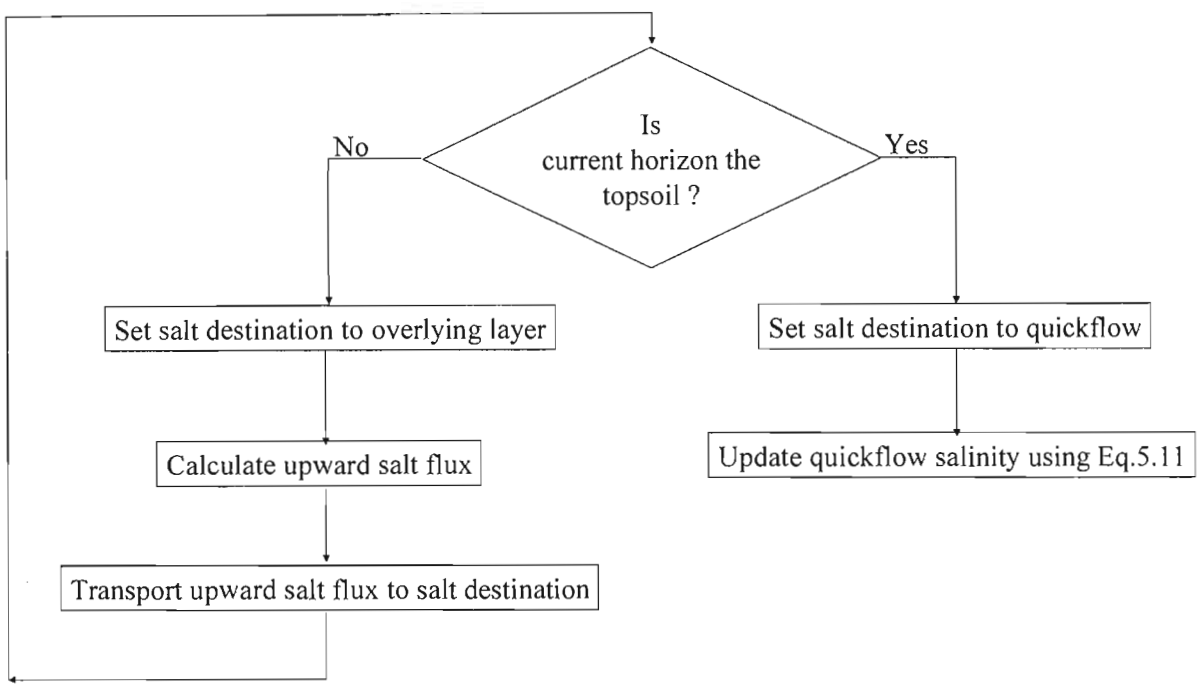

Figure 5.7 Flow diagram of upward salt movement in non-irrigated lands as represented in the *PUpwardSaltTransport* Process

The *PIrrigUpwardSaltTransport* Process also serves a similar task in irrigated lands. However, this process determines salt movement only from the topsoil to quickflow, with subsequent updating of the quickflow salinity and the salt load. This is so because of the presence of only a single layer as conceptualised in the *ACRU* model in the case of irrigated lands.

5.2.4 Salt generation

The process of salt generation involves complex weathering and soil-solute interaction mechanisms, which in turn are influenced by hydrological, climatic, geochemical and anthropogenic factors. Thus, among other factors, an adequate description of this process includes the detailed chemical reactions taking place at individual element level. This requires knowledge on such detailed processes and extensive data for each solute species, which is beyond the scope of this research. Hence, a simplified modelling approach of the salt generation mechanism is adopted in *ACRUSalinity*.

As mentioned in Section 5.3.2, computations to update TDS concentration of each horizon and the groundwater store to account for the increased salt concentration due to salt generation, take place in a separate process class. This allows for re-use of the same algorithm to determine the updated salt concentration of each soil horizon and the groundwater store both for irrigated and non-irrigated lands. Moreover, placing this process into a separate class minimises the complexity of processes performing subsurface salt balance and movement. Furthermore, any changes required for the future in the expressions describing the increased salt concentration as a result of salt generation processes can be made in this process only with little or no change to any of the other processes.

The salt generation process and subsequent update in salt concentration of each layer is carried out in the *PSaltUptake* Process. This process receives information from the calling class, which can either be the *PSubsurfaceSaltTra* or *PIrrigSubsurfSaltTransport*. The information includes identity of the layer in which salt generation is to take place, salt concentration of the layer before salt generation and area of the irrigated or non-irrigated land in which salt generation is to take place. This process then updates the salt concentration of the current layer based on the above and other relevant information according to first order rate kinetics as proposed by Ferguson *et al.* (1994).

As described in chapter 3, the first order rate kinetics equation assumes that the rate of increase over time in the concentration of a solute is proportional to how far the current concentration falls short of its equilibrium value. Equation 5.12 describes an initially rapid, but progressively slower, salt generation such that the concentration approaches the equilibrium value asymptotically. In the absence of any dilution by rainfall, irrigation water or

percolation and "evapoconcentration", the increase in subsurface TDS concentration with time from its initial value (C_i) to the saturation (C_{sat}) value due to salt generation is represented as in Figure 5.8.

$$C_{upd\_i} = C_i + (C_{sat} - C_i)[1 - \exp(-k)] \tag{5.12}$$

where C_{upd_i} = updated salt concentration of the i-th horizon or groundwater store (mg/l)

C_i = salt concentration of the i-th horizon or groundwater store before salt generation (mg/l)

C_{sat} = the equilibrium value (mg/l) and

k = rate constant.

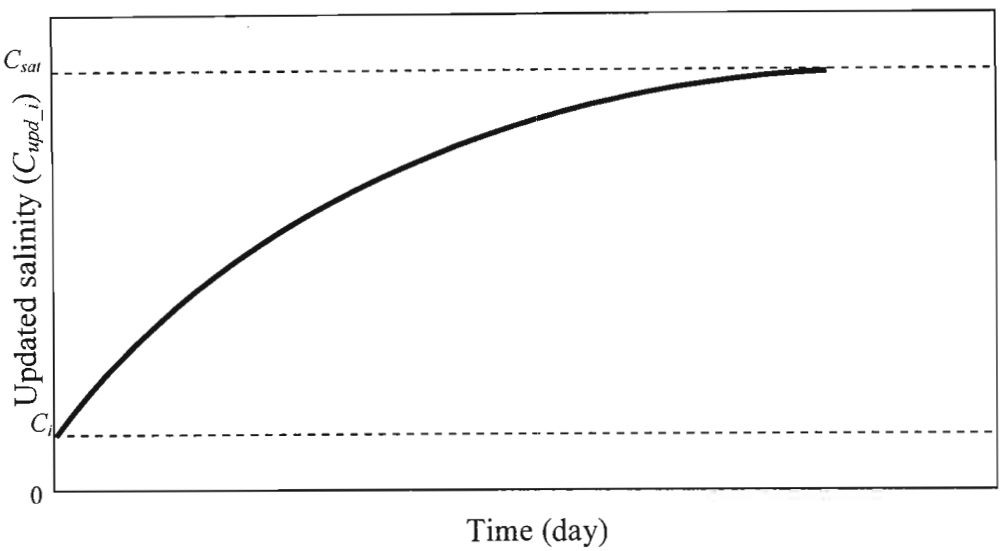

Figure 5.8 An increase in subsurface TDS concentration with time based on the first order rate kinetics

The first order rate kinetics equation is adopted in *ACRUSalinity* with some assumptions. Originally, this equation was proposed for use in estimating solute enrichment of the soil solution due to soil water uptake of individual solute species. However, in this case the equation is used for estimating the increased total dissolved solutes (TDS) value. This is based on the assumption that the quantity of total dissolved solutes, which is the salinity of a given layer, is the sum total of the major individual solute species in the soil solution. Thus, the

increase in total dissolved solute concentration follows a trend similar to that of the individual solute species and hence it can be described by a similar equation. The time parameter (t) in the original equation is omitted in Equation 5.12, since in this case the time step between successive salt generation computations is fixed to a single day. Hence, its value is 1.

The equilibrium value and the rate constant for each horizon and groundwater are inputs to the model by the user and are stored in the *DSaltSat* and *DUptakeRateConstant* data objects. The equilibrium value refers to the maximum salt concentration of the layer at which saturation level is reached. The rate constant (k) controls the rate of salt generation from each horizon and the groundwater store. Although the rate constant is expected to vary between solute species, for this purpose its value is assumed to be similar for all solute species and is represented by a single averaged value.

Once the updated salt concentration is determined by this process, the generated salt load is calculated in *PIrrigSubsurfSaltTransport* and *PSubsurfaceSaltTra* for irrigated and non-irrigated lands respectively. It is calculated as the difference between the salt load of a particular layer before and after update of the salt concentration has taken place. The generated salt load is stored in *DGeneratedSaltLoad* Data Object.

5.2.5 Effect of total evaporation on subsurface TDS balance

Different studies have shown the presence of some chemical constituents in irrigation and rainwater. The loss of this water through evaporation from the soil and vegetation tend to increase salinity. Dissolved solids are added to agricultural land by way of irrigation and rainwater. However, neither surface evaporation nor absorption by plants appreciably reduces the amount of these salts added to the soil (Kay, 1986). Rather, the continuous upward movement of water from a subsurface system results in salt accumulation near the soil surface as water is lost by evaporation (Hoffman *et al.*, 1990). Thus *ACRUSalinity* also attempts to take into account the effect of total evaporation based on this concept. On each day of simulation, evaporation taking place both through the plant and from the soil surface is assumed to leave the salts behind, thereby resulting in an increased TDS concentration of the soil solution from which water is removed through this process. The removal of evaporated water from the soil is undertaken by the soil water budgeting modules of *ACRU*.

5.3 Determination of Surface Flow Salt Balance

The interactions between hydrological and geochemical processes are fundamental in determining the stream water chemistry of many catchments (Chen *et al.*, 2002). Hence, any process that affects runoff generation is likely to influence runoff salinity. As described in the following section, stormflow generation in *ACRU* and other functional models is often expressed by adaptation of the SCS equation. Similarly, baseflow release can be estimated by one dimensional Dupuit approximations (as used in DISA model), or as a product of groundwater store and baseflow response coefficient (as used in *ACRU* model). However, in most cases the salinity level of stormflow is assumed to be equal to rainfall or irrigation water salinity.

5.3.1 Stormflow generation mechanism in *ACRU*

In *ACRU* the term stormflow refers to the flow generated from a rainfall event. Thus the applied irrigation water does not contribute to stormflow generation. Part of the stormflow generated on non-irrigated lands leaves the land on the same day and hence is referred to as quickflow. Whereas, the remaining quantity is delayed for release on subsequent days and is called delayed stormflow.

5.3.1.1 Stormflow generation

The SCS equation is based on the principle that runoff potential is inversely related to the soil's relative wetness. The stormflow depth, Q (mm), is expressed as (Schulze *et al.*, 1992):

$$Q = \frac{(Pg - Ia)^2}{Pg - Ia + S} \qquad \text{for } Pg > Ia \tag{5.13}$$

where Pg = gross daily precipitation amount (mm)
Ia = initial abstractions (mm) before stormflow commences and
S = potential maximum retention of the soil (mm).

The initial abstraction, Ia consists mainly of interception, initial infiltration and depression storages. In the *ACRU* model (Schulze, 1995a), however, interception is abstracted separately

and before the commencement of potential runoff producing rainfall. Initial abstraction is computed as a product of a variable coefficient and potential maximum retention (soil moisture deficit), i.e. $Ia = cS$. The regression coefficient c is referred to as the coefficient of initial abstraction and it depends on vegetation, site and management characteristics. The default value of the coefficient in *ACRU* is 0.2. However, it can be increased for conditions immediately after ploughing when surface roughness is high, or under forested conditions and reduced under conditions of soil compaction or convective rainfall.

The potential maximum retention (S) is taken as the difference between the soil water content at porosity and that held by a soil column of user specified critical depth prior to a rainfall event. The critical depth is a threshold depth for which the soil water deficit is calculated for stormflow generation. In *ACRU* the critical soil depth may vary and is used to account for different dominant runoff producing mechanisms prevailing in different climates, rainfall intensities, vegetation conditions and for different soil properties, as shown by the following diagram.

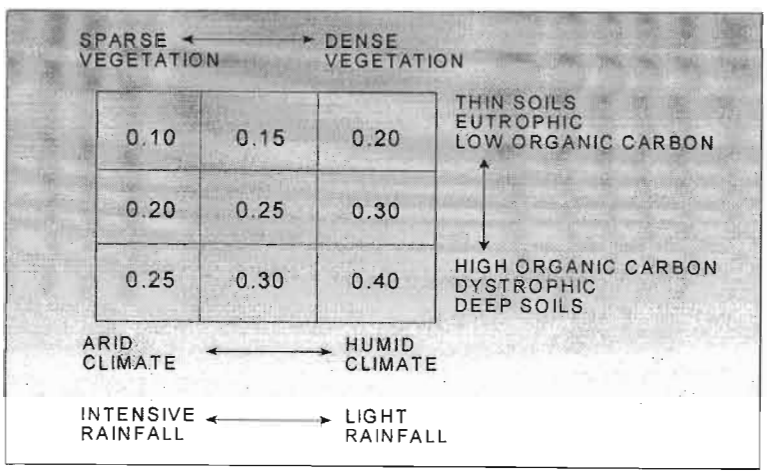

Figure 5.9 Suggested values of critical stormflow response soil depth (m) according to climatic, vegetation and soil characteristics (Schulze, 1995b)

5.3.1.2 The concept of delayed stormflow

In the *ACRU* model, the total stormflow generated from irrigated lands is assumed to leave the land on the same day. On the other hand, in non-irrigated areas a fraction of the generated flow is assumed to flow for subsequent days. According to Schulze (1995b), the generated total stormflow response from non-irrigated lands may be rapid or slow. Soils with a high

interflow potential would respond rapidly, as would small and/or steep and/or urbanised catchments when compared with relatively larger ones and/or catchments with gentle gradients or dense land cover, where infiltration is high and lateral flow occurs more slowly. For this reason a stormflow response coefficient is included in *ACRU* model, which controls the "lag" of the delayed (interflow) component of stormflow on the day of the event and determines what fraction of stormflow generated from an event is same-day runoff. In this document this is referred to as "actual quickflow". The remaining stormflow is "retained" to the next day, when again the fraction of the remaining is discharged into the stream, giving rise to an exponentially declining recession limb of a hydrograph. The sum of the "actual quickflow" and the fraction of the delayed stormflow discharged in a particular day is referred to in this document as quickflow. Furthermore, it is assumed in this research that the delayed stormflow does not include any interflow from subsurface components and thus it is having the same salinity level as the rain falling over the area.

5.3.2 Stormflow and quickflow salinity

The origin of dissolved solutes in surface water is assumed to be mainly from wet atmospheric deposition, i.e. the salt load associated with the rain falling on the area, and from the applied irrigation water. Salt input from these sources to the topsoil and its impact on the subsurface salt balance are described in Section 5.2.2. The present section describes the influence of salt input from these sources on the surface flow TDS balance in general, and on stormflow and quickflow salinity in particular.

The source of TDS in quickflow is expected to be both from rainfall and applied irrigation water as well as enrichment from the soil surface. However, because of the difficulty involved in estimating the quantity of solutes diffused to stormflow and as a result of the insignificant effect on stormflow TDS balance of such contributions, most models tend to ignore the diffused salt load contribution from the soil surface. According to Rhoades *et al.* (1997), prevalent "textbook" logic would lead to the conclusion that salt pickup via stormflow should be negligible because the "leaching edge" of the water that flows over the soil is thought to infiltrate into the soil and to "carry" the readily soluble salt with it. The salt in the soil is not expected to diffuse upwards significantly when the water is percolating downwards. With this prevalent view of the transport processes, one would not expect to find a significant increase in the salinity of stormflow compared to that of the applied water, other than that which might

be derived from the dissolution of suspended sediment gained through erosion. Mironenko and Pachepsky (1998) further suggest that ignoring vertical transport of the chemicals in surface water is obviously a viable approach for a thin water layer in rainfall-induced stormflow. Hence, the stormflow salinity is assumed to have the same value as the rainfall's average salt concentration on a site. However, quickflow salinity depends not only on the rainfall's salinity, but also on the salt concentration of delayed stormflow as well. The influence of delayed stormflow is described in the next section. The assumption that stormflow salinity is having the same TDS concentration as the rainfall average salinity may not hold true in areas characterised with significant salt crusts. In such areas the stormflow salinity may rise sharply with the rising limb of a hydrograph especially on the first flush of rainfall following a prolonged dry spell.

Determination of the salt balance and movement in stormflow generated from irrigated areas follows a similar approach to that from non-irrigated lands. However, in irrigated areas stormflow generated on a particular day is assumed to leave the area on the same day. Thus, unlike in non-irrigated lands, quickflow TDS concentration for irrigated lands is not influenced by TDS concentration of stormflow from previous days. In *ACRU2000,* stormflow generation from irrigated land is based on the assumption that it occurs only during a rainfall event and irrigation water *per se* does not make a direct contribution to stormflow generation. Therefore, in *ACRUSalinity* the stormflow generated on a particular day is assumed to have the same salinity as the average rainfall TDS concentration for the area. Salt concentration and salt load associated with the stormflow from irrigated lands is determined by the *PIrrigStormflowSalinity* Process.

5.3.3 The effect of delayed stormflow on TDS balance determination

The concept of delayed stormflow in *ACRU* complicates determination of TDS concentrations and salt loads associated with quickflow. Thus, to accommodate this concept an algorithm is included in *PStormflowSalinity*, where quickflow salinity is determined through simple mixing of the fraction of delayed stormflow and the fraction of generated stormflow leaving the area on the same day. Mathematically this is expressed as:

$$C_{qf} = \frac{(QF_a * C_{sf}) + (SF_d * C_{dsf})}{QF_a + SF_d} \qquad (5.14)$$

where C_{qf} = quickflow salinity (mg/l)

QF_a = actual quickflow, i.e. fraction of the stormflow leaving the land on the same day (l)

C_{sf} = stormflow salinity (C_{sf} = rainfall average salinity)(mg/l)

SF_d = fraction of delayed stormflow contributing to quickflow (l) and

C_{dsf} = salt concentration of delayed stormflow (mg/l).

Once the quickflow TDS concentration is determined, the salt load associated with quickflow is estimated by the following equation:

$$SL_{qf} = QF * C_{qf} \tag{5.15}$$

where SL_{qf} = salt load associated with the total quickflow volume for the day (mg) and

QF = total quickflow volume, i.e. $QF_a + SF_{cd}$ (l).

In *ACRU2000* a fraction of the stormflow delayed on a particular day is referred to as Carryover. The salt load associated with this Carryover is calculated based on the stormflow salinity and Carryover volume. The salt load associated with the Carryover is then added to the *DSurfaceSaltFluxRecord* Data Object to be released for subsequent days, in proportion to the discharged fraction of delayed stormflow volume.

As mentioned in Section 5.2.3.2, upward salt transport from the topsoil horizon to quickflow can take place when upward saturated flow occurs due to low drainage of the soil horizons and subsequent filling of topsoil pore spaces to their saturation. Thus, if on a particular day, a salt contribution occurs to quickflow due to upward flow, the salt concentration of quickflow is updated in the *PUpwardSaltTransport* and *PIrrigUpwardSaltTra* processes to account for the effect of this phenomenon.

5.3.4 Runoff salinity and salt load

The salt concentration and salt load of runoff water from non-irrigated lands is determined by the *PRunoffSalinity* Process. This process obtains the required data such as baseflow and

quickflow depths and their associated salinity from relevant data objects as shown in Figure 5.10. Once this process has received the required data, it determines runoff salinity through simple instantaneous baseflow and quickflow mixing using Equation 5.16. The associated salt load is then calculated using Equation 5.17. It stores runoff salinity and salt load in *DRunoffSalinity* and *DRunoffSaltLoad* data objects respectively for subsequent computations and for an output at the end of each day. Thus,

$$C_{run} = \frac{(BF * C_{bf}) + (QF * C_{qf})}{QF + BF} \tag{5.16}$$

$$SL_{run} = C_{run} * (BF + QF) \tag{5.17}$$

where C_{run} = salt concentration of runoff water (mg/l) and

SL_{run} = the salt load associated with runoff water (mg).

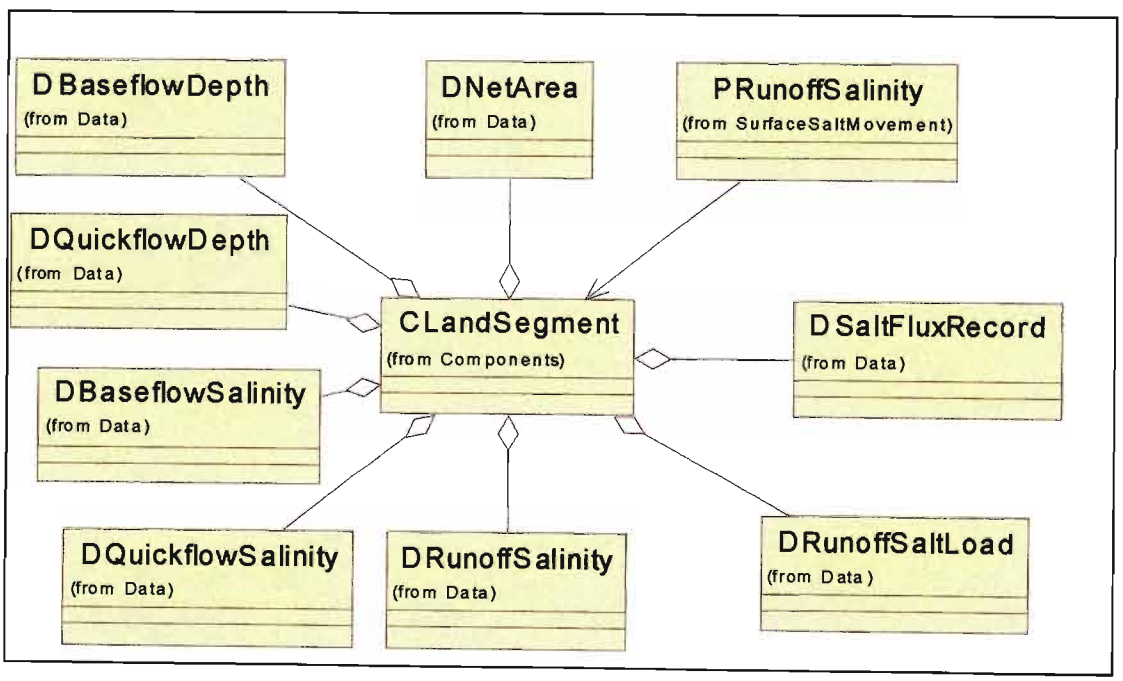

Figure 5.10 Class diagram of *PRunoffSalinity* Process and its associated component and data objects

Runoff salinity and the salt load from irrigated areas are determined in the *PIrrigRunoffSalinity* Process. This process generally follows a similar approach to the one

already described to compute salt concentration and salt load associated with runoff water in non-irrigated lands.

5.4 Salt Distribution to Reservoir and Channel Reaches

Salt load associated with runoff water from non-irrigated land, irrigated land and impervious areas is distributed to an appropriate destination component based on the direction of flow configured by the user for water quantity. Thus, the salt allocating processes distribute the stored salt load onto a particular component after they receive relevant information regarding the direction of water flow from the component object under consideration.

5.4.1 Runoff distribution in *ACRU*

The mass of salt load to be allocated to a particular outflow reach depends on the volume of runoff entering the reach and its salt concentration. Runoff volume in turn is a function of area of the contributing land. In the *ACRU* model a reservoir may be situated within or at the outlet of a sub-catchment. If it is located at the outlet of the sub-catchment, the entire sub-catchment area is assumed to contribute its flow to the dam. If, on the other hand, it is located within the sub-catchment, it functions as an internal dam and only a fraction of the sub-catchment area contributes to the dam. In the case of irrigated areas, the total flow from the land enters either the dam or the channel reach. In the case of non-irrigated lands and adjunct impervious areas only part of the total flow enters an internal dam while the remaining fraction enters the channel reach. Thus, to determine the volume of runoff contributing to a particular outflow reach, the net area (non-irrigated area) of a particular sub-catchment (land segment) is divided into an upper and lower net land segment area. In this case, the total net land segment area refers to the gross sub-catchment area excluding the dam, irrigated and impervious areas. The upper net land segment area refers to the fraction of net land segment area upstream of an internal dam, whereas, the lower net land segment area refers to that fraction of the total net land segment area downstream of an internal dam. In *ACRU2000* the upper and lower net land segment areas are calculated based on the following three possible sub-catchment configurations.

I. If no irrigated area exists in the sub-catchment

$$UNLSA\_1 = (A_{gls} - A_{adj} - A_{disj}) * f_{dam} - A_{dam} \quad (5.18)$$

$$LNLSA\_1 = (A_{gls} - A_{adj} - A_{disj}) * (1 - f_{dam}) \quad (5.19)$$

II. If an irrigated area exists in the sub-catchment and irrigation return flows enter the system downstream of an internal dam

$$UNLSA\_2 = UNLSA\_1$$
$$LNLSA\_2 = (A_{gls} - A_{adj} - A_{disj}) * (1 - f_{dam}) - A_{irrig} \quad (5.20)$$

III. If an irrigated area exists in the sub-catchment and irrigation return flows enter the system upstream of an internal dam

$$UNLSA\_3 = (A_{gls} - A_{adj} - A_{disj}) * f_{dam} - A_{dam} - A_{irrig} \quad (5.21)$$
$$LNLSA\_3 = LNLSA\_1$$

where
- A_{gls} = gross net land segment area (km^2)
- A_{dam} = dam area (ha)
- A_{irrig} = irrigated land area (ha)
- f_{dam} = fraction of the gross catchment area contributing its flow to the dam
- A_{adj} = adjunct impervious area (km^2) and
- A_{disj} = disjunct impervious area (km^2).

UNLSA_1, *UNLSA_2* and *UNLSA_3* refer to upper net land segment areas under the three different sub-catchment configurations in km^2, whereas, *LNLSA_1*, *LNLSA_2* and *LNLSA_3* refer to lower net land segment areas under the three different sub-catchment configurations in km^2.

The volume of runoff from non-irrigated areas entering an internal dam is expressed as the product of the upper net land segment area and the runoff depth from that area. The volume of runoff entering to the channel reach, in turn, is expressed as the product of the lower net land segment area and the runoff depth.

The preceding concepts for distribution of runoff water from non-irrigated and irrigated lands to the dam and/or channel reaches can be represented by a flow diagram as in Figure 5.11.

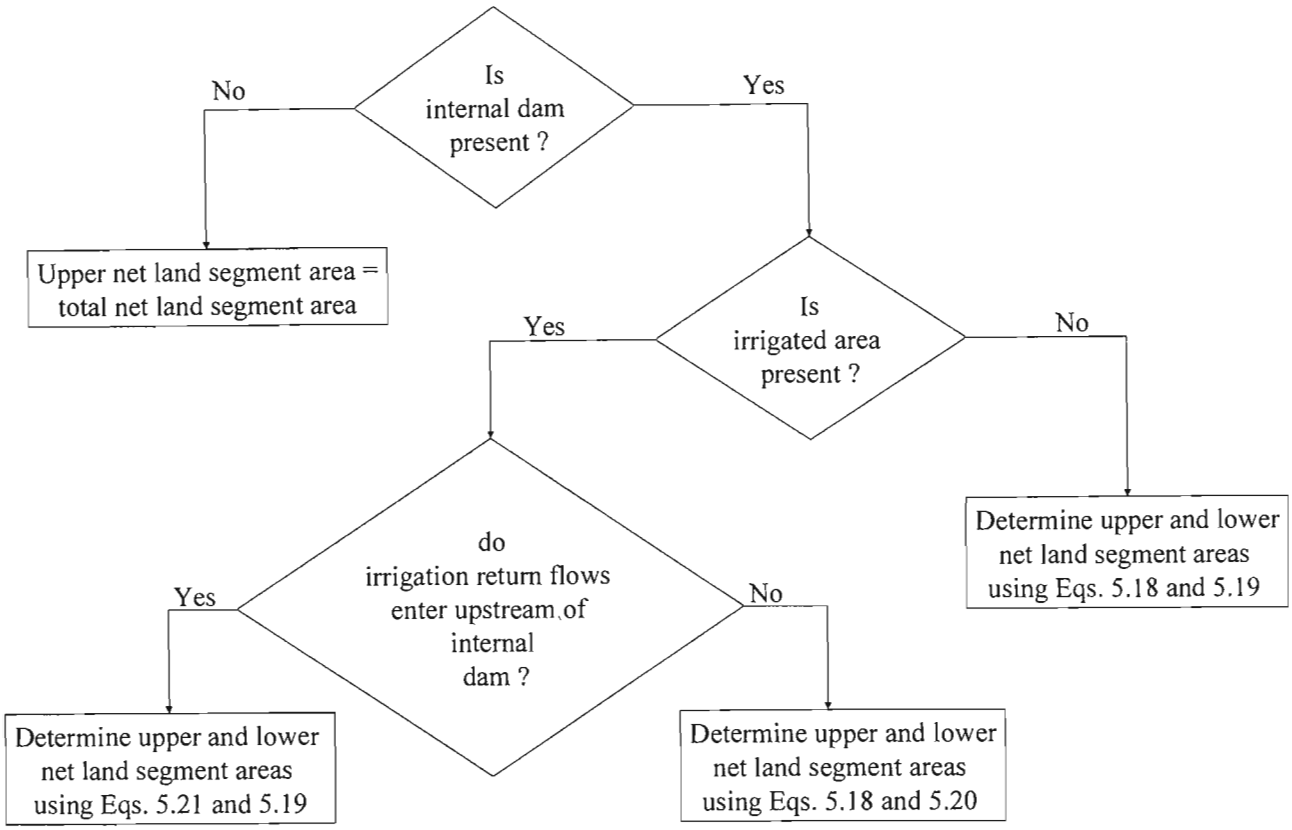

Figure 5.11 Flow diagram for determination of upper and lower net land segment areas

5.4.2 Salt distribution from non-irrigated lands

The process of salt distribution from non-irrigated areas to the appropriate outflow component is carried out by the *PLandSegSaltMovement* Process Object. This process distributes the runoff salt load from non-irrigated areas in a way similar for runoff distribution from these areas. In this process, runoff salt load ends up in a channel reach and/or in a reservoir. However, it assumes that only a single reservoir exists within a sub-catchment (land segment) to which a fraction of the runoff salt load is allocated. This process also assumes that the salt load from non-irrigated land is not distributed to more than one channel reaches. Hence, it considers only a single channel reach at a sub-catchment's outlet, where the remaining runoff salt load ends up. The *PLandSegSaltMovement* and its relationship with the various data and component objects are depicted in Figure 5.12.

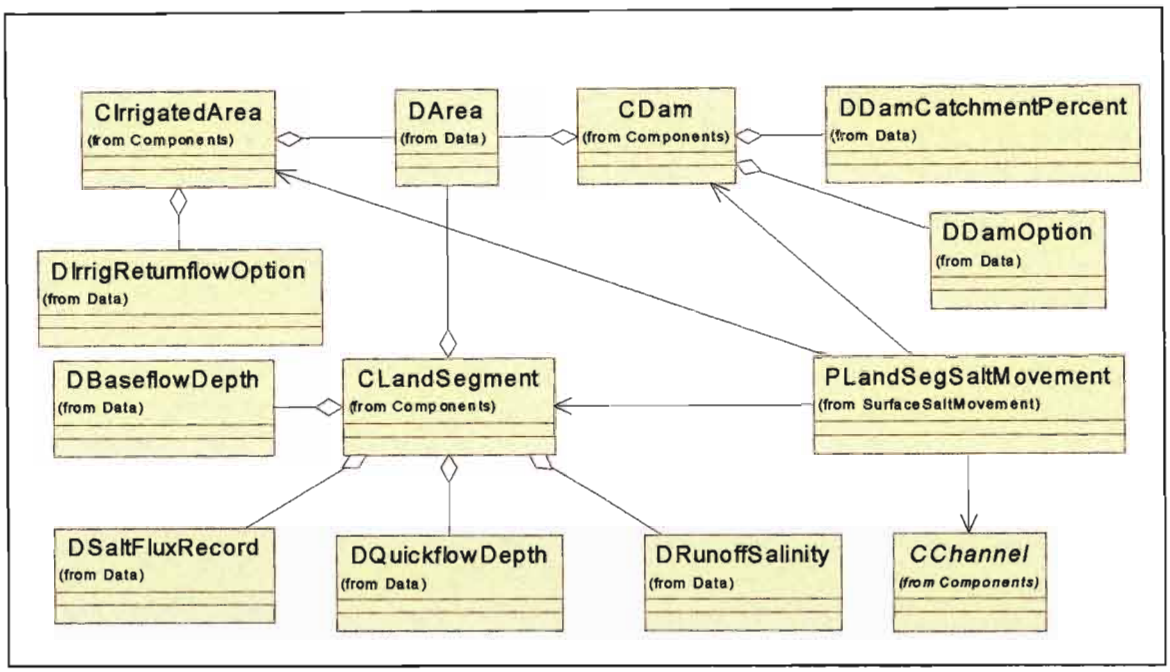

Figure 5.12 Class diagram of the *PLandSegmentSaltMovement* Process and associated component and data objects

Partitioning of the total non-irrigated area in a sub-catchment into that contributing its flow to the dam (upper net land segment area) and that contributing its flow to the channel reach (lower net land segment area) is carried out using a similar algorithm to that used for runoff distribution in hydrological process objects of *ACRU* (Section 5.4.1). After determination of the areas of non-irrigated land contributing to channel and dam reaches, the volume of runoff and its associated salt load entering the dam are calculated as follows:

$$RUN_{dam} = (BF + QF) * UNLSA\_i * 10^9 \tag{5.22}$$

$$SL_{dam} = RUN_{dam} * C_{run} \tag{5.23}$$

where RUN_{dam} = runoff volume entering to the dam (l)

$UNLSA\_i$ = upper net land segment area (km^2) under the i-th sub-catchment configuration and

SL_{dam} = salt load inflowing to the dam (mg).

The other variables have been defined in the previous sections, but BF and QF in this case represent baseflow and quickflow depths (m) respectively. Similarly, the remaining volume of

runoff and its salt load flowing into the channel reach are calculated using the following equations:

$$RUN_{chnl} = (BF + QF) * LNLSA\_i * 10^9 \quad (5.24)$$

$$SL_{chnl} = RUN_{chnl} * C_{run} \quad (5.25)$$

where RUN_{chnl} = runoff volume inflowing to the channel (l)

$LNLSA\_i$ = lower net land segment area (km^2) under the i-th sub-catchment configurations and

SL_{chnl} = salt load entering to the channel (mg).

The calculated masses of salt load flowing into the reservoir and/or channel reaches are then transported from the non-irrigated land to their respective destination components. However, if no dam exists in the sub-catchment or if the dam is situated at the sub-catchment's outlet, the total runoff generated from the sub-catchment flows into the channel reach. Hence, the salt load associated with this runoff is expressed as the product of the total runoff volume from non-irrigated lands and its salinity, as follows:

$$RUN = (BF + QF) * NLSA * 10^9 \quad (5.26)$$

$$SL = RUN * C_{run} \quad (5.27)$$

where RUN = the total runoff volume from non-irrigated land in a sub-catchment (l)

$NLSA$ = total area of the non-irrigated land in a sub-catchment (km^2) and

SL = total salt load associated with runoff from the non-irrigated land (mg).

Figure 5.13 shows the flow diagram of runoff salt load allocation from non-irrigated areas into a dam and/or channel reaches as represented in the *PLandSegSaltMovement* Process.

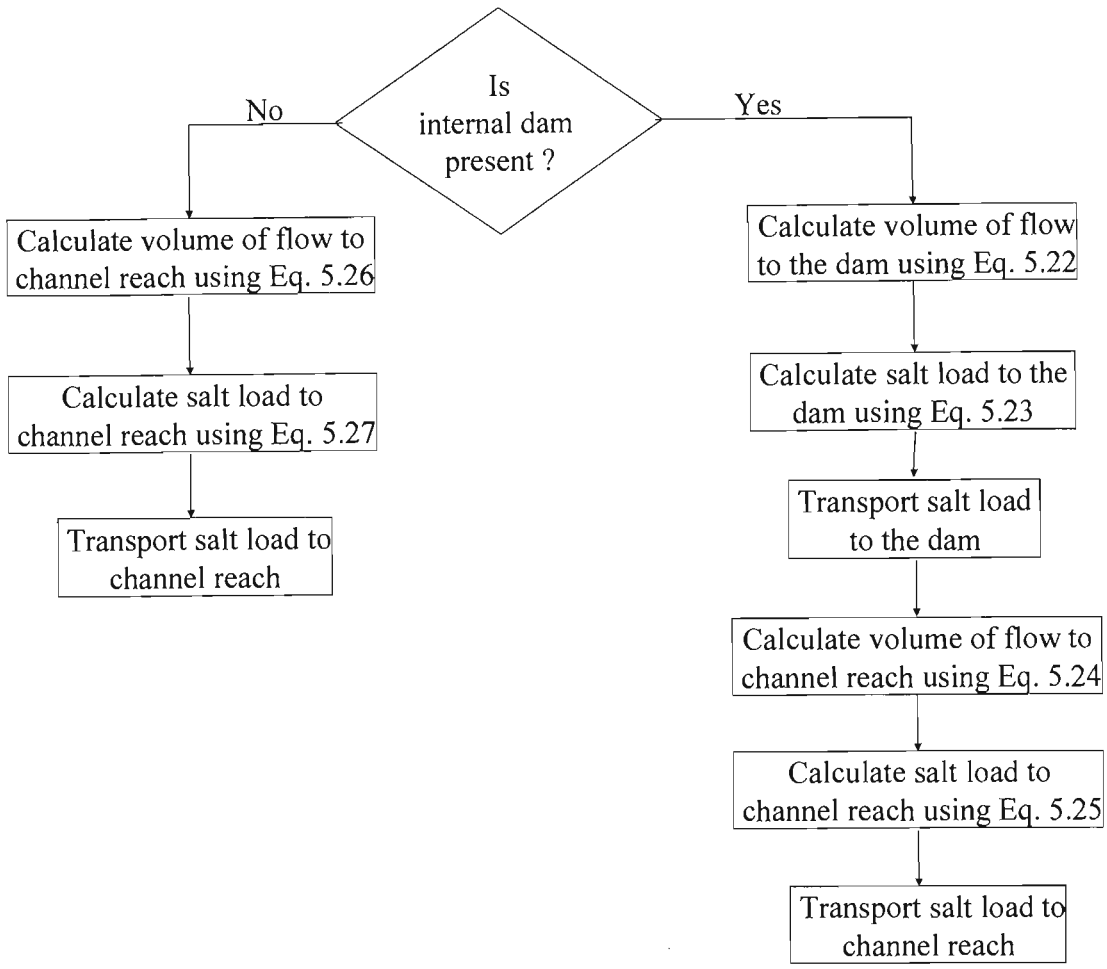

Figure 5.13 Flow diagram of runoff salt load allocation from non-irrigated areas

5.4.3 Salt distribution from irrigated lands

The process of salt distribution from irrigated lands is carried out by the *PIrrigatedAreasSaltMovement* Process. In this process, salt distribution follows the direction of runoff flow from the irrigated land. The allocation of runoff salt load from irrigated lands does not involve the partitioning of salt load to that flowing into the reservoir and channel reaches. Rather, it either ends up in a reservoir or in a channel reach, depending on the location of the irrigated land in relation to an internal dam. If the irrigated land is situated upstream of the dam, then the total salt load associated with runoff water from the irrigated land enters to the dam. If it is located downstream of an internal dam, the total salt load from the irrigated land enters to the channel reach. The *PIrrigatedAreasSaltMovement* and its relationship with the various data and component objects are shown in Figure 5.14.

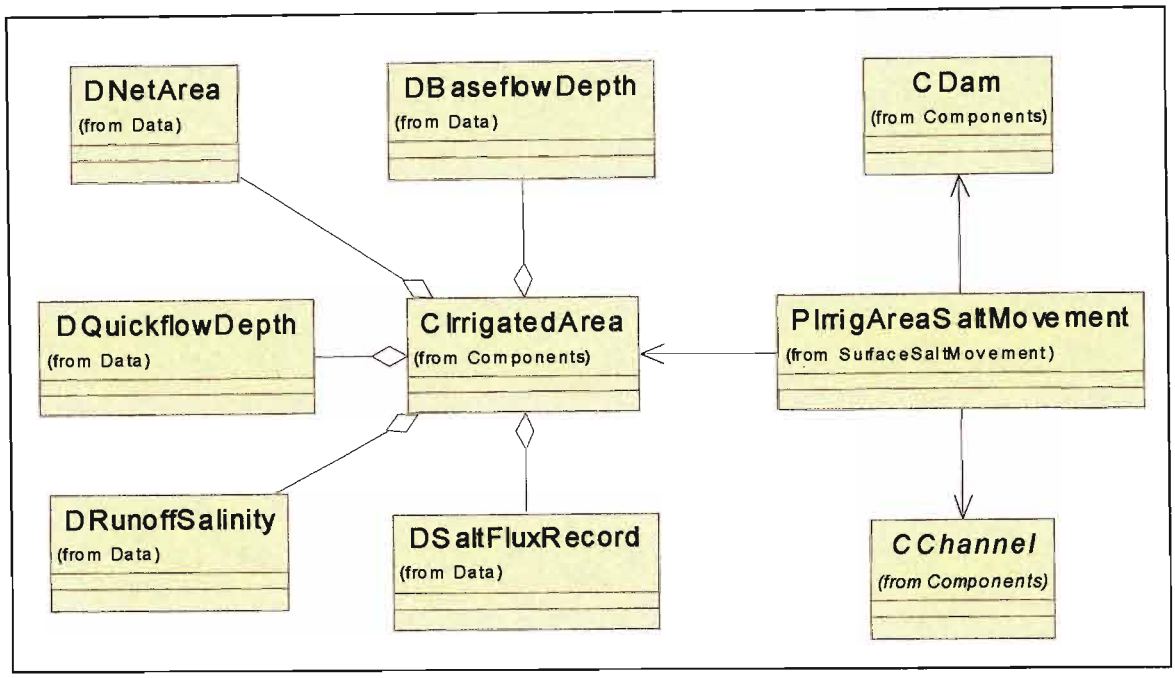

Figure 5.14 Class diagram of *PIrrigatedAreaSaltMovement* Process and associated data and component objects

5.4.4 Salt distribution from impervious areas

The increased need for applying the *ACRU* model to entirely urbanised catchments or to areas where the urban component is significant enough to influence runoff responses initiated the development of a routine that enables the model to simulate runoff from such areas (Schulze and Tarboton, 1995). This routine considers a number of urban land use categories such as business district, industrial and residential areas. These land use types vary according to their percentages of impervious areas to the total area. Since runoff salt load and concentration are directly influenced by runoff volume, the various urban land use categories and their hydrological responses are also likely to have an impact on hydrosalinity processes of these areas.

5.4.4.1 Hydrological responses of impervious areas as conceptualised in *ACRU* model

Impervious areas in the *ACRU* model are described as either adjunct or disjunct. Adjunct impervious areas are those parts of impervious areas adjunct, i.e. connected directly, to a water course, storm water drain or channel. Thus, runoff from adjunct impervious areas contribute directly to streamflow or the storm water system. On the other hand, disjunct

impervious areas represent those parts of the impervious area that are disconnected from the water course. Runoff from disjunct impervious areas initially flows into a pervious area and thereby contribute to the soil water budget and runoff response of that pervious area.

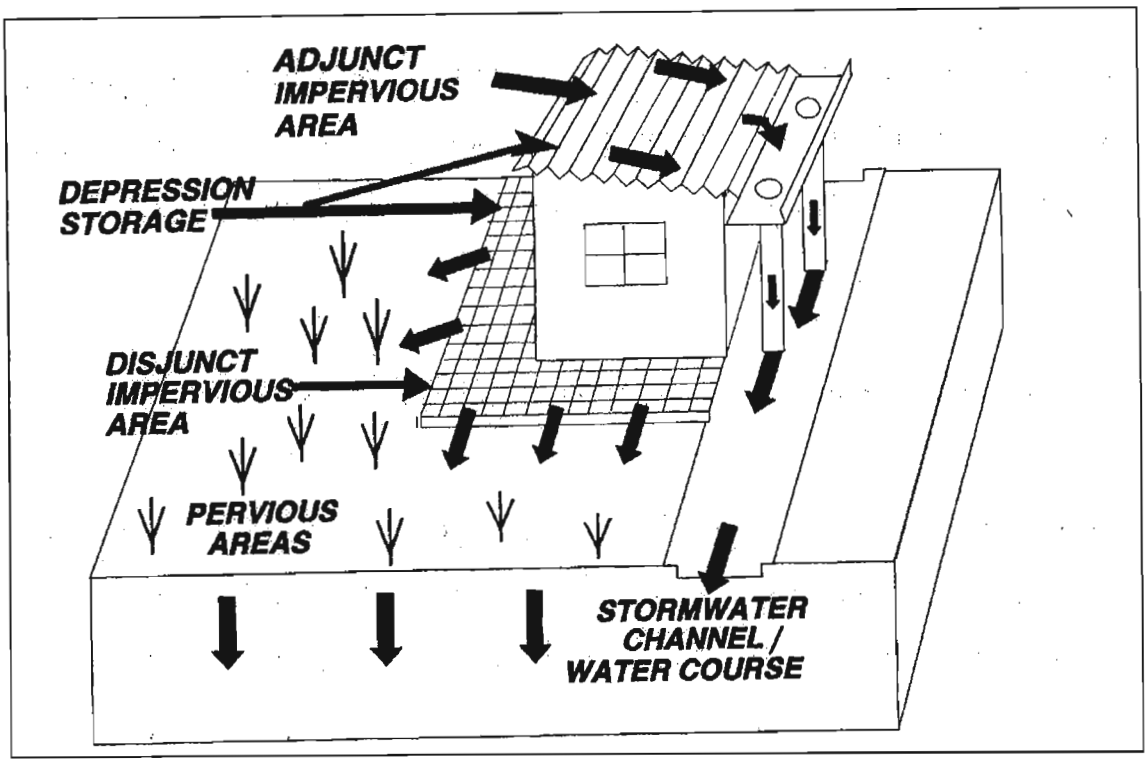

Figure 5.15 Runoff generation from impervious areas as conceptualised in *ACRU* model (Schulze and Tarboton, 1995)

5.4.4.2 Determination and allocation of runoff salt load from impervious areas

Determination of runoff salt loads from adjunct and disjunct impervious areas and their subsequent allocation to an appropriate destination reach is carried out in a single process object, using *PImperviousAreaSaltMovement*. Figure 5.16 shows a class diagram of this process and associated objects. As it can be seen from that figure, both adjunct and disjunct impervious areas are "types of" impervious area (*CImperviousArea*). Hence, it is possible and consistent to represent processes taking place in these areas in a single process object, as done for the runoff component. This process is responsible for distributing salt loads from an impervious area into a channel reach, in the case of adjunct impervious areas, or onto the surrounding non-irrigated area in the case of disjunct impervious areas. Once runoff depth is retrieved from the relevant data object, runoff volume from adjunct and disjunct impervious

areas is expressed by two distinct equations. If the impervious area under consideration is disjunct, runoff from such areas is calculated using Equation 5.28.

$$RUN_{dis} = RUN_{imp} * A_{dis} * 10^6 \qquad (5.28)$$

where RUN_{dis} = runoff volume from disjunct impervious area (l)

RUN_{imp} = depth of runoff from impervious area (mm) and

A_{dis} = disjunct impervious area (km^2).

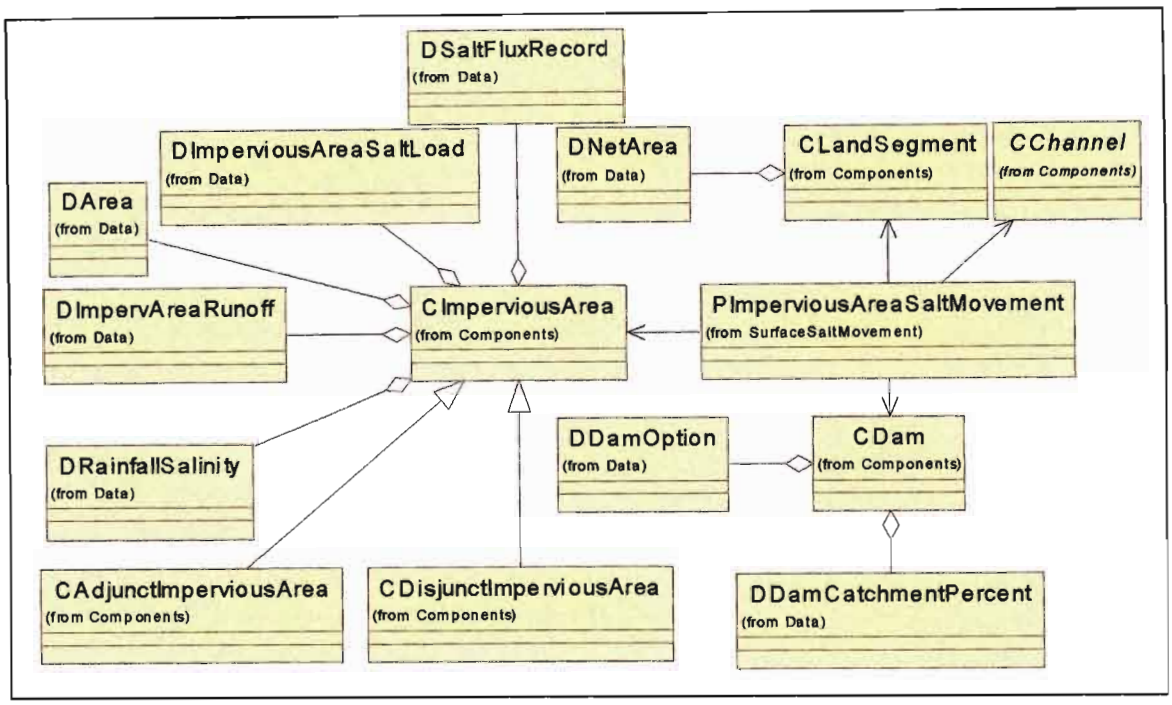

Figure 5.16 Class diagram of *PImperviousAreaSaltMovement* Process and associated objects

In impervious areas the only source of quickflow considered in *ACRU* is from rainfall i.e. there is no contribution from the topsoil as a result of saturated upward, and hence overland, flow. Some urban impervious areas may experience significant salt input due to dry atmospheric deposition with subsequent salt enrichment of the quickflow from such sources. However, due to the complications involved in programming, the present hydrosalinity module of *ACRU* does not account for this phenomenon. Thus, the salt concentration of quickflow from impervious areas is assumed to have the same TDS concentration as that of

the rain falling on the area. Similarly, runoff from impervious areas does not include any baseflow component in *ACRU*. Therefore, salt concentration of runoff water from impervious areas is assumed to have the same salinity as the quickflow from the area, which in turn has the same TDS concentration as the rain falling on that area. The salt load associated with runoff from disjunct impervious areas is calculated using Equation 5.29. The calculated salt load is then stored in *DImperviousAreaSaltLoad*.

$$SL_{dis} = RUN_{dis} * C_{run\_imp} \tag{5.29}$$

where SL_{dis} = salt load associated with runoff from disjunct impervious areas (mg) and

C_{run_imp} = salt concentration of runoff water from impervious areas (mg/l), with C_{run_imp} having the same value as the average TDS concentration of rainfall.

The effect of this salt load on surface and subsurface salt balance of the adjacent non-irrigated land is accounted indirectly in the *PStormflowSalinity* and *PSaltInput* processes. The daily stormflow in the hydrological modules of *ACRU* and hence the associated salt load in *ACRUSalinity*, are computed not only from the rain falling on the area for the day but also it includes the surface flow from disjunct impervious areas. Similarly, the daily infiltration to the topsoil of non-irrigated areas is partly comprised of the flow from adjunct impervious areas. Hence, the salt load associated with the infiltration water is partly comprised of the salt load from disjunct impervious areas. On the other hand, if the impervious area is an adjunct type, runoff volume is calculated as in Equation 30 by

$$RUN_{adj} = RUN_{imp} * A_{adj} * 10^6 \tag{5.30}$$

where RUN_{adj} = runoff volume from the adjunct impervious areas (l) and

A_{adj} = adjunct impervious area (km^2).

Furthermore, in the presence of an internal dam, the volume of runoff from adjunct impervious areas, and thus the total salt load, are partitioned into that entering the dam and channel reaches. In this case, the volume of runoff from adjunct impervious areas flowing into

the dam (RUN_{adj_dam}) is calculated as the product of the total runoff volume from the adjunct impervious area and the fraction of the land segment contributing to the dam (f_{dam}), as specified by the user. The remaining volume then enters the channel (RUN_{chnl}). The salt load flowing into the dam (SL_{adj_dam}) and channel (SL_{adj_chnl}) reaches are expressed using Equations 5.33 and 5.34.

$$RUN_{adj\_dam} = RUN_{adj} * f_{dam} \tag{5.31}$$

$$RUN_{adj\_chnl} = RUN_{adj} * (1 - f_{dam}) \tag{5.32}$$

$$SL_{adj\_dam} = RUN_{adj\_dam} * C_{run\_imp} \tag{5.33}$$

$$SL_{adj\_chnl} = RUN_{adj\_chnl} * C_{run\_imp} \tag{5.34}$$

The calculated salt load is then transported to its destination component (to the dam or channel reach). However, if no dam exists in the sub-catchment, the total runoff salt load from the adjunct impervious area is calculated using Equation 5.35 and is transported to the channel reach.

$$SL_{adj\_chnl} = RUN_{adj} * C_{run\_imp} \tag{5.35}$$

The preceding concepts of salt load determination and distribution from impervious areas are summarised in the following flow diagram.

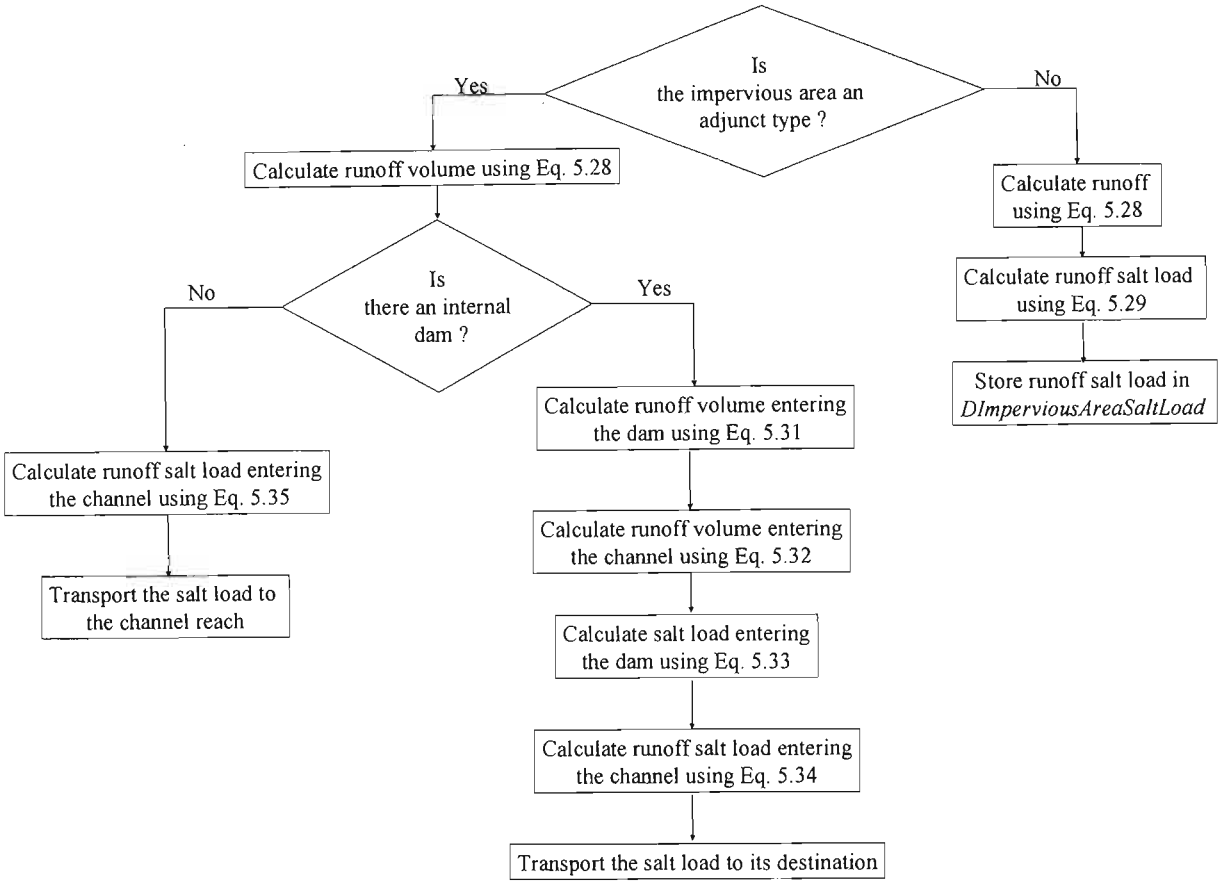

Figure 5.17 Flow diagram of salt load determination and distribution from impervious areas

5.5 Reservoir Salt Budget and Salt Routing

According to Bath *et al.* (1998), water quality models for reservoirs are developed for two main reasons. First, they can be used as research tools to establish an understanding of the complex interactions taking place between various processes. Secondly, these models are used as management and planning tools to provide necessary information for decisions on the abatement of water quality problems. These include short-term operational decisions to provide water quality and hydrological information and long term planning or design decisions where information is required on the influence of water resources developments and blending options.

Reservoir hydrosalinity models can be used to provide information on the governing processes and their influences on salt concentrations of reservoir storage and the various outflows. Such information is in turn frequently used to provide information on the design of

water treatment works and design operational and management guidelines for the reservoirs and its associated upstream areas. These include extracting useful information from model output that can be employed on timing of freshwater imports and downstream releases.

5.5.1 Reservoir water budgeting in *ACRU*

As accounted in the reservoir yield analysis section of the *ACRU* model (Schulze *et al.*, 1995d), the main components of reservoir water budget can be broadly classified as gains (inflows) and losses (outflows) from the system. Gains to the system include streamflows, inter-catchment transfers and precipitation onto the reservoir water surface. The loss component comprises evaporation from the water surface, legal water releases, seepage losses, overflows and irrigation as well as other abstractions. The various gains and losses from a reservoir system as conceptualised in *ACRU* model are shown in Figure 5.18.

5.5.1.1 Gains to the system

The following are gains to the reservoir system:

i. Streamflow: This is usually the major gain to the system and includes both stormflow and baseflow.
ii. Precipitation: This constitutes a second gain to the system. In *ACRU* all precipitation falling onto the entire surface area at full capacity is added. This is based on the assumption that when the reservoir is not at full storage, the adjacent dry parts are compacted and surface sealing has taken place. In some hydrosalinity models the salt contribution of precipitation is neglected, however, it can have significant effect particularly in areas where atmospheric deposition is dominant source of salt input.
iii. Inter-catchment transfers to the reservoir: This input to the reservoir is from outside the catchment which contributes streamflow. The present reservoir salt budget and salt routing routine of *ACRUSalinity*, however, does not account for inter-catchment salt load transfers.

5.5.1.2 Losses from the system

The following are losses from the reservoir system:

i. Abstractions from the reservoir: These include losses from the system and they include irrigation, domestic and other abstractions.
ii. Seepage losses: Daily seepage from earth-walled and unlined reservoirs may be estimated as equivalent to 0.0006 of the storage capacity (Schulze *et al.*, 1995d). This approximates that the reservoir empties about once in every five years as a result of seepage losses, disregarding any other losses or gains.
iii. Evaporation losses: Reservoir evaporation takes place from a large and usually relatively deeper water body, while the A-pan equivalent evaporation is subjected to local climatic and advective fluctuations. Therefore, in order to account for the varying relationship between a large water body and the A-pan, *ACRU* uses seasonally and regionally dependent month by month adjustment coefficients that are input by the user.
iv. Legal flow releases: This is a legal release of water from the reservoir for downstream riparian and other users.
v. Overflow: *ACRU* treats the temporal distribution of overflow in two ways. When the hydrograph routing option is not invoked, the reservoir water budget is calculated on a daily basis. In this case, the assumption is made that storage in excess of the maximum capacity spills from the reservoir on the same day. Thus, the maximum storage possible at the end of the day is equal to maximum capacity. If the hydrograph routing option is invoked, the upstream hydrograph, and the other gains to the system, are routed in sub-daily time steps through the reservoir using the storage indication method. Since this method accounts for storage above the full capacity level, for large dams the storage in the dam at the end of the day may be greater than the maximum reservoir capacity (Schulze *et al.*, 1995d). The current reservoir salt budget routine in *ACRUSalinity,* however, considers salt routing only at a daily time step and not at sub-daily ones.

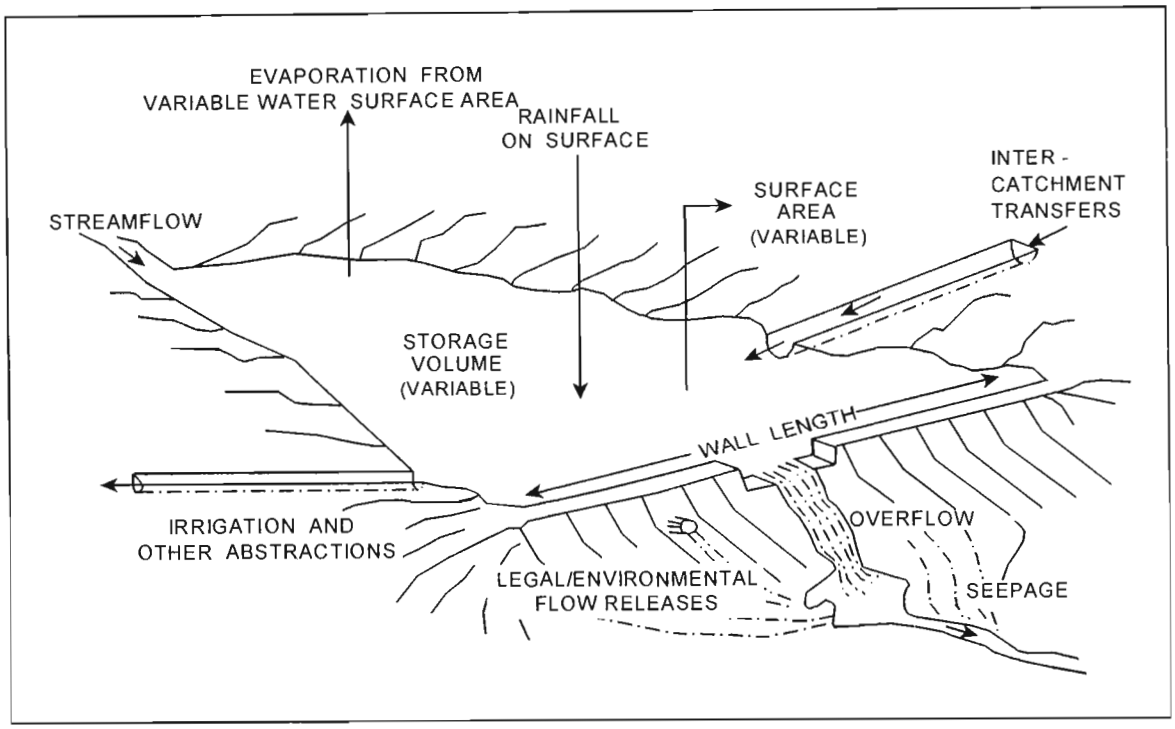

Figure 5.18 Reservoir water budget as conceptualised in *ACRU* model (Schulze and Smithers, 2002)

5.5.1.3 Surface area to storage relationship

Computations on the evaporation loss from a reservoir system and thereby its effect on salt concentration require knowledge of the surface area at various storage volumes of the reservoir. This can be estimated in *ACRU* with and without reservoir basin survey information (Schulze *et al.*, 1995d). The surface area to storage volume relationship, when the reservoir basin has been surveyed, is determined from the relationship that $A_s = a\ (Sv)^b$, where A_s stands for surface area of water (m^2) on a given day, Sv = storage (volume) of water (m^3) calculated from the previous day's final reservoir water budget, and "*a*" and "*b*" are the constant and the coefficient of the equation respectively, determined from the survey. According to Arnold *et al.* (1996), the coefficient "*b*" is a fairly constant parameter (0.9) and thus the constant "a" can be determined using maximum surface area and maximum storage of the reservoir. On the other hand, if no basin survey exists for the reservoir, *ACRU* computes the default surface area to storage relationship for different shapes of surface area from the reservoir wall length.

5.5.2 Determination of TDS concentration of reservoir storage and outflows

The reservoir salt budgeting computations are carried out by the *PReservoirComponSalinty* Process. This process operates in conjunction with the *PSaltStacking* Process to determine the reservoir's current storage salinity and salt load as well as TDS concentration of the various outflows from the reservoir system.

This process prepares the main data input requirements of the *PSaltStacking* Process. These include total volume of water flowing into the reservoir and its salinity, as well as total volume of water flowing out from the reservoir, excluding evaporation losses. The total volume of water flowing into the reservoir system, which comprises runoff from irrigated and non-irrigated lands, adjunct impervious areas as well as rain falling on the surface of a reservoir, is obtained from the daily total water influx record of the reservoir, as determined by the hydrological modules of *ACRU*. However, the salt load associated with the various inflow sources varies depending on the flow volume and salinity of each source. Hence, the required data for these flow components are also retrieved from the relevant individual data objects, as shown in Figure 5.19. As in the case of salt input to irrigated and non-irrigated lands, here again, a steady state rainfall salt concentration is assumed. The average TDS concentration of the total inflow from the various sources is then determined through instantaneous mixing of the different inflows using Equation 5.36. The salinity level of reservoir inflows is computed not only for use as a major input to the advection model, but also to help the user to anticipate the average salt concentration of reservoir inflows under different combinations of hydrological, climatic and catchment conditions, including upstream land use practices. Therefore, the average TDS concentration and salt load of the total reservoir inflow are stored in the *DResInflowSalinity* and *DInflowSaltLoad* data objects respectively for use in other computations and an output at the end of the day. Thus,

$$Cin_i = \frac{(RUN_{ni} * C_{run\_ni}) + (RUN_{irr} * C_{run\_irr}) + (RFL_{dam} * C_r) + (RUN_{adj\_dam} * C_{run\_adj})}{I_{dam}} \qquad (5.36)$$

where Cin_i = average salt concentration of water flowing into the dam (mg/l)

RUN_{ni} = runoff flowing into the dam from non-irrigated lands (l)

C_{run_ni} = Salt concentration of runoff from non-irrigated lands (mg/l)

RUN_{irr} = runoff from irrigated areas (l)

C_{run_irr} = salt concentration of runoff water from irrigated areas (mg/l)

RFL_{dam} = volume of rain falling on the dam surface (l)

C_r = rainfall salt concentration (mg/l)

RUN_{adj_dam} = runoff from adjunct impervious areas inflowing to the dam (l)

C_{run_adj} = salt concentration of runoff from adjunct impervious areas (mg/l) and

I_{dam} = total water inflow to the dam on the day including rain falling on surface of the dam (l).

The total outflow from the reservoir system that comprises legal flow releases (normal flow), abstractions from the reservoir, spillway overflow, seepage and evaporation from reservoir surface is obtained from the total outflux record of the reservoir, as determined by the hydrological processes of *ACRU*. This record includes evaporation from the reservoir surface. However, this process assumes that evaporation losses from the reservoir system have a salt concentrating effect by leaving the salts behind. Therefore, in order to accommodate this assumption, the total outflow from the reservoir which influences the salt load released from the system is reduced as described by the following equation:

$$Total\ outflow = total\ reservoir\ out\ flux\ record - reservoir\ evaporation \quad (5.37)$$

The TDS concentration at reservoir current storage is then computed in the *PSaltStacking* Process based on the information sent from this process on total inflow and outflow volumes, as well as the average salt concentration of the total inflow to the reservoir, as described by equation 5.36. One of the basic assumptions in the reservoir salt budget computations is a complete mixing of the reservoir at the end of each time step. Thus, no stratification in salt concentration is assumed to occur through out the depth of the reservoir. Hence, the outflow components that include legal flow releases, abstractions from the reservoir, spillway flow and seepage are assigned an average TDS concentration value as determined by the *PSaltStacking* Process. The corresponding salt load associated with the various outflow components is then calculated in this process as the product of the volume of water in the particular outflow component and the outflow salinity as determined by the *PSaltStacking* process. The *PReservoirComponSalinty* and its relationship with the various component, data and process objects is depicted in Figure 5.19.

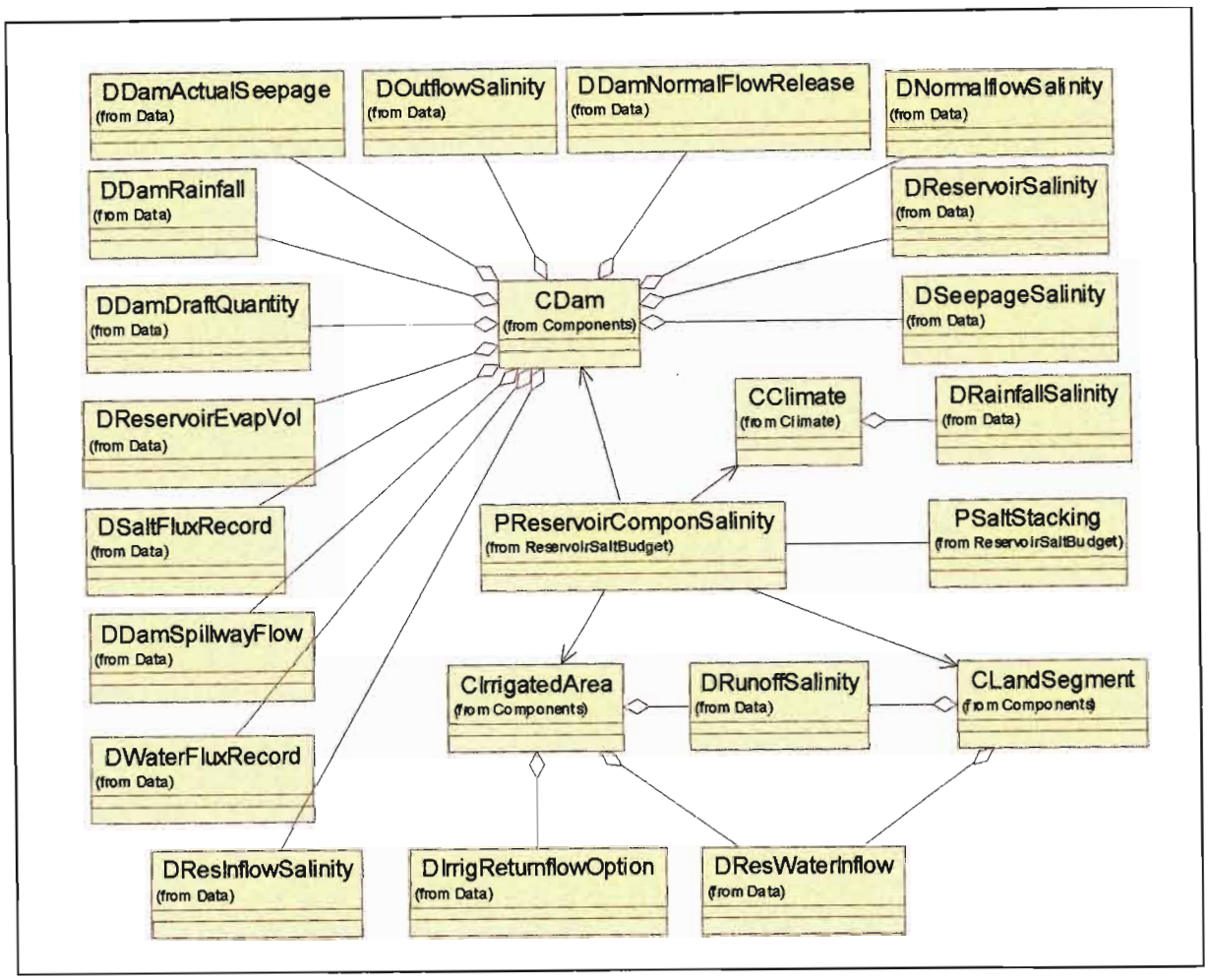

Figure 5.19 Class diagram of *PReservoirComponSalinity* Process and associated data and component objects

5.5.3 The *PSaltStacking* Process Object

Transport and mixing mechanisms of water and solutes in a stream or reservoir can be categorised as advective and dispersive. According to Michael (1997b), a stream that exhibits purely advective flow is said to undergo "plug-flow". Under ideal plug-flow, the length, shape and peak concentration of a dye tracer cloud will remain unchanged during transport downstream. On the other hand, dispersive transport moves solutes from areas of higher concentration to areas of lower concentration. Thus, with dispersive transport a dye tracer cloud will expand in length and reduce in peak concentration over time. This section describes reservoir storage salinity and salt concentration of an outflow from the dam based on the reservoir water budget and the two-cell plug-flow models.

The *PSaltStacking* Process Object in *ACRUSalinity* determines the average TDS concentration of the current storage and outflows from the reservoir. This process performs its computations when invoked by the *PReservoirComponSalinity* Process. It is thus not a stand-alone process. However, the main reasons for making this process take place in a separate class are to avoid complexity of the *PReservoirComponSalinity* and to facilitate re-use of the algorithm in the future for other processes that involve advective transport and mixing of salts. As mentioned in the previous section, this process obtains daily data on the volume of water inflowing to the dam and its salinity, as well as an outflow volume from the dam as determined by the *PReservoirComponSalinity* Process. Furthermore, this process also obtains other required data for reservoir storage salinity and outflow salinity computations from relevant data objects. The bi-directional association between the two process objects is shown in the UML diagram making up Figure 5.20.

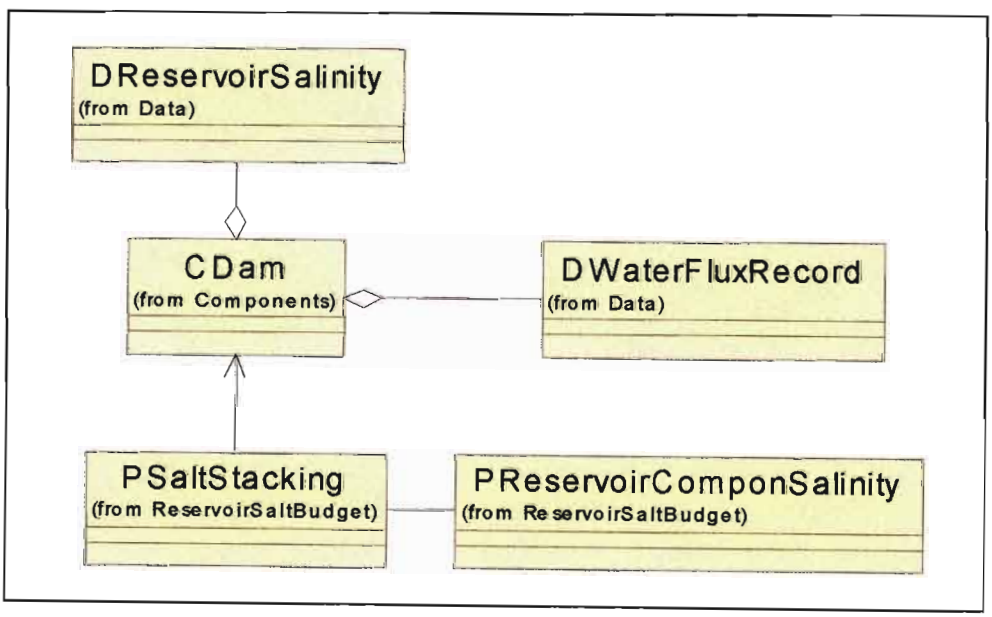

Figure 5.20 Class diagram of *PSaltStacking* Process and associated data and component objects

TDS concentration computations for the reservoir's current storage and outflows are accomplished using a simplified mixing and routing procedure as employed by Herold (1980). The method is based on the assumption that complete mixing occurs within the time step and advection is described by means of a two-cell plug-flow model. The first cell contains the mixed contents of the reservoir at the end of the previous day, while the second cell comprises all the inflows to the reservoir during the day being simulated. This process considers two

cases. The first arises when outflow of water from the dam is less than the storage at the end of previous time step (Figure 5.21 a). In that case, the salinity of water leaving the reservoir is set equal to reservoir salinity at the end of the previous day and the reservoir salinity at the end of the day is calculated as follows:

$$C_i = \frac{Qin_i * Cin_i + C_{i-1} * (S_{i-1} - Qout_i)}{S_i} \tag{5.38}$$

where C_i = reservoir salinity at the end of the current day of simulation (mg/l)

Qin_i = water inflow to the reservoir on the current day of simulation (l)

Cin_i = salt concentration of inflowing water on the current day of simulation (mg/l)

C_{i-1} = reservoir salinity at the end of the previous day (mg/l)

S_{i-1} = volume of water stored in the reservoir at the end of the previous day (l)

$Qout_i$ = water outflow from the reservoir for the current day of simulation (excluding evaporation loss) (l) and

S_i = volume of water stored in the reservoir at the current day of simulation (l).

The second case arises when outflow of water from the dam is greater or equal to the storage at the end of the previous day (Figure 5.21 b). In that case, the average TDS concentration of an outflow from the reservoir is described by Equation 5.39 and the reservoir salinity at the end of the day is calculated using Equation 5.40.

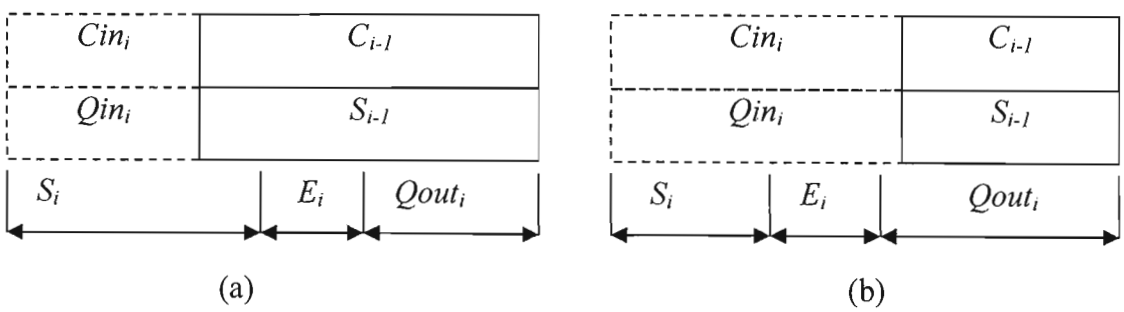

Figure 5.21 Plug-flow cells for the cases (a) when outflow is less than storage and (b) when outflow is greater or equal to storage (after Herold, 1980)

$$Cout_i = \frac{C_{i-1} * S_{i-1} + Cin_i * (Qout_i - S_{i-1})}{Qout_i} \tag{5.39}$$

$$C_i = \frac{Cin_i * (Qin_i - (Qout_i - S_{i-1}))}{S_i} \quad (5.40)$$

This process generally assumes that evaporation losses take place at the end of the day. It is also based on the assumption that evaporation losses from the reservoir surface tend to concentrate the salts in the reservoir by leaving the salts behind. The basic steps followed by this process are shown in the following flow diagram.

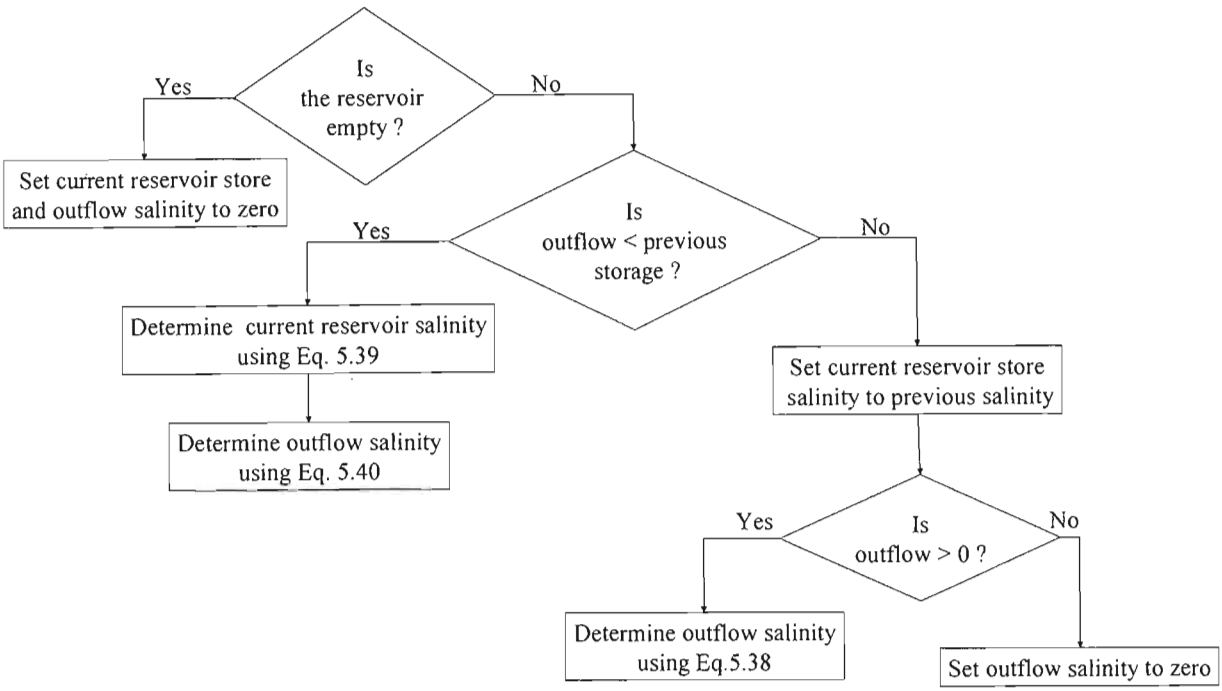

Figure 5.22 Flow diagram of the *PSaltStacking* Process

5.6 Channel Salt Movement and Distributed Hydrosalinity Modelling

As mentioned in Section 5.1.3, *ACRU2000* is structured in a way that, on each day of simulation, all processes taking place in *CReach* type (for example, in channel reaches) are executed only after processes for the land segment have been executed, starting from the edge towards an exit of the simulated catchment. Processes for each *CReach* type in turn are executed starting with reaches on the edge of the flow network and moving progressively downstream. Thus, salt balance computations for a channel reach of a particular sub-catchment are also carried out after all other *ACRUSalinity* processes operating in the sub-catchment have been executed.

The *PCatchmentSalinity* Process determines the salt load and concentration of the water flowing out of a particular channel reach. The salt load from the different sources in a sub-catchment such as irrigated and non-irrigated lands, reservoirs as well as impervious areas, entering the channel reach is determined and transported to the channel reach in relevant process classes. This process then determines the total salt load stored at the channel reach at the end of the day and the streamflow salinity as calculated in the reach. The average TDS concentration of streamflow at the channel reach is determined by using Equation 5.41:

$$C_{chnl} = \frac{SL_{inf\_t}}{STFL} \tag{5.41}$$

where C_{chnl} = TDS concentration of flow at the channel reach (mg/l)
SL_{inf_t} = daily total salt load stored in the channel reach (mg) and
$STFL$ = volume of streamflow at the channel reach (l).

In the case of distributed hydrosalinity modelling, where more than one sub-catchment is considered, the channel reach in a sub-catchment receives salt load not only from sources within the sub-catchment, but also from upstream sub-catchments. Therefore, in the case of distributed hydrosalinity modelling, the salt load stored in a particular channel reach is transported as salt influx to a downstream reach. The *PCatchmentSalinity* Process carries out the transport of salt load in the channel reach to a downstream channel or reservoir reaches. The *PReservoirComponSalinity* Process also performs a similar function if a particular reservoir is situated at sub-catchment outlet and a downstream reach exists in the catchment being simulated. In this case the total salt load associated with overflow, seepage and legal flow release from the reservoir is computed using Equation 5.42 and is transported to an appropriate downstream reach.

$$SL_{dam\_of} = (OF_{dam} * C_{of}) + (SEEP_{dam} * C_{seep}) + (NF_{dam} + C_{nf}) \tag{5.42}$$

where SL_{dam_of} = total salt load released from the dam to downstream reaches (mg)
OF_{dam} = overflow volume (l)
C_{of} = salt concentration of overflow (mg/l)
$SEEP_{dam}$ = volume of seepage water from the dam (l)
C_{seep} = salt concentration of seepage water (mg/l)

NF_{dam} = legal (normal) flow release volume (l) and

C_{nf} = salt concentration of legal flow (mg/l).

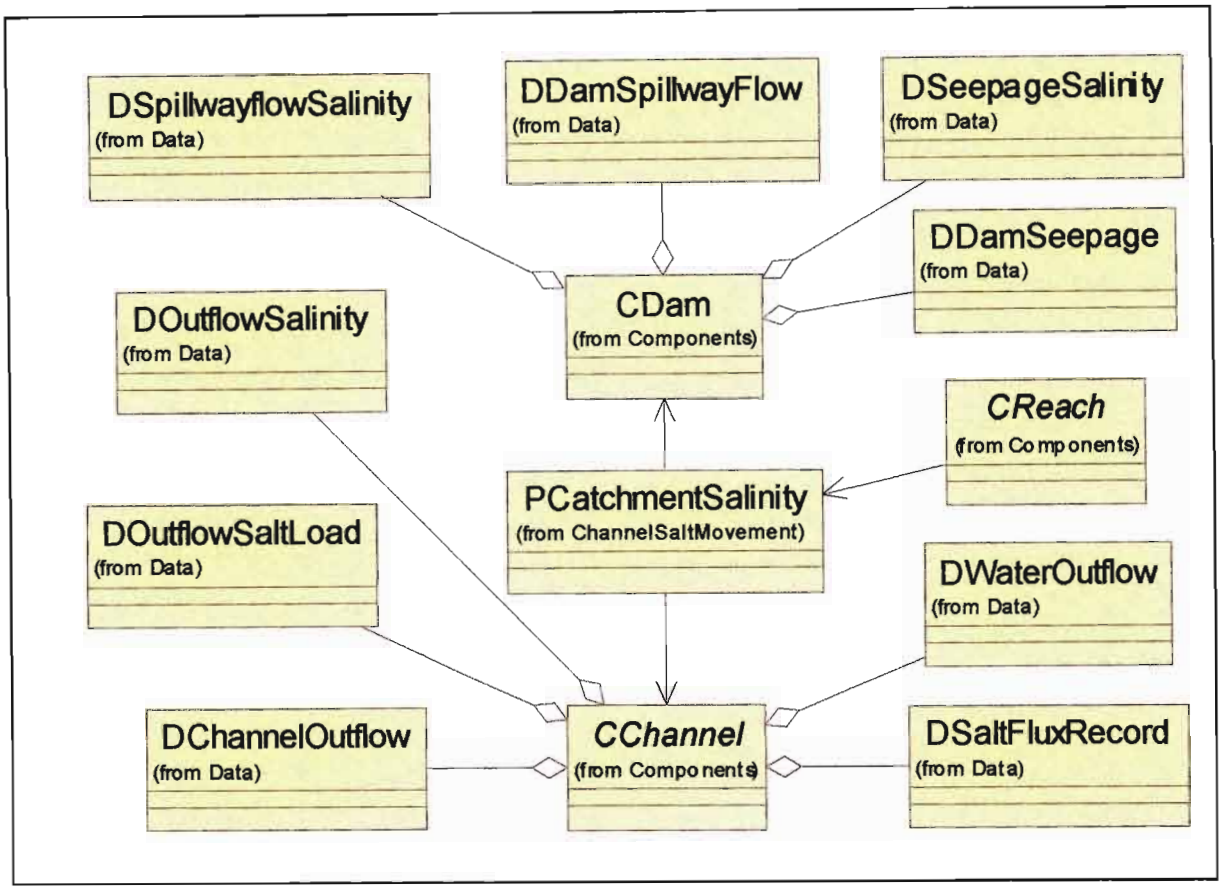

Figure 5.23 Class diagram of *PCatchmentSalinity* and associated component and data objects

To sum up, one of the basic assumptions in *ACRUSalinity* is that solutes are transported along with the moving water and in the direction of water flow (advection). Therefore, salt load transport in subsurface components, i.e. from rainfall salt input through soil horizons to the groundwater store and runoff, as well as the allocation of this runoff salt load to various destination components within a sub-catchment and to downstream reaches follows the direction of water flow as specified by the user and / or as determined by the hydrological modules of *ACRU2000*.

This chapter has reviewed the development of the hydrosalinity module of *ACRU* with special emphasis on how the various hydrosalinity processes are represented in the module. Following the development of *ACRUSalinity*, a verification study was carried out to see how

the new module performed under catchment conditions. This phase involved two main steps. The first step was code validation and the second step was comparison of module outputs against observed data. The validation and verification procedures, and subsequent sensitivity analysis of the major inputs to the module as well as a case study that shows some potential applications of the module for planning, design and management of water resource developments will be the subjects of discussion of the next two chapters.

6. VALIDATION AND VERIFICATION

Development of the hydrosalinity module of *ACRU, viz. ACRUSalinity* is followed by validation and verification of output from the module to see how it performs under field conditions. The validation process involved code validation followed by verification of simulated results through comparison against observed data from the Upper Mkomazi Catchment in KwaZulu-Natal province, South Africa.

Scientists and decision makers need assurances that the model they apply is valid. According to McLaughlin (1988), from a technical or scientific point of view a model is validated when it properly describes the physical processes. From a regulatory point of view, however, it is validated when the model yields adequate predictions with the main goal being to reduce the risk of making inappropriate decisions from the model results. Loague *et al.* (1998) suggest that a model is a good representation of reality, and hence valid, if it can be used to predict certain observable phenomena within acceptable accuracy and precision. However, according to Herald (1999), there is no defined procedure or technique that is widely accepted to do this. Furthermore, the level of acceptable inaccuracy will vary with applications. Hence, one model may be valid for a situation requiring general trends and qualitative information, such as irrigation management and educational purposes, but invalid for pure scientific research.

The approach employed to validate the hydrosalinity module of *ACRU* involved salt balance computations for different components with the help of a spreadsheet. This was done to validate the algorithms underlying the various hydrosalinity processes in terms of mass conservation. This step is not intended for generating outputs to be used for comparison against the observed data. Therefore, some of the salinity related inputs to the model were hypothetical values. The approach to verify the model's output involved use of hydrological and salinity related data specific to the Upper Mkomazi Catchment and the model outputs are graphically and analysed statistically for comparison against observed data. This chapter therefore presents the following:

- A general description of the Upper Mkomazi Catchment
- Code validation of the *ACRUSalinity* module and

- Verification through comparison of model output against observed streamflow salinity data.

6.1 Description of the Upper Mkomazi Catchment

The Upper Mkomazi Catchment constitutes the upstream part of the Mkomazi Catchment draining to the U1H005 weir (flow gauge). The Mkomazi Catchment is located in KwaZulu-Natal province in South Africa. The Upper Mkomazi Catchment is used during the evaluation phase of the hydrosalinity module of *ACRU* which is developed in this project. Although, salinity is not a threat to this catchment, some of the criteria considered when selecting the catchment are:

- The entire catchment was previously configured for *ACRU 300* version of the *ACRU* model (Taylor, 2001) and
- In comparison with many of the other catchments that are configured for the *ACRU* model (including the Lower Mkomazi Catchment), this catchment has good streamflow TDS concentration data.

What follows is a general description of the Upper Mkomazi Catchment. Detailed information about the catchment can be obtained from reports of other studies undertaken for the area, e.g. Dickens (1998), IWR (1998) and Taylor (2001).

6.1.1 Climatological and hydrological conditions

Climatically the Mkomazi Catchment is classified as a humid zone (IWR, 1998). Rainfall distribution is reasonably consistent throughout the catchment, ranging from nearly 1300 mm per annum (p.a) at the headwaters to 1000 mm p.a in the middle and 900 mm p.a in the lower reaches of the catchment. The Mean Annual Precipitation (MAP) for the entire catchment is 981mm. However, the MAP is higher in the upstream parts of the catchment (1000-1287 mm) and correspondingly most of the runoff is generated upstream (IWR, 1998). The mean monthly A-pan equivalent evaporation ranges from a minimum value of 59 mm for June to a maximum of 150 mm for December (Schulze, 1997).

The Mkomazi River flows from the foothills of the Drakensberg Mountains towards the east. Two streamflow gauges with flow records dating from early 1960s exist along the river. The first, U1H005 commands the upstream part of the catchment (1744 km^2) and the second, U1H006 is close to the estuary (4349 km^2) and records flow from the entire catchment. The historical records for the upstream gauge (Figures 6.1, 6.2) have few gaps due to missing data. The downstream gauge, however, has unreliable high flow measurements (IWR, 1998).

Figure 6.1 The U1H005 gauging weir at Camden

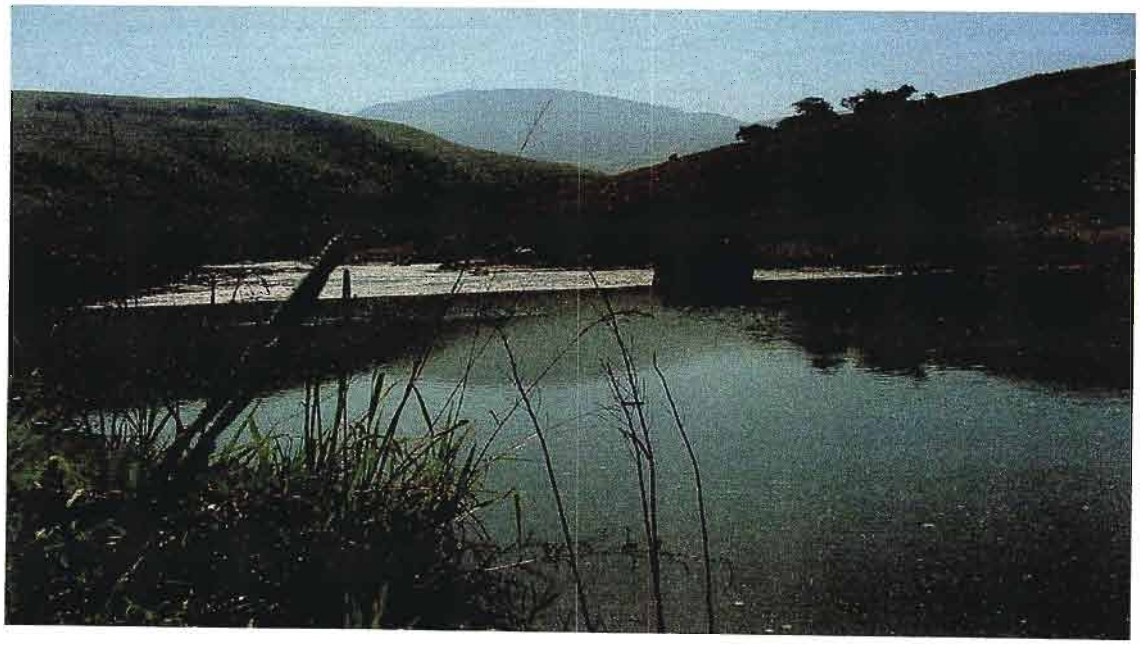

Figure 6.2 Mkomazi River from upstream of the U1H005 gauging weir

6.1.2 Physiography

The great Escarpment around Sani Pass forms the headwaters of the Mkomazi, which exits into the Indian Ocean at Umkomaas (IWR, 1998). Table 6.1 provides some sub-catchment physiographic information of the Upper Mkomazi Catchment. The catchment's altitude ranges from 2165 m in the north western part of the catchment (sub-catchment 5) to 1339 m in the south eastern part of the catchment (sub-catchment 14).

Table 6.1 Sub-catchment physiographic information of the Upper Mkomazi Catchment (after Taylor, 2001)

Sub-catchment No	Longitude (degree, decimal)	Latitude (degree, decimal)	Area (km^2)	Mean Altitude (m)
1	29.38	29.51	162.91	2124
2	29.39	29.59	63.32	1959
3	29.54	29.58	141.69	1533
4	29.64	29.61	29.22	1373
5	29.49	29.41	142.97	2165
6	29.46	29.47	57.76	2088
7	29.60	29.50	208.01	1639
8	29.71	29.59	47.09	1410
9	29.71	29.49	189.23	1851
10	29.79	29.56	77.44	1643
11	29.38	29.62	93.12	2104
12	29.60	29.71	32.87	1685
13	29.60	29.69	148.15	1568
14	29.79	29.64	29.97	1339
15	29.90	29.60	18.87	1680
16	29.84	29.64	70.94	1492
17	29.71	29.72	69.99	1678
18	29.81	29.72	158.55	1310

6.1.3 Land use and land cover

Under natural conditions, the upper catchment vegetation would be dominated by pure grassveld and temperate and transitional forest and scrub, with false grassveld and coastal tropical forest dominating the middle and lower catchment (IWR, 1998). However, a survey conducted by Edward (1998) has shown that the Mkomazi Catchment is a highly modified one due to excessive levels of utilisation. As a consequence of this disturbance, the river system has been heavily infested with alien plant species and the diversity of the riparian

vegetation has been drastically reduced. The riparian zone is characterised by considerable infestation of wattle which has resulted in a loss of the local riparian species. This phenomenon was noticed during the field visits undertaken by Taylor in 2001 and by the author in 2003. Only a few remnants of the riparian vegetation remain. The large number and diversity of pioneer species indicates high levels of disturbance (Edward, 1998).

The present land use from satellite imagery in 1996, which was used previously as input to the *ACRU* model for hydrological simulation of the Mkomazi Catchement, includes a number of land use categories (Taylor, 2001). Land use classes of the Upper Mkomazi Catchment are shown in Figure 6.3. As it can be seen from the figure, the Upper Mkomazi Catchment is mainly dominated by unimproved grassland but with a significant proportion of the area being degraded due to overgrazing coupled with the steep gradient of the landscape. Forest plantations and subsistence dryland agriculture are other land uses in the catchment. Human activity along the river varies from low in the upper reaches, to diverse agriculture in the middle to lower reaches.

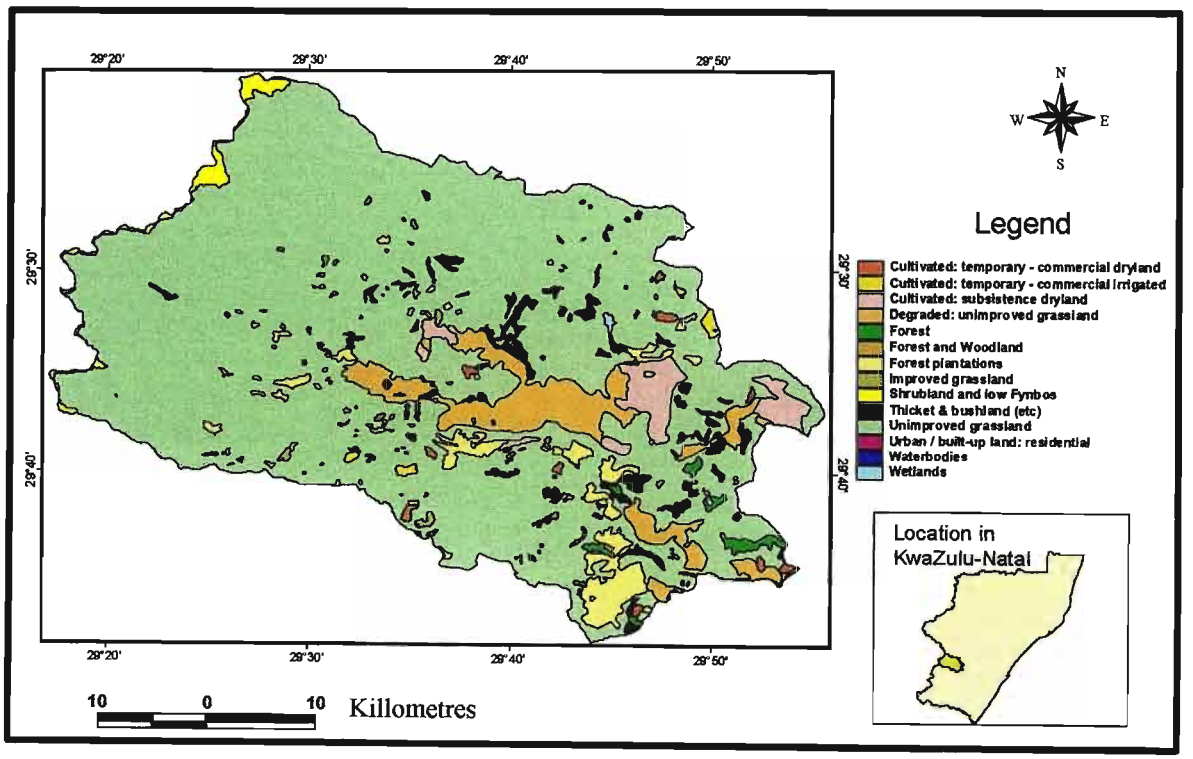

Figure 6.3 Land use classes of the Upper Mkomazi Catchment (after Taylor, 2001)

6.1.4 Geological formations

The Upper Mkomazi contains a wide range of geological formations from igneous rocks in its upper reaches to sedimentary rocks in its middle and lower reaches. The upper part of the catchment is dominated with Basalts and Arenites. Mudstones occupy most of the middle and lower part of the catchment's geology. Dolerite also characterises the middle lower part of the catchment's geology. According to Rowntree and Dollar (1998), the faulted terrain feature of the catchment signifies structural control of the channel and the effect of basement geology can be noticed from the general relief. The upper catchment has steep relief, while the middle and lower-middle catchment can be classified as undulating. Steep relief in the lower part of the catchment is a function of the undulating lithology. The lithology produces clay to clay loam soils (Rowntree and Dollar, 1998). Figure 6.4 shows major geological formations in the Upper Mkomazi Catchment.

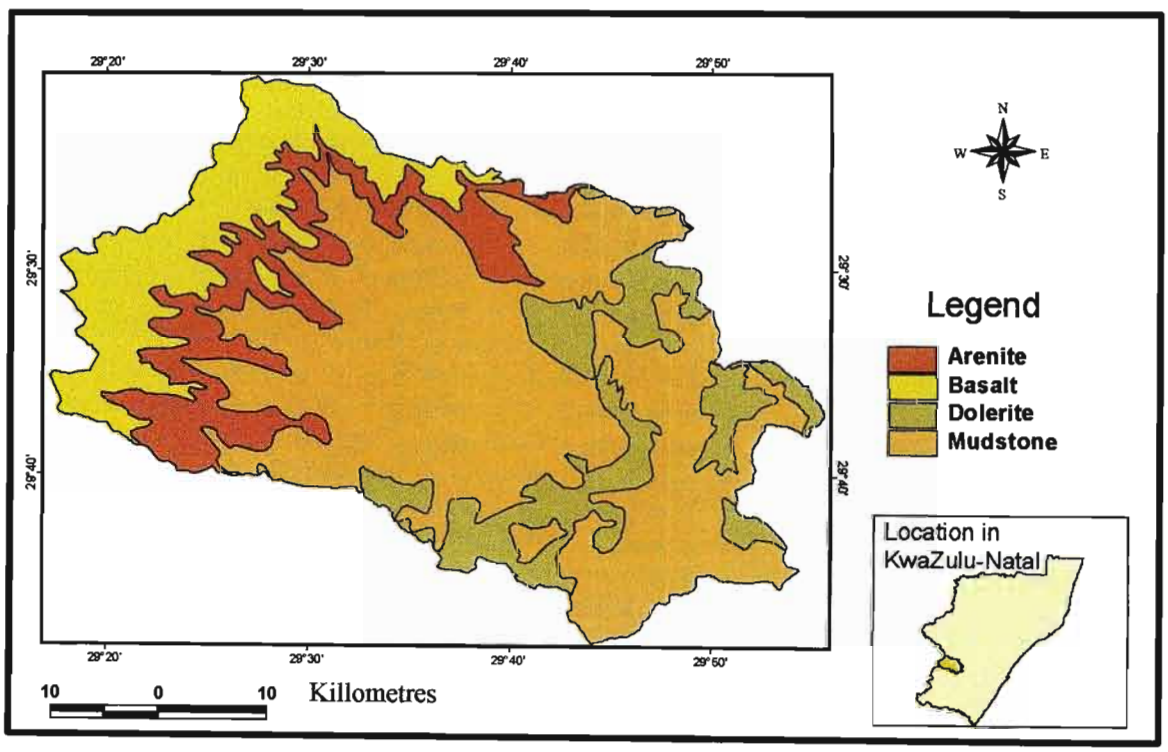

Figure 6.4 Major geological formations of the Upper Mkomazi Catchment (after Council for Geoscience, 1999)

6.1.5 Salinity in the catchment

The current levels of salinity in the Upper Mkomazi Catchment are not a threat for most uses of the water in the catchment. However, the increased TDS concentration of water flowing at the catchment outlet compared to rainfall TDS concentration in the catchment implies that both natural and anthropogenic factors are causing an impact that generally results in the differences in TDS concentration between the rainfall and outflowing water.

The natural and human-induced salinity in the catchment result from point and non-point sources. The natural sources of salinity in the catchment generally originate from the weathering and dissolution of underlying rocks or soils overlying the rocks. Although, when compared to the lower parts of the Mkomazi Catchment, the Upper Mkomazi Catchment is influenced less by human activities, agricultural land use still constitutes a substantial part of the catchment. Agricultural practices in the catchment may result in increased salt concentrations and salt loading in draining streams. Total evaporation from crops result in concentrating dissolved solids in the remaining return flows. Irrigation practices also increase the flow through soils, which is expected to increase the total salt loading from previous natural salt loading levels.

DWAF salinity data from 1985 to 1995 that included EC values for weirs U1H005 and U1H006 have been assessed to identify seasonal fluctuations and any general long term trend. The results are shown in Figure 6.5. The EC values do not show significant increases with time at either weir. Seasonal fluctuations in EC, however, are evident at both stations, mainly as a result of seasonal changes in natural processes. During the rainy season, TDS concentrations drop due to the dilution effect of rain falling on the area, whereas during the dry season salt concentration starts to increase due to the "evapoconcentration" processes. The comparison of EC values between U1H005 and U1H006 weirs has shown that TDS concentrations increase downstream in the catchment. This can be attributed to the re-use of water as it flows downstream and due to the increased human influences in the lower parts of the catchment.

In general, this assessment of historical EC data between the period of 1985 to 1995 for both the upper and lower sampling sites (U1H005 and U1H006 respectively) did not show any significant increases with time. However, the seasonal fluctuations in EC values observed in

both stations are in response to changes with time of natural and/or anthropogenic factors influencing the hydrosalinity processes. Hence, any activity that facilitates these processes would possibly increase the currently low streamflow TDS concentrations of the catchment to an extent that could limit the domestic and/or agricultural and/or industrial uses of the water.

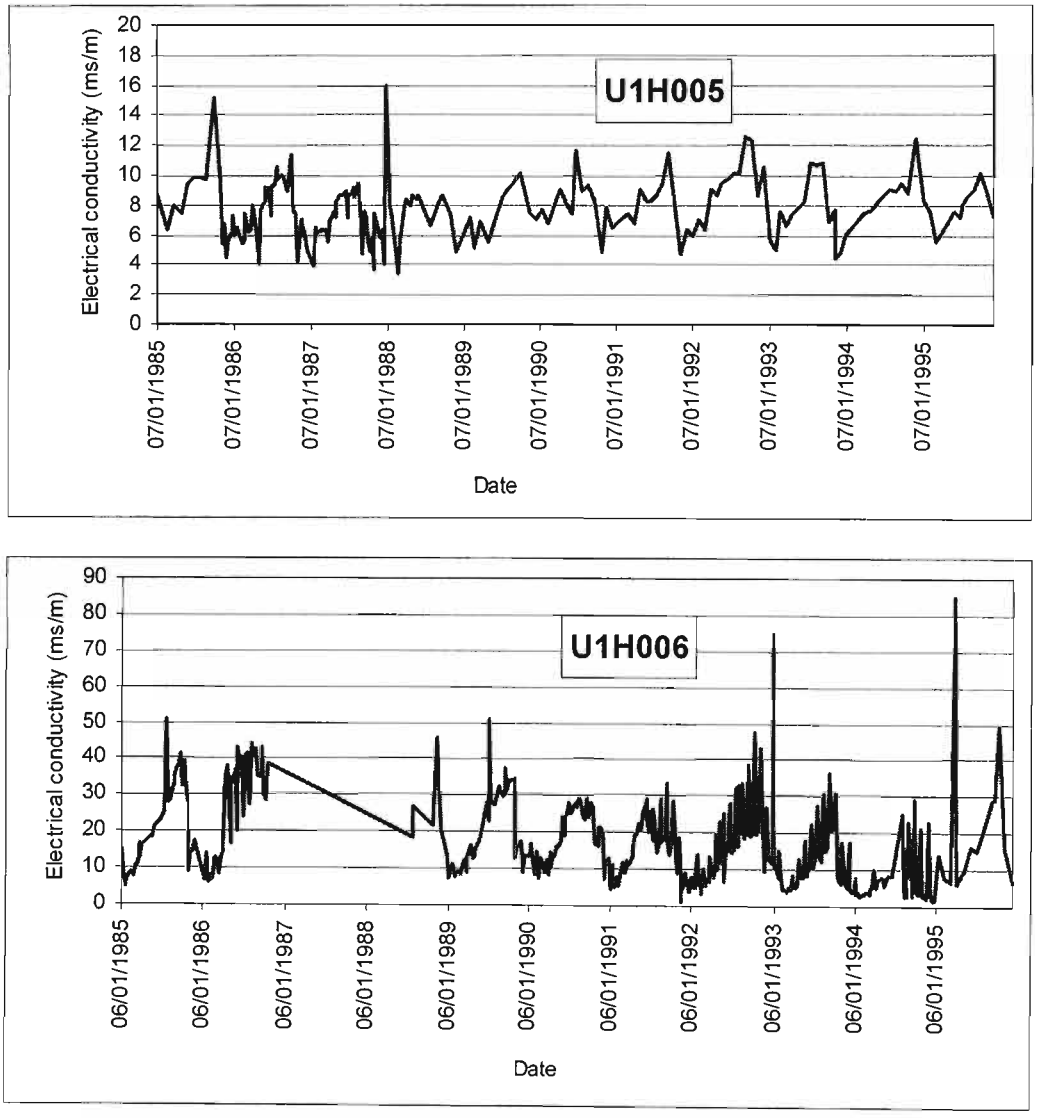

Figure 6.5 Intra-and inter-annual trends of streamflow salinity in the Upper (U1H005) and Lower (U1H006) Mkomazi Catchments

6.2 Previous Modelling Efforts in the Upper Mkomazi Catchment

Some researchers have conducted modelling based hydrological studies in the Mkomazi Catchment. These studies, undertaken by DWAF and the School of Bioresources Engineering

and Environmental Hydrology at the University of Natal include detailed modelling studies in the catchment and are outlined below.

6.2.1 DWAF pre-feasibility study

A general pre-feasibility study was conducted in the Mkomazi Catchment by DWAF for the Mkomazi-Mgeni Transfer Scheme. The objective of this study was to select an optimal transfer scheme for the Mkomazi through identification and evaluation of a number of potential schemes, eliminating those that have little merit, and carrying out a reconnaissance survey of the remaining schemes (NSI, 1998).

The study includes modelling present and future scenarios on the impact of domestic, agriculture, forestry, industrial as well as environmental demands on the available water resources. The hydrological models employed in the study were the Water Resources Yield Model (WRYM) and the BKS AFFDEM program for modelling forestry demands. This study disaggregates the Mkomazi Catchment into the 12 DWAF Quaternary Catchments in order to model the impact of forestry and irrigation at this level of spatial disaggregation. Furthermore, this study of DWAF investigated various water resources development schemes such as the Impendle and Smithfield dam schemes and their potential hydrological impact on downstream water resources.

6.2.2 *ACRU* based simulation study

A comprehensive hydrological modelling study using the *ACRU* model was conducted by Taylor (2001) with the general aim of assessing water resources management scenarios in the Mkomazi Catchment. The simulation includes daily flows for use in assessing the streamflow characteristics associated with the in-streamflow requirements. The study also includes modelling the impacts of land use change and water resources development on the availability of water resources. This study delineates the Mkomazi Catchment into 52 sub-catchments. This was done in order to represent the different land use and management practices as discrete units as well as considering proposed developmental concerns within the catchment (Taylor, 2001).

6.3 Setup of *ACRU2000* For the Upper Mkomazi Catchment

As stated in Section 6.2.2, the *ACRU* model was previously configured for the Mkomazi Catchment by Taylor (2001). This configuration of the *ACRU* model for the Mkomazi Catchment, through further refinements of the 12 Quaternary Catchments, delineates the whole Mkomazi Catchment into 52 sub-catchments. The first 18 sub-catchments representing the Upper Mkomazi Catchment are shown in Figure 6.6. Figure 6.7 also shows the flow direction and thus salt transport route between sub-catchment cells.

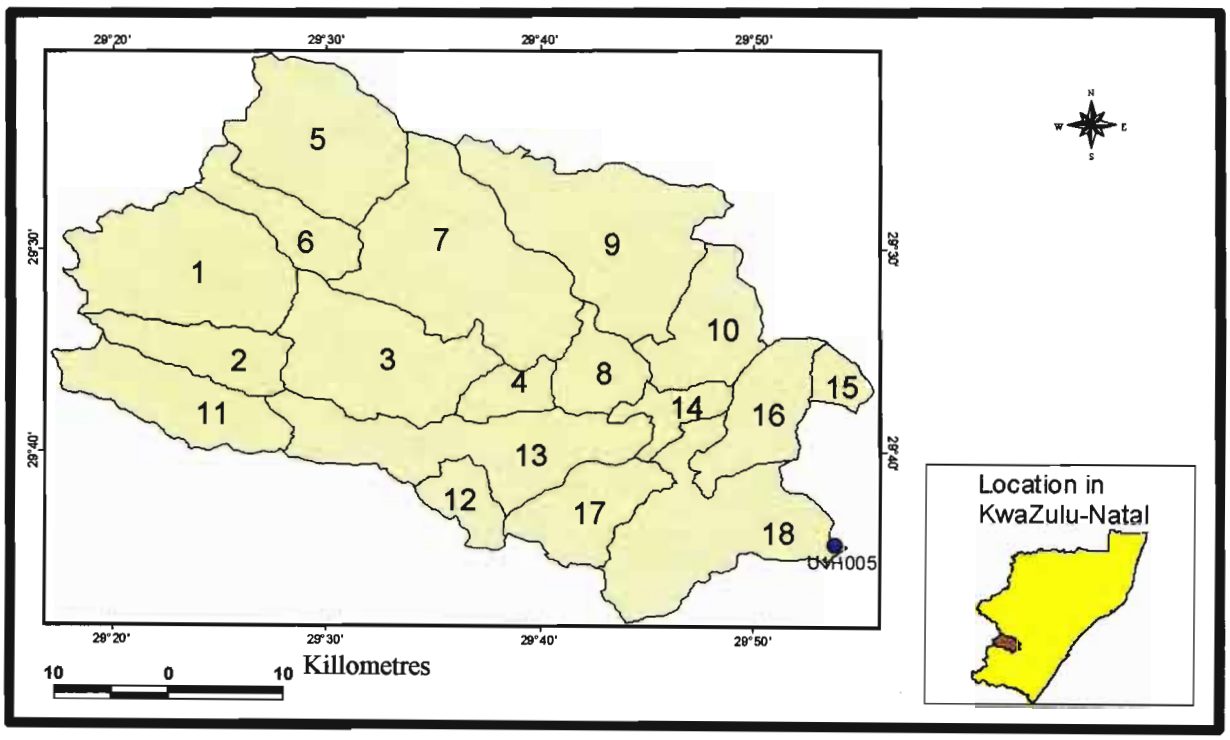

Figure 6.6 *ACRU* sub-catchment delineation of the Upper Mkomazi Catchment (after Taylor, 2001)

The Mkomazi Catchment was configured for the FORTRAN based *ACRU 300 series*. The *ACRU 300 series* uses a single Menu file that holds most of the input data information for all sub-catchments and hydrological response units. *ACRU2000*, there against, requires a separate input file for each hydrological response unit within a sub-catchment and a control file that holds general information about the simulation such as sub-catchment specifications and the start and end dates of simulation. Thus the *ACRU* Menu file was converted to *ACRU2000*

input files and a control file using one of the *ACRU* Utilities, *viz.* the *ACRU* Menu Converter program.

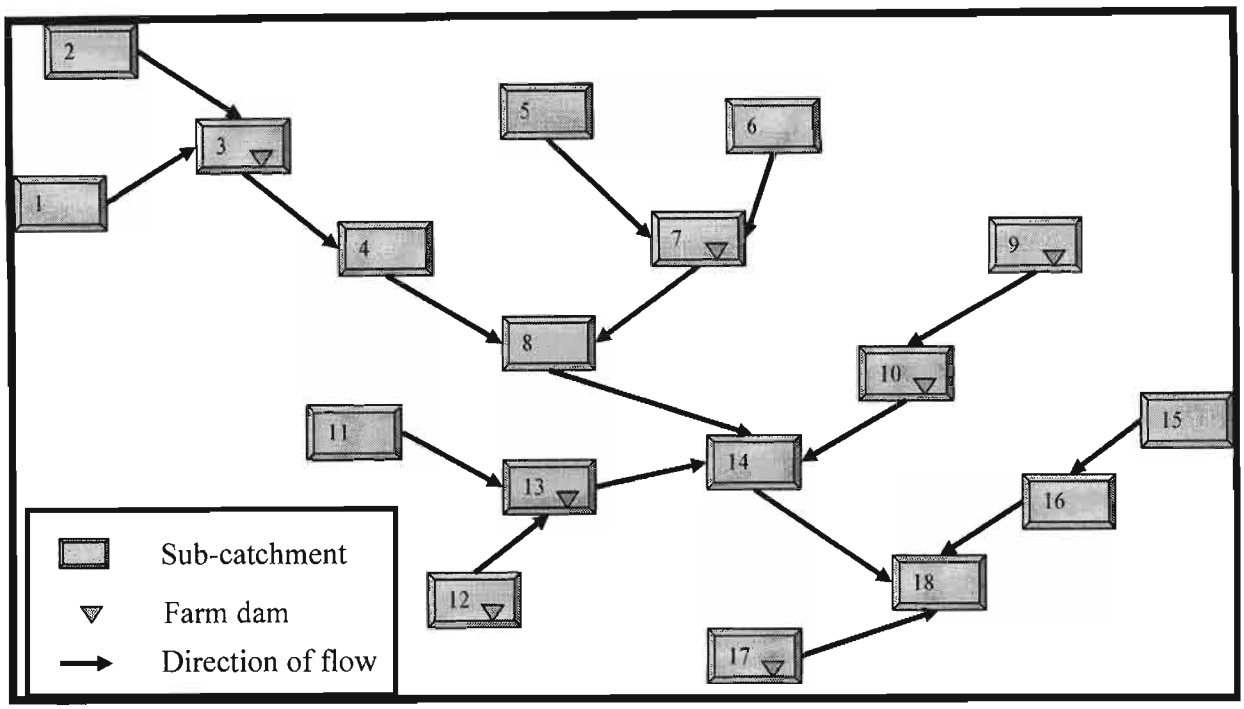

Figure 6.7 Diagram of sub-catchment configuration for the Upper Mkomazi Catchment (after Taylor, 2001)

Each sub-catchment of the Mkomazi Catchment is composed of nine hydrological response units (land use categories) as shown in Table 6.2. In *ACRU2000* each of these units has its own input file. Therefore, for the first 18 sub-catchments included in the Upper Mkomazi Catchment, a total of 162 input files (18 x 9) are generated from the original Menu file. The input parameters specific to *ACRUSalinity* are then added at the end of each of the 162 input files in accordance with the *ACRU2000* input format.

Table 6.2 Hydrological response units in each sub-catchment of the Upper Mkomazi Catchment (after Taylor, 2001)

Sub-catchment No	Total area (km^2)	Forest (km^2)	Plantation (km^2)	Valley Bushveld (km^2)	Dryland (km^2)	Urban (km^2)	Grassland (km^2)	Wetland (km^2)	Channel (km^2)	Dams & Irrigation (km^2)
1	162.914	0.000	0.401	0.866	0.000	0.000	160.538	0.000	1.095	0.010
2	63.323	0.000	0.806	0.000	0.000	0.000	61.635	0.000	0.867	0.010
3	141.668	0.000	6.659	4.196	0.636	15.269	113.357	0.000	1.535	0.032
4	29.216	0.000	1.952	0.833	0.000	17.551	8.156	0.000	0.712	0.010
5	142.968	0.237	0.000	0.000	0.000	0.000	141.636	0.000	1.081	0.010
6	57.758	0.825	0.173	0.000	0.000	0.000	55.799	0.000	0.946	0.010
7	208.006	0.268	2.804	12.608	5.258	11.196	172.560	0.946	2.712	0.597
8	47.091	0.000	0.000	0.046	0.007	25.206	20.334	0.000	1.484	0.010
9	189.227	0.000	0.545	5.806	0.649	0.000	179.017	0.000	1.464	0.801
10	77.443	0.000	4.191	1.879	19.236	4.029	44.327	0.000	1.137	2.641
11	93.123	0.208	1.569	0.000	0.000	0.000	89.965	0.000	1.367	0.010
12	32.865	0.140	0.606	0.000	1.084	0.000	29.126	0.000	0.360	1.546
13	148.147	0.000	12.190	1.323	4.685	0.318	123.587	0.000	2.144	3.898
14	29.970	0.000	2.026	0.289	6.071	3.478	17.607	0.000	0.487	0.010
15	18.867	0.000	0.001	0.000	10.052	0.229	8.378	0.000	0.195	0.010
16	70.939	1.337	0.422	7.124	1.990	8.517	50.614	0.000	0.924	0.010
17	69.655	1.214	3.213	3.537	0.350	0.351	59.695	0.000	0.618	0.676
18	158.546	8.802	27.145	7.589	2.276	22.561	86.517	0.000	3.644	0.010

6.4 Basic Data Input Requirements and Data Preparation for *ACRUSalinity*

Model predictions are commonly compared with measured data in order to prove that the model output is a realistic representation of field processes. However, in order to compare model simulations with measured data, model input parameters must be known and field data to compare with model outputs must also be available. Thus, the first step towards the verification phase was to obtain the required raw data inputs and subsequent preparation of these data in a way that can be used by the model. Data relating to the hydrological aspect were already available. However, data that are specific to the new module (*ACRUSalinity*) still needed to be input. These were obtained from various sources. The following sections will discuss the methodology followed and the assumptions taken to derive values of particular parameters.

6.4.1 Rainfall and irrigation water TDS concentrations

As described in Section 2.2.2, rainfall is the fundamental driving force and pulsar input to most hydrological processes (Schulze *et al.*, 1995c), resulting also in water quality impacts from non-point sources (Pegram and Görgens, 2001). Rainfall plays a major role during wet atmospheric deposition. This is particularly true in areas with low salinity waters. In such areas the chemical composition is controlled mainly by the amount of dissolved salts furnished by precipitation. On the other hand, rainfall has a dilution effect on areas with high TDS concentration.

Salt input to the topsoil of irrigated and non-irrigated lands is computed in *ACRUSalinity* from the volume of rainfall and irrigation water as well as their associated TDS concentrations. This module assumes a single average representative rainfall salt concentration value for each sub-catchment. Analysis of rainfall samples by Simpson (1991) collected over a period of seven months at Cedara meteorological station (located in U2H016 catchment) in the neighboring Mgeni Catchment reveals that the average TDS concentration on the area to be 11.3 mg/l. The measured rainfall TDS concentration ranges from 2.7 mg/l to 27 mg/l. A similar study carried out by Flügel (1995) in the Western Cape province from an analysis of 67 rainfall samples has shown rainfall salt concentrations varying between 14 and 125 mg/l with an average value of 37 mg/l. Görgens (2003) suggests that rainfall TDS concentration of the Mkomazi Catchment would be lower than the Western Cape province.

Therefore, based on the above information the rainfall TDS concentration of the Mkomazi Catchment is assumed to have the same value as its neighboring Mgeni Catchment, and as measured at the Cedara meteorological station. Hence, a value of 11.3 mg/l is taken as the average rainfall TDS concentration for the Upper Mkomazi Catchment. Similarly, no data was found for the catchment's irrigation water TDS concentration. Hence, assuming the main source of irrigation water supply in the catchment to be from the river, the average TDS concentration of streamflow at U1H005 *viz.* 58 mg/l, is taken as a representative value.

6.4.2 Initial TDS concentrations of subsurface and reservoir water storage

In *ACRU*, the initial soil water content of the topsoil and subsoil at the start of a simulation are input to the model. Therefore, in order to account for the impact of this subsurface water storage at the start of a simulation on surface and subsurface TDS balance, it is important to determine the salt load associated with the initial soil moisture. The initial salt load of these subsurface systems is computed and set before any of the other hydrosalinity processes are executed for the simulation period. From assessment of the historical record of the streamflow salinity, the average maximum value during the dry season was found to be 100 mg/l. Therefore, based on the assumption that streamflow during the dry season is composed of only subsurface flow and hence its salinity reflects the average TDS concentration of the subsurface system, the initial salt concentration of the topsoil and subsoil is taken as 100 mg/l. A sensitivity test of this variable has shown that the impact of this variable on surface and subsurface TDS balance decreases with time and it would have little effect after three months (Section 7.1.3). Therefore, a warm up period of three months is also used in all simulations to minimise errors emanating from data uncertainty of the initial TDS concentration.

ACRU also considers the initial volume of water stored in reservoirs at the start of a simulation. Thus, in order to conserve the salt mass, *ACRUSalinity* also computes and stores the initial salt load of a reservoir at the start of a simulation. This salt load is computed from the initial volume of water stored in the dam and its salinity which is input to the model by the user. Hence, the initial TDS concentration of a reservoir needs to be known. For the purpose of this dissertation this value is assumed to have the same value as the streamflow average TDS concentration. Therefore, the initial stored water in the reservoir at the start of simulation is assumed to have TDS concentration of 58 mg/l. Similar to that of initial subsurface TDS concentration, the initial reservoir water TDS concentration value was also found to have little

effect on simulated daily TDS concentration values after a few days following the start of the simulation (Section 7.1.4). This is particularly true for small reservoirs draining big catchment areas where the whole initial storage of the reservoir may even get replaced with "new" water after only few high events.

6.4.3 Salt uptake rate and equilibrium values

ACRUSalinity uses a first order rate kinetics equation to describe the salt generation process in subsurface components. Data requirements of this process include the salt concentration of the specific layer before salt generation, the equilibrium value (saturation value) and the rate constant. The first parameter is calculated internally from the daily salt and water balances. The equilibrium value and the rate constant, however, are inputs to the model.

Estimated values of these parameters can be determined if daily soil salinity data are available for the area. However, no such time series records are found for the Mkomazi Catchment. An attempt was made to derive estimated values for the salt uptake rate constant parameter from the available streamflow salinity records measured during the dry season. This is based on two basic assumptions. First, during the dry season the streamflow is composed of only subsurface flow and hence, during this period, the streamflow has the same salt concentration as the subsurface water. Secondly, the Upper Mkomazi Catchment is less influenced by human activity, thus there is little or no effluent discharge to the stream. Historical streamflow and salinity data in U1H005 are then assessed to extract data that can fulfill the abovementioned requirements.

Regression analysis based on the extracted data sets was conducted with the help of GENSTAT Software (McConway *et al.*, 1999). The data sets are fitted into the first order rate kinetics equation in the form of Equation 3.9 and assuming a C_e value of 3000 mg/l (a lower range of the global average maximum soil salinity values (Aswathanarayana, 2001)). The difference between this maximum soil salinity and the daily salinity values is then treated as the explanatory variable (x). Similarly, the difference in TDS concentration between successive days is treated as the response variable (y). Further, the y-intercept term is omitted from the model to express the equation in its original form. The GENSTAT output for this analysis is shown in Appendix F. Output from this regression analysis shows that, the slope of the curve that represents the rate constant, k, is $3.4 * 10^{-4}$ at a significance probability of less

than 0.001 and standard error of observations of 0.534. Both parameters indicate that the first order rate kinetics model is adequate to describe the increase in streamflow TDS concentration with time. The regressed k value is also not far from the range of theoretically expected values of this parameter (i.e. 10^{-4} - 10^{-7} day^{-1}) for individual solute species, as suggested by Ferguson *et al.* (1994). However, the regression analysis has shown an extremely low accounted percentage of variance. This can be attributed to the low number of observations used in the regression analysis (only 15 records), due to limitations in the availability of daily streamflow TDS concentration data recorded between two rainfall events. Therefore, it was decided that the rate constant and equilibrium values had to be derived by calibration against observed TDS values.

6.5 Code Validation of the Major *ACRUSalinity* Process Objects

One measure of model validity is the ability of the model to conserve mass (Konikow, 2002). This can be measured by comparing the net fluxes calculated or specified in the model, e.g. inflow and sources minus outflow and sinks with changes in storage (accumulation or depletion). The mass balance computations can thus be used to assess whether the algorithms describing various processes yield the desired results.

It is time intensive to make a detailed code validation of the algorithms underlying each process in the module. Therefore, this section validates the code underlying only the key processes which might likely have errors due to the relatively complicated algorithms describing them. This mainly occurs on these processes that involve transport of salts from one component to another, or that receive TDS concentration or salt load information from two or more components. However, during the development process of the hydrosalinity module, mass balance computations were done after every change or new addition made to process objects, so as to track and correct such errors over time.

6.5.1 Code validation of subsurface salt movement processes

Mass conservation computations in any of the subsurface components consider salt gains (inflows) to, and losses (outflows) from, the components under consideration. *ACRUSalinity* assumes that the sources of salt gains to a subsurface component (a soil horizon or the groundwater store) are:

- salt input through wet atmospheric deposition (rainfall salt input)
- salt input from applied irrigation water, and
- salt generated as a result of *in situ* weathering processes.

The term salt input in the Table 6.3 and 6.4 refers to the salt input from both irrigation and rain water. Similarly, losses from any of the subsurface components are assumed to be as a result of:

- downward salt transport associated with the saturated downward flow of water
- salt load associated with baseflow release, in the case of groundwater system, and
- upward salt transport along with upward saturated flow of water.

The mass of salt stored on a particular day in any of the subsurface components (topsoil, subsoil or groundwater store) is computed from consideration of the previous day's salt load, gains to the system and losses from the system as follows:

calculated current salt load = previous day's salt load + total gain - total loss

Outputs obtained from the model are used for these mass balance computations, as shown in Tables 6.3 and 6.4. The salt load associated with the upward flow of water for the three consecutive days selected for this computation was zero. The salt input column, for the case of topsoil refers to the salt load added from rainfall or irrigation water, whereas, for subsequent layers, it refers to salt load associated with percolation water from the overlying layer.

The calculated current salt load is compared against the simulated value and the error is then expressed as a percentage difference between the calculated and simulated values. Only minor differences (of an order of less than 10^{-9}) between calculated and simulated values can be noticed from the "Error" column of both tables. This is attributed to rounding errors.

Table 6.3 Mass balance for code validation of subsurface salt movement processes in non-irrigated land

Component	Date	Previous day's salt load (mg)	Salt input (mg)	Generated salt load (mg)	Percolated/ Baseflow salt load (mg)	Calculated current salt load (mg)	Simulated current salt load (mg)	Error (%)
Topsoil	09/04/95	16085289.81	2822982.34	57354.79	2121598.59	16844028.35	16844028.35	2.21E-14
	10/04/95	16844028.35	738574.00	55884.66	1851271.79	15787215.22	15787215.22	-1.18E-14
	11/04/95	15787215.22	102796.00	49223.82	1102430.26	14836804.78	14836804.78	-1.26E-14
Subsoil	09/04/95	26339019.30	2121598.59	55467.52	1277067.58	27239017.83	27239017.83	0.00E+00
	10/04/95	27239017.83	1851271.79	58847.14	1844888.75	27304248.01	27304248.01	1.36E-14
	11/04/95	27304248.01	1102430.26	58525.42	1751281.39	26713922.30	26713922.30	-1.39E-14
Groundwater	09/04/95	58423586.14	1277067.58	80043.85	932578.88	58848118.69	58848118.69	0.00E+00
	10/04/95	58848118.69	1844888.75	82517.21	948098.18	59827426.47	59827426.47	0.00E+00
	11/04/95	59827426.47	1751281.39	84828.09	961951.16	60701584.79	60701584.79	-1.23E-14

Table 6.4 Mass balance for code validation of subsurface salt movement processes in irrigated land

Component	Date	Previous day's salt load (mg)	Salt input (mg)	Generated salt load (mg)	Percolated/ Baseflow salt load (mg)	Calculated current salt load (mg)	Simulated current salt load (mg)	Error (%)
Topsoil	09/04/95	3433643113.07	18996567.25	54315547.83	28707284.68	3478247943.46	3478247943.47	-2.88E-10
	10/04/95	3478247943.46	11887930.01	54790044.42	39045159.05	3505880758.85	3505880758.84	2.85E-10
	11/04/95	3505880758.85	1676000.00	53885607.92	20438115.81	3541004250.96	3541004250.96	0.00E+00
Groundwater	09/04/95	1900848972.32	28707284.68	26075587.33	39112636.89	1916519207.44	1916519207.44	1.24E-14
	10/04/95	1916519207.44	39045159.05	26149707.83	39634281.49	1942079792.83	1942079792.83	0.00E+00
	11/04/95	1942079792.83	20438115.81	25928168.40	39768921.54	1948677155.50	1948677155.50	0.00E+00

6.5.2 Code validation of surface salt movement processes

The salt load associated with runoff water from irrigated and non-irrigated lands comprises salt load from baseflow and quickflow. Therefore, the "Calculated runoff salt load" column shown on Table 6.5 is computed as the sum of the baseflow salt load and quickflow salt load columns. This calculated salt load on a particular day is compared against the simulated output from the model. The "Error" column is then determined as the percentage difference between the runoff salt load as calculated on a spreadsheet and that simulated by the model. The result from this comparison shows that the algorithms involved in runoff salinity and salt load computations are yielding the required results with only minor errors. These minor errors are attributed to rounding errors.

Table 6.5 Mass balance for code validation of surface salt movement processes

Component	Date	Baseflow salt load (mg)	Quickflow salt load (mg)	Calculated runoff salt load (mg)	Simulated runoff salt load (mg)	Error (%)
Non-irrigated land	09/04/1995	932578.88	135068.07	1067646.95	1067646.95	0.00E+00
	10/04/1995	948098.18	94547.65	1042645.83	1042645.83	1.12E-14
	11/04/1995	961951.16	66183.35	1028134.51	1028134.51	0.00E+00
Irrigated land	09/04/1995	39112636.89	2548432.75	41661069.64	41661069.64	0.00E+00
	10/04/1995	39634281.49	222069.99	39856351.48	39856351.47	2.51E-08
	11/04/1995	39768921.54	0.00	39768921.54	39768921.54	0.00E+00

6.5.3 Code validation of reservoir salt budgeting processes

The major sources of salt input to an internal reservoir system accounted in *ACRUSalinity* are:

- runoff salt load from irrigated lands
- runoff salt load from non-irrigated lands
- runoff salt load from adjunct impervious areas and
- salt input through wet atmospheric deposition (salt load associated with the rain falling on the surface of the reservoir).

Similarly, the total salt outflow from a reservoir system comprises salt load associated with:

- seepage water
- overflow from the reservoir
- domestic or irrigation water abstracted from the reservoir and
- legal flow (normal) flow release.

The current salt load stored in the reservoir is calculated from considerations of the total inflow, total outflow and salt load stored in the reservoir at the end of the previous time step as:

calculated current salt load = previous day's salt load + total inflow – total outflow

The calculated current salt load is then compared against the simulated current salt load. The error value which is calculated as the percentage difference of the calculated and simulated current salt load is found to be minor. This minor difference shown on the "Error" column of Table 6.6 is due to rounding errors. Therefore, the algorithms describing the reservoir salt budget are performing the required tasks almost perfectly.

Table 6.6 Mass balance for code validation of reservoir salt budgeting processes

Reservoir inflow and outflow components		**Date**				
		07/04/1995	08/04/1995	09/04/1995	10/04/1995	11/04/1995
Salt inflow sources	irrigated	39050607.60	39111977.90	41661069.60	39856351.50	39768921.50
	non-irrigated	223842940.99	222263205.68	237597563.92	249456786.95	257730309.21
	rainfall	0.00	44400000.00	69264000.00	39072000.00	5683200.00
	impervious	0.00	39.35	63.09	34.26	2.37
	total salt inflow (mg)	262893548.61	305775222.92	348522696.66	328385172.68	303182433.12
salt outflow	seepage	1012.14	1056.84	1023.14	926.58	897.88
	overflow	0.00	413370181.63	850371375.03	456820732.84	115589219.49
	abstraction	33738035.34	35228150.71	34104644.47	30886105.40	29929333.62
	legal flow	1012.14	0.00	0.00	0.00	0.00
	total salt outflow (mg)	33740059.62	448599389.18	884477042.64	487707764.82	145519450.99
Previous day's salt load (mg)		5592810179.80	5821963668.80	5679139502.53	5143185156.54	4983862564.40
Calculated current salt load (mg)		5821963668.79	5679139502.54	5143185156.55	4983862564.40	5141525546.53
Simulated current salt load (mg)		5821963669.00	5679139503.00	5143185157.00	4983862564.00	5141525547.00
Error (%)		1.43937E-10	-1.5921E-10	-1.07398E-10	7.85119E-11	-1.29895E-10

6.5.4 Code validation of channel salt movement and distributed hydrosalinity modeling processes

In the presence of an internal dam the salt load associated with runoff from non-irrigated land and adjunct impervious areas of a sub-catchment is allocated to an internal dam and a channel reach. On the other hand, if no reservoir exists in the sub-catchment, or if it is situated at the sub-catchment's outlet, the total salt load associated with the runoff water from the sub-catchment is allocated to a channel reach. In the previous section's mass balance computation for a reservoir salt budget an internal dam was considered and in this case an external dam will be considered.

For the purpose of this code validation of channel and distributed hydrosalinity modelling processes, a simple catchment composed of four sub-catchments with one external dam situated at the outlet of Sub-catchment 3 is used. Layout of the sub-catchments and the direction of water flow and salt transport between the sub-catchments are shown in Figure 6.8.

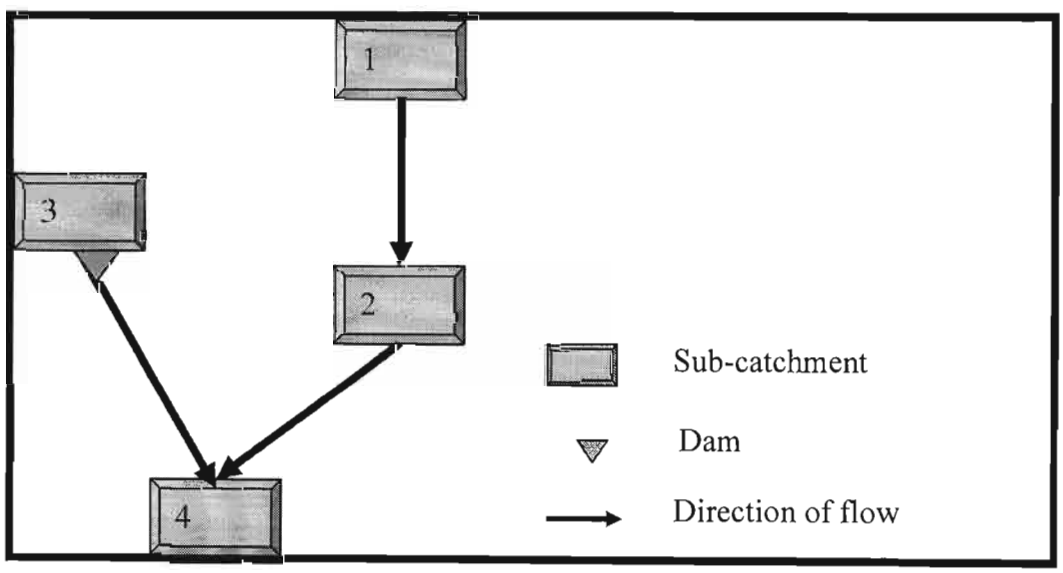

Figure 6.8 Layout and direction of salt transport for the catchment used in code validation of channel and distributed hydrosalinity modelling processes

On each sub-catchment the sources of salt input to a channel reach are:

- salt load associated with runoff water from adjunct impervious areas
- salt load associated with runoff water from non-irrigated lands
- salt load associated with runoff water from irrigated lands and
- salt load transported from upstream reaches, in the case of distributed hydrosalinity modeling.

No channel reach salt storage is assumed in *ACRUSalinity*. Therefore, on a particular day, the total salt load that enters the channel reach is transported to a destination reach on the same day. Thus, the total salt load at the river (channel) reach of Sub-catchment 2 (River_2) is calculated as the sum total of:

- streamflow salt load from river reach 1 (River_1)
- runoff salt load from adjunct impervious area in Sub-catchment 2
- runoff salt load from irrigated land in Sub-catchment 2 and
- runoff salt load from non-irrigated land in Sub-catchment 2.

Based on configuration of the four sub-catchments used for this purpose (Figure 6.8), the salt load from River_2 is transported to River_4. Similarly, the salt load associated with the total outflow from the external reservoir of Sub-catchment 3 (Dam_3) is allocated to River_4. Therefore, the calculated total salt load at River_4 in Table 6.7 is computed from the sum total of:

- salt load from River_2
- salt load from Dam_3
- salt load associated with runoff water from adjunct impervious area of Sub-catchment 4
- salt load associated with runoff water from irrigated lands of Sub-catchment 4, and
- salt load associated with runoff water from non-irrigated land of Sub-catchment 4.

The calculated total salt load at river reaches 2 and 4 are compared against the simulated values on these reaches. As shown on the "Error" column of Table 6.7, only minor rounding errors can be noticed. This reveals that the algorithms describing channel salt movement and

distributed hydrosalinity modelling processes, except for the minor rounding errors, are also considered free from coding error and are performing the tasks for which they are intended.

Table 6.7 Mass balance in mg for code validation of channel and distributed hydrosalinity modelling processes

Component		Date		
		28-Dec	29-Dec	30-Dec
Total salt load at River_1		51466.7	55904.8	51561.1
Sub-catchment 2	Adjunct impervious area	0.0	1942228.5	303144.0
	Irrigated land	0.0	0.0	0.0
	Non-irrigated land	19634302.6	19684233.0	19562181.3
	Calculated total salt load at River_2	19685769.3	21682366.3	19916886.4
	Simulated total salt load at River_2	19685769.3	21682366.3	19916886.4
	Error (%)	3.97E-13	-8.59E-14	-2.24E-13
Outflow salt load from Dam_3		1745659.2	1753324.9	1707290.0
Sub-catchment 4	Adjunct impervious area	0.0	20457862.4	3206056.8
	Irrigated land	0.0	0.0	0.0
	Non-irrigated land	210476751.0	242962956.0	236110333.0
	Calculated total salt load at River_4	231908179.4	286856509.0	260940567.0
	Simulated total salt load at River_4	231908179.4	286856509.0	260940567.0
	Error (%)	1.28509E-13	-8.3114E-14	-2.3984E-13

6.6 Verification Against Observed Data

Discrepancies between observed and simulated responses of a system can be the manifestation of errors in the mathematical model. Simulation results are often less accurate than desired due to uncertainty in the input data provided to the model as well as uncertainties in the modelled processes (Rossouw and Kamish, 2001). According to Konikow (2002), in applying hydrological models to field problems, there are three sources of errors.

- One source consists of conceptual errors, i.e., theoretical misconceptions about the basic processes that are incorporated in the model. Conceptual errors include both neglecting relevant processes as well as representing inappropriate processes.
- A second source of error involves numerical errors arising in the equation-solving algorithm.
- A third source of error arises from uncertainties and inadequacies in the input of data that reflect our inability to describe comprehensively and uniquely attributes of the system.

In most model applications conceptualisation problems and uncertainties concerning data are the most common sources of error (Konikow, 2002). *ACRUSalinity* is validated for the second source of error (coding error) as described in the previous section. This section, therefore, presents the assessment made on the combined effects of the first source of error (conceptual error) and the third source of error (data uncertainty). A sensitivity analysis is also undertaken (Chapter 7), in order to assess the effects of data uncertainty and errors on module outputs.

6.6.1 Observed daily flow and TDS concentration

Observed data from the Mkomazi Catchment were used for data patching and comparison of simulated model outputs. The observed data used for these purposes include daily flow and its TDS concentration value. Daily streamflow depth for the U1H005 gauging weir, where the Upper Mkomazi Catchment drains, was obtained from DWAF. Similarly, the streamflow salinity data for this station is obtained from the "Water Quality on Disc" CD-ROM (CSIR, 2002). This disc gives access, on a PC, to many of the macro-chemical water quality data-bases for the area, such as EC, TDS, PH and most base elements. Streamflow TDS concentration grab samples collected on a weekly basis from January 1986 to December 1987 are used for calibration (1986) and verification (1987) purposes. This period is chosen because it has relatively few missing records compared to data records of the remaining years for the station.

6.6.2 Observed data conversion and patching

The salinity data, in mg/l, for the calibration and verification periods is based on weekly grab samples. Hence, conversion to daily values was necessary so as to be used for comparison with the daily model output. Therefore, filling of missing values and subsequent conversion to daily data are done in two steps. The first step involved patching missing TDS values from the EC record, if the EC value was available for the given day. The second step involved data patching using the TDSGEN program which has been developed by Ninham Shand Consulting Engineers. This program infills missing data based on flow-TDS relationships recorded in the area.

The patching of missing TDS values from EC values was based on a regression equation established using observed TDS and EC values. The relationship between TDS (mg/l) and EC

(ms/m) as recorded at gauge U1H005 is plotted in Figure 6.9. The linear regression analysis yielded the following relationship with coefficient of determination (R^2) of 0.79:

$$TDS = 6.388 * EC + 8.256 \quad (6.1)$$

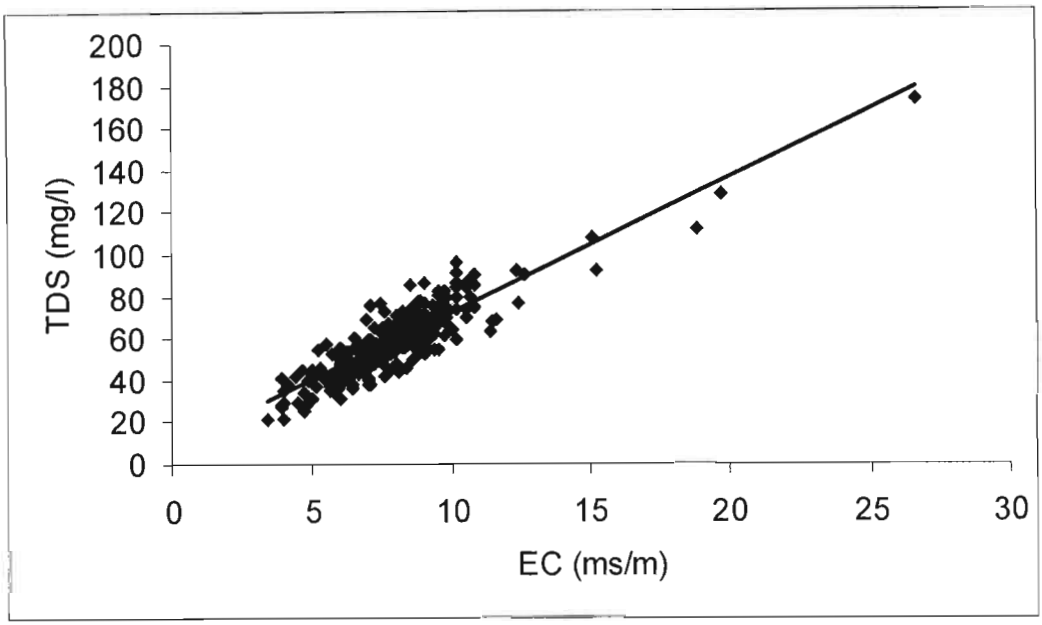

Figure 6.9 TDS versus EC relationship as recorded at U1H005 (Camden)

First, available conductivity measurements for the area are converted to TDS values by using Equation 6.1. Then, if on a particular day, a recorded TDS value does not exist while a conductivity value does, the converted EC value is used to fill the missing TDS value. However, if neither TDS nor EC values are recorded on the particular day the missing values are infilled by use of the TDSGEN program.

6.6.3 Calibration of the *ACRUSalinity* module

According to Konikow (2002) model calibration may be viewed as an evolutionary process in which successive adjustments and modifications to the model are made based on the results of previous simulations. The modeller decides when sufficient adjustments have been made to the representation of parameters and processes and at some time accepts the model as being adequate (or perhaps rejects the model as being inadequate and seeks alternative approaches). This decision is often based on a mix of subjective and objective criteria. Some of these

criteria include the visual fit between plots of time series of simulated and observed salt concentrations and through comparison of statistical outputs such as means, standard deviations and correlation coefficients of simulated and observed values. In general the objective of model calibration is to minimise differences between the observed data and simulated values. Usually the model is considered calibrated when it reproduces historical data within some acceptable level of accuracy. The acceptable level is determined subjectively (Konikow, 2002).

As mentioned in Section 6.3.2.3, the attempt to derive values of the salt uptake rate constant (k) through fitting a regression equation to an observed streamflow TDS concentration data was not successful owing to the lack of a daily soil moisture salinity data. Hence, an attempt was made to obtain a representative rate constant (k) and equilibrium (C_e) value for the area through calibration of the module. This was achieved by changing these values in an attempt to optimise the module predictions of the streamflow salinity against the observed data. The graphical and statistical methods employed for the calibration purpose are outlined below.

6.6.3.1 Time series and percentile curves

Both time series and percentile curves are used to estimate values of the rate constant and equilibrium parameters that yield the best fit between observed and simulated streamflow TDS concentration values. Figures 6.10 and 6.11 show the time series and percentile curves respectively for the calibration period (from 01 January, 1986 to 31 December, 1986). From the various calibration trials undertaken to obtain a representative uptake rate constant (k) and an equilibrium (C_e) values for the Upper Mkomazi Catchment, the best fit (Figures 6.10 and 6.11) is attained at a k value of 4.5E-5 and C_e value of 3000 mg/l. During the calibration trials constant values of k and C_e parameters are used in all sub-catchments.

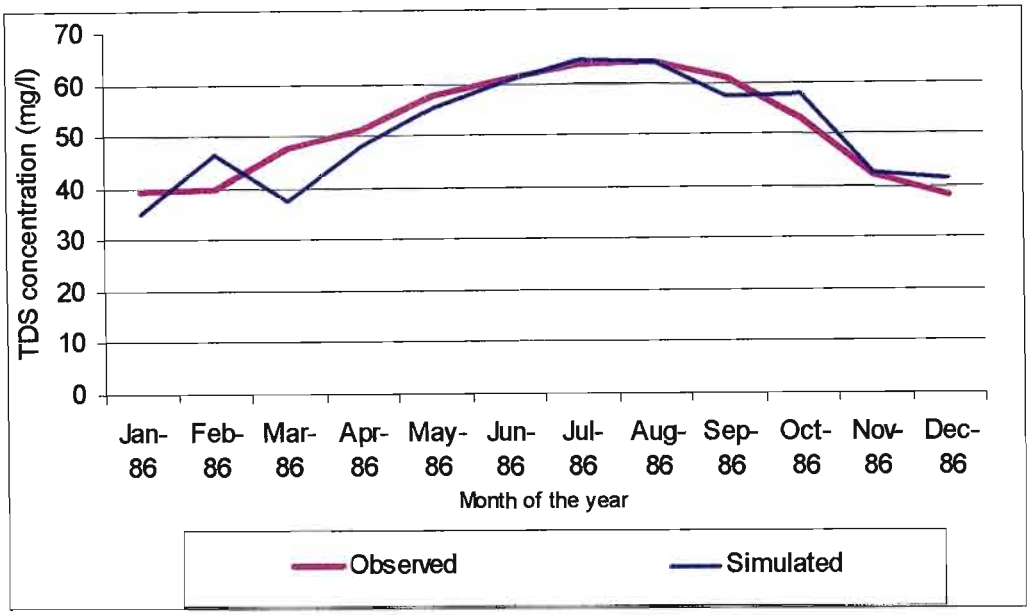

Figure 6.10 Monthly means of daily observed and simulated streamflow TDS concentration at Camden for the calibration period (U1H005)

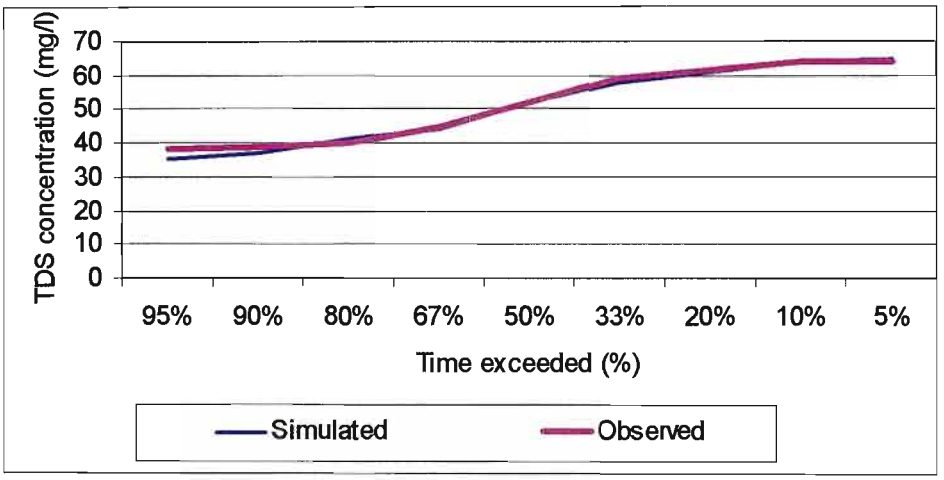

Figure 6.11 Percentile curves for observed and simulated monthly means of daily streamflow TDS concentration at Camden for the calibration period (U1H005)

6.6.3.2 Statistical analysis

According to Schulze *et al.* (1995), the general aim of a good simulation is a one to one correspondence between simulated and observed values, with a high correlation, a minimum symmetric error and the conservation of means, deviations and other statistics. The wide

range of goodness-of-fit statistics comparing observed and simulated values can be categorised into conservation statistics and regression statistics. The conservation statistics that include mean, standard deviation and skewness coefficient are employed in this dissertation for comparison of observed and simulated values. A summary of these statistics for the calibration period are shown in Table 6.8. Similarly, regression statistics for comparison of observed and simulated values including correlation coefficient, coefficient of determination, slope as well as y-intercept for the scatter plot of observed versus simulated values are also given in Table 6.9.

The general aim during the procedure with regard to the conservation statistics was to minimise:

- the percentage difference between means of observed and simulated values
- the percentage difference in standard deviation, i.e. in minimising the difference in dispersion of the observed and simulated data about their mean values and
- the percentage difference in skewness coefficient, i.e. the symmetry of the observed and simulated values.

Conversely, the aim with regard to the regression statistics used was to:

- maintain a slope as close as possible to 1.0 since a slope value greater than one indicates over-simulation whereas a slope value less than 1.0 indicates under-simulation (Schulze *et al.*, 1995)
- minimise the base constant (y-intercept) to zero
- maximise the correlation coefficient to unity and
- maximise the coefficient of determination to unity.

Table 6.8 Conservation statistics of streamflow salinity at Camden (U1H005)

Statistical parameter	Observed	Simulated	Difference %
Mean (mg/l)	51.67	51.00	-1.30
Standard deviation	9.96	10.30	3.41
Skewness Coefficient	-0.12	-0.14	16.67

Table 6.9 Regression statistics of streamflow salinity at Camden (U1H005)

Statistical parameter	Value
Slope	0.94
Base constant (y-intercept)	2.65
Correlation coefficient	0.90
Coefficient of determination	0.82

As it can be seen from the time series and percentile curves, the simulated streamflow TDS concentration has shown good fit with the observed values at U1H005 when a salt uptake rate constant of 4.5E-5 and an equilibrium value of 3000 mg/l are used. This is also confirmed from the statistical analysis shown in Tables 6.8 and 6.9. Therefore, these values are taken as representative values for k and C_e parameters in the catchment.

6.6.4 Verification result and discussion

The uptake rate constant (k) and the equilibrium values as determined from the calibration result are used as input in simulating streamflow TDS concentration for the verification period (January to December, 1987). Both graphical and statistical methods are then used to evaluate the module performance using the same criteria as considered for calibration.

6.6.4.1 Time series and percentile curves

The daily simulated TDS concentration values and the observed values from the weekly samples are plotted in the same graph (Figure 6.12). From Figure 6.12 it can be seen that the

simulated values follow the observed seasonal fluctuations remarkably well. Similarly, the monthly mean of daily observed TDS concentrations which are patched from the weekly grab samples are plotted in the same graph with the simulated values as shown in Figure 6.13. From Figure 6.13 it can be seen that the simulated TDS concentration follow the observed seasonal fluctuations remarkably well. However, the monthly mean of daily simulated TDS concentration values, especially from April to August of the verification year (1987), have slightly exceeded the observed streamflow salinity values. On the other hand, the simulated streamflow TDS concentration values for the period of October to December have shown very good fits with the observed values (Figure 6.13).

Figure 6.14 shows observed and simulated percentile curves of the daily streamflow TDS concentration at Camden for the verification period. In general, the percentile curve for simulated values has followed the trend of observed streamflow TDS concentration curve very well. However, the graph shows an overall slight over-simulation of streamflow TDS concentrations, especially for those with relatively higher values (values that would be exceeded in less than 50 % of the time).

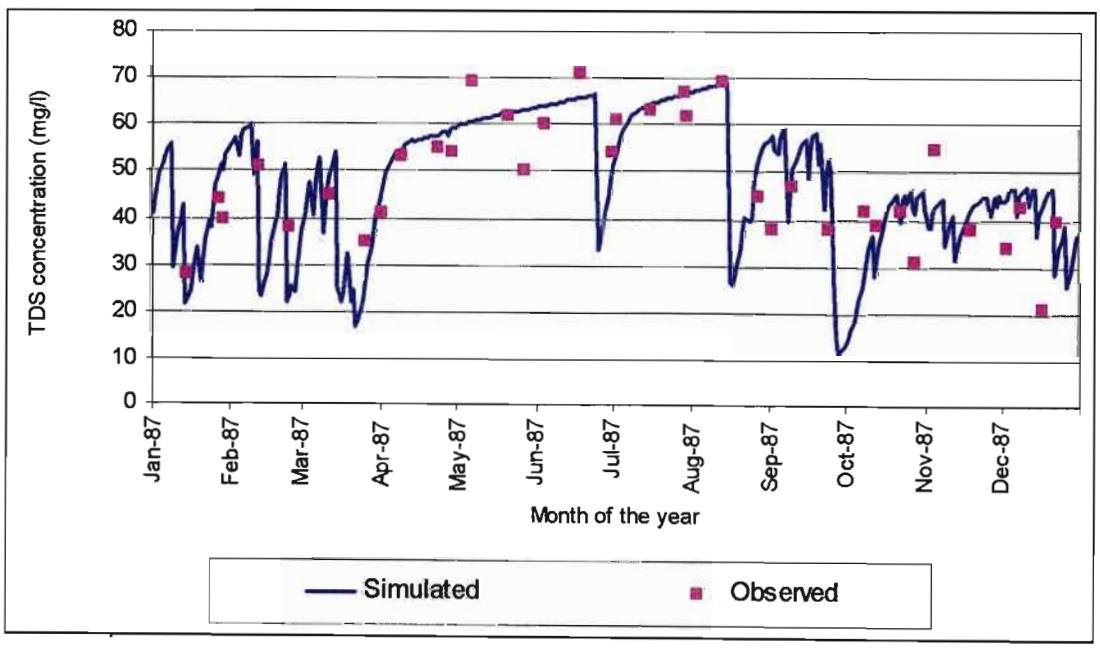

Figure 6.12 Observed (weekly grab of samples) and daily simulated streamflow TDS concentration values at Camden (U1H005)

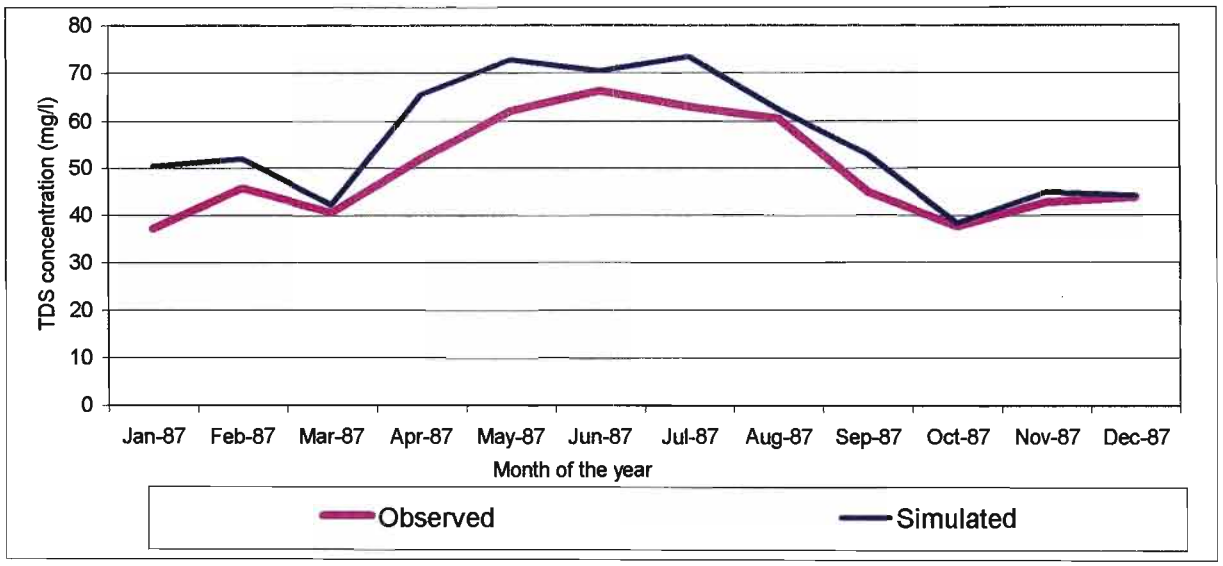

Figure 6.13 Monthly means of daily observed (patched with TDSGEN) and simulated streamflow TDS concentration values at Camden for the verification period (U1H005)

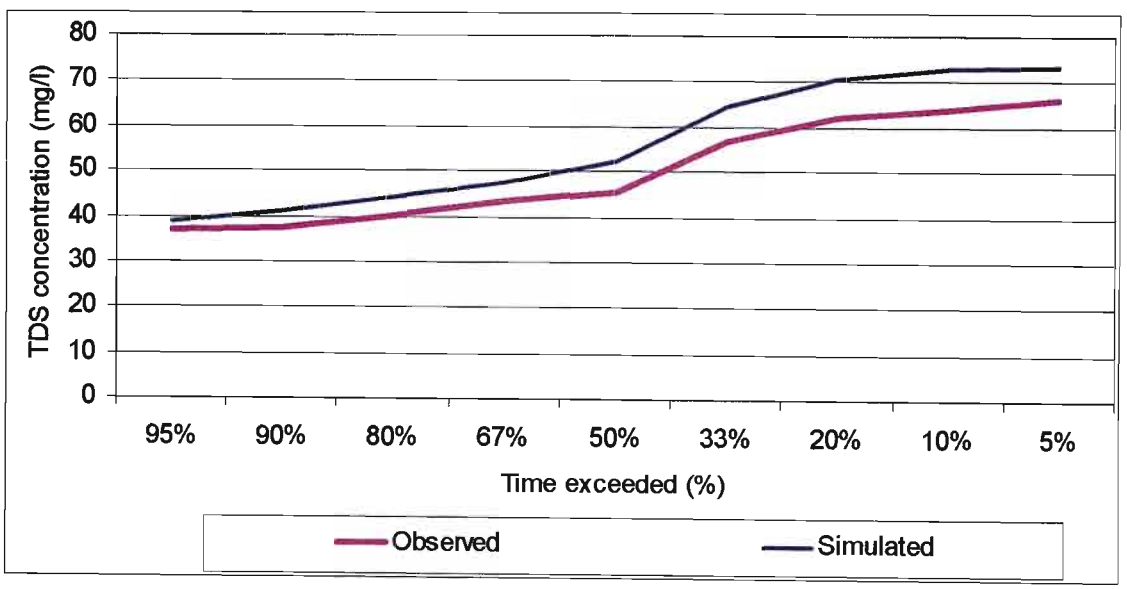

Figure 6.14 Percentile curves of observed (patched with TDSGEN) and simulated TDS concentration values at Camden for the verification period (U1H005)

6.6.4.2 Statistical analysis

Both conservation and regression statistics are used to compare the simulated and observed streamflow TDS concentrations. Results from the statistical analysis are shown in Tables 6.10

and 6.11. In both tables the "Daily" Column refers to value of the statistical parameter determined using daily simulated values and daily observed values which are patched using the TDSGEN program from the weekly grab of samples, whereas the "Weekly" Column refers to value of the statistical parameter calculated using only the weekly grab of samples and the simulated values for the particular day. In general the conservation and regression statistics show a fair ability of the hydrosalinity processes encoded in *ACRUSalinity* to mimic the natural processes taking place in the catchment.

- The conservation statistics, save for the skewness coefficient, do not indicate high divergence between observed and simulated values. The high difference observed between the skewness coefficients, however, reveals a considerable difference in the symmetry of the observed and simulated salinity distributions.

- The regression statistics show a very good fit with:

    - the slope showing a slight over-simulation of the model,
    - the Y-intercept having a value close to 0, showing a slight over-simulation, and
    - the correlation coefficient and coefficient of determination showing a high degree of association between observed and simulated values.

Table 6.10 Conservation statistics of streamflow TDS concentration at Camden (U1H005)

Statistical parameter	**Observed**		**Simulated**		**Difference %**	
	Daily	**Weekly**	**Daily**	**Weekly**	**Daily**	**Weekly**
Mean (mg/l)	49.81	48.12	55.82	48.33	12.07	0.44
Standard deviation	10.57	10.18	12.57	12.49	18.92	22.69
Skewness Coefficient	0.45	0.42	0.21	-0.31	-53.33	173.81

Table 6.11 Regression statistics of streamflow TDS concentration at Camden (U1H005)

Statistical parameter	Value	
	Daily	Weekly
Slope	1.11	0.97
Base constant (y-intercept)	0.33	1.52
Correlation coefficient	0.92	0.79
Coefficient of determination	0.87	0.63

6.7 Conclusions

This chapter has discussed the code validation and verification of the hydrosalinity module of *ACRU*. The code validation which was undertaken based on the principle of mass conservation has shown that the major algorithms of the new module are free of errors emanating from incorrect computer coding, except for minor rounding errors. Similarly, the verification undertaken to evaluate how this module performs under field conditions through comparison of model simulation against observed data has yielded good result when taking into account the data limitations for some of the hydrosalinity input parameters for the Mkomazi Catchment, and considering the complex nature of actual hydrosalinity processes, as they involve geochemical processes in addition to all of the other processes influencing water quantity.

The next chapter reviews the various sensitivity tests undertaken in this project in order to examine model response to changes in values of the main input parameters of *ACRUSalinity* and a case study in the Mkomazi Catchment to demonstrate some potential applications of the module.

7. SENSITIVITY ANALYSIS AND CASE STUDY

Sensitivity analysis of the main input parameters to the new module, and a case study on land use change and water resources development scenarios are undertaken following the validation and verification of *ACRUSalinity*. The case studies are carried out for the same catchment used in the verification process, *viz.* the Upper Mkomazi Catchment in KwaZulu-Natal province, South Africa. This chapter therefore describes the following:

- A sensitivity analysis of the main *ACRUSalinity* module parameters
- Case studies that include an assessment of temporal and spatial changes in streamflow salinity, as well as
- Modelling the impacts of land use change and water resources developments on the catchment's TDS balance.

7.1 Sensitivity Analysis of the Basic *ACRUSalinity* Parameters

The testing of a model's performance is only considered to be complete once a careful and detailed sensitivity analysis has been conducted. This is also a very useful tool for building confidence in the model's structure (Schulze, 1995). Sensitivity analysis helps to examine the impact of less accurate data on model outputs. Görgens *et al.* (2001) suggest that, where sound data are not available from field observations or theoretical knowledge, those model components which are affected should be subjected to well designed sensitivity tests.

A sensitivity analysis is performed by assuming various values for given parameters. According to Konikow (2002), this helps to determine the sensitivity of the model to factors that affect flow and transport and to errors and uncertainty in data. Evaluating the relative importance of each factor helps determine which data must be defined most accurately and which data are already adequate or require minimal further definition. If additional data can be collected in the field, such a sensitivity analysis helps to decide which types of data are most critical and how to get the best return on the costs of additional data collection. If additional data can not be collected, then the sensitivity tests can help to assess the reliability of the model by demonstrating the effect of a given range of uncertainty or error in the input data on the output of the model.

Four input parameters that are specific to the hydrosalinity module are considered in this sensitivity analysis. Each of these parameters, in turn, is varied between extremes of plus or minus 50% of the base value. For the purpose of this dissertation the rate constant (k) and the salt saturation (equilibrium) parameters are assumed to remain constant down the soil profile and groundwater store. Thus, in most of the sensitivity tests the same value is used for topsoil, subsoil and groundwater store. The following sections discuss the sensitivity of model outputs to these parameters.

7.1.1 Effect of the salt uptake rate constant on subsurface water and runoff salinity

The salt uptake rate parameter is used in salt generation computations. The value of this parameter can be estimated through fitting a regression equation to a time series soil moisture and groundwater store TDS concentration values measured between two rainfall events. However, owing to the limitations in the availability of such data for the Mkomazi Catchment its value was estimated through calibration of the model. Therefore, a sensitivity analysis was performed to evaluate the effect of errors in this parameter on the topsoil, subsoil and groundwater stores as well as on runoff salinity.

Runoff salinity is the result of the combined effect of quickflow and baseflow as well as their associated TDS concentrations. In the case of quickflow, unless there is a contribution otherwise from saturated upward flow, its TDS concentration is neither directly nor indirectly influenced by the value of the salt uptake rate constant, whereas, baseflow salinity is affected directly by the value of this parameter. Therefore, based on this idea, one would expect to see a major deviation in the curves representing change in baseflow salinity and change in runoff salinity in response to changes in the salt uptake rate parameter. However, no significant difference can be noticed between the two curves (Figure 7.1). This phenomenon is attributed to the nature of the land use of the sub-catchment used for simulation of this sensitivity test. The first *ACRU* sub-catchment in the Upper Mkomazi Catchment is used for the various sensitivity test simulations. The land use of this sub-catchment is dominated by forest. Forest plantations are generally characterised as having high interception levels and increased rates of infiltration that result in reduced stormflows. Therefore, runoff volumes from these areas are mainly comprised of baseflow. The simulated stormflow, for example, was found to be only 5 % of the total runoff from the sub-catchment used in this sensitivity test. This results to closer TDS concentration values between runoff and baseflow from such areas (Figure 7.1). A

small difference can be noticed only at the two extremes of change in k values. This small difference reveals that runoff salinity is relatively less sensitive than baseflow salinity to changes in salt uptake rate constant. In general both output parameters, baseflow and runoff salinity, have shown low sensitivity to changes in the value of the salt uptake rate constant.

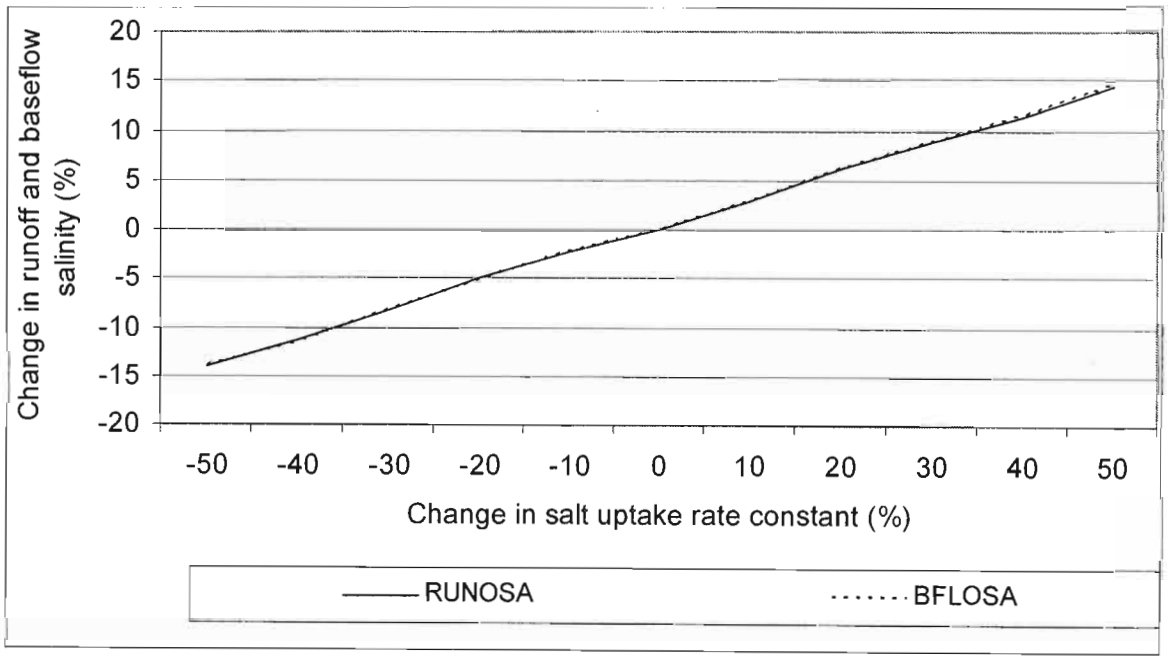

Figure 7.1 The effect of changes in salt uptake rate constant, k, on baseflow salinity (BFLOSA) and runoff salinity (RUNOSA)

Figure 7.2 shows the effect of change in salt uptake rate constant on topsoil, subsoil and groundwater store salinity. As it can be seen from the various curves, the sensitivity to changes in salt uptake rate constant increases from the topsoil down to groundwater store. Thus the topsoil moisture salinity (TOPSSA) is less sensitive to changes in the salt uptake rate constant than the subsoil moisture salinity (SUBSSA). The subsoil moisture salinity in turn is less sensitive than the groundwater store salinity (GWSA). The difference in sensitivity between the different subsurface components can be attributed to the variation in "evapoconcentration" and the degree of dilution by rainfall between these components. In general, the three subsurface components have shown low sensitivity to changes in the salt uptake rate constant.

Another remarkable observation that can be noticed from Figures 7.1 and 7.2 is that the change in surface and subsurface water salinity response to changes in salt uptake rate

constant increases at a decreasing rate. This phenomenon can be described by the fact that, as the salt uptake rate increases it results in increased subsurface TDS concentrations. The upper limit of subsurface water salinity (salt saturation) value then starts to take control of the amount of salt that can be generated on a particular day, where a further increase in the value of salt uptake rate results in lower increase in subsurface water salinity. A similar trend can also be noticed of the effect of decreasing values of the salt uptake rate constant on subsurface water salinity. In this case, however, the change in subsurface water salinity decreases at an increasing rate. This can also be explained by a similar reason, where at low values of subsurface water salinity (as compared to the salt saturation value) salt generation is less constrained by the salt saturation value and hence a small decrease in the value of salt uptake rate constant results in a significant difference in subsurface TDS concentration . Therefore, the sensitivity of subsurface water salinity to salt uptake rate constant increases with a decrease in *k* value and decreases with increase in *k* value.

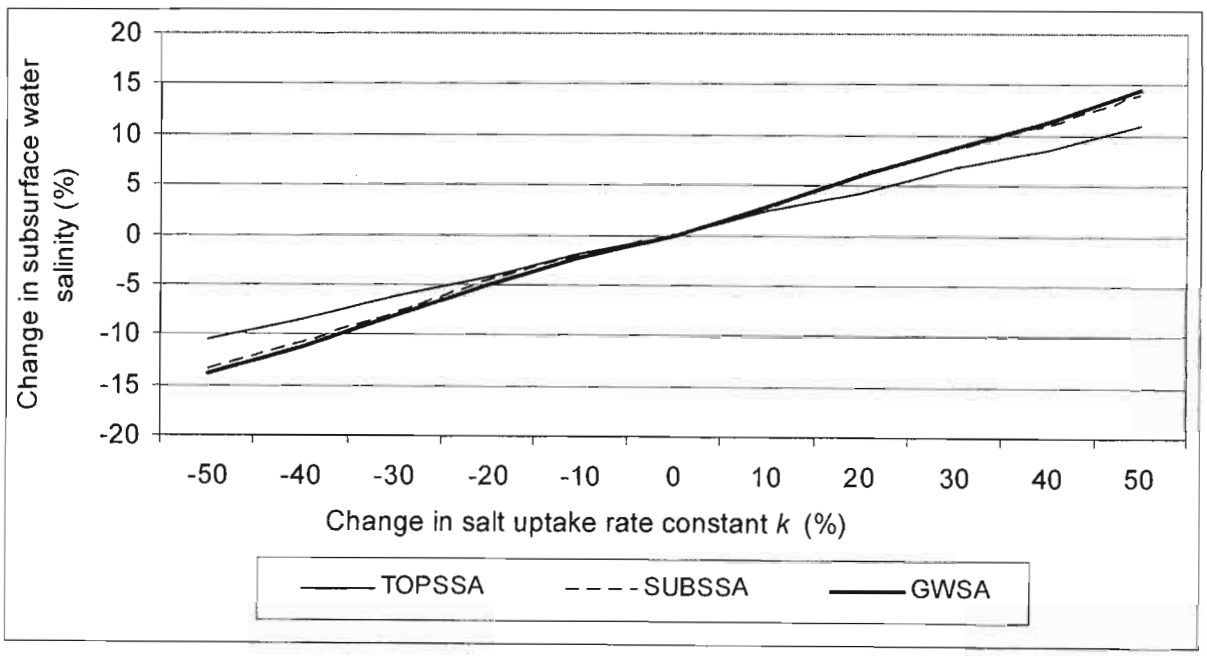

Figure 7.2 The effect of change in salt uptake rate constant on the topsoil salinity (TOPSSA), subsoil salinity (SUBSSA) and groundwater salinity (GWSA)

7.1.2 The influence of changes in salt saturation values on runoff and subsurface water salinity

Salt saturation is one of the major input parameters to the salt generation equation. This value represents the maximum subsurface water salinity beyond which no salt generation takes place. As can be observed from Figure 7.3, baseflow and runoff salinity have shown almost the same sensitivity for changes in the salt saturation value. This is due to the reason mentioned in the previous section, which is attributed to the nature of the land use in the sub-catchment used for the sensitivity test simulations. In general, both curves show low sensitivity of baseflow and runoff salinity to changes in value of the salt saturation parameter.

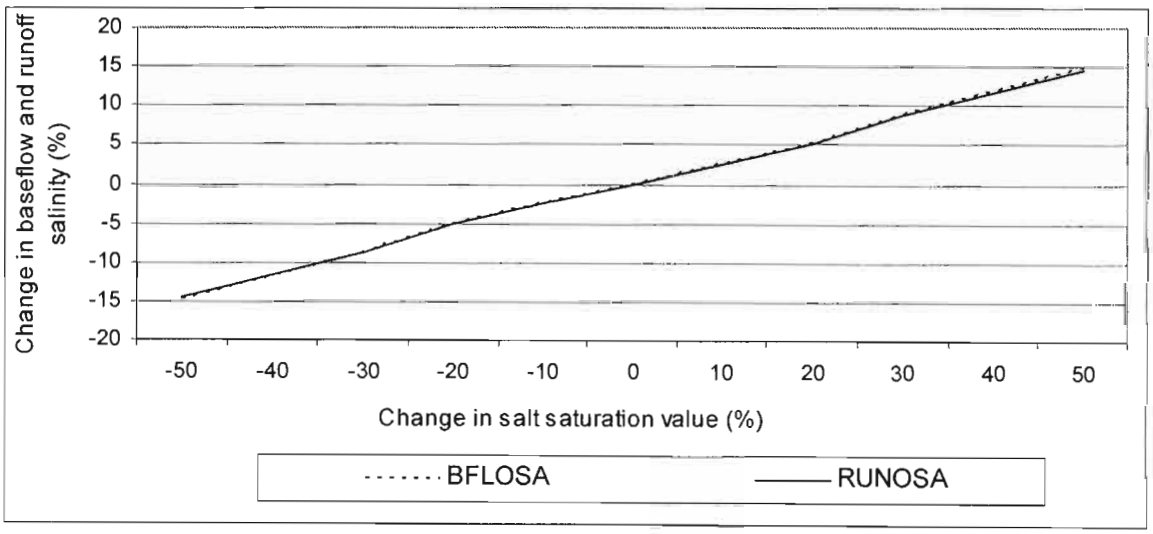

Figure 7.3 The impact of changes in value of the salt saturation parameter on runoff salinity (RUNOSA) and baseflow salinity (BFLOSA)

Figure 7.4 shows the effect of changes in salt saturation value on subsurface water salinity. The different curves reveal that groundwater TDS concentration (GWSA) is relatively more sensitive than subsoil water salinity (SUBSSA) which in turn is more sensitive that the topsoil water salinity (TOPSSA). The difference in sensitivity between the three subsurface components can be attributed to the variation in "evapoconcentration" and the degree of dilution by rainfall between these components. In general, the topsoil, subsoil and groundwater salinity have shown low sensitivity to changes in value of the salt saturation parameter.

All the curves in Figures 7.3 and 7.4 show a certain degree of upward curvature. This curvature shows an increase in subsurface water salinity at an increasing rate with an increase in the salt saturation value. This can be explained by the fact that as the salt saturation value increases, the asymptotic value (the maximum TDS concentration value) at which, the salt generation becomes zero, is pushed forward resulting in an increased rate of change in subsurface water salinity. Similarly, a decreasing change in salt saturation value results in a decrease in subsurface water salinity at a decreasing rate. This can also be explained by the same reason. As subsurface water salinity decreases, the salt generation mechanism is less governed by value of the salt saturation parameter. Rather, the other parameters of the equation, such as the salt uptake rate constant, will have more control on the salt generation processes, as described in the previous section.

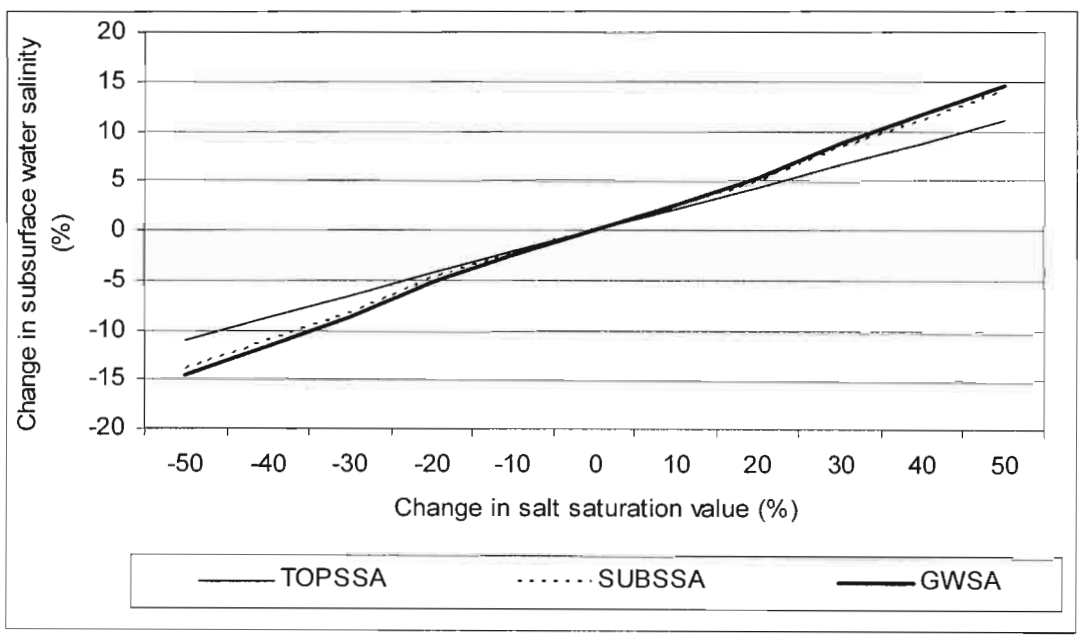

Figure 7.4 Sensitivity of the topsoil salinity (TOPSSA), subsoil salinity (SUBSSA) and groundwater salinity (GWSA) to changes in values of the salt saturation parameter

7.1.3 Effect of initial soil water salinity on time series subsurface water and runoff salinity

The initial soil moisture salinity parameter is one of the basic inputs to the module. This parameter is input to the module in order to account the effect of the initial soil moisture at the

beginning of the simulation period on surface and subsurface TDS balance. A sensitivity test was conducted to assess the impact of this parameter on topsoil, subsoil, groundwater store and runoff salinity.

Figure 7.5 shows sensitivity of baseflow and runoff average salinity to changes in initial soil moisture salinity. Only a minor difference can be noticed between the sensitivity curves of baseflow and runoff salinity. As explained in the previous sections, the reason for this phenomenon is associated with the nature of the land use in the simulated catchment. However, baseflow salinity (BFLOSA) shows relatively higher sensitivity than runoff salinity (RUNOSA).

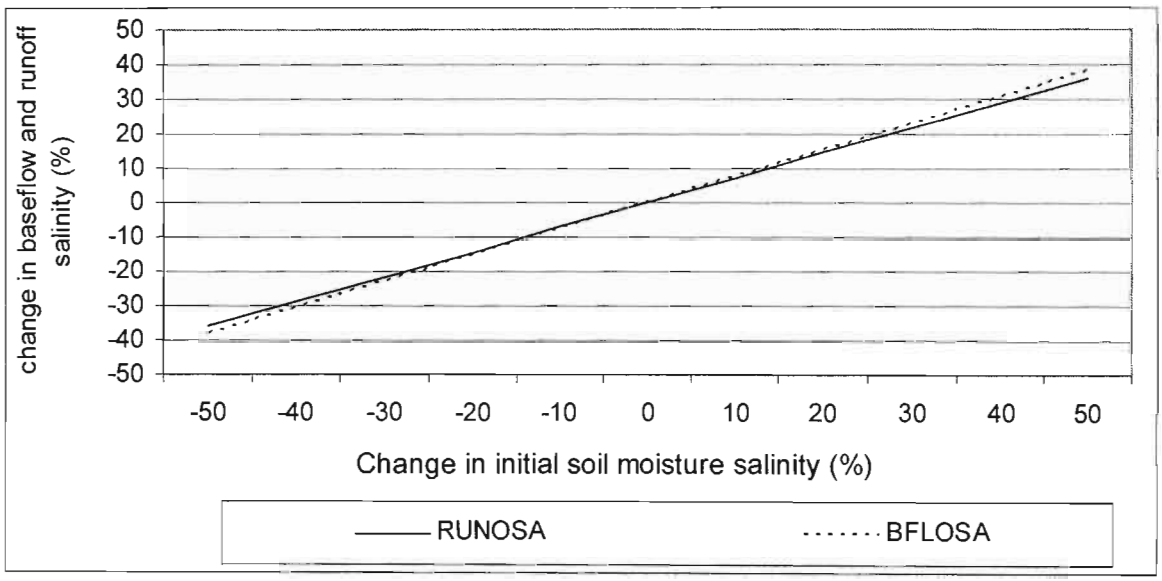

Figure 7.5 Sensitivity of baseflow salinity (BFLOSA) and runoff salinity (RUNOSA) in response to changes in initial soil horizon salinity

Simulated time series TDS concentration values of the topsoil horizon at different initial TDS concentration values (INITOPSSA) are plotted on the same graph to view the general trend in subsurface water TDS concentration with time in response to changes in value of this parameter (Figure 7.6). For the first few months of the simulation period, a considerable difference can be noticed between the five curves representing daily topsoil TDS concentration outputs simulated at different initial TDS concentration values. However, this difference between these curves decreases with time. Therefore, the impact of initial topsoil TDS concentration values on subsequent daily TDS concentration values shows a decreasing

trend with time. The impact of initial subsoil salinity on subsequent daily subsoil TDS concentration values has also shown a similar trend with time (Figure 7.7).

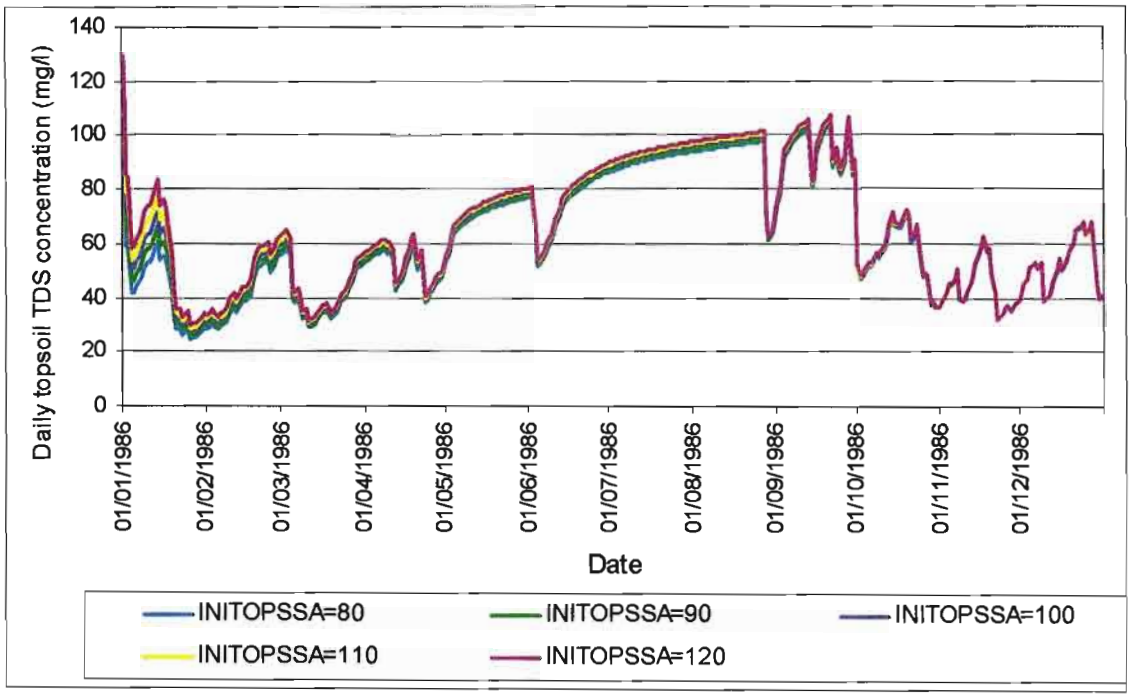

Figure 7.6 Daily simulated topsoil TDS concentration curves at different initial topsoil salinity (INITOPSSA) values

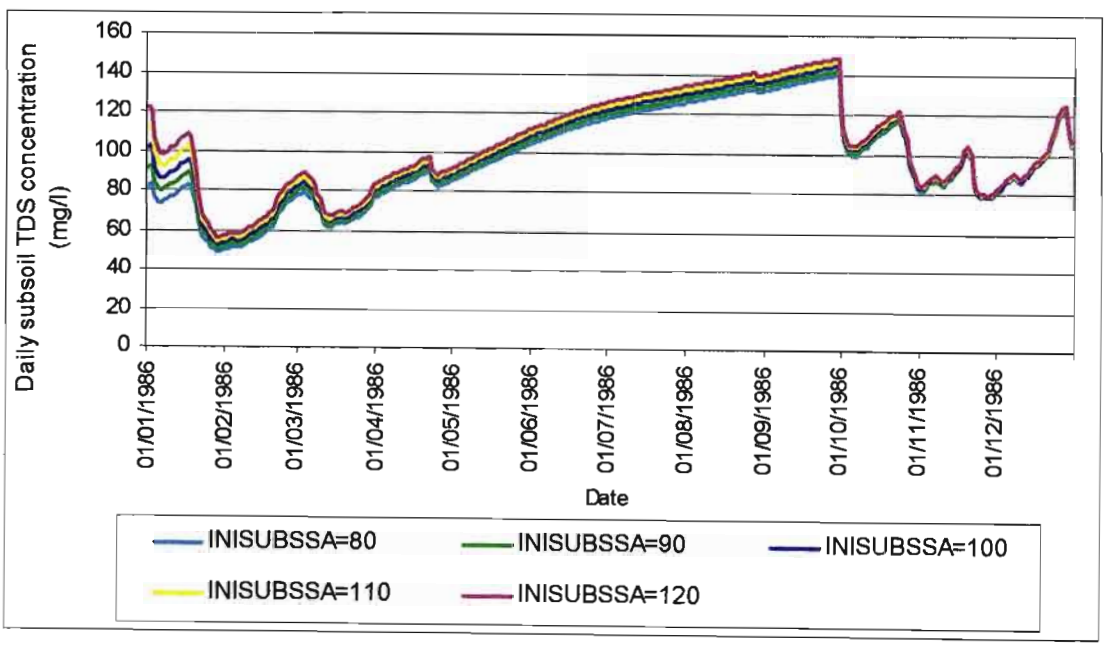

Figure 7.7 Daily simulated subsoil TDS concentration curves at different initial subsoil salinity (INISUBSSA) values

The decreasing impact of changes in the initial topsoil salinity value on subsequent days' TDS concentration with time initiated the idea of conducting separate sensitivity tests for different periods of the year. Therefore, the simulation period was divided into four quarters, each quarter representing three months of the simulation period. Figure 7.8 shows sensitivity of daily soil moisture salinity to changes in the value of initial soil moisture salinity. The result shows that topsoil TDS concentration is highly sensitive to changes in initial soil moisture TDS concentration in the first three months of the year (first quarter) compared to subsequent periods of the year. Although the remaining quarters of the year show similar sensitivity of the topsoil TDS concentration to changes in initial soil moisture TDS concentration, the sensitivity does decrease from the third quarter to the fourth quarter of the year. Sensitivity of the subsoil and groundwater store TDS concentration to changes in this parameter are also shown in Figures 7.9 and 7.10. From comparisons of these three graphs, it can be concluded that sensitivity of subsurface TDS concentration to changes in initial soil moisture salinity decreases with time and increases downward from topsoil to groundwater store. This can be explained by the following reasons:

- With time, part of the initially stored soil moisture is displaced by the infiltrated rainfall or irrigation water applied on the area resulting to dilution and subsequent reduced impact of the initial value on daily TDS concentration.
- The topsoil's TDS concentration is more frequently diluted through rainfall or irrigation water recharge as compared to subsoil or groundwater store. This is because the topsoil horizon is almost always recharged during a rainfall event or during irrigation. However, the recharge of subsoil and groundwater store is controlled not only by the quantity of water stored in the topsoil horizon but also by the physical characteristics of the topsoil horizon that control its moisture release characteristics. Therefore, impact of the initial TDS concentration value on subsoil and groundwater store lasts for a longer period of time than on topsoil horizon.

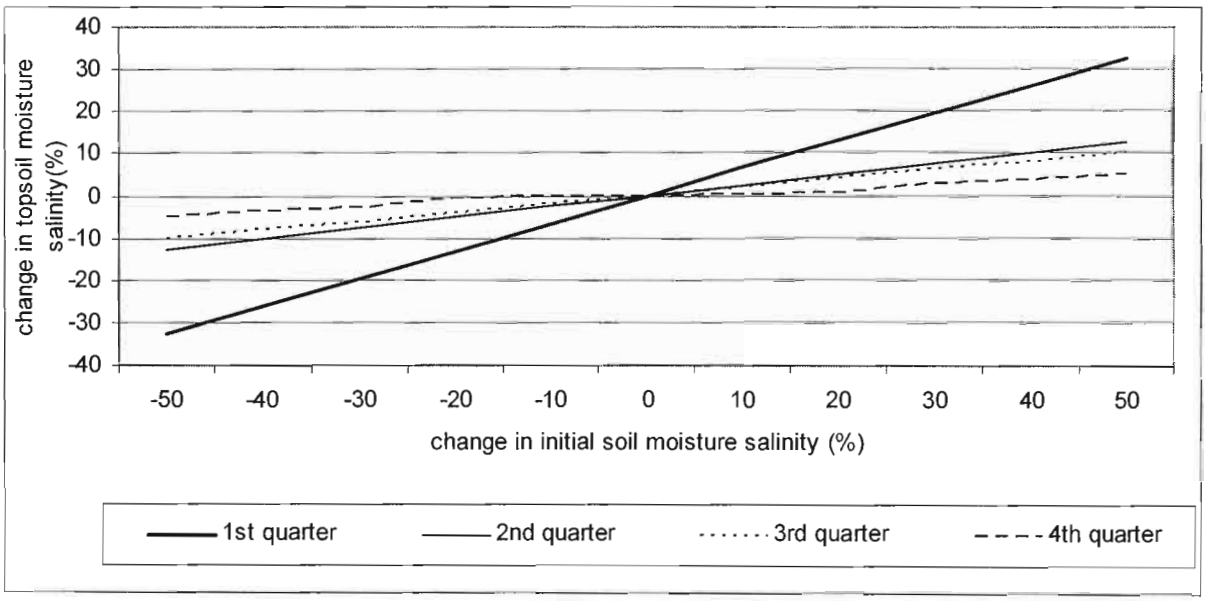

Figure 7.8 The influence of changes in initial soil moisture salinity on topsoil moisture average salinity at different times during the year

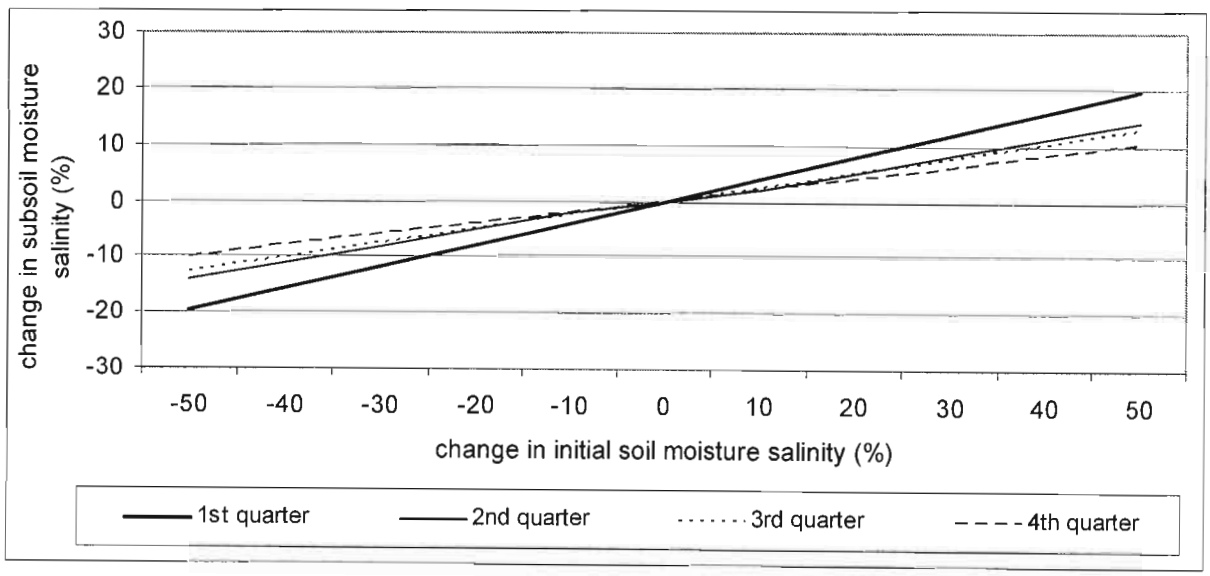

Figure 7.9 The influence of changes in initial soil moisture salinity on subsoil moisture average salinity at different times during the year

The preceding relevant graphs are also displayed in the same graph (Appendix E) for the ease of comparison of model sensitivities between parameters.

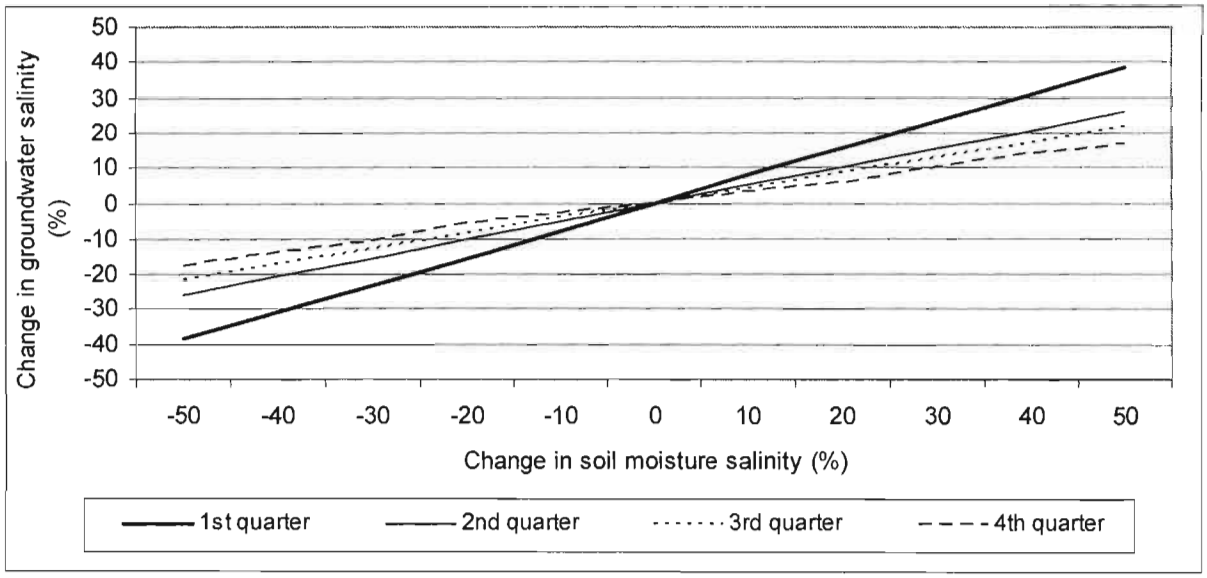

Figure 7.10 The influence of changes in initial soil moisture salinity on groundwater average salinity at different times during the year

7.1.4 Effect of initial reservoir storage salinity on time series reservoir storage and outflow salinity

The initial reservoir storage salinity value is an important input for reservoir TDS balance computations in *ACRUSalinity*. Hence, it is appropriate to conduct sensitivity tests on this parameter. To assess if a certain trend exists in the impact of the initial reservoir storage salinity, INIRESSA, on daily TDS concentration values, as in the case of subsurface salinity, the daily TDS concentration outputs from the module are plotted in the same graph (Figure 7.11).

From this figure it can be seen that no significant difference can be observed between the various reservoir storage TDS concentration curves simulated at different initial reservoir salinity values varying between 46.4 mg/l and 69.6 mg/l, i.e. plus or minus 20 % of its base value (58 mg/l). Therefore, there was no need to conduct different sensitivity tests at various intervals of the year as was done for the case of soil moisture salinity.

The impact of changes in initial reservoir salinity on mean reservoir storage and outflow salinity is shown in Figure 7.12. The figure shows that the TDS concentration of water discharged from the reservoir (OUTFSA) is relatively more sensitive to changes in reservoir

initial storage salinity than the reservoir storage TDS concentration (RESSA). However, the overall sensitivity of the reservoir storage and outflow salinity to changes in initial storage salinity is very low.

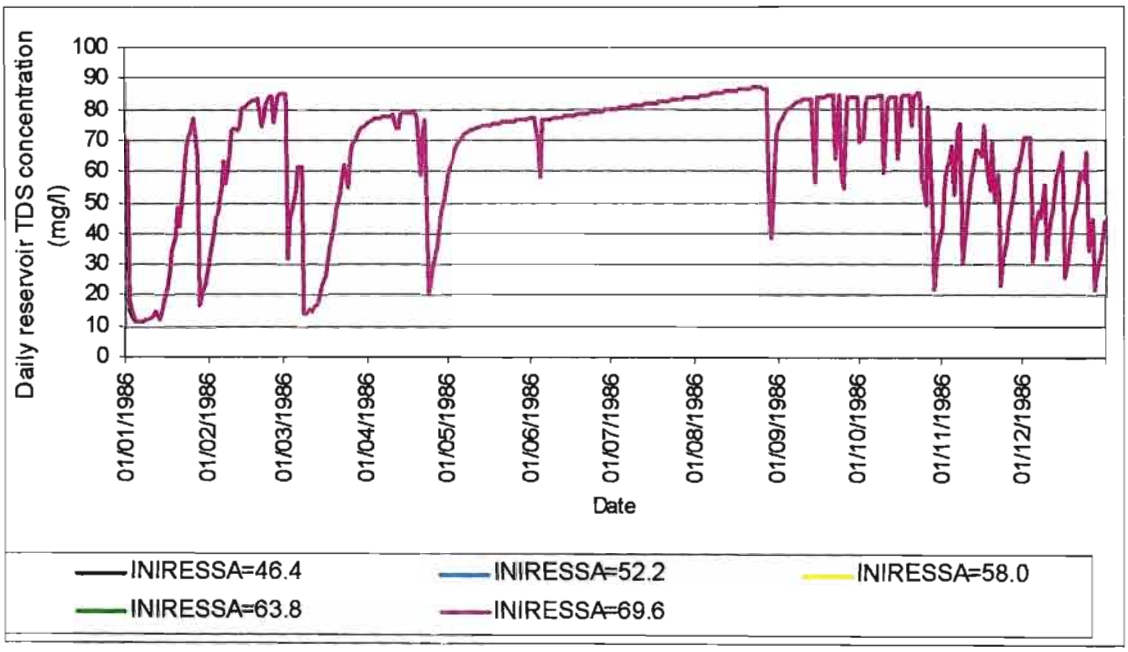

Figure 7.11 The impact of initial reservoir storage salinity on simulated daily reservoir storage average salinity

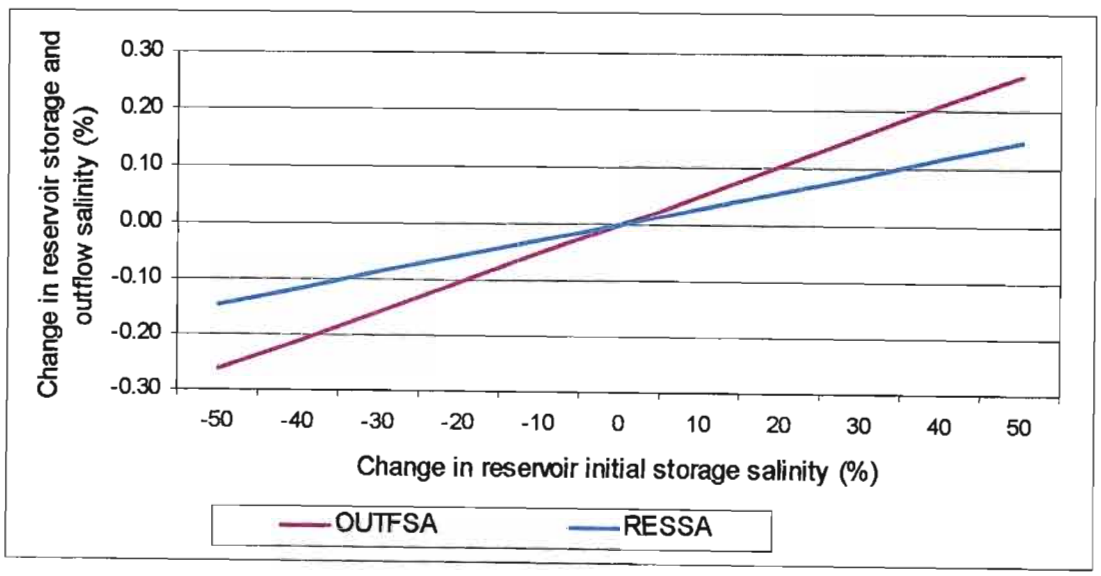

Figure 7.12 Sensitivity of reservoir storage and outflow average salinity to changes in reservoir initial storage salinity

7.2 Some Applications of *ACRUSalinity*: Case Study in the Upper Mkomazi Catchment

This section demonstrates some applications of the hydrosalinity module of *ACRU* with scenarios and case studies in the Upper Mkomazi Catchment. The scenarios and case studies include:

- spatial change in streamflow TDS concentration and salt load at various sub-catchment outlets
- seasonal and long term temporal changes in streamflow TDS concentration and salt load at the catchment outlet
- the impact of a new reservoir on downstream TDS concentration and
- the influence of future land use change on downstream TDS concentration.

7.2.1 Spatial and temporal variations in streamflow salinity within the catchment

One of the major applications of hydrological and water quality models is for an assessment of temporal and spatial changes in values of a variable of interest (for example streamflow and its TDS concentration). This allows catchment managers to anticipate the duration of elevated salinity and salt load and to identify which part of their catchment is likely to have a greater or lesser contribution to the total salt load at the catchment outlet. Such information may then be used to take appropriate measures or management options at the right place. Similarly, the result from an assessment of temporal changes in salt load and concentration may help to understand the general long term trend and seasonal fluctuations in TDS concentration and salt load. Model outputs with seasonal TDS concentration trend might, for example, help to identify months of the year on which various management options such as blending options should be considered.

7.2.1.1 TDS concentration at sub-catchment outlets and reaches

An assessment at various reaches of the Upper Mkomazi Catchment based on simulations undertaken with *ACRUSalinity* for a period of 10 years, i.e. from 1986 until 1995, shows that streamflow TDS concentration spatially varies within the catchment and it is generally higher

at downstream than at upstream end of the catchment. This can be attributed partly to the re-use of water for irrigation and subsequent enrichment in dissolved solutes as it flows downstream. Figure 7.13, shows the relative TDS concentration at the outlet of each sub-catchment. The corresponding simulated mean TDS concentration and salt load values at the outlet of each sub-catchment are given in Table 7.1.

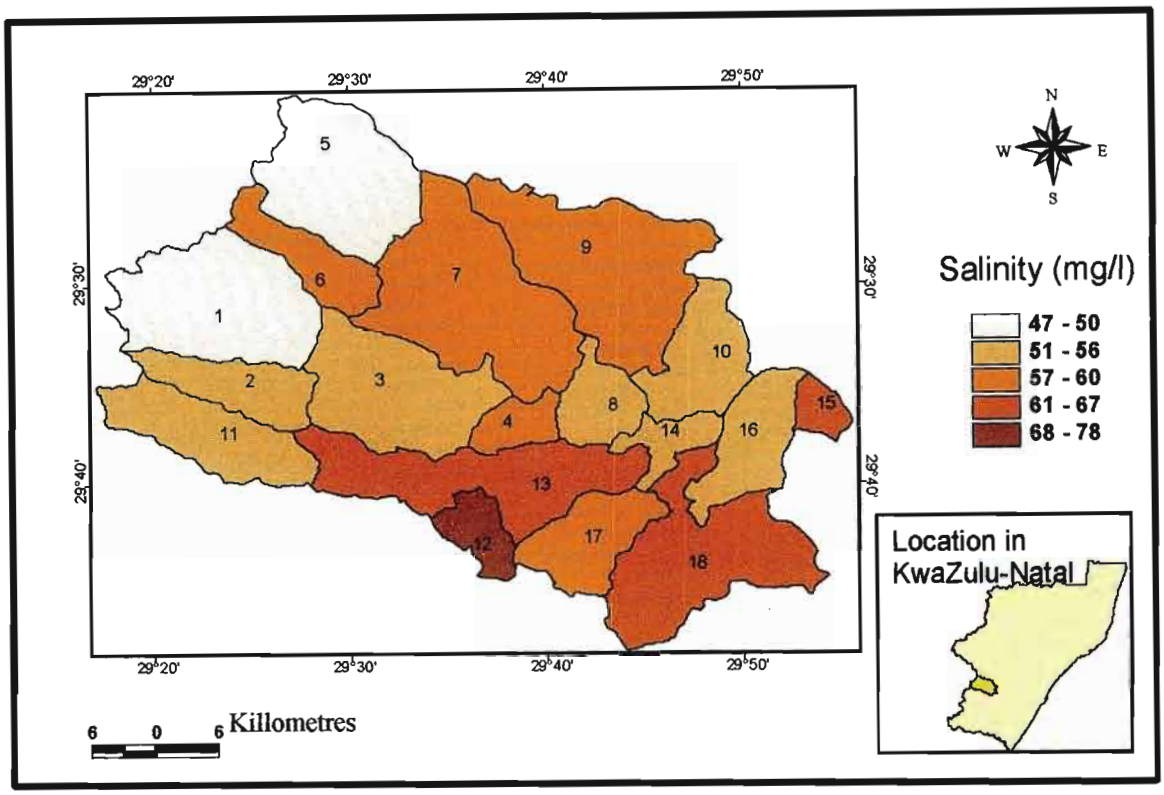

Figure 7.13 Spatial variation of mean TDS concentration at sub-catchment outlets of the Upper Mkomazi Catchment based on the simulation from 1986 to 1995

The difference in streamflow salinity between the various sub-catchments is as a result of the spatial variation in hydrologic, climatic and physiographic factors within the catchment. For example, Sub-catchments 1 and 12 have the lowest and highest simulated streamflow TDS concentration respectively (Figure 7.13). The main reason for the difference in streamflow salinity between the two sub-catchments is found to be as a result of the spatial variation in precipitation, evaporation, land use and other hydrologic, climatic and physiographic factors as shown in Appendix D. Sub-catchment 12 has the highest percentage of irrigated land compared to the other sub-catchments. Similarly, this sub-catchment has lower mean annual precipitation but higher mean annual evaporation compared to Sub-catchment 1. All these

factors together with the other factors result in relatively higher TDS concentration in Sub-catchment 12 compared to Sub-catchment 1.

The streamflow salt load increases downstream at various reaches of the main channel. For example, as it can be seen from Table 7.1 the streamflow salt load at the outlet of Sub-catchment 3 is less than that of Sub-catchment 4 which in turn has lower salt load than Sub-catchment 8. This is attributed mainly to the increase in streamflow volume downstream at various reaches along the main channel. The direction of flow and salt transport within the Upper Mkomazi Catchment is shown in Figure 6.6.

Table 7.1 Simulated average TDS concentration and salt load at the outlet of sub-catchments in the Upper Mkomazi Catchment

Sub-catchment No.	Average TDS concentration (mg/l)	Average Salt load (kg)
1	50.26	7761.5
2	57.05	3108.7
3	58.38	18490.0
4	57.92	20002.6
5	47.21	7351.9
6	53.04	3089.2
7	54.07	21578.6
8	55.65	44449.4
9	55.25	9157.6
10	54.37	13344.6
11	54.46	4357.6
12	64.04	1742.4
13	60.88	14547.3
14	56.47	74470.5
15	63.18	1137.9
16	67.83	5149.8
17	78.23	3885.3
18	59.30	92120.5

7.2.1.2 Temporal variations in streamflow salinity and catchment salt export

A preliminary assessment of salinity in the Mkomazi Catchment based on observed TDS concentration values is described in Section 6.1.5. However, most of the observed records used for that assessment were monthly samples, and at irregular intervals of time. Therefore, this topic will examine the temporal variations in TDS concentration of streamflow from the

Upper Mkomazi Catchment based on model outputs at a daily time step. Similarly, in this section the salt load export to the Lower Mkomazi Catchment will also be discussed.

Figure 7.14 shows the seasonal and long term variations in monthly averages of daily streamflow TDS concentrations (mg/l) and salt load (mg) at the outlet of the Upper Mkomazi Catchment. Seasonal fluctuations in TDS concentration can be noticed from the figure that can be attributed mainly to "evapoconcentration" and the dilution effect of rain falling on the area. The long term trend (ten years) for the area reveals an increasing streamflow TDS concentration with time. This can be due to an increase in reuse of water with time for irrigation and other purposes. Similarly, the salt load export of the catchment has shown seasonal fluctuations, although, the long term trend shows a decreasing trend with time. The decreasing trend in streamflow salt load, despite of increase in streamflow salinity, is attributed to the decrease in streamflow volumes.

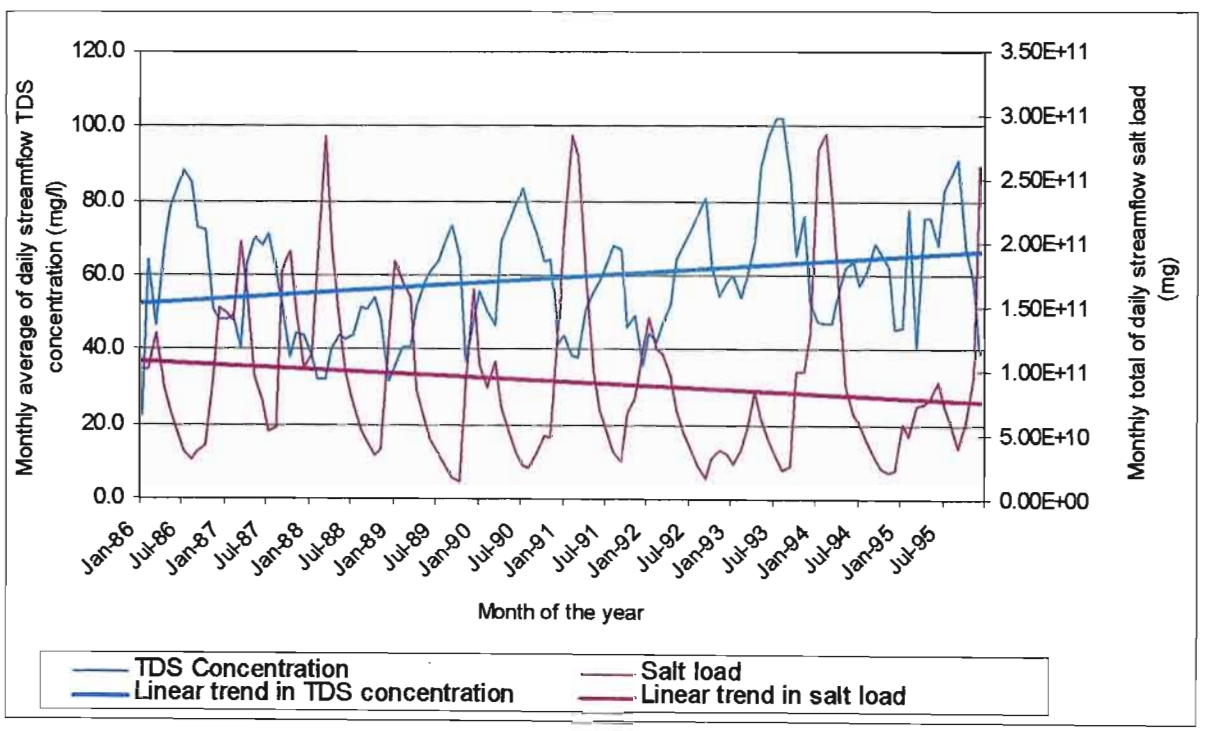

Figure 7.14 Simulated monthly average of daily TDS concentration and salt load at the outlet of the Upper Mkomazi Catchment (U1H005)

7.2.2 Modelling future scenarios

In order to demonstrate some potential applications of the new module, this section will attempt to examine scenarios of future water resource development and land use change in regard to their effects on downstream TDS concentration, *viz.* evaluating the impact of a proposed reservoir and the impact of land use changes from grassland to forest and to irrigated areas.

7.2.2.1 Evaluating the impact of a proposed reservoir on downstream TDS concentration

The Impendle is one of the proposed dams in the Mkomazi Catchment under the Mkomazi-Mgeni transfer scheme. This reservoir will be situated at the outlet of the 14th *ACRU* sub-catchment (Taylor, 2001). An analysis to optimise reservoir size was carried out by Ninham Shand Consulting Engineers. The first two reservoir sizes considered under this study for the Impendle Reservoir are 135 and 270 million m^3 (10^6 m^3). The impact of this proposed reservoir on downstream streamflow TDS concentration was assessed using simulation results from the hydrosalinity module of *ACRU*. This assessment considers impacts of the reservoir at the two sizes (135 and 270 million m^3) assuming the present land use (baseline).

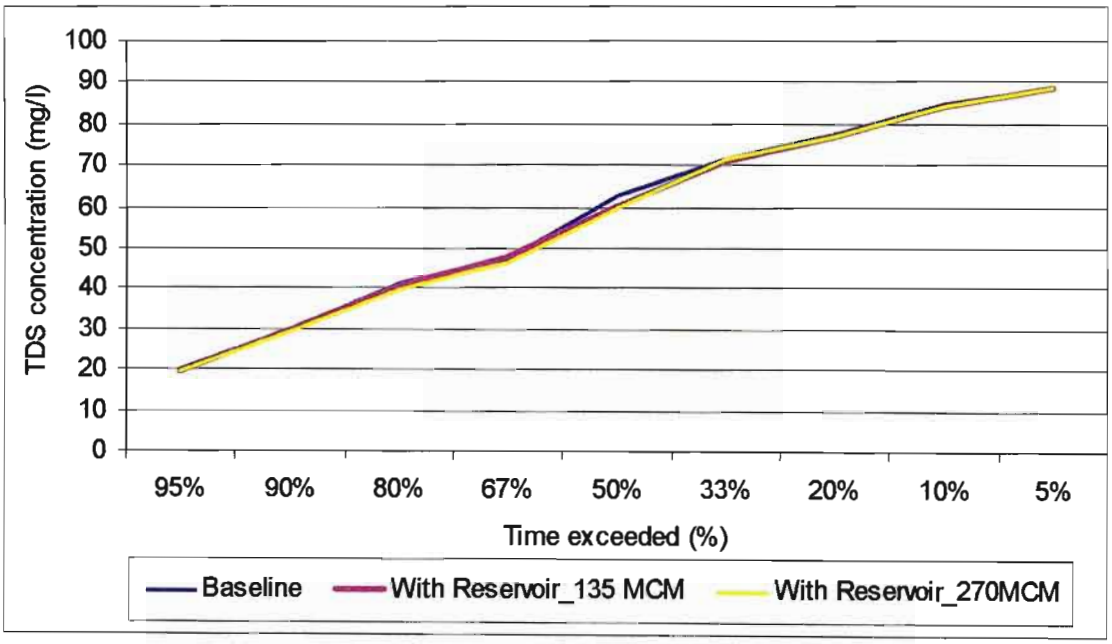

Figure 7.15 Impact of the proposed Impendle Reservoir on streamflow TDS concentration as simulated at the outlet of Sub-catchment 13 at two reservoir sizes

There is little difference on downstream streamflow TDS concentration as a result of the presence of the reservoir at the two different sizes. From Figure 7.15 it can also be seen that no significant difference exists between the two curves and the baseline. Only a minor difference can be noticed around the median TDS concentration values. Therefore, the proposed dam will not have significant impact on downstream streamflow TDS concentration both at reservoir size of 135 and 270 million m^3 especially on high and low TDS concentrations. This can be attributed to the low evaporation that characterises the Mkomazi Catchment, compared to many arid and semi-arid areas, where evaporation is a major cause of increased salinity due to "evapoconcentration" effect. The little "evapoconcentration" in the reservoir that could have resulted in increased downstream streamflow salinity is offset by the reduced area of the grassland where subsurface salt uptake and increased soil and groundwater salinity as a result of evaporation from the soil surface and transpiration from the plant could have been imposed.

7.2.2.2 The impact of land use change on downstream TDS balance

Any activity that alters the water balance of an area also alters its salt budget. Therefore, a change in land use practice is expected to result in a subsequent shift in downstream TDS concentration and salt load. For example, in the Murray-Darling Basin of Australia, the formation and growth of dryland salinity has been mainly attributed to land use changes from native forest vegetation to grazing and irrigated lands (Blackmorea *et al.*, 1999).

An assessment of the impact of commercial forest on downstream TDS concentration is undertaken through replacement of the original grassland (baseline) with forest in the sub-catchment chosen for this purpose (*ACRU* sub-catchment No. 13). The area coverage of the various land uses in this sub-catchment is shown in Table 6.2. The scenarios included in this assessment are what would be the impact on downstream streamflow TDS concentration if:

- 50 % of the sub-catchment was afforested and
- 75 % of the sub-catchment was afforested with eucalyptus.

The simulated average streamflow TDS concentration downstream of the afforested sub-catchment shows relatively lower values compared to those of the baseline grassland. This can be seen from the curves in Figure 7.16. Forest plantations consume much water and from

a greater soil depth as compared to grasses. This results in very low baseflow discharge. Therefore, flow from the other land use categories, such as impervious urban areas will constitute most of the streamflow at the sub-catchment's outlet. In *ACRU* the flow from impervious areas does not include baseflow. Hence, it is characterised with low TDS concentration. In general, from these scenarios it can be noticed that afforestation of grasslands especially in high water table areas, which are prone to dryland salinity, might be a viable management option to prevent land and water salinisation. On the other hand, these scenarios show that land clearing for grazing purposes might have a significant impact on dryland salinity.

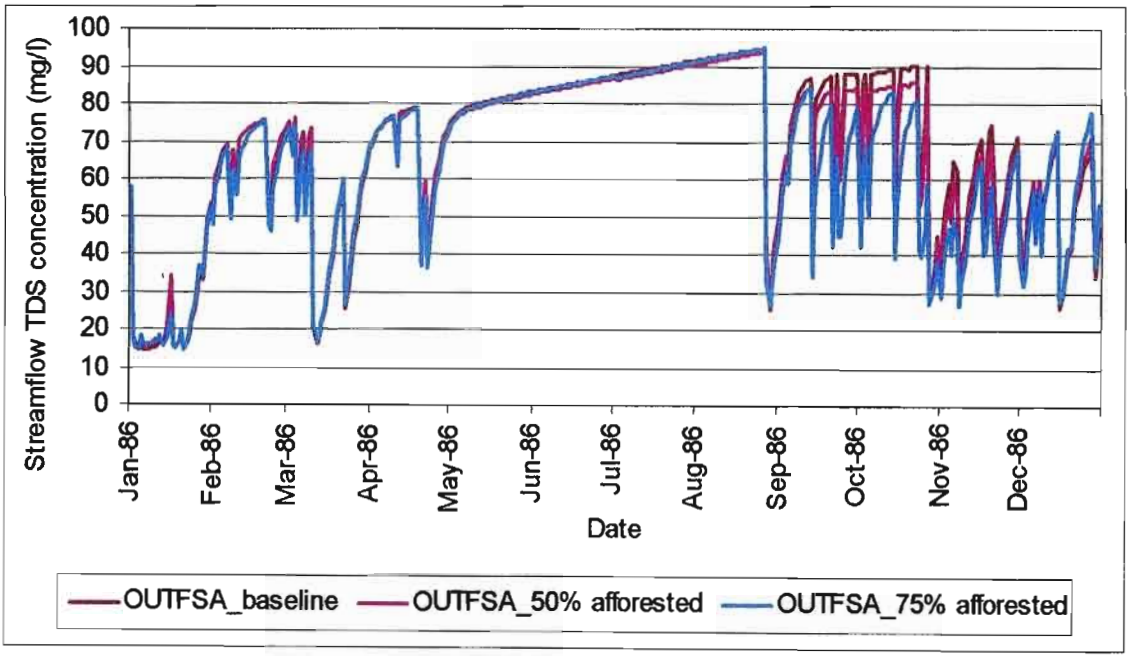

Figure 7.16 The impact of forests on downstream streamflow TDS concentration at the outlet of Sub-catchment 13

A numerical break down of the runoff constituents before and after afforestation is shown in Table 7.2. The results from this analysis show that water consumption as estimated by the actual evapotranspiration (AET) has increased as a result of afforestation with subsequent decrease in baseflow and quickflow depths. This in turn has resulted to an increase in baseflow and runoff TDS concentration. However, the streamflow salinity has decreased as a result of the decreased volume of runoff from the afforested land with subsequent reduction in runoff salt load contributed to the total streamflow.

Table 7.2 Flow components and their salinities of the runoff from the afforested area and the streamflow volume and its salinity at the outlet of Sub-catchment 13

Land use	Baseflow (average)		Quickflow (average)		Runoff (average)		Streamflow (average)		Aver-age AET (mm)
	Flow (mm)	Salinity (mg/l)	Flow (mm)	Salinity (mg/l)	Flow (mm)	Salinity (mg/l)	Flow (mm)	Salinity (mg/l)	
Baseline	0.54	85.02	0.52	11.30	1.06	73.55	0.28	67.54	1.43
50% afforested	0.28	101.10	0.12	11.30	0.40	94.99	0.24	66.61	1.59
75% afforested	0.28	101.10	0.12	11.30	0.40	94.99	0.23	64.26	1.59

Land use change from natural vegetation for extension of irrigation practices have also been a major cause of salinity in most arid and semi-arid areas of the world. This problem of land and water salinisation due to increased irrigation practices is aggravated when the irrigation management is poor. The hydrosalinity module of *ACRU* can aid in providing information for efficient management of irrigated lands with the objective of reducing the impact of the irrigation activity and management on land and stream salinity. To demonstrate the applicability of *ACRUSalinity* for this purpose a simulation study is undertaken to assess the impact of increasing irrigated area under different irrigation scheduling practices. The simulation study was undertaken by converting part of the grassland in *ACRU* Sub-catchment No. 13 of the Upper Mkomazi Catchment to an irrigated land. Streamflow TDS concentration at the outlet of this sub-catchment for the present land use is represented in Figure 7.17 by "OUTFSA_baseline". Monthly totals of daily rainfall events on the irrigated area (RFLIR) are also included in Figure 7.17, for ease of comparison of the TDS trend with rainfall events.

In this land use change scenario an assessment was made of the impact of an increase in irrigation activity from the present area of 350 ha to 4000 ha, i.e. 25 % of the total sub-catchment area on downstream TDS concentration for two irrigation scheduling practices. The irrigation scheduling practices considered are:

- applying irrigation water to refill the soil profile to the drained upper limit as soon as plant stress sets in (its impact on streamflow TDS concentration being represented in Figure 7.17 by OUTFSA_ISCHED=1) and
- applying a fixed amount of irrigation water, 15 mm, in a fixed irrigation cycle of 5 days (OUTFSA_ISCHED=2).

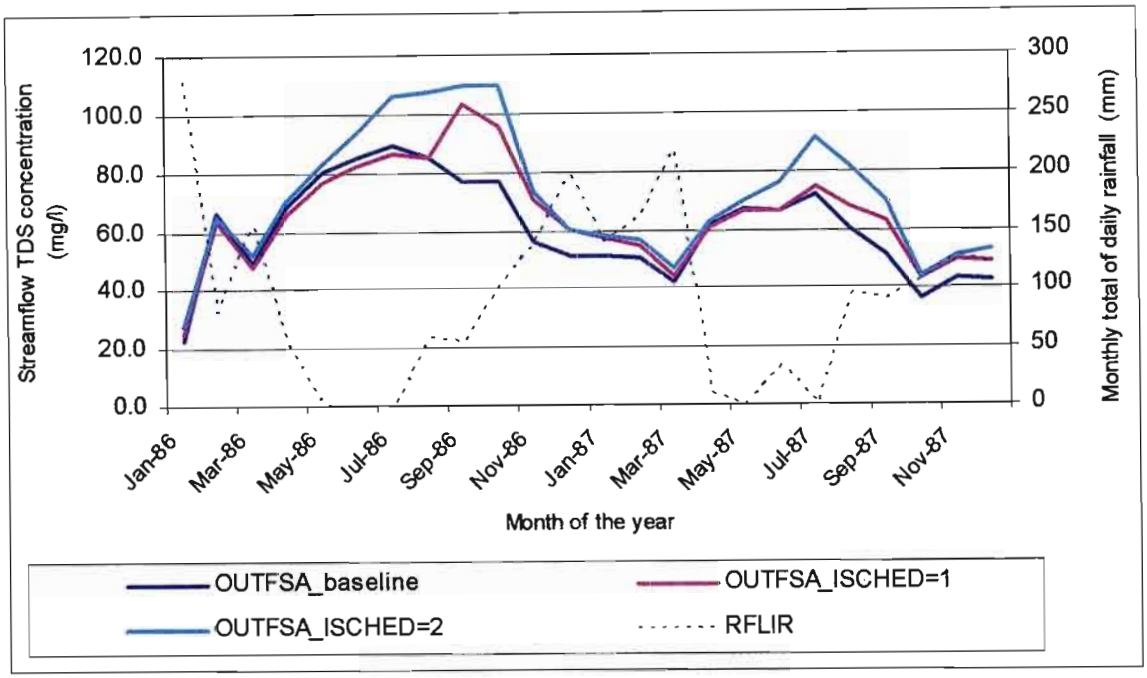

Figure 7.17 Impact of irrigation on downstream streamflow TDS concentration under different irrigation scheduling practices

The above graphical analysis of model outputs shows that increasing irrigated land generally results to increased downstream streamflow TDS concentration. However, the increased irrigation activity has less impact when irrigation water is applied to refill the soil profile to its drained upper limit than when using the irrigation scheduling with a fixed amount of irrigation water (15 mm) in a fixed irrigation cycle (5 days). The reasons for the differences in streamflow TDS concentration under the two irrigation scheduling practices are explained below.

The irrigation scheduling to refill the soil profile to the drained upper limit implies that little water percolates from the soil horizon to the groundwater store. This results in a relatively low contribution of baseflow to the total runoff from the irrigated land. Furthermore, when the

soil profile is recharged by rain water to its drained upper limit, no irrigation water is applied to the soil and hence no salt is added from irrigation water. This further results in low streamflow TDS concentration especially, during the dry season where the streamflow TDS concentration is even less than under the previous natural land use (grassland). However, the limited leaching when using this irrigation scheduling practice results in salt accumulation in the soil profile. Thus, the accumulated effect of the salt in the soil profile and groundwater store appears when flushing occurs due to a rainfall event (RFLIR). This effect can be noticed on the falling limbs of the streamflow TDS concentration curves in Figure 7.17. On the other hand, the fixed amount-fixed cycle irrigation scheduling results in increased flow through the soil profile and percolation out of it throughout the year. This generally leads to more salt loading when compared to the previous natural salt loading and the salt loading when using the irrigation scheduling to drained upper limit.

7.3 Conclusions

The various sensitivity tests described in this chapter give some information on the relative importance of the major hydrosalinity input parameters in terms of their impact on surface and subsurface water TDS concentration. However, results from these sensitivity tests should not be taken as conclusive, since some of these results are expected to change from one catchment to another and with time, depending on the prevailing climatic, hydrological and catchment conditions. The case study on the Upper Mkomazi Catchment has also demonstrated the wide range application of *ACRUSalinity* that include for an assessment of temporal and spatial changes in TDS concentration and salt load, the impact of water resources developments such as the construction of a reservoir and its size on downstream TDS concentration as well as the impact of land use change on streamflow TDS concentration and salt loading. Although, this and the previous chapters are based on discussions, and conclusions were also given at the end of each chapter, the next chapter will focus on some points that need further discussion and will present a general conclusion.

8. DISCUSSION AND CONCLUSIONS

Discussions with regard to a specific topic are detailed in each of the preceding chapters of the dissertation and conclusions have also been drawn at the end of each chapter. Therefore, the main aim of this chapter is to discuss points which require further detail, to compare some features of the hydrosalinity module of *ACRU* against other existing hydrosalinity models and to present a general conclusion based on the results of the research project.

In the last few decades increasing demands on limited water resources and increasing pollution of these resources (especially in terms of salinity) have been great cause for concern in many arid and semi-arid areas of the world, including South Africa (Cowan and Skivington, 1993). The sustainability of agriculture and the preservation of soil and water resources in these areas require an appropriate balance between the potentially negative on-site and off-site effects of salinity. In order to achieve these goals, catchment modelling plays an important role in assessing future trends in salt load and land salinisation as well as the impacts of different management options. However, this in turn requires an understanding of the different sources and processes involved in hydrosalinity. In order to understand the main sources and controlling processes of hydrosalinity and to explore some modelling techniques employed to describe the interaction between the various sources and hydrosalinity processes, an extensive literature review was undertaken in Chapters 2 and 3.

The various sources and processes of hydrosalinity are interrelated. The salinity hazard posed on a given land and water resource is influenced by various processes that are responsible for the release, transport, and deposition of salts related to each source. Hence, modelling of hydrosalinity processes requires a comprehensive approach that takes into account salt inputs from various sources such as atmospheric deposition, irrigation water and fertilizer application; salt uptake by plants and precipitation; release of salts from weathered soil and rock materials as well as transportation mechanisms through the soil profile to receiving streams and reservoirs. Therefore, catchment managers and other practitioners generally need to consider the interaction between factors such as climate, hydrology and catchment characteristics, including land use practices, for proper management of their land and water resources. Despite the fact that most of the sources and processes of hydrosalinity are highly

interrelated, knowledge about the main sources and the manner in which the dominating processes influence water salinity is vitally important for the development of hydrosalinity models.

As noted by Jayatilaka and Connel (1995), different modelling approaches can each play a role in some hydrological simulation. However, in developing a model or when applying an existing model to handle a particular problem, it is important to consider several factors that determine model suitability. Some of these factors are: the scale of the problem (be it field or catchment), the type of simulation (event or continuous) and the accuracy of the output required. In addition, the availability of data, both for model calibration and for verification, needs to be taken into account. Therefore, the basic types of water quality and quantity models are reviewed in Chapter 3 followed by how the various hydrosalinity processes are represented in these models, with special emphasis on soil salt balance and movement. Review of the various hydrosalinity models has shown that most of these models operate in lumped mode. However, hydrosalinity studies at a catchment scale usually require discretisation of the catchment into a number of (usually relatively homogenous) sub-catchments in order to accurately model the salinity level and salt loading in bigger catchments or in catchments with complex land uses and soils. Therefore, there is a research need to develop catchment based distributed hydrosalinity models. The hydrosalinity module of *ACRU, viz. ACRUSalinity,* can simulate TDS concentrations and salt loading both in single catchment (lumped mode) and in multiple sub-catchments (distributed mode), with salt transport occurring from one sub-catchment to another based on the direction of flow as determined by the cascading sub-catchment configuration. Therefore it is hoped that, the development of *ACRUSalinity* will make a significant contribution towards filling the abovementioned research needs in the facet of hydrosalinity modelling.

ACRUSalinity is developed in the object-oriented version of *ACRU, viz. ACRU2000.* This version has a modular structure, where new modules can be added to the model with little or no interference with the existing modules. The modular structure of *ACRU2000* has facilitated the development of *ACRUSalinity* because, with the new structure, any new module can easily inherit much of the basic structure and many of the objects of *ACRU2000.* This is possible in *ACRU2000* since it is implemented with an object-oriented programming technique. Therefore, the role of object-oriented programming tools such as the Java programming

language and Rational Rose Software were important in the development of *ACRUSalinity,* both when building new objects and when defining the relationship of these objects with the existing hydrological modules of *ACRU2000* for an easy flow of information and data between the various objects.

Although the object-oriented programming technique has significant merits over the procedural programming languages such as BASIC and FORTRAN, it is not without limitations. Some of the problems encountered during the development of *ACRUSalinity* were the low speed of execution and problems related with precision limits. It was noticed that *ACRU2000* takes a longer time for execution than the FORTRAN based *ACRU 300.* The second problem is attributed mainly to rounding errors. As described in Chapters 4 and 5, certain data objects such as *DWaterFluxRecord* and *DSaltFluxRecord* serve not only to store data, but also to conduct internal water and salt balance computations with the help of their parent classes. Therefore, if a new process under development attempts to transport salt from one component to another, and if the salt loading in the supplying (owner) component is lower than the salt load requested for transfer, then an error message is sent and execution halts. Such problems were encountered mainly during the distribution of the salt load from adjunct impervious and non-irrigated areas to a reservoir and to channel reaches in the presence of an internal reservoir. Therefore, in these processes dealing with salt load distribution, an attempt was made to avoid this type of problem through introduction of a "correction value" of plus or minus the difference between the quantity of salt stored in the owner component and the requested quantity of salt load for transport to a destination component. However, this correction value is added to, or subtracted from, the owner/destination component if, and only if, the difference ("correction value") is between -0.001 mg and 0.001 mg, since a difference outside of this limit might also be caused due to incorrect computer coding.

The subsurface TDS balance in *ACRUSalinity* generally adopts the technique employed by the DISA hydrosalinity model (Görgens *et al.*, 2001). However, subsurface salt movement is based primarily on the principle of conservation of mass and thus it depends mainly on the water balance and the direction of flow as conceptualised in the hydrological modules of *ACRU.* For example, subsurface salt movement associated with saturated upward and downward soil water flow depends mainly on the quantity and direction of flow as determined by the hydrological modules of *ACRU.* The subsurface component of a non-irrigated land is

represented in *ACRU* with two soil horizons (topsoil and subsoil) and an intermediate/groundwater store. The subsurface system of an irrigated land is represented with only a single soil horizon and a groundwater store. Therefore, the Lagrarian salt lagging approach used in the DISA model to account the impact of a difference in TDS concentration of percolation water entering into a layer and whose origin is from more than one overlying layers, is not employed in *ACRUSalinity*. This is based on the assumption that since the soil profile is divided into only two layers (in the case of non-irrigated lands), the depth of water percolating to the groundwater system on a particular day is less than the soil moisture content of the subsoil at the end of the previous day. Thus, the origin of the daily percolation water into the groundwater store is assumed to be only from its immediate overlying layer (i.e. the subsoil).

The process of salt generation in the DISA model is described by an empirical equation (Chapter 3, Section 3.4.3.1). However, this equation was reported not to be entirely successful in a realistic simulation of subsurface salt generation processes (Görgens *et al.*, 2001). Therefore, an attempt was made in *ACRUSalinity* to find an alternative equation that could describe this process. The first order rate kinetics equation was employed by Ferguson *et al.* (1994) to describe an enrichment of individual solute species in soil water. This equation was adopted in *ACRUSalinity* to describe salt generation in subsurface components. It describes the salt generation process in the soil and groundwater system fairly well. The problem in using this equation is, however, to obtain values for its parameters from physical measurements. Values of these parameters for most of the individual solute species can be obtained from literature (Ferguson *et al.*, 1994). However, no such data are available for total dissolved solutes, since this is probably the first research of its kind to apply this equation on total dissolved solutes. Estimated values of these parameters can be determined if time series of soil salinity data are available for the area. The rate constant, k, may be estimated from fitting a regression equation to observed data measured at below drained upper limit (DUL), i.e. when there is no significant mixing taking place due to percolation from an upper layer. Below DUL, drainage ceases and the water remaining is held by capillary forces which are sufficient enough to resist gravity (Schulze *et al.*, 1995b). Similarly, the equilibrium concentration of respective horizons may be estimated from salinity data recorded after a long spell of dry weather.

Runoff salinity depends on the volume and TDS concentration of stormflow and baseflow. Therefore, runoff TDS concentration is determined in *ACRUSalinity* based on an instantaneous mixing of surface and subsurface flows. The value of baseflow salinity is determined from the consideration of the combined effects of water and salt balance in the subsurface system. However, stormflow is assumed to have the same TDS concentration as the average salinity of rainfall in the catchment. This is based on the report from some researchers who have indicated that stormflow salinity is not expected to show a significant difference when compared to TDS concentration of the rain falling on the land, or the applied irrigation water (for example, Rhoades *et al.*, 1997; Mironenko and Pachepsky, 1998). The assumption that stormflow salinity as having the same TDS concentration as the rainfall salinity may not hold true in areas characterised with significant salt crusts. In such areas the stormflow salinity may initially rise with the rising limb of a hydrograph on the first flush of rainfall following a prolonged dry spell.

The salt load associated with runoff water is distributed to channel and/or reservoir reaches depending on the catchment configuration. In general, the determination of baseflow and stormflow salinity, as well as runoff salinity and salt loading and the subsequent salt allocation to a destination reach, is based on physical processes. Thus, the hydrosalinity module of *ACRU* is suitable for testing various "what if" scenarios to assess the impact of changes in land use, climatic and hydrologic as well as water resources developments such as construction of reservoirs, on future catchment TDS balance including surface and subsurface TDS concentration and salt export to downstream reaches.

The module evaluation phase of this research has involved code validation and verification against observed data. The code validation was undertaken mainly to detect errors emanating from incorrect computer coding through using the principle of mass conservation. The code validation has proved that the main algorithms describing the various hydrosalinity processes in *ACRUSalinity* are safe from such errors, except for minor rounding errors. The verification result through comparison of model simulation against observed streamflow TDS concentrations at Camden (U1H005) gauging weir in the Upper Mkomazi Catchment has shown good results. Both the graphical and the statistical analysis of observed and simulated values have indicated that the simulated streamflow salinity values mimic the observed values remarkably well.

A sensitivity analysis was carried out to assess model responses to changes in the values of the major hydrosalinity input parameters. From the sensitivity tests, it was noticed that runoff water salinity was less sensitive to changes in salt uptake rate constant (k) than baseflow salinity, although both parameters have also shown low sensitivity to changes in the value of k. However, a significant difference in sensitivity of TDS concentration of various subsurface components to changes in k was observed with an increasing sensitivity from topsoil down to the groundwater store. A similar result was also obtained from a sensitivity test on the impact of changes in value of the salt saturation (equilibrium) parameter on surface and subsurface components. The model has also shown a relatively high sensitivity to changes in initial subsurface TDS concentration for the first three months of the simulation period, but thereafter, the value of this parameter had little impact on surface and subsurface TDS concentrations. The model has shown low sensitivity to changes in initial reservoir water TDS concentrations. Therefore, no single input parameter dominantly impacts the surface and subsurface water TDS concentrations. Rather, TDS concentration in these components is a function of all the water quantity and salinity related parameters.

Because these are general observations from the sensitivity analysis, it is difficult to assume results from these sensitivity tests as being conclusive and applicable under all conditions. Rather, the sensitivity result for most of the parameters is expected to change, depending on climatic, hydrological and catchment conditions of an area. For example, results from an assessment of the impact of initial subsurface and reservoir TDS concentration on daily TDS concentration vary, depending on such factors as the volume and timing of rainfall events. If a high rainfall event occurs at the beginning of the simulation period then the initial TDS concentration is expected to have little impact on the subsequent days' TDS concentration, whereas, in the absence of any dilution by rainfall or irrigation water, in the case of subsurface components, the subsurface water salinity increases according to the first order rate kinetics and thus the model response would be high to changes in value of the initial subsurface water salinity.

Although, for a more accurate simulation and improved applications of the module, it is necessary to conduct further research and additions to the module, the present hydrosalinity module of *ACRU* comprises several process objects that can be used to provide a reasonable first order approximation in a number of hydrosalinity studies. The present applications of the new module include for an assessment of:

- the impact of changes in future climatic and hydrological changes on TDS concentration and salt loading
- the impact of forest plantations or clearing of forests on dryland salinity
- the on-site and off-site impacts of irrigation on surface and subsurface water salinity as well as its impact on downstream TDS concentrations in streamflow and salt loading
- the impact of water resources developments, such as a reservoir, on downstream TDS concentration or
- the impact of different management options on reservoir TDS concentration and salt loading.

In general, the new module generates a number of output information that could be used in the above-mentioned and other applications, whereas, the input information specific to the new module are very few compared to the extent of output information (Appendix A). Therefore, considering the module's intended use as a catchment scale hydrosalinity simulation tool mainly for application in developing countries where limited data is a major problem, the module is designed so that it can run using the minimum input information and yet provide reasonably adequate information for use in planning, design and management of land and water resources with the purpose of preventing land and water salinisation. Further research to enhance the performance of the newly developed hydrosalinity module is recommended in the next chapter.

9. RECOMMENDATIONS FOR FUTURE RESEARCH

Hydrosalinity processes are complicated since they involve the interaction between various sources and controlling factors, in addition to all the factors impacting water quantity. Hence, the adequate modelling of these processes, especially at a catchment scale, requires a comprehensive approach that accounts for the impacts of the various point and non-point sources of salinity. Most of the non-point sources and the basic hydrosalinity processes are included in the present hydrosalinity module of *ACRU, viz. ACRUSalinity*. Yet, inclusion of some processes and research on deriving the value of input parameters to the module need to be undertaken for more accurate and improved applications of the module in diverse catchments. The following important sources and associated processes of hydrosalinity could be accommodated in *ACRUSalinity* in the future:

- The present hydrosalinity module of *ACRU* does not take into account the impact of fertilizer and gypsum application on the TDS balance. However, this may have a substantial effect on surface and subsurface TDS balance, if the simulated catchment is dominated by irrigated lands. Therefore, the effects of fertilizer and gypsum application may need to be accommodated in the module.

- Industrial and urban effluents are important non-point sources of salt loading. However, the current hydrosalinity module of *ACRU* does not include the impact of urban and industrial effluents. Therefore, the effect of salt loading from these sources on urban runoff TDS concentration and salt loading need also be accommodated in the future.

- Currently *ACRUSalinity* simulates TDS concentration and salt loading of outflows from a reservoir and at river reaches downstream of the reservoir on daily basis. However, in order to capture the intra- daily differences in TDS concentrations and salt loadings, an algorithm needs to be included in the module in order for it to simulate salt routing through reservoirs and rivers at sub-daily time steps.

- Water which flows directly below the root zone through cracks (by-pass flow) on a heavy clay soil is reported to provide an important mechanism for solute leaching. Therefore, the

impact of cracking on surface and subsurface TDS balance, in general, and on the delayed stormflow in particular, also needs to be accommodated in the future.

- Further, in order to realistically simulate the movement of salts in sloping topography, *ACRU* needs to consider multiple terracing in the riparian zone and the interactions between these terraces. Thereafter, *ACRUSalinity* also needs to handle the movement of salts between the terraces.

- At present the daily stormflow salinity is assumed to have the same value as rainfall salinity. Therefore, *ACRUSalinity* needs to accommodate in the future for the impact of near surface flows and salt crusting on surface TDS balance.

- The present hydrosalinity module of *ACRU,* uses an irrigation water salinity as inputted by the user on monthly basis. Although it might result to a cumulative error, the module can also get this value from the TDS series generated at each point of abstraction of an irrigation water. Therefore, the module also needs to include an option where salt balance computations can use daily irrigation water salinity from the TDS series generated at each point of abstraction of the irrigation water.

- At this stage, the total stormflow generated in irrigated areas leaves the catchment on the same day. However, similar to the case of non-irrigated areas, stormflow generated from irrigated areas may take many days before the total stormflow leaves the catchment. Therefore, a lag function needs to be included for a stormflow generated from irrigated areas with subsequent incorporation of its impact on surface and subsurface TDS balance.

- In some areas surface dry atmospheric deposition from oceanic aerosols, continental dust, active volcanoes and/or anthropogenic inputs can have substantial impact on surface and subsurface water TDS balance. Therefore, the impact of dry atmospheric deposition on surface and subsurface TDS balance needs to be accommodated in *ACRUSalinity.* Similarly the impact of surface salt accumulation on TDS balance due to a capillary action also needs to be accommodated in the future.

- Finally, research needs to be conducted on the salt saturation (equilibrium) and salt uptake rate constant (k) parameters, both of which are employed during salt generation computations in *ACRUSalinity*. These two parameters are the most important parameters in describing salt generation processes in subsurface components. However, it is difficult to obtain values for these parameters through physical measurements. Therefore, research needs to be undertaken to derive a representative value from a combination of geological formations or soil types as well as hydrological and climatic conditions of an area, since the two parameters are expected to be influenced mainly by these factors. An expression with one or more variable from the above factors can then be included in *ACRUSalinity* so that the salt uptake rate and salt saturation parameters can be internally derived from the hydrological inputs of *ACRU*.

10. REFERENCES

Addiscot, T. M. and Wagenet, R. J. 1985. Concepts of solute leaching in soils: a review of modeling approaches. Journal of soil science. Vol. 36. 411-424.

Archeimer, B., Anderson, L. and Lepisto, A. 1996. Variation of nitrogen concentration in forest streams-influence of flow, seasonality and catchment characteristics. Journal of hydrology. Vol.179. 281-304.

Arnold, J. G., Williams, J. R., Srinivasan, R. and King, K. W. 1996. *Soil and water assessment tool (SWAT)*. USDA, Agricultural research service. Texas.

Aswathanarayana, U. 2001. *Water resources management and the environment*. A. A. Balkema publishers. The Netherlands.

Ayers, R. S. and Westcot, D. W. 1985. Water quality for agriculture. Irrigation and drainage paper No. 29. FAO. Rome.

Bath, A. J., Smidt, K. O., Görgens, A. H. M. and Larsen, E. J. 1998. Applicability of hydrodynamic reservoir models for water quality management in stratified water bodies in South Africa: Application of DYRESM and CE-QUAL-W2. Water Research Commission, Pretoria, Report No. 304/2/97.

Billett, M. F., Lowe, J. A., Black, K. E. and Cresser, M. S. 1996. The influence of parent material on small-scale spatial changes in stream water chemistry in Scottish upland catchments. Journal of hydrology. Vol. 187. 311-331.

Blackmorea, D. J, Goss, K. F, Newman, R. J. and Powell, J. 1999. Salinity management in the Murray Darling Basin [Internet]. Department of land and water conservation (NSW), Australia. Available from: <:http//www.atse.org.au/publications/symposia/proc-1999p17.htm> [accessed 12 August 2002].

Borland Software Corporation. 2001. *JBUILDER'5 Professional*. Borland Software Corporation. USA.

Bresler, E. 1981. Transport of salts in soils and subsoils. In *Land and stream salinity*, eds. J . W. Holmes and T. Talsma. 35-62. Elsevier scientific publishing Co. Amsterdam.

Butler, A. J. E. 2001. The development and evaluation of an operating rule framework for the *ACRU* Agrohydrological Modelling System. MSc thesis. School of Bioresources Engineering and Environmental Hydrology. University of Natal. Pietermaritzburg.

Campbell, K. L., Kiker, G. A. and Clark, D. J. 2001. Development and testing of a nitrogen and phosphorous process model for Southern African water quality issues. ASAE Paper No. 01-2085. Michegan, USA.

Chen, J., Wheater, H. S. and Lees, M. J. 2002. Identification of processes affecting stream chloride response in the Hafren Catchment, mid-Wales. Journal of hydrology. Vol. 264. 12-33.

Clark, D. J., Kiker, G. A. and Schulze, R. E. 2001. Object-oriented restructuring of the *ACRU* agrohydrological modelling system. In *Proc. of the tenth South African National hydrological symposium*. University of Natal, Pietermaritzberg, South Africa. 26-28 September.

Collins, R. and Jenkins, A. 1996. The impact of agricultural land use on stream chemistry in the middle hills of the Himalayas, Nepal. Journal of hydrology. Vol. 185. 71-86.

Connel, L. D., Jayatilaka, C., Gilfedder, M., Mein, R. G., and Vandervaere, J. P. 2001. Modelling flow and transport in irrigation catchments : Development and testing of sub-catchment model. Water Resources Research. Vol. 37. 949-963.

Council for Geioscience. 1999. Geological map of Kwazulu Natal. Council for Geoscience, Pretoria, South Africa.

Cowan, J. A. and Skivington, P. 1993. Assessment of the feasibility and impact of alternative water pollution control options on TDS concentrations in the Vaal Barrage and Middle Vaal. Water Research Commission, Pretoria, Report No. 326/1/93.

Crabtree, R. W. 1986. Spatial distribution of solutional erosion. In *Solute processes*, ed. S. T. Trudgil. 329-361. John Willey and Sons Ltd. Chichester.

Crescimanno, G., Provenzano, G., and Booltink, H. W. G. 2002. The effect of alternating different water qualities on accumulation and leaching of solutes in a Mediterranean cracking soil. Hydrologic processes. Vol. 16. 717-730.

Cryer, R. 1986. Atmospheric solute inputs. In *Solute processes*, ed. S. T. Trudgil. 15-64. John Willey and Sons Ltd. Chichester.

CSIR. 2002. Water quality on disc: Water quality data from the hydrological information system. Version 1.

Datta, P. S. 1983. Trend analysis of water quality in the Sabarmati River at Ahmedabed for a decade. In *Proc. 18th general assembly of the international union of geodesy and geophysics*. 71-78. Hamburg. 15-27 August.

Davis, J. S. and Keller, H. M. 1983. Dissolved loads in streams and rivers-discharge and seasonally related variations. In *Proc. 18th general assembly of the international union of geodesy and geophysics*. 79-90. Hamburg. 15-27 August.

Department of Environmental Affairs and Tourism (DEAT). 1996. Integrated pollution control and waste management: The need for integrated pollution control in South Africa. ed. D. Cloete. Johannesburg.

Dickens, C. 1998. Mkomazi IFR study: starter document for IFR workshop. Scottburgh. 24-27 March.

Edward, T. J. 1998. Preliminary survey of riparian vegetation on the Umkomazi River system. In *Mkomazi IFR study: starter document for IFR workshop*. Scottsburgh. 24-27 March.

Ferguson, R. I., Trudgill, S. T. and Ball, J. 1994. Mixing and uptake of solutes in catchments: Model development. Journal of hydrology. Vol. 159. 223-233.

Flügel, W. A. 1987. Dryland salinity research in the Western Cape Province. In *Proc. of the 1987 hydrological sciences symposium*. Vol. 1. 113-132. Rhodes University, South Africa. 6-9 September.

Flügel, W. A. 1995. River salination due to dryland agriculture in the Western Cape Province, Republic of South Africa. Environmental International. Vol. 21. 679-686.

Forster, S. F. 1987. IRRIS: Model background and description (Draft). Department of Water Affairs, Pretoria.

Foster, I. D., Carter, A.D. and Grieve, I.C. 1983. Biogeochemical controls on river water quality in a forested drainage basin, Warwickshire, UK. In *Proc. 18th General Assembly of the International union of Geodesy and Geophysics.* 241-253. Hamburg. 15-27 August.

Froehlich, W.1983. The mechanisms of dissolved solids transport in Flysch drainage basins. In *Proc. 18th General Assembly of the International union of Geodesy and Geophysics.* 99-108. Hamburg. 15-27 August.

Furness, H. D. 1989. Catchment water quality. In *Proc. of the fourth South African National hydrological symposium*. 355-363. University of Pretoria, South Africa. 20-22 November.

Gibbs, R. J. 1992. Mechanisms controlling world water chemistry. Science. Vol. 170,1088-1090.

Görgens, A. H. M., Jonker, V., and Beuster, H. 2001. The DISA hydrosalinity model. Water Research Commission, Pretoria, Report No. 369/1/01.

Görgens, A. H. M. 2003. Mail communication.

Hall, D. G. 1993. An amended functional leaching model applicable to structured soils. Journal of soil science. Vol. 123. 579-588.

Hall, G. C. and Du Plessis, H. 1981. User's guide to FLOSAL. Vol. 3. Water Research Commission, Pretoria.

Herald, J. 1999. Hydrosalinity studies in the Coerney valley. Water Research Commission, Pretoria, Report No. 195/1/99.

Herbert, F. W. and Mary, P. A. 1982. *Introduction to groundwater modelling*. Academic press. New York.

Herold, C. E. 1980. A model to compute on a monthly basis diffuse salt loads associated with runoff . Hydrological Research Unit. Report No. 1/80.

Herold, C. E. 1981. A model to simulate daily river flows and associated diffuse source conservative pollutants. Hydrological Research Unit. Report No. 3/81.

Herold, C. E. and Eeden, P. H. 2001. The feasibility of using low cost modelling techniques to relate river water quality and diffuse loads to a range of land uses. Water Research Commission, Pretoria, Report No. 796/1/01.

Hillman, R. M. 1981. Land and stream salinity in Western Australia. In *Land and stream salinity*, eds. J. W. Holmes and T. Talsma. 11-18. Elsevier scientific publishing Co. Amsterdam.

Hoffman, G. J. Howell, T. A. and Solomon, K. H. 1990. *Management of farm irrigation systems*. The American Society of Agricultural Engineers Inc. USA.

Institute for Water Research (IWR). 1998. Mkomazi IFR study: specialist meeting proceedings. Scottburgh. 24-27 March.

Jayatilaka, C. and Connel, L. D. 1995. A review of catchment scale hydrologic modelling approaches. Cooperative Research Centre for Catchment Hydrology. Report No. 95/5.

Johnston, M. A. 1994. An evaluation of the four electrode and electromagnetic induction techniques of soil salinity measurements. Water Research Commission, Pretoria, Report No. 269/1/94.

Johnston, W. R. 1993. Changes in subsurface drainage water salinity and boron concentrations. Journal of irrigation and drainage engineering. Vol. 119. 201- 213.

Jolankai, G. 1997. Basic river water quality models: description of the CAL program on water quality modelling. IHP-V/Technical documents in hydrology No. 13, UNESCO, Paris.

Jonker, V. 1995. Improvements to the DISA hydrosalinity model and its application to the Vaalharts Irrigation Scheme. MSc thesis. University of Stellenbosch.

Kay, M. 1986. *Surface irrigation systems and practices*. Oxford. UK.

Kelbe, B. and Germishuyse, T. 1999. A study of the relationship between hydrological processes and water quality characteristics in the Zululand coastal region. Water Research Commission, Pretoria, Report No. 361/1/99.

Kienzle, S. W., Lorentz, S. A. and Schulze, R. E. 1997. Hydrology and water quality of the Mgeni Catchment. Water Research Commission, Pretoria, Report No. TT87/97.

Kiker, G. A. and Clark, D. J. 2001. The development of a Java-based, Object-oriented modelling system for simulation of Southern African Hydrology. ASAE Paper No. 01-2030. Michegan, USA.

Kinross, J. 2001. Freshwater Acidification and 'Acid Rain': The effect of trees. Napier University, Edinburgh.

Konikow, L. F. 2002. Use of numerical models to simulate ground water flow and transport. In *Environmental isotopes in the hydrological cycle: principles and applications.* ed. Yurtsever, Y. Vienna.

Laudelout, H. 1975. Modelling of salt movement through the soil profile. In *Prognosis of salinity and alkalinity.* 213-240. Land and water development division. FAO Soils bulletin, No. 31. Rome.

Leij, F. J. and Genuchten, M. T. 1999. Principles of solute transport. In *Agricultural drainage*, eds. R. W. Skaggs and J. V. Schilfgaarde. 331-356. American Society of Agronomy Inc. USA.

Loague, K. M., Green, R. E. and Mulkey, L. A. 1998. Evaluation of mathematical models of solute migration and transformation. In *International conference and workshop on the validation of flow and transport models for the unsaturated zone.* ed. P. J. Wierenga. 231-248. New Mexico. 22-25 May.

Loah, I. C. and Stoikes, R. A. 1981. Predicting stream salinity changes in South Western Australia. *In Land and stream salinity*, eds. J. W. Holmes and T. Talsma. 227-253. Elsevier scientific publishing Co. Amsterdam.

Lorentz, S. A. 1986. Solute transport in variably saturated flow in porous media with dual porosity. MSc thesis. Department of Agricultural and Chemical Engineering. Colorado State University. Colorado.

Lorentz, S. A. 1987. Laboratory column tests on various oil shale materials. In *Proc. of the seventh annual AGU front range branch hydrology days.* eds. J. Hubert, M. Seytanx and G. S. Thomas. 167-174. Colorado. 21-23 April.

Luthin, J. N. 1997. *Drainage of agricultural lands.* Madison Inc. California.

Matos, A. T. Costa, L. M., Fontes, M. P. F. and Martinez, M. A. 1999. Retardation factors and the dispersion-diffusion coefficients of Zn, Cd, Cu, and Pb in soils from Vicosa-Mg, Brazil. Transactions of the ASAE, Vol. 42. 903-910.

McConway, K. J., Jones, M. C. and Taylor, P. C. 1999. *Statistical modelling using GENSTAT.* USA.

McLaughlin, D. 1988. Developing a systematic approach to model validation. In *International conference and workshop on the validation of flow and transport models for the unsaturated zone*. ed. Wierenga, P. J. New Mexico. 22-25 May.

Meybeck. M. 1981. Pathways of major elements from land to ocean through rivers. In *River inputs to ocean systems*. UNESCO report. 18-30.

Meybeck. M.1983. Atmospheric input and river transport of dissolved substances. In *Proc. 18th General Assembly of the International union of Geodesy and Geophysics.* 173-192. Hamburg. 15-27 August.

Michael, A. M.1997a. *Irrigation theory and practice*. Pashupatic printers. Delhi.

Michael, G. W. 1997b. R-ToT: River time of travel model. Center for Louisiana inland water studies, University of South Western Louisiana. Technical Report series 97-110.

Miller, M. R., Brown , P. L., Donovan, J. J., Begatino, R. N., Sonderegger, J. L. and Schimidt, F. A. 1981. Saline seep development and control in the North American great plains - hydrological aspect. In *Land and stream salinity*, eds. J. W. Holmes and T. Talsma. 115-142. Elsevier scientific publishing Co. Amsterdam.

Mironenko, E. V. and Pachepsky, Y. A. 1998. Estimating transport of chemicals from soil to ponding water. Journal of Hydrology. Vol. 208. 53-61.

Moolman, J. H. 1993. An evaluation of a range of computer models simulating the transport of solutes and water in the root zone of irrigated soils. Water Research Commission, Pretoria, Report No. 196/1/93.

Nativ, R., Adar, E., Dahan, O. and Nissim, I. 1997. Water salinization in arid regions: observation from the Negev desert, Israel. Journal of hydrology. Vol. 196. 271-296.

New South Wales Department of Land and Water Conservation (NSW). 2000. Salinity in New South Wales. New South Wales, Australia.

Ninham Shand Inc. (NSI). 1990. Breede River System: Development of a daily hydrosalinity model (DISA). Department of Water Affairs. Report No. H 000/00/0790.

Ninham Shand Inc. (NSI). 1998. Mkomazi-Mgeni transfer scheme pre-feasibility study (main report). Department of Water Affairs and Forestry. Report No. 2787/7856.

Njitchoua, R., Dever, L., Fotes. J. C. and Naah, C. 1997. Geochemistry, origin and recharge mechanisms of ground water from the Garoua sandstone aquifer. Journal of hydrology. Vol.190. 123-140.

Pegram, G. C., and Görgens, A. H. M. 2001. A guide to non-point source assessment in South Africa. Water Research Commission, Pretoria, Report No. TT 142/01.

Pegram, G. C., Görgens, A. H. M. and Quibell, G. E. 1998. Policy considerations for non-point source management in South Africa: As input to the water law review process. Water Research Commission, Pretoria, Report No. TT 696/1/98.

Quatrani, T. 1998. *Visual Modelling with Rational Rose and UML*. Addison Wesley Longman Inc. Massachusetts. USA.

Quilez, D., Aragues, R. and Tanji, K. K. 1992. Salinity of rivers: Transfer function-noise approach. Journal of irrigation and drainage engineering. Vol. 118-357.

Rational Software Corporation. 1998. *Rational Rose 98*. Rational Software Corporation Cupertino. USA.

Raymond, P. F. 2001. Surficial and near surficial geologic processes [internet]. University of Georgia. Available from<: http://www.arches.urga.edu/GEOL-5rivers.html >[accessed 10 Augest 2002].

Reichert, P., Borchardt, D., Henze, M., Rauch, W., Shanahan, P., Somlyody, L. and Vanrolleghem., P. 2001. River water quality model No. 1. Scientific and technical report No. 12. IWA publishing.

Reynolds, B., Fowler, D., Smith, R. I. and Hall, J. R. 1997. Atmospheric inputs and catchment solute fluxes for major ions in five Welish upland catchments. Journal of hydrology. Vol. 194. 305-329.

Rhoades, J. D., Lesch, S. M., Burch, S. L., Letey, J., LeMert, R. D., Shouse, P. J., Oster, J. D. and O'Halloran, T. 1997. Salt distribution in cracking soils and salt pickup by runoff waters. Journal of irrigation and drainage engineering. Vol. 123. 323-328.

Ross, S. 1989. *Soil processes: A systematic approach*. Routledge, Chapman and Hall Inc. USA.

Rossouw, J. N. and Kamish, W. 2001. Assessing the impact of environmental reservoir releases using a two-dimensional reservoir water quality model. In *Tenth South African National Hydrological Symposium*. University of Natal, Pietermaritzburg. 26-28 September.

Rowntree, K. and Dollar, E. 1998. Geomorphology. In *Mkomazi IFR study: starter document for IFR workshop*. Scottsburgh. 24-27 March.

Runkel, R. L. 1998. One-Dimensional Transport With Inflow and Storage (OTIS): A solute transport model for streams and rivers. U.S. Geological Survey. Report No. 98-4018.

Russo, D. 2002. A note on effective parameters of the convection-dispersion equation. Water Resources Research. Vol. 38. 9.1-9.7.

Schulze, R. E. 1975. Catchment evapotranspiration in the Natal Drakensburg. Unpublished PhD thesis. Department of Geography. University of Natal. Pietermaritzburg.

Schulze, R. E., Schmidt, E. J. and Smithers, J. C. 1992. SCS-SA Users Manual, PC-based SCS Design flood estimates for small catchments in southern Africa. Department of Agricultural Engineering University of Natal. Pietermaritzburg.

Schulze, R. E. 1995a. Hydrology, agrohydrology and agrohyrological simulation modelling. In *Hydrology and Agrohydrology : A Text to Accompany the ACRU 3.00 Agrohydrological Modelling System*. ed. R. E. Schulze. Water Research Commission, Pretoria, Report TT69/95. pp AT1-1 to AT1-13.

Schulze, R. E. 1995b. Streamflow. In *Hydrology and Agrohydrology : A Text to Accompany the ACRU 3.00 Agrohydrological Modelling System*. ed. R. E. Schulze. Water Research Commission, Pretoria, Report TT69/95. pp AT10-1 to AT10-6.

Schulze, R. E. 1995c. Soil water budgeting and total evaporation. In *Hydrology and Agrohydrology: A Text to Accompany the ACRU 3.00 Agrohydrological Modelling System*. ed. R. E. Schulze. Water Research Commission, Pretoria, Report TT69/95. pp AT7-1 to AT7-21.

Schulze, R. E. 2001. Modelling of hydrological design-lecture note.

Schulze, R. E. and Smithers, J. C. 2002. The *ACRU* agrohydrological modelling system as of 2001: Background, concepts, structure, output, typical applications and operations. In *Modelling as a tool in integrated water resources management: Conceptual issues and case study applications*. ed. R.E. Schulze. Water Research Commission, Pretoria, Project K/749. pp 47-84.

Schulze, R. E. and Tarboton, K. C. 1995. *ACRU*: Hydrological responses from urbanised areas. In *Hydrology and Agrohydrology : A Text to Accompany the ACRU 3.00 Agrohydrological Modelling System*. ed. R. E. Schulze. Water Research Commission, Pretoria, Report TT69/95. pp AT11-1 to AT11-6.

Schulze, R. E. Angus, G. R. Lynch, S. D. and Smithers, J. C. 1995a. *ACRU*: Concepts and Structure. In *Hydrology and Agrohydrology : A Text to Accompany the ACRU 3.00 Agrohydrological Modelling System*. ed. R. E. Schulze. Water Research Commission, Pretoria, Report TT69/95. pp AT2-1 to AT2-26.

Schulze, R. E. Angus, G. R. and Guy, R. M. 1995b. *ACRU*: Soils. In *Hydrology and Agrohydrology : A Text to Accompany the ACRU 3.00 Agrohydrological Modelling System*. ed. R. E. Schulze. Water Research Commission, Pretoria, Report TT69/95. pp AT5-1 to AT5-40.

Schulze, R. E., Dent, M. C., Lynch, S. D., Schafer, N. W., Kienzle, S. W. and Seed, A. W. 1995c. Rainfall. In *Hydrology and Agrohydrology : A Text to Accompany the ACRU 3.00 Agrohydrological Modelling System*. ed. R. E. Schulze. Water Research Commission, Pretoria, Report TT69/95. pp AT3-1 to AT3-33.

Schulze, R. E., Smithers, J. C., Lecler, N. L., Tarboton, K. C. and Schmidt, E. J. 1995d. Reservoir yield analysis. In *Hydrology and Agrohydrology : A Text to Accompany the ACRU 3.00 Agrohydrological Modelling System*. ed. R. E. Schulze. Water Research Commission, Pretoria, Report TT69/95. pp AT14-1 to AT14-17.

Schulze, R. E. 1997. South African atlas of agrohydrology and climatology. Water Research commission, Pretoria, Report TT82/96.

Schwartz, R. C., Mcinnes, K. J., Juo, A. S. R., Wilding, L. P. and Reddell, D. L. 1999. Boundary effects on solute transport in finite soil columns. Water Resources Research. Vol. 35. 671-681.

Seelig, B., Scherer, T. and Rutten, L. 2001. Managing irrigation water salinity in the lower Rio Grande Valley. Texas agricultural extension service.

Shouse, P. J., Lettey, J., Jobes, J., Fargerlund, J., Burch, S. L., Oster, J. D., Rhoades, J. D. and O'halloran, T. 1997. Salt transport in cracking soils: Bromide tracer study. Journal of irrigation and drainage engineering. Vol. 123. 329-335.

Shukla, M. K. and Cepuder, P. 2000. Anion exclusion during transport of chloride through soil columns. Transactions of the ASAE. Vol. 43. 1425-1430.

Silvert, W. 1993. Object-oriented ecosystem modelling. Ecological Modelling. Vol. 68. 91-118.

Simpson, D. E. 1991. Quantification of the effects of land-use on runoff water quality in selected catchments in Natal. Water Resources Commission, Pretoria, Report No. 237/1/91.

Smettem, K. R. 1986. Solute movement in soils. In *Solute processes*. ed. S. T. Trudgill. 141-162. John Wiley and Sons Ltd. Chichester.

Song, Z. D. and James, L. D. 1992. An objective test for hydrologic scale. Water Resources Bulletin. Vol. 28. 833-844.

Spears, D. A. 1986. Mineralogical control of the chemical evolution of groundwater. In *Solute processes*, ed. S. T. Trudgil. 167 – 192. Chichester: John Willey and Sons Ltd.

Taylor, V. 2001. Hydrological modeling applications for water resources management in the Mkomazi catchment. MSc thesis. School of Bioresources Engineering and Environmental Hydrology. University of Natal. Pietermaritzburg.

Tedeschi, A., Beltran, A. and Aragues, R. 2001. Irrigation management and hydrosalinity balance in a semi-arid area of the middle Ebro river basin (Spain). Agricultural Water Management. Vol. 49. 31-50.

Wagenet, R. J. and Hutson, J. L. 1989. LEACHM (Version 2). Water Resources Institute, Cornell University, New York.

Walling, D. E. and Webb, B.W. 1986. Solutes in river systems. In *Solute processes*, ed. S. T. Trudgil. 251-317. John Willey and Sons Ltd. Chichester.

Wiechers, H. N., Freeman, M. J. and Howard. 1996. The management of urban impoundments in South Africa. Vol. 1.Water Resources Commission, Pretoria, Report No. TT77/96.

Wild, A. 1981. Mass flow and diffusion. In *The chemistry of soil processes*, eds. D. J. Greenland and M. H. B. Hayes. 37-80. John Willey and Sons Ltd. Chichester.

Wolf-Piggott, B. 1995. Demonstrating the potential of GIS technology in hydrosalinity modelling through interfacing the DISA model and a GIS. Water Resources Commission, Pretoria, Report No. 588/1/95.

11. APPENDICES

Appendix A New data objects added to *ACRU2000* in this project

Table A1 Definition of the general data objects in *ACRUSalinity*

Class Name	Abbreviation	Definition	Remark
DSalinityOption	SALINITY	An option whether the hydrosalinity module is to be executed in a particular simulation	Input
DReservoirSalinityOption	RESSALINITY	An option whether the reservoir salt budget routine is to be executed in a particular simulation	Input

Table A2 Definition of data objects that belong to non-irrigated areas

Class Name	Abbreviation	Definition	Remark
DActualQuickflowDepth	AQFLDE	Depth of the generated stormflow that leaves non-irrigated land on the same day	Internal
DBaseflowSalinity	BFLOSA	TDS concentration of baseflow release from non-irrigated areas	Output
DBaseflowSaltLoad	BFLSL	The salt load associated with the baseflow releases from non-irrigated areas	Output
DGeneratedSaltLoad	GENSL01	The salt load generated in the topsoil horizon of non-irrigated areas	Output
DGeneratedSaltLoad	GENSL02	The salt load generated in the subsoil horizon of non-irrigated areas	Output
DGeneratedSaltLoad	GENSLGW	The salt load generated in the groundwater store of non-irrigated areas	Output
DGroundwaterSalinity	GWSA	TDS concentration of the groundwater store in non-irrigated areas	Output

Table A2 Continued

Class Name	Abbreviation	Definition	Remark
DInitialSalinity	INISUBSSA	TDS concentration of the soil moisture of the subsoil horizon in non-irrigated areas at the start of a simulation	Input
DInitialSalinity	INITOPSSA	TDS concentration of the soil moisture of the topsoil horizon in non-irrigated areas at the start of a simulation	Input
DInitialSaltLoad	INISUBSSL	Salt load of the soil moisture of subsoil horizon in non-irrigated areas at the start of a simulation	Output
DInitialSaltLoad	INITOPSSL	Salt load of the soil moisture of the topsoil horizon in non-irrigated areas at the start of a simulation	Output
DPercSaltConc	PERCSA01	TDS concentration of percolation water from the topsoil to subsoil in non-irrigated areas	Output
DPercSaltConc	PERCSA02	TDS concentration of percolation water from the subsoil to groundwater store in non-irrigated areas	Output
DPercSaltLoad	PERCSL01	Salt load associated with percolation water from the topsoil to the subsoil in non-irrigated areas	Output
DPercSaltLoad	PERCSL02	Salt load associated with percolation water from the subsoil to the groundwater store in non-irrigated areas	Output
DQuickflowSalinity	QFLOSA	TDS concentration of the quickflow from non-irrigated areas	Output
DQuickflowSaltLoad	QFLOSL	The salt load associated with quickflow from non-irrigated areas	Output
DRainfallSalinity	RSALIN	TDS concentration of the rain falling on non-irrigated areas	Input

Table A2 Continued

Class Name	Abbreviation	Definition	Remark
DRainfallSaltLoad	RFLSL	Salt load associated with the rain falling on non-irrigated areas	Output
DRunoffSalinity	RUNOSA	TDS concentration of runoff water from non-irrigated areas	Output
DRunoffSaltLoad	RUNOSL	The salt load associated with runoff water from non-irrigated areas	Output
DSaltFluxRecord	SALTFL01	Salt load associated with the topsoil moisture in non-irrigated areas	Output
DSaltFluxRecord	SALTFL02	Salt load associated with the subsoil moisture in non-irrigated areas	Output
DSaltFluxRecord	SALTFLGW	Salt load associated with the groundwater store in non-irrigated areas	Output
DSaltInput	SALTINP	Total salt input to non-irrigated areas	Output
DSaltSat	SALTSAT01	The salt saturation value of the topsoil horizon in non-irrigated areas	Input
DSaltSat	SALTSAT02	The salt saturation value of the subsoil horizon in non-irrigated areas	Input
DSaltSat	SALTSATGW	The salt saturation value of groundwater store in non-irrigated areas	Input
DSubsoilSalinity	SUBSSA	TDS concentration of the subsoil horizon in non-irrigated areas	Output
DSurfaceSaltFluxRecord		Salt load associated with surface flows	Internal
DTopsoilSalinity	TOPSSA	TDS concentration of the topsoil horizon in non-irrigated areas	Output
DUptakeRateConstant	SALTUPT01	The rate of salt generation in the topsoil horizon of non-irrigated areas	Input
DUptakeRateConstant	SALTUPT02	The rate of salt generation in the subsoil horizon of non-irrigated areas	Input
DUptakeRateConstant	SALTUPTGW	The rate of salt generation in the groundwater store of non-irrigated areas	Input

Table A2 Continued

Class Name	Abbreviation	Definition	Remark
DUpwardSaltFlux	UPSF02	Salt load associated with upward water movement from the subsoil horizon to the topsoil horizon in non-irrigated areas	Output
DUpwardSaltFlux	UPSF02	Salt load associated with upward water movement from the subsoil horizon to the topsoil horizon in non-irrigated areas	Output

Table A3 Definition of data objects that belong to irrigated areas

Class Name	Abbreviation	Definition	Remark
DBaseflowSalinity	BFLOSA	TDS concentration of baseflow releases from irrigated areas	Output
DBaseflowSaltLoad	BFLSL	The salt load associated with the baseflow releases from irrigated areas	Output
DGeneratedSaltLoad	GENSL01	The salt load generated in the topsoil horizon of irrigated areas	Output
DGeneratedSaltLoad	GENSLGW	The salt load generated in the groundwater store of irrigated areas	Output
DGroundwaterSalinity	GWSA	TDS concentration of the groundwater store in irrigated areas	Output
DInitialSalinity	INITOPSSA	TDS concentration of the soil moisture of topsoil horizon in irrigated areas at the start of a simulation	Input
DIrrigationWaterSalinity	IRRWASA	TDS concentration of the applied irrigation water	Input
DIrrigationWaterSaltLoad	IRRWASL	Salt load associated with the applied irrigation water	Output
DPercSaltConc	PERCSA01	TDS concentration of percolation water from the topsoil to the subsoil in irrigated areas	Output

Table A3 Continued

Class Name	Abbreviation	Definition	Remark
DPercSaltLoad	PERCSL01	Salt load associated with percolation water from the topsoil to the subsoil in irrigated areas	Output
DQuickflowSalinity	QFLOSA	TDS concentration of the quickflow from irrigated areas	Output
DQuickflowSaltLoad	QFLOSL	The salt load associated with quickflow from irrigated areas	Output
DRainfallSaltLoad	RFLSL	Salt load associated with the rain falling on irrigated areas	Output
DRunoffSalinity	RUNOSA	TDS concentration of runoff water from irrigated areas	Output
DRunoffSaltLoad	RUNOSL	The salt load associated with runoff water from irrigated areas	Output
DSaltFluxRecord	SALTFL01	Salt load associated with the topsoil moisture in irrigated areas	Output
DSaltFluxRecord	SALTFLGW	Salt load associated with the groundwater store in irrigated areas	Output
DSaltInput	SALTINP	Total salt input to irrigated areas	Output
DSaltSat	SALTSAT01	The salt saturation value of the topsoil horizon in irrigated areas	Input
DSaltSat	SALTSATGW	The salt saturation value of the groundwater store in irrigated areas	Input
DTopsoilSalinity	TOPSSA	TDS concentration of the topsoil horizon in irrigated areas	Output
DUptakeRateConstant	SALTUPT01	The rate of salt generation in topsoil horizon of irrigated areas	Input
DUptakeRateConstant	SALTUPTGW	The rate of salt generation in the groundwater store of irrigated areas	Input
DUpwardSaltFlux	UPSF01	Salt load associated with upward water movement from the topsoil horizon to surface flow (quickflow) in irrigated areas	Output

Table A4 Definition of data objects that belong to the reservoir component

Class Name	Abbreviation	Definition	Remark
DAbstractionSaltLoad	ABSRSL	The salt load associated with the water abstracted from the reservoir for irrigation, domestic and other uses	Output
DInflowSaltLoad	INFSL	The salt load associated with the total inflow to a reservoir	Output
DInitialSalinity	INIRESSA	TDS concentration of the water stored in a reservoir at the start of a simulation	Input
DInitialSaltLoad	INIRESSL	Salt load of the water stored in a reservoir at the start of a simulation	Output
DNormalflowSalinity	NORMFLSA	TDS concentration of the legal flow releases from the reservoir	Output
DNormalflowSaltLoad	NRMLFLSL	Salt load associated with the legal flow releases from the reservoir	Output
DOutflowSalinity	OUTFSA	Average TDS concentration of the total outflow from the reservoir	Output
DOutflowSaltLoad	OUTFSL	Salt load associated with the daily total outflow from a reservoir	Output
DRainfallSalinity	RSALIN	TDS concentration of the rain falling on a reservoir surface	Input
DReservoirEvapVol		The daily volume of evaporated water from a reservoir surface	Internal
DReservoirSalinity	RESSA	TDS concentration of the water stored in a reservoir	Output
DResInflowSalinity	RESINFSA	Average TDS concentration of the total inflow to a reservoir	Output
DSaltFluxRecord	SALTFLRES	Salt load associated with the water stored in a reservoir	Output
DSaltInput	SALTINP	Total salt input to a reservoir	Output
DSeepageSalinity	SEEPAGESA	TDS concentration of seepage water from a reservoir	Output

Table A4 Continued

Class Name	Abbreviation	Definition	Remark
DSeepageSaltLoad	SEEPAGESL	Salt load associated with seepage water from a reservoir	Output
DSpillwayflowSalinity	OFLSA	TDS concentration of an overflowing water from the reservoir	Output
DSpillwayflowSaltLoad	OVERFLSL	Salt load associated with an overflowing water from the reservoir	Output

Table A5 Definition of data objects that belong to impervious areas (adjunct and disjunct impervious areas)

Class Name	Abbreviation	Definition	Remark
DImperviousAreaSaltLoad	RUNOSL	The salt load stored in adjunct or disjunct impervious areas	Output
DRainfallSalinity	RSALIN	TDS concentration of the rain falling on adjunct and disjunct impervious areas	Input

Table A6 Definition of data objects that belong to the channel

Class Name	Abbreviation	Definition	Remark
DOutflowSaltLoad	OUTFSL	Salt load associated with the daily total outflow from a channel reach	Output
DSaltFluxRecord		The daily total salt load inflowing to a channel reach	Internal
DWaterOutflow	OUTFLV	The daily volume of water outflowing from a channel reach	Output

Appendix B Main data objects used in *ACRUSalinity* from the hydrological modules of *ACRU*

Class Name	Definition
DActualIrrigApplic	The quantity of irrigation water applied to the field, excluding the various losses
DArea	Area of a component such as catchment area or impervious area
DBaseflowDepth	Baseflow depth in irrigated or non-irrigated areas
DChannelOutflow	Depth of water outflowing from a particular channel reach
DDamActualSeepage	Daily seepage loss from a reservoir
DDamCatchmentPercent	Percentage of the total catchment area being simulated that is contributing its flow to the reservoir
DDamDraftQuantity	The daily quantity of water abstracted from a reservoir
DDamNormalFlowRelease	The quantity of water released for downstream users (legal flow releases)
DDamOption	An option about the existence and location of a reservoir in a catchment
DDamRainfall	The quantity of rain falling on a reservoir surface
DDamSpillwayFlow	The quantity of water outflowing from a reservoir through the spillway
DEffectiveRainfall	The quantity of rain infiltrated to the topsoil of irrigated or non-irrigated areas
DImpervAreaRunoff	The quantity of runoff water from impervious areas
DIrrigMonth	The month in which irrigation takes place
DIrrigReturnflowOption	An option whether an irrigation return flows upstream or downstream of an internal reservoir
DNetArea	The area of a particular component
DQuickflowDepth	The depth of quickflow from irrigated or non-irrigated area
DSaturatedFlow	The quantity of percolated water from one layer to an underlying layer in irrigated or non-irrigated areas
DWaterFluxRecord	The quantity of water on a particular component, for example in reservoir and soil horizons of irrigated or non-irrigated areas

Appendix C Major component objects used in *ACRUSalinity* from the hydrological modules of *ACRU*

Class Name	Definition
CClimate	The component (physical feature) that represents the general climate of an area
CIrrigatedArea	The component representing irrigated areas
CLandSegment	The component that represents non-irrigated areas, or in some cases a sub-catchment
CChannel	The component that represents a stream or river
CDam	The component representing a reservoir
CImperviousArea	The component representing total impervious areas
CAdjunctImperviousArea	The component that represents adjunct impervious areas
CDisjunctImperviousArea	The component that represents disjunct impervious areas
CReach	The component that represents an inflow or outflow reach, for example, a river or reservoir reach

Appendix D Some of the factors and their magnitude resulting in the spatial variation of salinity betweens Sub-catchments 1 and 12

Factors affecting salinity		Sub-catchment No. 1	Sub-catchment No. 12
Mean annual precipitation (mm)		1107	945
Mean annual evaporation (mm)		1503.7	1588.6
Irrigated area as percentage of the total area		0	5
Impervious area as percentage of the total area	Adjunct	0.015	0.028
	Disjunct	0.198	0.045
Elevation (m)		2123.6	1684.6
Slope (%)		26.5	11.3
Depth of A-horizon (m)		0.22	0.26
Depth of B-horizon (m)		0.22	0.38
Porosity (m/m)	Topsoil	0.438	0.432
	Subsoil	0.420	0.413
Drained upper limit (m/m)	Topsoil	0.229	0.225
	Subsoil	0.244	0.256
Wilting point (m/m)	Topsoil	0.138	0.137
	Subsoil	0.147	0.171

Appendix E Sensitivity analysis of the major *ACRUSalinity* input parameters

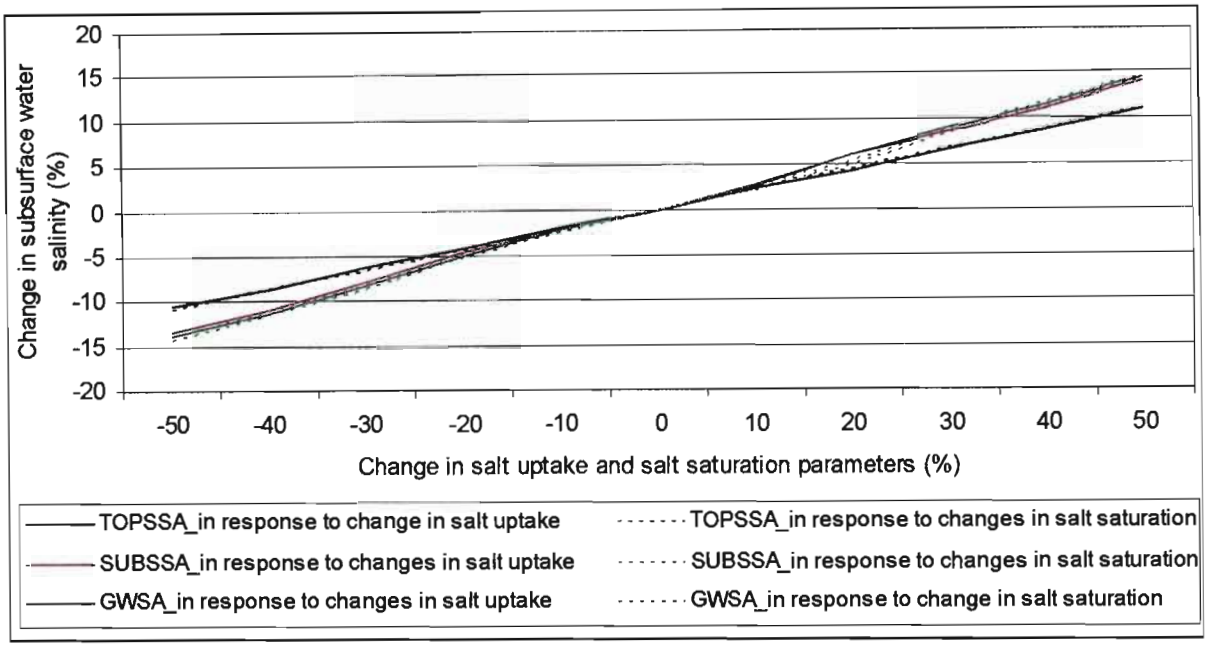

Figure E1 The impact of changes in salt uptake and salt saturation parameter values on subsurface water salinity

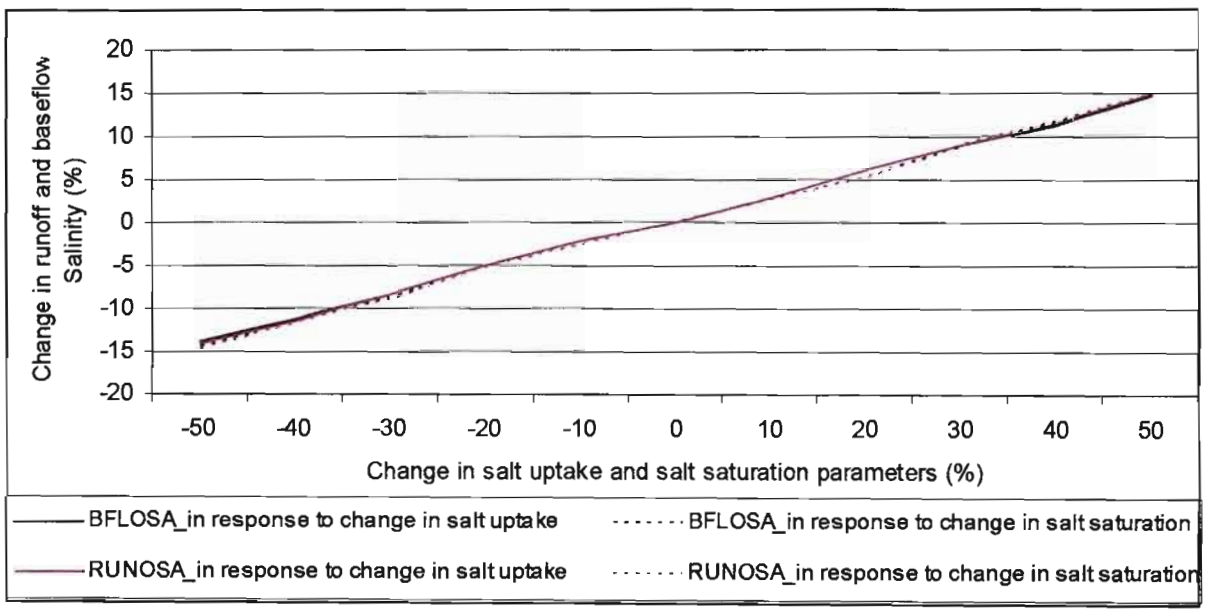

Figure E2 The impact of changes in salt uptake and salt saturation parameter values on runoff and baseflow salinity

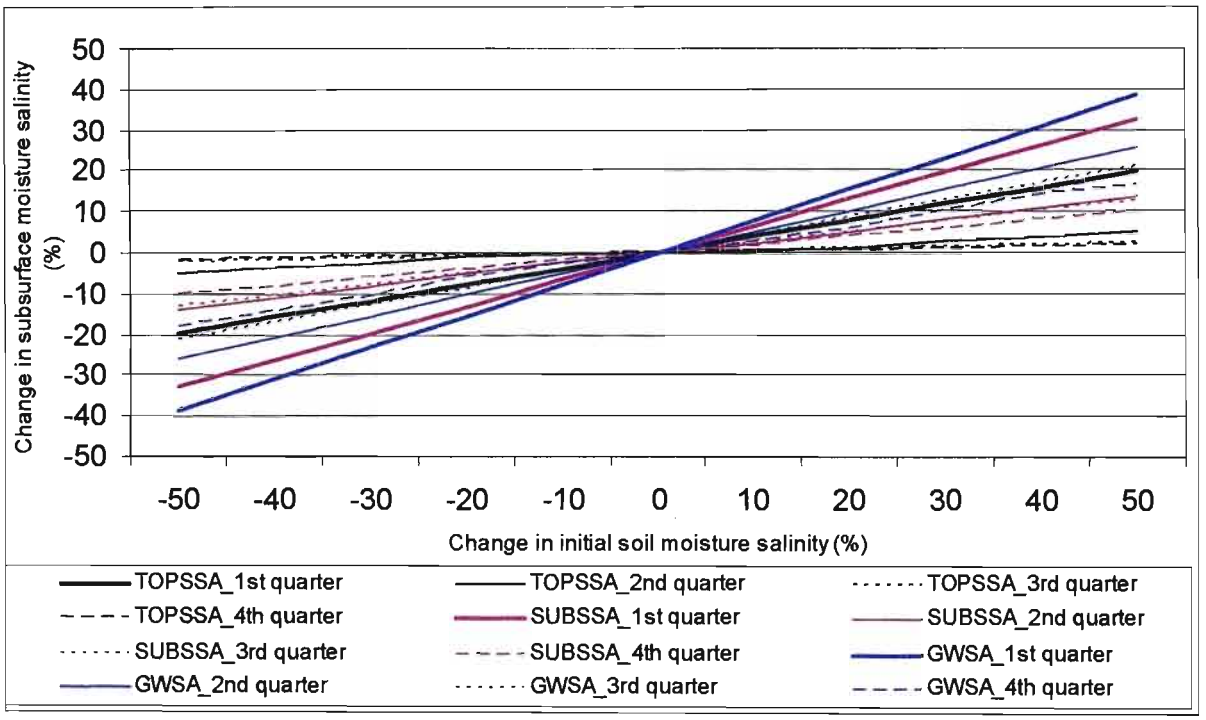

Figure E3 The impact of changes in initial soil moisture salinity value on subsurface water salinity

Appendix F GENSTAT output of the regression analysis for determination of the salt uptake rate constant for the Upper Mkomazi Catchment

```
***** Regression Analysis *****

 Response variate: changeInCwithTime
     Fitted terms: ChangeInC


*** Summary of analysis ***

             d.f.  s.s.         m.s.         v.r.         F pr.
Regression   1     15.001       15.0006      52.51        <.001
Residual     14    3.999        0.2857
Total        15    19.000       1.2667

Change       0     -0.001       *

Percentage variance accounted for 0.0
Standard error of observations is estimated to be 0.534


*** Estimates of regression coefficients ***

             estimate     s.e.         t(14)        t pr.
ChangeInC    0.0003401    0.0000469    7.25         <.001
```

NB. changeInCwithTime represents the difference in TDS concentration between successive days over the time interval (in days), and changeInC represents the difference between the maximum soil TDS concentration and the observed TDS concentration for the day

Appendix G API specification of *ACRUSalinity*

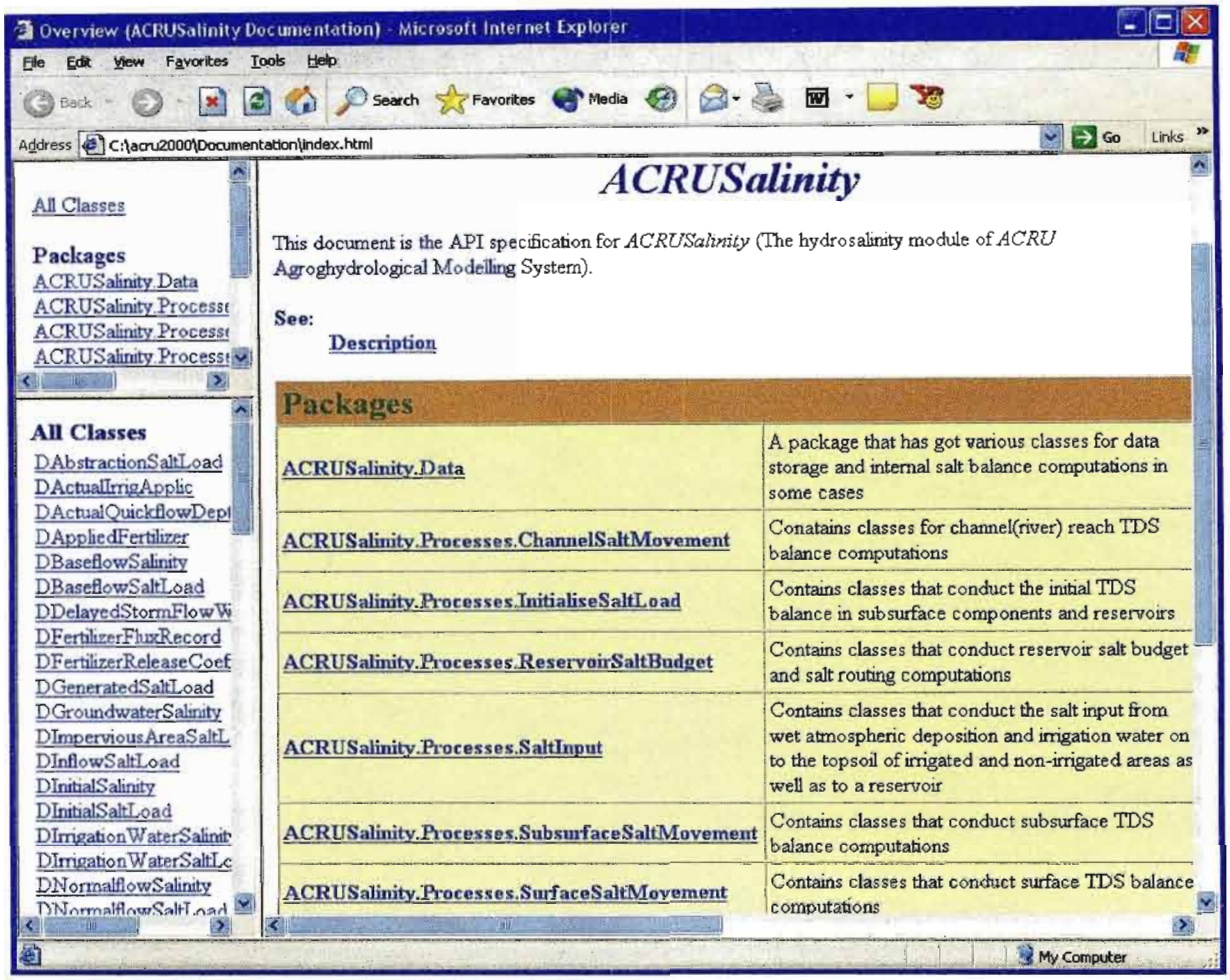

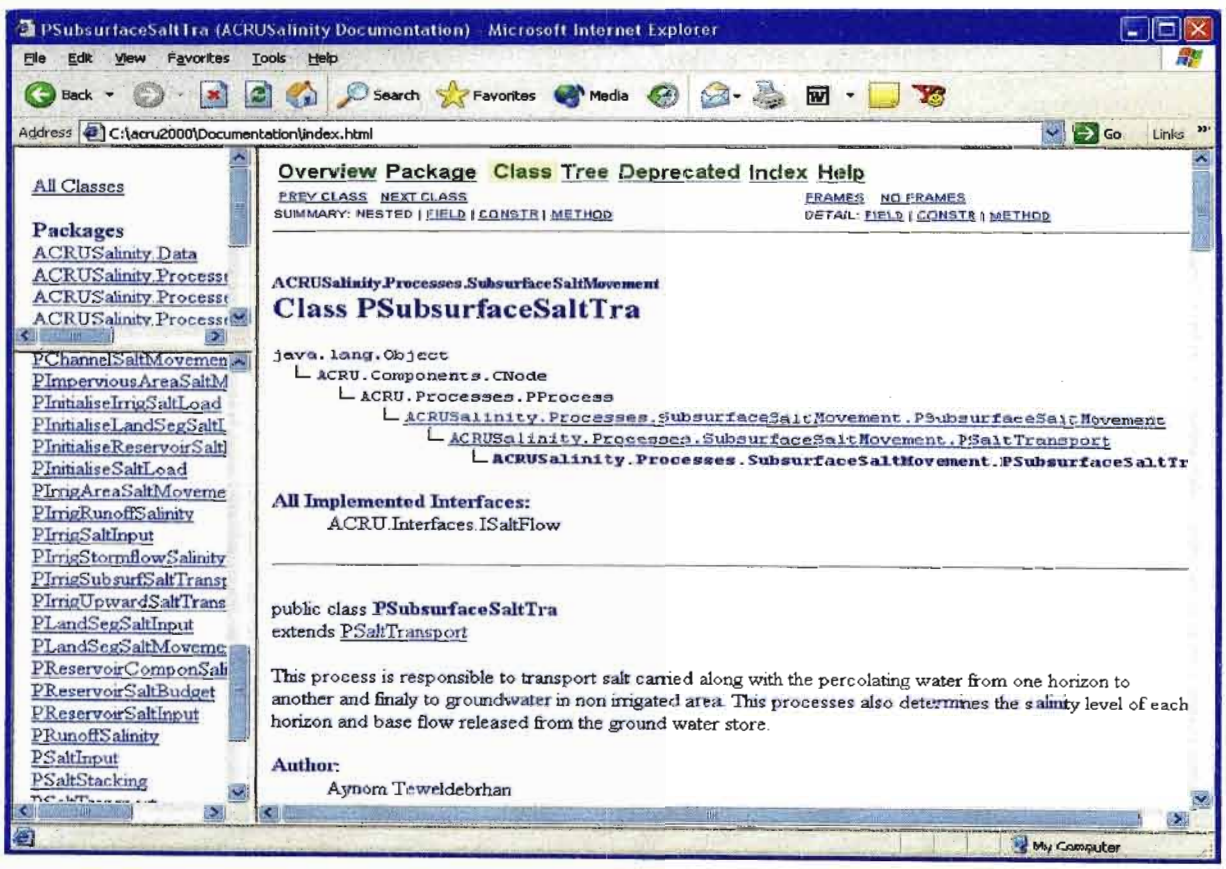

Appendix H A sample Java code and packages in *ACRUSalinity*

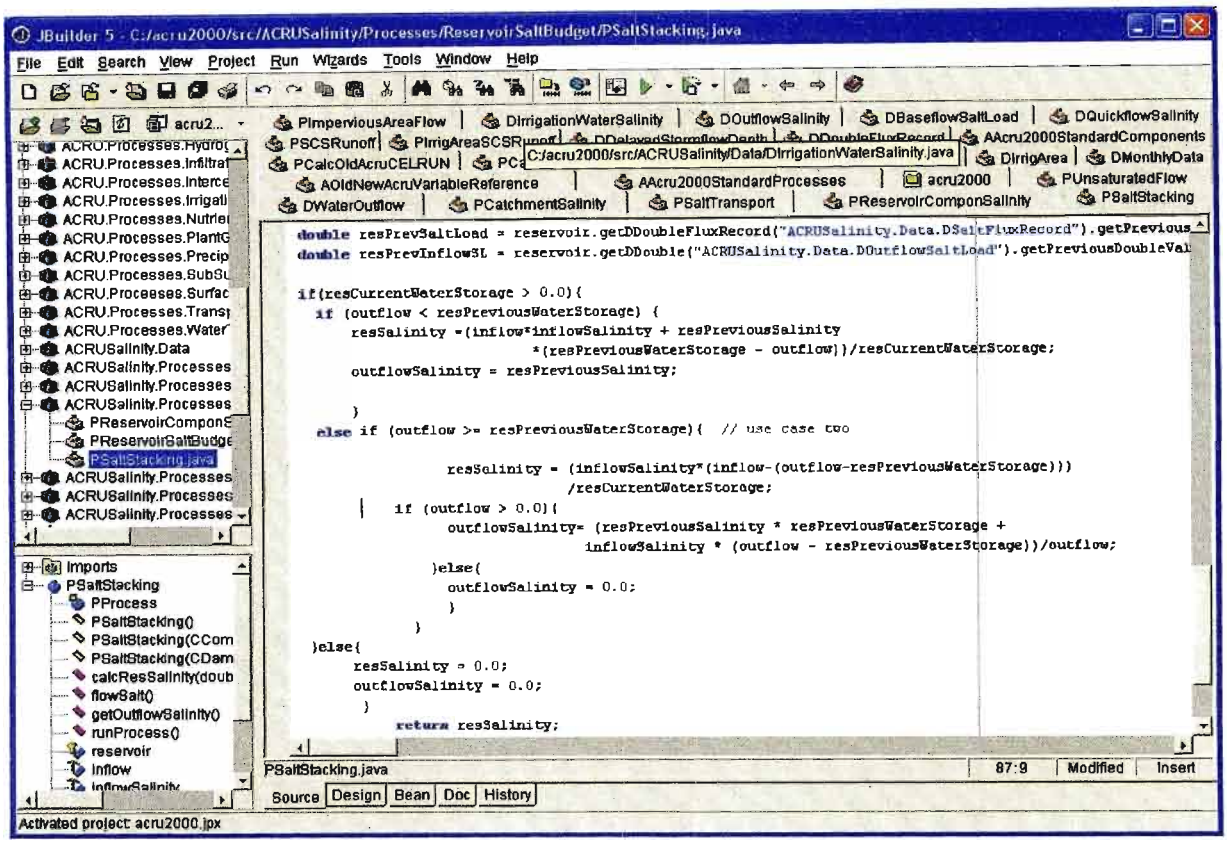

Appendix I *ACRUSalinity* output variables in the output variable selector of *ACRU*

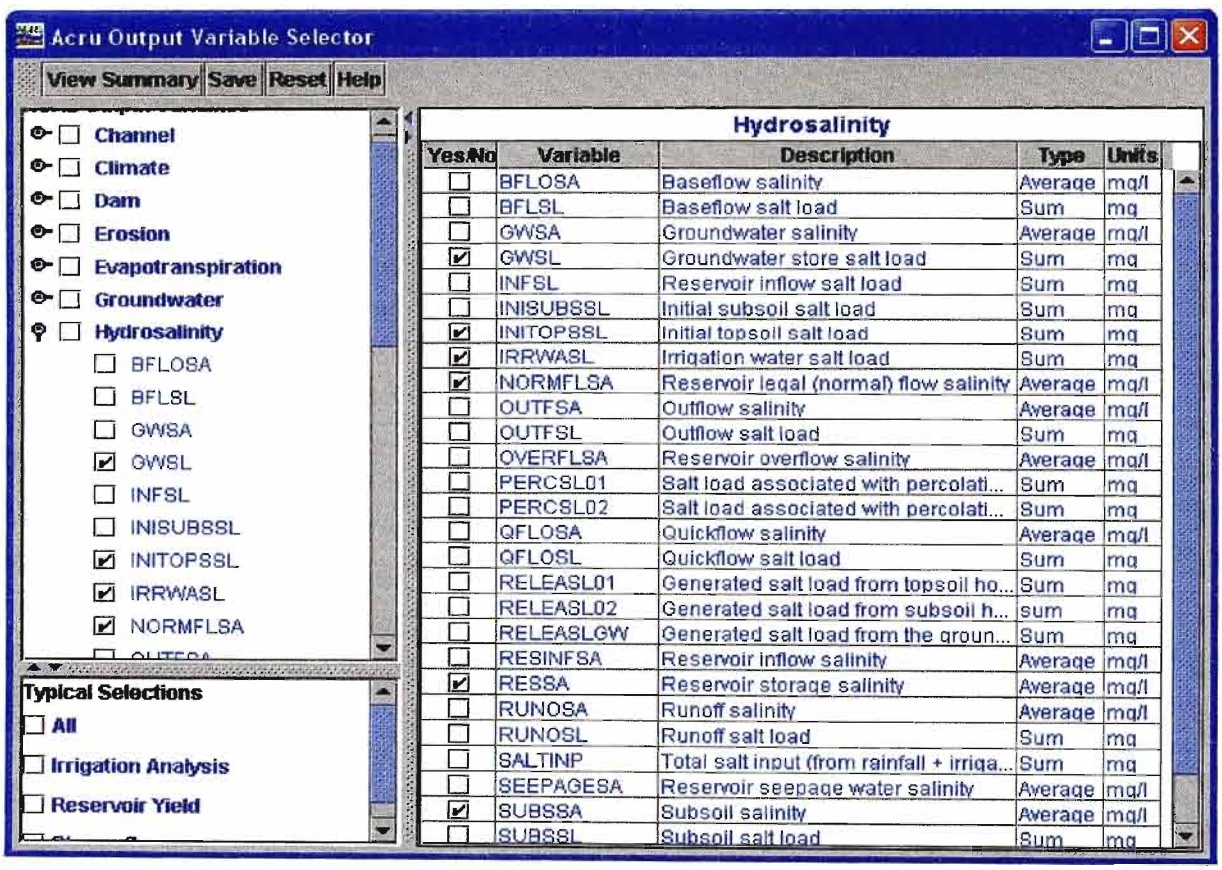

Yes/No	Variable	Description	Type	Units
☐	BFLOSA	Baseflow salinity	Average	mg/l
☐	BFLSL	Baseflow salt load	Sum	mg
☐	GWSA	Groundwater salinity	Average	mg/l
☑	GWSL	Groundwater store salt load	Sum	mg
☐	INFSL	Reservoir inflow salt load	Sum	mg
☐	INISUBSSL	Initial subsoil salt load	Sum	mg
☑	INITOPSSL	Initial topsoil salt load	Sum	mg
☑	IRRWASL	Irrigation water salt load	Sum	mg
☑	NORMFLSA	Reservoir legal (normal) flow salinity	Average	mg/l
☐	OUTFSA	Outflow salinity	Average	mg/l
☐	OUTFSL	Outflow salt load	Sum	mg
☐	OVERFLSA	Reservoir overflow salinity	Average	mg/l
☐	PERCSL01	Salt load associated with percolati...	Sum	mg
☐	PERCSL02	Salt load associated with percolati...	Sum	mg
☐	QFLOSA	Quickflow salinity	Average	mg/l
☐	QFLOSL	Quickflow salt load	Sum	mg
☐	RELEASL01	Generated salt load from topsoil ho...	Sum	mg
☐	RELEASL02	Generated salt load from subsoil h...	sum	mg
☐	RELEASLGW	Generated salt load from the groun...	Sum	mg
☐	RESINFSA	Reservoir inflow salinity	Average	mg/l
☑	RESSA	Reservoir storage salinity	Average	mg/l
☐	RUNOSA	Runoff salinity	Average	mg/l
☐	RUNOSL	Runoff salt load	Sum	mg
☐	SALTINP	Total salt input (from rainfall + irriga...	Sum	mg
☐	SEEPAGESA	Reservoir seepage water salinity	Average	mg/l
☑	SUBSSA	Subsoil salinity	Average	mg/l
☐	SUBSSL	Subsoil salt load	Sum	mg